DISTRIBUTION OF GAP JUNCTION PROTEINS IN VASCULAR TISSUE IN NORMAL AND DISEASED STATES

Nicole M. Rummery

A thesis submitted for the degree of Doctor of Philosophy

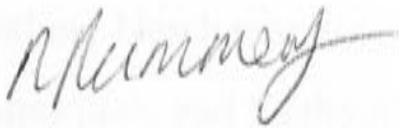**of the**

Australian National University

October 2003

Division of Neuroscience

John Curtin School of Medical Research

Australian National University

Canberra

STATEMENT

The contents of this thesis are original and all experiments were planned and carried out by the author under the supervision of Professor Caryl Hill, except where otherwise stated or referenced.

The preparation and Western blotting of cells transfected with DNA for vascular connexins was performed by Dr Hilton Grayson, while Western blotting of rat tissues was performed by Dr Gordon McGurk. Oligonuclotide primers used in this thesis were designed by Professor Caryl Hill. Electrophysiological experiments performed in Chapter 5 were carried out by Dr Narelle Bramich, while tension myography was performed with the assistance of Dr Shaun Sandow. In Chapter 7, experiments concerning conducted hyperpolarization and relaxation in the caudal artery were performed by Dr Kenichi Goto, and electron microscopy was performed by Dr Therese Brackenbury.

Nicole M. Rummery

ACKNOWLEDGMENTS

ABSTRACT

Gap junctions are intercellular ion channels comprised of molecules known as connexins (Cxs), and are important for the coordination and conduction of endothelial vasomotor responses and the maintenance of vascular tone. Gap junctions are found in the vascular wall connecting adjacent endothelial cells, and adjacent smooth muscle cells (Christ *et al.* 1996), while myoendothelial gap junctions are found connecting the two cell layers (Sandow *et al.* 2000). Four Cxs, Cx37, 40, 43 and Cx45, have been identified in the vascular wall (Severs, 1999; Krüger *et al.* 2000). Changes in endothelial function and signal conduction via gap junctions may be involved in the pathology of disease states such as hypertension. In the aorta of hypertensive rats, changes have been reported in the expression of Cx43, suggesting some coincidence between pressure and Cx expression in blood vessels (Haefliger *et al.* 1999).

Real-time polymerase chain reaction (PCR) and immunohistochemistry, using Cx specific antibodies, was used to quantify the expression of mRNA and protein for Cxs 37, 40, 43 and 45, separately in the smooth muscle and endothelium of two functionally different arteries, the thoracic aorta and caudal artery of young normotensive Wistar rats. Furthermore, changes in Cx expression were examined in these vessels during the development of hypertension and were correlated with changes in morphology of the smooth muscle and endothelium. Endothelial cell morphology and Cx expression was also assessed in other blood vessels known to be involved in the control of peripheral resistance. Finally, the effect any such changes may have on vascular function was examined in the caudal and mesenteric arteries during hypertension.

In young Wistar rats, results show that Cx37 was the major Cx present in gap junctions in the media of the caudal artery, while Cx43 was important in gap junctional coupling within the media of the thoracic aorta. Cxs 37, 40 and 43 were present in the endothelium of both arteries, while Cx45 was absent. These results highlight the heterogeneity of Cx expression amongst functionally different vascular beds.

The effect of blood pressure on vascular morphology and Cx expression, was examined in the thoracic aorta, caudal, mesenteric and basilar arteries of the spontaneously hypertensive rat (SHR) in comparison to the Wistar-Kyoto (WKY). The development of hypertension in the SHR was shown to begin at approximately 4 weeks of age with animals becoming hypertensive compared to age matched control WKY at 9 weeks of age.

Endothelial cell size was decreased in the caudal and mesenteric arteries of the SHR and this was accompanied by a decrease in the expression of Cx40 in the endothelium of the caudal artery and Cx37 in the mesenteric artery. Endothelial cell size was not altered in the thoracic aorta or basilar artery of the SHR; however expression of Cx37 in the endothelium was reduced in both arteries. Remodeling of the vascular media was also observed in both the caudal and mesenteric arteries, both vessels undergoing medial hypertrophy. In the caudal artery, such remodeling occurred in association with a reduction in the expression of Cx45. Medial remodeling was not observed in either the aorta or the basilar artery, however, in the aortic media expression of Cxs 43 and 45 was significantly reduced.

In the caudal artery of the WKY, endothelial cell size and the expression of Cxs 37, 40 and 43 was maximal at 3 weeks, while in the SHR cell size and the expression of Cx40 decreased during the development of hypertension. In the thoracic aorta, endothelial cells increased in size during development in both the WKY and SHR. Similarly, the expression of Cxs 37, 40 and 43 also was also increased in both strains. In the media of the caudal artery, the increase in expression of Cx45 during development was greater in the WKY than in the SHR, while in the aortic media, expression of Cxs 43 and 45 increased in the WKY during development but not in the SHR.

Vascular function during hypertension was examined in the caudal and mesenteric arteries of the SHR using tension myography and electrophysiology. In the caudal artery, results demonstrated that endothelium-derived hyperpolarizing factor (EDHF)-mediated hyperpolarization of the vascular media was reduced in the SHR, however there was no change in vessel relaxation. During examination of nerve-mediated excitatory junction potentials in the caudal artery, reduced radial coupling of the media in the SHR was demonstrated. In the mesenteric artery, conducted EDHF-mediated hyperpolarization and relaxation was reduced in the SHR; however, evidence suggests that this may be due to the involvement of K_{IR} channels during hypertension.

Changes in Cx expression and remodeling of the vascular smooth muscle and endothelium occur in some blood vessels during hypertension, however there is extensive heterogeneity amongst different vascular beds. In the caudal artery, vascular remodeling and altered Cx expression may have a causative role in the development of hypertension. The changes described here have demonstrated that vascular remodeling in combination with reduced cellular coupling could contribute significantly to endothelial dysfunction and altered vascular function during hypertension.

PUBLICATIONS ARISING FROM DATA PRESENTED IN THESIS

The following papers resulting from work presented in this thesis have been published:

Sandow SL. Bramich N, Bandi HP, Rummery N and Hill CE. (2003). Structure, function and EDHF in the caudal artery of the SHR and WKY rat. *Arterioscler. Thromb. Vasc. Biol.* 23:822-828.

Sandow SL, Bramich NJ, Bandi HP, Rummery N, Hill CE. (2002). Endothelium-derived hyperpolarizing factor, myoendothelial gap junctions and hypertension. In: EDHF 2002. Vanhoutte PM (ed.). Taylor and Francis Publishers. UK. Pp. 108-116.

Rummery NM, Hickey H, McGurk G, Hill CE. (2002). Connexin 37 is the major connexin expressed in the media of the caudal artery. *Arterioscler. Thromb. Vasc. Biol.* 22:1427-1432.

Hill CE, Rummery N, Hickey H, Sandow SL. (2002). Heterogeneity in the distribution of vascular gap junctions and connexins: implications for function. *Clin. Exp. Pharmacol. Physiol.* 29:620-625.

Rummery NM, McKenzie K, Whitworth JA, and Hill CE. (2002). Decreased endothelial cell size and connexin expression in rat caudal arteries during hypertension. *J. Hypertension.* 20:247-253.

A number of presentations of this work were made at scientific meetings. The following abstracts were published in conjunction with these presentations:

Rummery NM, Sandow SL, Brackenbury T and Hill CE. (2003). Vascular remodeling and changes in cellular coupling during vascular disease. Meeting of the Australian Physiological and Pharmacological Society, Sydney, NSW.

Rummery NM, Sandow SL, Brackenbury T and Hill CE. (2003). Variabiltiy in vascular remodeling and cellular coupling during hypertension. 11th Symposium of the Australian and New Zealand Microcirculation Society, Fraser Island, Qld.

Rummery NM, Hickey H, McGurk G, Hill CE. (2002). Connexin 37 is the major connexin expressed in the media of the caudal artery. *Journal of Vascular Research.* (22nd meeting of the European Society for Microcirculation), 39:S1.

Sandow SL, Rummery NM, Hill CE. (2002). Endothelium-derived hyperpolarizing factor and myoendothelial gap junctions are upregulated in the femoral artery of the juvenile rat. *Journal of Vascular Research.* (22nd meeting of the European Society for Microcirculation), 39:S1.

Sandow SL, Bramich NJ, Bandi HP, Rummery N, Hill CE. (2002). Structural changes maintain endothelium-derived hyperpolarizing factor activity in hypertensive caudal artery. *4th Workshop on EDHF.Abbaye des Vaux de Cernay (France)*, 4:53.

Hill CE, Bramich N, Rummery N, and Sandow SL. (2001). Heterogeneity in gap junctions contributes to function in normal and diseased arteries. *7th World Congress for Microcirculation.* 7:29-2.

Rummery NM, and Hill CE. (2001). Evidence against connexin43 expression in smooth muscle of tail artery. *Proc. Aust. Neuroscience Soc.* 12.

Rummery NM, McKenzie K, Whitworth J, Hill CE. (2001). Changes in cell size and connexin expression in the endothelium of the rat tail artery during the development of hypertension. The Canberra hospital region Annual scientific meeting. Canberra, Australia.

Hill CE, McKenzie K, Rummery NM*, and Whitworth J. (2001). Changes in cell size and connexin expression in the endothelium of the rat tail artery during the development of hypertension. Congress of International Union of Physiological Sciences, Christchurch, New Zealand. (*First author of abstract, authors are arranged alphabetically for conference requirements).

Sandow SL, Bramich N, Rummery N, and Hill CE. (2001). Correlation of myoendothelial gap junctions and EDHF-activity in the caudal artery during hypertension. Congress of International Union of Physiological Sciences, Christchurch, New Zealand.

Hill CE, Hong T, Rummery N, Francki K, Hickey H, Sandow SL. (2000). Heterogeneity in the distribution of vascular gap junctions and connexins: implications for function. *Proc. Aust. Phys. Pharm. Soc.* 31:133P.

ABBREVIATIONS

The following is a list of abbreviations used in the text of this thesis:

ACh	acetylcholine
ATP	adensoine triphosphate
BA	basilar artery
bp	base pairs
BSA	bovine serum albumin
CA	caudal artery
Ca^{2+}	calcium
cAMP	cyclic 3',5'-adenosine monophosphate
cDNA	complementary DNA
cGMP	cyclic 3',5'-guanosine monophosphate
Ct	threshold cycle
C-terminal	carboxyl-terminal
Cx(s)	connexin(s)
dATP, dCTP, dGTP, dTTP	deoxynucleotide (adenosine, cytidine, guanosine, thymidine) triphosphate
DNA	deoxyribonucleic acid
DNaseI	deoxyribonuclease I
DOCA	deoxycorticosterone acetate
EC	endothelial cell
EDTA	ethylenediaminetetra-acetic acid
EDHF	endothelium-derived hyperpolarizing factor
EJP(s)	excitatory junction potential(s)
FITC	fluorescein iso-thiocyanate
GA	glycyrrhetinic acid
IEL	internal elastic lamina
Kb	kilobases
K_{Ca}	calcium activated potassium channel
K_{IR}	inwardly rectifying potassium channel
L-NAME	N^{G}-nitro-L-arginine methyl ester

MA	mesenteric artery
MEGJ(s)	myoendothelial gap junction(s)
mmHg	millimetres of mercury
mRNA	messenger RNA
NO	nitric oxide
NOS	nitric oxide synthase
N-terminal	amino-terminal
PAGE	polyacrylamide gel electrophoresis
PBS	phosphate buffered saline
PCR	polymerase chain reaction
RNA	ribonucleic acid
RNase	ribonuclease
ThA	thoracic aorta
tRNA	transfer RNA
SHR	spontaneously hypertensive rat
SHR-SP	stroke-prone spontaneously hypertensive rat
SMC	smooth muscle cell
VDCC	voltage dependent calcium channel
vWF	von Willebrand factor
WKY	Wistar-Kyoto rat

TABLE OF CONTENTS

CHAPTER 1

INTRODUCTION

1.1 STRUCTURE AND FUNCTION OF GAP JUNCTION CHANNELS

Gap junction channels are expressed in almost all mammalian tissues where they facilitate chemical and electrical communication between adjacent cells. As such, gap junctions are essential for a number of functions, including the maintenance of homeostasis, embryonic development, cellular differentiation, proliferation and migration (Loewenstein, 1979; Kumar & Gilula, 1996; Delorme *et al.* 1997). Gap junction communication has also been demonstrated in inflammatory processes and wound healing (Larson & Haudenschild, 1988; Beyer & Steinberg, 1991). In electrically excitable tissues such as the myocardium and vascular tissue, gap junctions are essential for cellular communication via the propagation of action potentials. In a similar manner, metabolites and second messengers including cyclic adenosine monophosphate (cAMP), inositol triphosphate and calcium (Ca^{2+}) are able to pass though gap junction channels from one cell to another (Gilula *et al.* 1972; Tsien & Weingart, 1976; Saez *et al.* 1989; Veenstra *et al.* 1995; Carter *et al.* 1996).

1.1.1 Gap junction structure

Gap junctions are intercellular channels formed in the plasma membrane, linking the cytoplasm of adjacent cells, allowing the direct transfer of electrical current and small molecules of less than one kilodalton (1 kD) in molecular weight, between coupled cells (Kumar & Gilula, 1996). Gap junction channels are comprised of a family of membrane proteins known as connexins (Cxs). Six individual Cx proteins oligomerize in the plasma membrane of one cell to form a connexon or hemichannel. A complete gap junction channel results from the docking of two connexons, one from each of two apposing cells (Musil & Goodenough, 1993; Falk *et al.* 1997). Each connexon may be comprised of a single Cx isotype or multiple isotypes, forming homomeric or heteromeric connexons, respectively. Consequently, gap junction channels may be either homotypic or heterotypic in nature depending on the type of connexon contributed from each cell (Goodenough *et al.* 1996; Brink *et al.* 1997; White & Paul, 1999) (Figure 1.1).

1

Figure 1.1

Figure 1.1.

Structure of gap junction channels. Six connexin proteins oligomerize forming a hemichannel or connexon in the plasma membrane of one cell. A complete gap junctional channel linking two adjacent cells results from the docking of two connexons, one from each of the two apposing cells. Connexons may be homomeric (A, B) or heteromeric (C, D) in nature depending of whether a single or multiple types of connexins are present in each connexon. Homotypic (A, D) or heterotypic (B, C) gap junction channels may also form depending on the Cx type in the two connexons.

A. Homomeric Homotypic **B. Homomeric Heterotypic** **C. Heteromeric Heterotypic** **D. Heteromeric Homotypic**

Plasma membrane cell 1

Intercellular gap

Plasma membrane cell 2

Connexon

Connexin
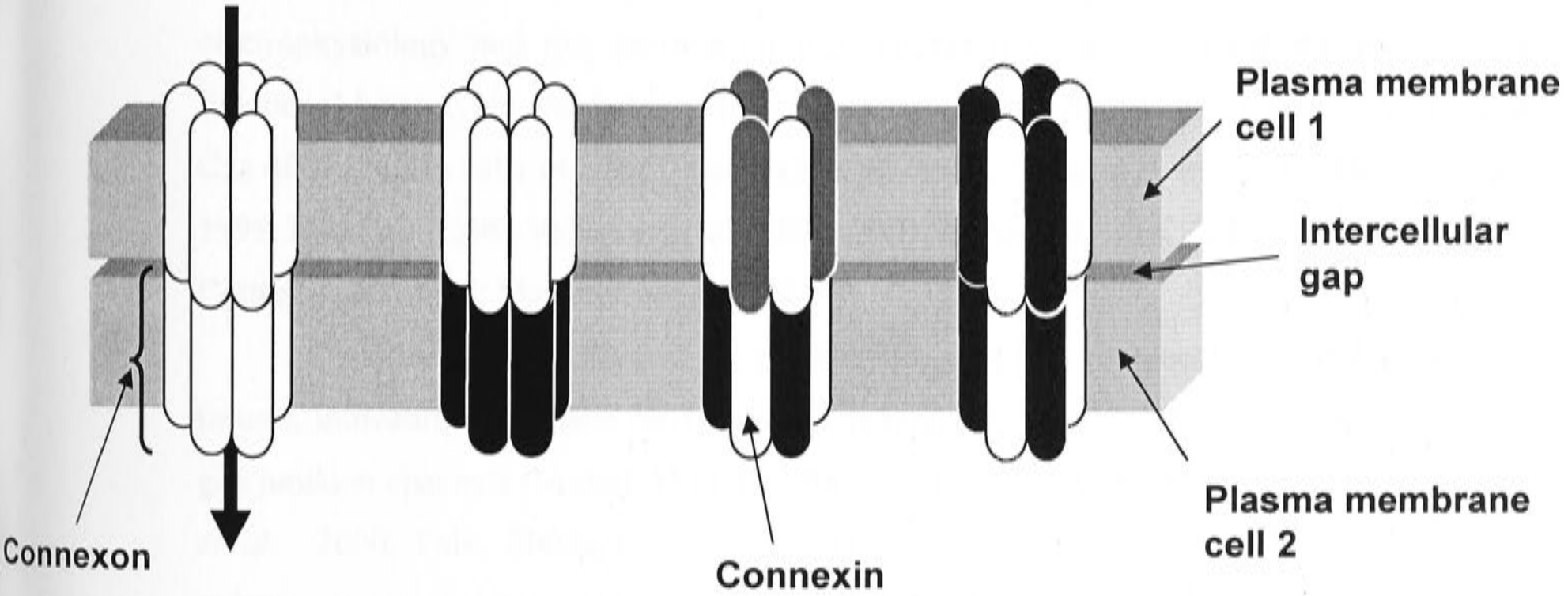
While the formation of homotypic or heterotypic gap junction channels has been demonstrated *in vitro*, less is known regarding their expression *in vivo*. The ability of a cell population to express each type of gap junction channel depends on the number of Cx proteins expressed within that population. Thus, heteromeric and heterotypic gap junctions may be formed when two or more Cx isotypes are expressed within the cell population. Brink *et al.* (1997) demonstrated that a cell population expressing more than one Cx isotype has the potential to form up to 196 structurally and physiologically distinct channel types, although it has been shown that not all Cx isotypes are able to form connexons, therefore limiting this theoretical number to less than 196 in practice (Brink *et al.* 1997). In cultured A7r5 cells, experiments have demonstrated the co-localization of Cxs 40 and 43 (He *et al.* 1999), while in HeLa cells the co-localization of both Cxs 40 and 43 have been demonstrated in some hemichannels (Valiunas *et al.* 2001). Furthermore, electrophysiology and dye permeation experiments have demonstrated the presence of functional heterotypic and heteromeric gap junction channels between Cxs 40 and 43, and Cxs 40 and 45 in cells *in vitro* (Steinberg *et al.* 1994; Elfgang *et al.* 1995; Moreno *et al.* 1995; He *et al.* 1999; Valiunas *et al.* 2000, 2001; Cottrell & Burt, 2001; Burt *et al.* 2001; Cottrell *et al.* 2002; Martinez *et al.* 2002).

Co-localization of several Cx proteins has also been demonstrated in a number of tissues, indicating that these cells have the potential to form heterotypic and heteromeric gap junction channels (Nicholson *et al.* 1987; Gros & Jongsma, 1996; Severs, 1999; Beyer *et al.* 2000; Falk, 2000a,b). For example, in endothelial cells of the rat aorta and pulmonary artery, immunohistochemical and ultrastructural studies have shown that Cxs 37, 40 and 43 are commonly co-localized in the same gap junctional plaque (Yeh *et al.* 1997a, 1998; Ko *et al.* 1999). A gap junction plaque may be formed by the aggregation of several to many thousands of gap junction channels (McNutt & Weinstein, 1970; Lagaud *et al.* 2002a). In a similar manner, Cxs 40 and 43 have been found to co-localize within the atrioventricular node and Purkinje fibres (Gourdie *et al.* 1993), while Cx43 has been found to co-localize with Cx45 in a restricted zone of the sinoatrial node of the rat heart (Coppen *et al.* 1999). In cultured cells, experiments have demonstrated that dye transfer is absent in the absence of Cx plaques and in the presence of very small plaques (Bukauskas *et al.* 2000). Dye transfer was present in cells displaying larger gap junction plaques estimated to contain at least 400 channels. In these plaques, it was found that only a small percentage of channels present within the plaque were open at the one time. These results suggest that

2

clustering of gap junction channels into plaques may be required for effective cellular coupling as smaller plaques contained fewer open gap junction channels at any one time.

1.1.2   Connexin proteins

To date, 20 Cx proteins have been identified in mammalian tissue (Willecke *et al.* 2002; Gustincich *et al.* 2003). Each protein, commonly named after its molecular weight in kDa, is encoded by a single gene consisting of one exon and one or two introns within the 5' untranslated region (White & Paul, 1999). All Cxs have the same basic molecular structure, each consisting of four α-helical membrane-spanning domains, two extracellular loops, one intracellular loop and three cytoplasmic regions (Yeager & Gilula, 1992; Falk *et al.* 1994). The distinct functional properties of each Cx protein arise from amino acid sequences specific for each Cx, located in the intracellular loop and carboxy terminus. The two extracellular loops contain highly conserved cysteine residues, which are involved in the docking of the two hemichannels the formation of heterotypic gap junction channels (Yeager & Nicholson, 1996; Sosinsky, 1996). The four α-helical membrane-spanning domains are highly conserved in their amino acid sequence. The second transmembrane domain contains a proline residue, shown to be important for voltage gating of the channel, while the third transmembrane domain is amphipathic in nature and is thought to line the central pore of the gap junction channel (Yeager & Nicholson, 1996; Kumar & Gilula, 1996; Tearle, 2002).

1.1.3   Functional properties of gap junction channels

Gap junction channels demonstrate unique electrical and biochemical properties depending on the constituent Cx isotypes present. Functional properties of gap junction channels such as unitary conductance, voltage gating and permeability have been studied using single Cx expression systems in cell culture (van Veen *et al.* 2001). For example, homotypic channels containing Cx37 have high unitary conductance values of approximately 300-400 picoSiemens (pS) (Veenstra *et al.* 1994b). Homotypic channels containing Cxs 40 or 43, have unitary conductance values of approximately 150-200 pS and 90-115 pS respectively (Veenstra *et al.* 1992; Moreno *et al.* 1994; Traub *et al.* 1994; Beblo *et al.* 1995), while Cx45 channels demonstrate low unitary conductance values of 25-30 pS (Veenstra *et al.* 1994a; Moreno *et al.* 1995). The permeability of gap junction

channels to dyes and small molecules also varies depending on the constituent Cxs. Homotypic channels formed in HeLa cells expressing Cx43 are non-ion selective and are readily permeable to dyes such as Lucifer yellow (Martinez *et al.* 2002). On the other hand, homotypic channels comprised of Cx45 show greater selectivity for cations than anions and are permeable to Lucifer yellow (van Veen *et al.* 2001), whilst Cx40 channels are cation selective and permeable to Lucifer yellow, 2'7'-dichlorofluorescein and 6-carboxyfluorescein (van Veen *et al.* 2001).

The formation of heterotypic and heteromeric channels, expressing more than one Cx, has been shown to confer channel properties that are distinct from homotypic channels formed from each of the individual Cxs (Brink, 1998; Beyer *et al.* 2000; Cottrel & Burt, 2001; Valiunas *et al.* 2000; Burt *et al.* 2001; Valiunas *et al.* 2002; Steinberg *et al.* 1994; Martinez *et al.* 2002). These studies suggest that the heteromeric nature of gap junction channels depends on the properties of the individual Cxs within the channel and the ratio in which each Cx is expressed. Recently, it has been demonstrated that altering the ratio of Cxs 40 and 43 expressed in cultured cells affects the chemical, but not the electrical permeability of the channel. Heterotypic channels were shown to adopt the biochemical characteristics of the more permeably restrictive channel (Burt *et al.* 2001; Cottrel *et al.* 2002). The above studies thus suggest that the functional properties of a cell population may be altered by changes in Cx expression (Beyer *et al.* 2000; Brink *et al.* 2000). Thus, this demonstrates the importance of determining the specific Cx composition of the gap junctional channels formed in any particular artery or arteriole, since this is likely to have a significant influence on vascular function.

1.2   GAP JUNCTION REGULATION

The electrical and biochemical properties of gap junction channels can be modulated in both the short or long term. Short-term regulation of gap junctions may involve rapid and reversible changes in channel conductance by altering channel open probability or channel turnover. Long-term regulation involves alterations in gene expression at the mRNA and protein levels. Gap junctional conductance may be modulated by a number of different mechanisms such as the phosphorylation of Cx proteins, changes in intracellular Ca^{2+} concentration and pH. Furthermore, Cx expression may also be

regulated by changes in Cx synthesis and turnover rates (Severs *et al.* 1996; van Veen *et al.* 2001).

1.2.1 Gap junction phosphorylation

Almost all Cx proteins can be characterized as phosphoproteins (Goodenough *et al.* 1996). It is likely that the phosphorylation occurs as a form of posttranslational modification that regulates gap junctional protein trafficking, assembly into gap junctional plaques, channel conductance and turnover (Musil & Goodenough, 1991; Saez, 1998). Phosphorylation has been demonstrated to both increase and decrease gap junctional communication depending on the cell type examined (Munster & Weingart, 1993; Kwak & Jongsma, 1996; Lampe & Lau, 2000). Cx phosphorylation is induced by the activation of various protein kinases such as protein kinase C (PKC) (Saez *et al.* 1997), PKA (Traub *et al.* 1994; van Rijen *et al.* 2000), PKG (Takens-Kwak & Jongsma, 1992), mitogen-activated protein (MAP) kinase (Warn-Cramer *et al.* 1996), as well as many unknown protein kinases (Lampe & Lau, 2000). Phosphorylation of Cx proteins occurs predominantly on serine residues, with tyrosine phosphorylation also occurring, although to a lesser extent (Crow *et al.* 1990; Laing *et al.* 1994; Kanemitsu *et al.* 1997; van Veen *et al.* 2000). For Cx43, the majority of these residues are putative sites for PKC phosphorylation, however there are also several sites known to be phosphorylated by PKA, PKG and MAP kinase (Kanemitsu & Lau, 1993; Lau *et al.* 1996; Warn-Cramer *et al.* 1996; Lampe & Lau, 2000). The number and location of specific phosphorylation sites for each Cx protein vary according to the species of sequence origin, although most serine phosphorylation sites are found within a highly conserved region of the carboxy terminus (Laing *et al.* 1994; Lampe *et al.* 2000; van Veen *et al.* 2001).

Just as phosphorylation of Cx proteins by protein kinases has profound effects on gap junctional communication, dephosphorylation of Cxs by protein phosphatases also has important modulatory effects on gap junction function, having been shown to have a role in trafficking and degradation of Cx proteins (Lampe & Lau, 2000). Inhibition of protein phosphatases has been shown to increase Cx43 phosphorylation and alter channel conductance *in vitro* (Moreno *et al.* 1994).

1.2.2 Intracellular calcium and pH

The diffusion of Ca^{2+} through gap junctions at concentrations outside normal physiological ranges has been shown to cause channel closure (Burt, 1987; Brink *et al.* 2000). Studies in lens epithelial cells demonstrate reduced gap junctional coupling following sustained increases in intracellular Ca^{2+} (Churchill *et al.* 2001), while other studies describe reduced Cx43 phosphorylation and gap junctional coupling following an increase in Ca^{2+} levels within physiological ranges (Crow *et al.* 1994).

Intracellular pH has also been shown to affect intercellular communication through gap junction channels (Morley *et al.* 1997). *In vitro*, lowering pH, significantly reduces channel conductance, while at very low pH, conductance is completely inhibited, likely a result of reduced channel open probability (Hermans *et al.* 1995; Morley *et al.* 1997). The sensitivity of gap junction channels to changes in pH depends on the particular Cx isotype (Werner *et al.* 1991; Stergiopoulos *et al.* 1999; Gu *et al.* 2000; Thomas *et al.* 2002). The cytoplasmic loop of the Cx protein, an area rich in proline residues, may be involved in the sensitivity of Cx43 to changes in pH (Ek-Vitorin *et al.* 1996; Calero *et al.* 1998). In a similar manner, histidine residues within this same region have been shown to be essential for both normal channel formation and pH gating (Spray & Burt, 1990; Ek *et al.* 1994; Hermans *et al.* 1995). Several studies have suggested that pH gating of Cxs involves interaction between the cytoplasmic loop of the protein and specific sequences in the pore region acting as a receptor site (Ek *et al.* 1994; Morley *et al.* 1996, 1997).

1.2.3 Synthesis, trafficking and degradation of gap junctions

Synthesis, aggregation and degradation of gap junction channels are all targets for the regulation of intercellular communication. Although, the formation of gap junction channels has been extensively studied, the process of Cx biosynthesis and assembly into gap junctions is complex and many unanswered questions remain.

Many studies have shown that the biosynthesis of Cx proteins is similar to that of other membrane proteins, in that synthesis occurs in the endoplasmic reticulum (ER) following translocation into the ER membrane (see Yeager *et al.* 1998; Falk, 2000a,b). Whether post-translational modification of Cx proteins and the formation of connexon hemichannels occurs in the ER or later in the Golgi apparatus is a point of some debate, as there is evidence in support of both pathways (Musil & Goodenough, 1993; Kumar *et al.* 1995; Ahmad *et al.* 1999). Transportation of Cxs from the ER to the plasma membrane via

6

the Golgi apparatus occurs predominantly via the secretory pathway (Musil & Goodenough, 1993; George *et al.* 1999; Martin *et al.* 2001), although it has been suggested that some Cxs use an alternative transportation mechanism dependent on microtubules and G proteins (George *et al.* 1999; Lampe *et al.* 2001; Martin *et al.* 2001). Thus, there is evidence that the exact location of hemichannel assembly and the mechanisms involved in their transportation to the plasma membrane may differ depending on the Cx isotype (Yeager *et al.* 1998; Geroge *et al.* 1999; Sarma *et al.* 2002).

As mentioned above, following insertion of Cxs into the plasma membrane, the formation of a complete gap junction channel requires the docking of two hemichannels within the plasma membrane of two apposing cells (Musli & Goodenough, 1993). Experiments using Cxs tagged with fluorescent proteins have demonstrated that hemichannels may be inserted either directly into a gap junction plaque or randomly into the plasma membrane, whereby they are able to move laterally along the plasma membrane and become integrated into the edge of an existing plaque (Yeager *et al.* 1998; Gaietta *et al.* 2002; Lauf *et al.* 2002). The formation of gap junctions and the clustering of channels into gap junction plaques may be facilitated by cell adhesion molecules including E-cadherin, liver cell adhesion molecule, and N-cadherin (Musil *et al.* 1990; Jongen *et al.* 1991; Meyer *et al.* 1992; Yeager *et al.* 1998). More recently a role for cytoskeletal proteins such as zonula occludens-1 (ZO-1) and α-spectrin have also been identified (Toyofuku *et al.* 1998). The exact mechanisms involved may depend on the Cx isotype, although this is currently unknown.

Unlike other membrane proteins, Cxs have a short half-life of between 1-5 hours (Darrow *et al.* 1995; Laird *et al.* 1991; Hertlein *et al.* 1998). Such rapid turnover presents a dynamic way of controlling cellular communication by up- or down-regulation of Cx synthesis, assembly, trafficking and degradation. The degradation of Cx proteins, like other plasma membrane proteins occurs either at the ER via proteasomal dependent mechanisms in response to protein mis-folding and improper oligomerization, or at the plasma membrane, resulting in the degradation of complete gap junction channels (Gropper *et al.* 1991; Musil *et al.* 2000; Jordan *et al.* 2001). Degradation of gap junction channels in the plasma membrane is not well understood. However, it is thought to involve both lysosomal and proteasomal pathways (Laing *et al.* 1997; Laing & Beyer, 1995; McGee *et al.* 1996; Musil *et al.* 2000). Double membrane vesicular bodies composed of gap junction channels, termed annular gap junctions (Naus *et al.* 1993) have been suggested to be initial

7

degradation products formed following the internalisation of gap junction channels or large fragments of gap junction plaques (Severs *et al.* 1989; Jordan *et al.* 2001; Gaietta *et al.* 2002). Gap junction channels contained within annular gap junctions are subsequently targeted for either protesomal or lysosomal degradation (Laing *et al.* 1997; Beardslee *et al.* 1998; Laing *et al.* 1998; Musil *et al.* 2000). Therefore, the formation of annular gap junctions may provide a mechanism by which large numbers of gap junction channels can be simultaneously degraded (Jordan *et al.* 2001).

Recently, there has been some suggestion that the processes involved in the synthesis, trafficking and degradation of gap junction channels present potential targets for therapeutic regulation of cellular coupling. However, drugs currently used to inhibit these mechanisms in experimental conditions are not specific for Cx proteins, having widespread effects on many cellular proteins (Brink, 2002; Beyer & Berthoud, 2002; Lagaud *et al.* 2002a). More recently, it has been suggested that modulation of gap junction gating, can be achieved using peptides synthesised to mimic sequences of the extracellular loops of Cx proteins (Berman *et al.* 2002). The application of such peptides has been shown to inhibit gap junctional communication *in vivo* and *in vitro*, while also being selective to specific Cx isotypes (Chaytor *et al.* 1997; Kwak & Jongsma, 1999; Berman *et al.* 2002).

1.3   GAP JUNCTION EXPRESSION IN VASCULAR TISSUE

Communication via gap junctions between cells in the vascular wall has been implicated in a range of functions, including coordination and conduction of endothelial cell responses modulating vasomotor tone (Christ *et al.* 1996). Studies involving immunofluorescence, electron microscopy and electrophysiology have identified gap junctions connecting adjacent endothelial cells (Ko *et al.* 1999), adjacent smooth muscle cells (Beny & Connet, 1992) and adjacent endothelial and smooth muscle cells via myoendothelial gap junctions (MEGJs, Sandow & Hill, 2000). At the ultrastructural level, gap junctions are identified by their electron dense pentalaminar structure, with a total thickness of approximately 9-10 nm, whereby the proximity of the outer membrane of the two apposing cells is seen as a single dark line. In some cases, at this point a gap of approximately 3 nm in width is visible (Unwin & Zampighi, 1980), which delineates the two adjacent connexon oligomers.

Within cardiovascular tissue, four Cxs have been reported, Cxs 37, 40, 43 and 45 (Severs, 1999; Hill *et al.* 2001). All four Cxs have been identified in vascular smooth muscle, while Cxs 37, 40 and 43 have been detected in the endothelium of most vessels (see Hill *et al.* 2001). More recently, two new Cxs have been identified in mouse and human vascular smooth muscle, Cxs 31.9 and 30.2 (White *et al.* 2002; Nielsen *et al.* 2002; Nielsen & Kumar, 2003). Overall, the current data suggests that there is significant heterogeneity in Cx expression within and between species and vascular bed, indicating that vessels of differing function may express different Cx isotypes (Hill *et al.* 2001). Localized differences in Cx expression have been described in the media and endothelium of the rat aorta and human internal mammary artery (Ko *et al.* 1999a,b; Ko *et al.* 2001), in the endothelium of afferent renal arterioles (Gabriels & Paul, 1998; Guo *et al.* 1998), and in areas of increased shear stress, such as at aortic branch points (Gabriels & Paul, 1998). Furthermore, the expression of Cx proteins in the aortic endothelium has also been shown to vary with age (Yeh *et al.* 2000).

Given that the different Cx isotypes may form channels with unique electrical and biochemical properties, the heterogeneity in Cx expression amongst different vessels may contribute to the heterogeneity in vascular responses (Severs, 1999; Hill *et al.* 2001).

1.3.1 Smooth muscle

Whilst the specific Cx composition in different arteries varies, Cx43 is the predominant Cx expressed in the vascular smooth muscle of large elastic arteries such as the thoracic aorta (Hong & Hill, 1998; Yeh *et al.* 1998; Nakamura *et al.* 1999; Hong & Hill, 1998; van Kempen & Jongsma 1999). Comparative studies of Cx43 expression in such large conduit arteries show that expression decreases with distance from the heart (Ko *et al.* 2001). Cx45 has also been detected in the media of the thoracic aorta (Ko *et al.* 2001; Li & Simard, 2002), although its expression is significantly less than that of Cx43. Interestingly, expression of Cxs 43 and 45 in the aorta seems to be dependent on smooth muscle cell phenotype. Smooth muscle cells of the synthetic phenotype express high levels of Cx43, while differentiated cells of the contractile phenotype express low levels of Cx43. Furthermore, Cx45 expression appears to be approximately inverse to that of Cx43 in most regions of the aorta (Ko *et al.* 2001). Fully differentiated smooth muscle cells of an adult non-diseased artery are predominately of the contractile phenotype. Together these studies suggest that Cx43 may be important for the synthesis and maintenance of the extracellular

matrix, while Cx45 may be more important in mature contractile smooth muscle cells (Rennick *et al.* 1993; Blackburn *et al.* 1997; Ko *et al.* 2001). Other Cxs found in the media of elastic arteries include Cx40, which has been described in the aorta of several animal species including cow and pig, although it is absent in the rat thoracic aorta (van Kempen & Jongsma, 1999). Studies have also described the presence of medial Cx37 in the aorta and pulmonary artery of the rat (Nakamura *et al.* 1999), although such observations have not been universally supported (van Kempen & Jongsma, 1999). Such discrepancies are likely to be due to the specificity of Cx antibodies used in each particular study (Severs *et al.* 2001). Recent studies have demonstrated the expression of protein for the newly identified Cx31.9 in smooth muscle cells of the human aorta (Nielsen *et al.* 2002).

Studies investigating the major Cx isoform within the media of muscular arteries provide evidence for a similar heterogeneity amongst different vascular beds and animal species. A number of studies have reported that Cx43 is absent in the media of muscular arteries, including the caudal, basilar, mesenteric and coronary arteries (Bastide *et al.* 1993; Bruzzone *et al.* 1993; Gros *et al.* 1994; Yeh *et al.* 1997b; Hong & Hill, 1998; Li & Simard, 1999). However, other studies have reported the presence of Cx43 in the media of pial and cremaster arterioles and the basilar artery of the rat and cheek pouch arterioles of the hamster (Li & Simard, 1999; Little *et al.* 1995a). Cx40 has been demonstrated in the media of the coronary artery in a number of species (van Kempen & Jongsma, 1999), as well as in the basilar artery (Li & Simard, 1999), in preglomerular and cremaster arterioles of the rat (Little *et al.* 1995a; Arensbak *et al.* 2001; Haefliger *et al.* 2001), and in hamster cheek pouch arterioles (Little *et al.* 1995a); although Cx40 is absent from mesenteric arterioles of the rat (Gustafsson *et al.* 2003). A number of studies have identified Cx45 in vascular smooth muscle of embryonic and adult mice (Krüger *et al.* 2000; Kumai *et al.* 2000; Alcoléa *et al.* 1999), while more recently, Cx45 has been demonstrated in the media of cerebral vessels of the rat (Li & Simard, 2002). While generally considered to be an endothelial Cx, Cx37 has been identified in the media of the coronary artery of the rat (van Kempen & Jongsma, 1999) and in collateral vessels during coronary arteriogenesis in the dog (Cai *et al.* 2001). Recently, studies have demonstrated the expression of the Cxs 31.9 and 30.2 in vascular smooth muscle cells of human and mouse testis and brain (Nielsen *et al.* 2002; White *et al.* 2002; Nielsen & Kumar, 2003).

The extent of Cx staining in the media of muscular arteries and arterioles suggests the incidence of gap junction channels may be less than that observed in the endothelium or in the media of conduit vessels (Xia *et al.* 1995; Beny, 1999). At the ultrastructural level, pentalaminar gap junctions between smooth muscle cells are rarely observed, and where described are smaller ($\leq$100 nm) than those observed in the endothelium (Berne & Rubio, 1979; Beny & Connat, 1992; Sandow & Hill, 2000; Sandow *et al.* 2003b). Interestingly, dyes such as Lucifer yellow readily pass between endothelial cells of large muscular arteries and arteries of the microcirculation (Emerson & Segal, 2000a,b; Sandow *et al.* 2003b), and between smooth muscle cells of large muscular arteries such as the caudal artery (Sandow *et al.* 2003b); which is in contrast to arterioles of the microcirculation where such dye movement between adjacent smooth muscle cells is absent (Segal & Beny, 1992; Emerson & Segal, 2000a,b). In the smooth muscle of the caudal artery, dye movement occurred in a preferential manner, between smooth muscle cells in a radial, but not a longitudinal direction (Sandow *et al.* 2003b). Results such as these further suggest differences between the coupling within the two cell layers.

Indeed, discrepancies in reported Cx staining in some vessels, such as the cheek pouch arteriole (Little *et al.* 1995a; Sandow *et al.* 2003d) are likely due to non-specificity of antibodies and /or poor experimental technique; thus accounting further for the range of reported heterogeneity in Cx expression (Hill *et al.* 2001; Severs *et al.* 2001). To date, there have been few studies which have systematically investigated the expression of all four Cxs in vascular tissue using rigorously tested antibodies.

1.3.2 *Endothelium*

In the vascular endothelium, Cxs 37, 40 and 43 have been commonly identified in both large and small arteries, but unlike vascular smooth muscle, Cx expression shows less variation amongst vascular bed and species. At the ultrastructural level, large areas of intact pentalaminar gap junctions, up to and more than 1 μm in length, have been found, confirming the view that endothelial cells are well coupled throughout the vasculature (Yeh *et al.* 1998; Ko *et al.* 1999; Sandow *et al.* 2003d). Similarly, at the light microscope level, gap junctions appear punctate, delineating the border of endothelial cells (Yeh *et al.* 1998).

The gap junction protein most widely expressed throughout the vasculature in a number of different animal species is Cx40. Expression of protein for Cx40 has been

identified in the aorta of the rat, cow, pig and embryonic mouse (Delorme *et al.* 1997; Yeh *et al.* 1997a, 1998; Gabriels & Paul, 1998; van Kempen & Jongsma, 1999), and in the carotid and pulmonary arteries of the rat (Ko *et al.* 1999; Yeh *et al.* 1998, 2000). Cxs 37 and 43 are also expressed in the endothelium of the aorta, carotid and pulmonary arteries of the rat (Hong & Hill, 1998; van Kempen & Jongsma, 1999; Yeh *et al.* 1997a; 1998, 2000; Gabriels & Paul, 1998; Nakamura *et al.* 1999). Cx43 expression is also found in the pig aorta (van Kempen & Jongsma, 1999). In the rat aorta and pulmonary artery, all three Cxs are frequently co-localized in the same gap junctional plaque, thus suggesting the ability of these tissues to form heteromeric gap junction channels (Ko *et al.* 1999; Yeh *et al.* 1997a, 1998). Some studies have found that the expression of Cx37 in the rat aorta is heterogeneous in nature, unlike the abundant expression of Cxs 40 and 43 (van Kempen & Jongsma, 1999; Yeh *et al.* 1997a). In contrast to these studies, Gabriels & Paul (1998) show that the expression of Cx43 is heterogeneous along the length of the rat aorta, with ten-fold greater expression in the thoracic aorta compared to the abdominal aorta. Expression of Cx37 was also detected in the aorta of the embryonic mouse, while Cx43 was absent (Delorme *et al.* 1997; Simon & McWhorter, 2003). In culture, Cx37 has been detected between endothelial cells derived from the porcine and bovine aorta (Reed *et al.* 1993; Carter *et al.* 1996), while Cx43 is present in cells from the porcine aorta and the bovine pulmonary artery (Lash *et al.* 1990; Pepper *et al.* 1992b). However, it should be noted that expression in culture has been shown to differ from that in intact vessels (van Kempen & Jongsma, 1999).

All three Cxs are also expressed in the endothelium of muscular arteries in a number of species, Cx40 being the most widely expressed of the three Cxs. Expression of Cx40 was detected in the coronary artery of the rat, mouse, bovine, pig and in collateral vessels of the dog (Bastide *et al.* 1993; Gros *et al.* 1994; Yeh *et al.* 1997a, 1998; van Kempen & Jongsma, 1999; Cai *et al.* 2001). The mesenteric and basilar arteries of the rat also expresses Cx40 (Li & Simard, 1999; Gustafsson *et al.* 2003), as do human umbilical arteries and the pial and cremaster arterioles of the rat and the cheek pouch arterioles of the hamster (Little *et al.* 1995; van Rijen *et al.* 1997). Vessels of the mouse renal vasculature including the interlobular arteries and the afferent and efferent arterioles also express Cx40 (Seul & Beyer, 2000). Like Cx40, expression of Cx37 is also found in the coronary artery of the rat, mouse, pig and collateral vessels of the dog (Yeh *et al.* 1997a, 1998; van Kempen & Jongsma, 1999; Cai *et al.* 2001), however the distribution of Cx37 is more

heterogeneous in nature compared to the abundant expression of Cx40 in these vessels. Cx37, while absent from the endothelium of the bovine coronary artery (van Kempen & Jongsma, 1999), is found in small arteries of the lung parenchyma in humans and rats (van Rijen *et al.* 1997). In the rat mesentery, expression of Cx37 was present in some, but not all vessels examined (Gustafsson *et al.* 2003). The distribution of Cx43 in muscular arteries is less than that of Cxs 37 and 40. While Cx43 was detected in the endothelium of the pig coronary artery, in the cow this expression was found only in the proximal vessels and was absent in the rat coronary artery except in areas towards the aortic junction (Yeh *et al.* 1997a, 1998; Hong & Hill, 1998; van Kempen & Jongsma, 1999). Cx43 was also detected in the mesenteric arteries and in pial and cremaster arterioles of the rat, in cheek pouch arterioles of the hamster (Little *et al.* 1995; Gustafsson *et al.* 2003), and in human umbilical artery endothelial cells (van Rijen *et al.* 1997).

1.3.3 *Myoendothelial gap junctions*

Myoendothelial gap junctions (MEGJs) form when projections arising from an endothelial cell or a smooth muscle cell abut the plasma membrane of a cell from the opposite layer (Sandow & Hill, 2000). MEGJs are smaller and less frequent than homocellular endothelial cell gap junctions and their incidence varies throughout the vasculature (Sandow & Hill, 2000; Sandow *et al.* 2002). For example, ultrastructural experiments have demonstrated that the number of MEGJs in the rat mesenteric artery varies along the length of the vessel, with significantly more MEGJs in the distal compared to the proximal mesenteric artery (Sandow & Hill, 2000). Furthermore, while MEGJs have been identified ultrastructurally in the caudal artery of the adult rat, no MEGJs were found in the rat femoral artery (Sandow *et al.* 2002, 2003b), while the incidence of MEGJs in the lateral branch of the saphenous artery is significantly greater in the juvenile than in the adult WKY rat (Sandow *et al.* 2003c). Furthermore, it has been shown that the incidence of MEGJs in the blood vessel wall increases as the size of the vessel decreases (Sandow & Hill, 2000; Hill *et al.* 2002; Sandow *et al.* 2003a). Coupling of the smooth muscle and endothelium has also been demonstrated electrophysiologically in the hamster cheek pouch arteriole and the porcine ciliary artery with the direct transfer of dye between the two cell layers, thus indicating the presence of MEGJs (Little *et al.* 1995b; Beny, 1999). In a similar manner, in the rat mesenteric and the hamster retractor feed arteries, resting membrane potential of endothelial and smooth muscle cells were not significantly different;

thus further supporting the presence of direct electrical coupling of the two cell layers (Emerson & Segal, 2000a, 2001; Sandow *et al.* 2002). Furthermore, in several vascular beds, agonist induced hyperpolarization of the endothelium evokes a similar hyperpolarization of the smooth muscle suggesting that the two cell layers are coupled (Sandow *et al.* 2002; Emerson & Segal, 2000a, 2001). At the ultrastructural level, MEGJs have been identified in several tissues in rat, human, rabbit and mouse vessels (Spagnoli *et al.* 1982; Aydin *et al.* 1991; Sandow & Hill, 2000; Sandow *et al.* 2003b; Dora *et al.* 2003), however, identification of the Cx isotype present at MEGJs is yet to be determined.

The above discussion highlights the significant heterogeneity of Cx expression amongst different vascular beds, and also between animal species. The presence of heterogeneity may contribute to the differences in functional characteristics present amongst these vascular beds.

1.3.4   *Variation in connexin expression due to physical factors*

The vascular endothelium consists of a single layer of cells, separated from the smooth muscle by the internal elastic lamina, and as such is exposed to varying hemodynamic forces arising from the flow of blood; a phenomenon known as shear stress (Davies & Tripathi, 1993; DePaola *et al.* 1992). Changes in blood flow and consequently shear stress have been shown to result in adaptive responses within the endothelium, including changes in endothelial cell morphology, gene expression and vascular function (Davies *et al.* 1992; Resnick *et al.* 2003). Thus, changes in shear stress can modulate vasomotor tone and blood flow. Blood flow within arteries is generally laminar, except in areas of bifurcation or in curved regions where blood flow is turbulent (Davies & Tripathi, 1993). Recent studies examining Cx expression in the vascular endothelium have shown that expression of Cx43 in the rat aorta is increased in areas of aortic bifurcation (Gabriels & Paul, 1998). Expression of Cx43 was specifically increased in areas downstream of vessel branch points. Cx37 was down-regulated upstream of aortic branch points, while Cx40 was constant along the length of the aorta. In a similar manner, when a segment of the abdominal aorta, devoid of branch points, was surgically ligated, reducing the diameter of the vessel and increasing shear stress, expression of Cx43 was significantly up-regulated downstream of the ligation site. In contrast, Cx37 expression was down-regulated at upstream sites, while the expression of Cx40 was not altered (Gabriels & Paul, 1998). Other experiments performed *in vitro* demonstrate that an increase in fluid shear stress

14

results in the up-regulation of Cx43 mRNA (Cowan *et al.* 1998; DePaola *et al.* 1999), with a corresponding increase in intracellular dye transfer (DePaola *et al.* 1999). In agreement with this, in cultured vascular smooth muscle cells subject to mechanical stretch, an increase in expression of Cx43 mRNA and protein occurs (Cowan *et al.* 1998). Mechanical strain and fluid shear stress used in these experiments mimic physiological conditions which occur during hypertension, where an increase in blood pressure corresponds to changes in total peripheral resistance and vessel distensibility (Resnick *et al.* 2003).

Atherosclerotic regions of blood vessels are subject to turbulent flow, and thus represent areas of altered shear stress (Davies, 1986). The development of atherosclerotic lesions also coincides with an increase in Cx43 expression in the blood vessel wall (Blackburn *et al.* 1995; DePaola *et al.* 1999). Several studies have demonstrated that an increase in shear stress can cause transient disruption to the plasma membrane of endothelial cells as seen in areas around arterial branch points (Davies *et al.* 1986; Yu & McNeil, 1992). Furthermore, mechanical injury of the vascular endothelium has been shown to increase the expression of Cx43 in endothelial cells in some studies (Pepper *et al.* 1992b; Yeh *et al.* 1997a), while others show no alteration in vascular Cx43 expression (Polacek *et al.* 1997). Yeh *et al.* (2000) demonstrated a significant decrease in the expression of Cxs 37, 40 and 43 immediately following mechanical injury of the aortic endothelium, followed by a slower progressive increase in the expression of all three Cxs as the endothelium regenerates. In cultured endothelial cells, the release of basic fibroblast growth factor following injury has been suggested to initiate an increase in Cx43 (Pepper *et al.* 1992a). Such injury corresponds with the mechanical disruption of endothelial cells, which may occur during angioplasty, and also results in the transformation of underlying smooth muscle cells from the contractile to the synthetic phenotype (Schwartz *et al.* 1978; Ross, 1995). As discussed in section 1.3.1, an increase in Cx43 expression in the vascular media has been shown to correspond with phenotypic transformation of smooth muscle cells (Rennick *et al.* 1993; Yeh *et al.* 1997b; Ko *et al.* 1999b).

Despite the many studies demonstrating an up-regulation of Cx expression in areas of shear stress and mechanical strain, the role of such up-regulation in blood vessel function is largely unknown. Gabriels & Paul (1998) suggest that the up-regulation of Cx43 may enhance cell communication with the vascular smooth muscle and cells of the immune

system also expressing Cx43, ultimately minimizing cell damage and thus restoring vascular function.

1.4 ROLE OF GAP JUNCTIONS IN REGULATING ARTERIOLAR TONE

The maintenance of arteriolar tone is achieved via a balance between vasoconstrictor and vasodilator responses. Alterations to this balance have been implicated in a number of disease states such as hypertension and atherosclerosis (Mombouli & Vanhoutte, 1999).

1.4.1 Vasodilator responses

Endothelium-dependent relaxation has an important function in the control of vascular tone through the release of several mediators that act on the underlying smooth muscle to cause a relaxation. The actions of such mediators, which include nitric oxide (NO), prostaglandins and endothelium-derived hyperpolarizing factor, are induced in response to hemodynamic forces such as shear stress, or in response to agonists such as acetylcholine (ACh) or bradykinin (EDHF, Palmer et al. 1988; Taylor & Weston, 1988). The role of each vasodilatory factor has been shown to vary depending on a number of variables including the vascular bed and animal species (Hill et al. 2001). Both NO and EDHF have been shown to play major roles in endothelium-dependent vasodilation, while prostaglandins may play a more minor role (Bauersachs et al. 1997).

1.4.1.1 Nitric oxide

NO is formed by the conversion of L-arginine to L-citrulline in a reaction catalyzed by NO synthase (NOS, Palmer & Moncada, 1989). Several isoforms of NOS have been identified, and are characterized according to where they were first demonstrated; endothelial NOS (eNOS), neuronal NOS and inducible NOS (Busse & Mulsch, 1990; Moncada et al. 1991). Endothelial NOS can be stimulated to produce NO in response to agonist or in response to increased vasoconstriction and shear stress (Fleming & Busse, 1995; Vargas et al. 1990). Basal production of NO in a number of vessels has also been demonstrated (Moncada et al. 1991). NO production in the endothelium is released to diffuse to the smooth muscle where it acts to relax the cells by initiating the guanylate cyclase production of cyclic 3'5' guanosine monophosphate (cGMP, Rapoport & Murad,

16

1983). While it is possible that in large vessels gap junctions within the media might be involved in the spread of vasodilatory responses to NO, this is unlikely to be so critical in the microcirculation, where the media is comprised of only one or two smooth muscle cell layers (Christ *et al.* 1996; Beny, 1999; Hill *et al.* 2001). Indeed, in the caudal artery of the rat, and in the rabbit iliac artery, NO-mediated relaxation was not affected by gap junction blockers (Chaytor *et al.* 2002; Sandow *et al.* 2003b).

1.4.1.2 Prostaglandins

Prostaglandins are derived from the cyclooxygenase metabolism of arachidonic acid, producing prostaglandin H2 (Smith *et al.* 1991). Cell specific synthesis of individual prostanoid products including the vasodilator, prostacyclin and vasoconstrictor, thromboxane A_2, occurs via the action of specific synthases (Smith *et al.* 1991; Smith, 1992). Prostaglandins have been shown to have a role in endothelium-dependent relaxation in several vascular beds; the endothelium is known to be a major site of prostacyclin production (Moncada *et al.* 1977; DeWitt *et al.* 1983). Like NO, the mechanism by which prostaglandins are involved in smooth muscle cell relaxation is through the regulation of cGMP synthesis (Smith, 1992). Prostaglandins are able to diffuse from the endothelium to activate receptors in the smooth muscle and initiate a hyperpolarization (Parkington *et al.* 1993). A role for gap junctions in the mediation of this response may be limited to large vessels containing several layers of smooth muscle.

1.4.1.3 Endothelium-derived hyperpolarizing factor (EDHF)

Endothelium-dependent relaxation in response to agonists may also be evoked by a factor independent of NO and prostaglandins (Bolton *et al.* 1984). This unknown factor has been termed EDHF (Taylor & Weston, 1988). To date, the identity of EDHF is still controversial, however, it is widely accepted that the actions of EDHF are mediated by the activation of Ca^{2+} activated potassium (K_{Ca}) channels, located on endothelial cells. The activation of K_{Ca} channels results in hyperpolarization of the endothelium, followed by the hyperpolarization and subsequent relaxation of the smooth muscle due to reduced Ca^{2+} influx through voltage dependent Ca^{2+} channels (VDCC, Garland *et al.* 1995; Tomioka *et al.* 1999; Bolz *et al.* 2001; Ohnishi *et al.* 2001). The inhibition of K_{Ca} channels with a combination of apamin and charybdotoxin, to inhibit small (S), intermediate (I) and / or large (B) conductance K_{Ca} channels, respectively, has been shown to prevent relaxation in a

17

number of vascular beds (Edwards & Weston, 1998). Indeed, in the absence of NO and prostaglandins, the action of these antagonists is considered to be the hallmark of EDHF-mediated responses. Several possible candidates for EDHF have been proposed. Putative candidates include chemical factors, such as cytochrome P450 metabolites of arachidonic acid (Bauersachs et al. 1994; Randall et al. 1996; Campbell & Harder, 1999), hydrogen peroxide (Matoba et al. 2002) and potassium ions (Edwards et al. 1998; Bussemaker et al. 2003). Alternatively, the direct electrical coupling of the smooth muscle and endothelium via MEGJs may account for EDHF activity (Beny & von der Wied, 1991; Sandow et al. 2002, 2003b). In this case, EDHF may be more accurately described as EDH.

Endothelium-dependent vasodilation, and specifically EDHF activity, has been shown to vary depending on the vascular bed (Shimokawa et al. 1996; Zygmunt et al. 1995; Hill et al. 2001). In general, the importance of EDHF as a vasodilator is increased as the vessel size and the number of smooth muscle cell layers decreases (Shimokawa et al. 1996; Urakami et al. 1997; Tomioka et al. 1999; Sandow et al. 2002; Berman et al. 2002; Hill et al. 2002). Thus, EDHF-mediated vasodilation is likely to play a significant role in the microcirculation (Shimokawa et al. 1998; Hill et al. 2001).

Evidence for the direct electrical coupling of the smooth muscle and endothelium has been demonstrated in a number of vascular beds from several species (von der Weid & Beny, 1993; Welsh & Segal, 1998; Chaytor et al. 1998, 2001, 2002; Taylor et al. 2001; Beny, 1997; Yamamoto et al. 1998; Edwards et al. 1998; Emerson & Segal, 2000; Coleman et al. 2001; Allen et al. 2002; Emerson et al. 2002; Goto et al. 2002; Sandow et al. 2002; Budel et al. 2003; Ujiie et al. 2003). For example, in the rat mesenteric artery, ACh induced hyperpolarization of the endothelium also evoked hyperpolarization of the smooth muscle. This data, coupled with the ultrastructural evidence of MEGJs, indicates electrical coupling of the two cell layers (Sandow et al. 2002). In parallel with the demonstrated role of EDHF in the microcirculation, the incidence of MEGJs has been shown to increase as vessel size decreases (Shimokawa et al. 1996; Sandow & Hill, 2000; Sandow et al. 2002; Sandow et al. 2003d). Indeed, in the rat femoral artery, no EDHF-mediated relaxation is present (Zygmunt et al. 1995; Wigg et al. 2001; Sandow et al. 2002), which correlates with an absence of MEGJs, while in the rat mesenteric artery, the presence of an EDHF-mediated relaxation is correlated with the presence of MEGJs (Sandow et al. 2002). Thus, several studies have provided support for the hypothesis that EDHF activity may simply be due to the direct passage of an endothelium-derived

18

hyperpolarization to the smooth muscle via MEGJs. In contrast to the studies described above, Savage *et al.* (2003) have demonstrated a significant EDHF-mediated relaxation in the femoral artery of the rat, which was not completely abolished by blockade of NO, prostaglandins and K_{Ca} channels. The reason for this discrepancy is unknown, although it may relate to the region of artery taken.

Further evidence for the importance of gap junctional coupling in EDHF activity has been provided via the use of gap junction inhibitors including the putative uncouplers, 18α- and 18β-glycyrrhetinic acid (18β-GA) and Cx-mimetic (Gap) peptides, which reportedly alter gap junctional aggregation and channel gating, respectively (Goldberg *et al.* 1996; Guan *et al.* 1996; Evans & Boitano, 2001; Berman *et al.* 2002). These inhibitors block endothelial-dependent hyperpolarization and subsequent relaxation of the smooth muscle in a variety of vascular beds (Yamamoto *et al.* 1998, 1999; Coleman *et al.* 2001; Sandow *et al.* 2002, 2003b; Chaytor *et al.* 2001; Griffith *et al.* 2002; Tare *et al.* 2002; De Vriese *et al.* 2002). Although in some vessels, including the guinea pig coronary artery, it has been shown that 18β-GA is able to inhibit endothelial hyperpolarization directly (Tare *et al.* 2002).

The above discussion provides evidence that electrical coupling between cells of the blood vessels wall occurs via gap junctions. MEGJ coupling has been demonstrated to be important for EDHF-mediated responses in small arteries and arterioles, and more recently in larger muscular arteries such as the caudal artery. Thus MEGJs are likely to contribute significantly to the coordination of vascular responses in these vessels (Chaytor *et al.* 1998, 2001; 2002; Griffith *et al.* 2002; Sandow *et al.* 2003b).

1.4.2 *Vasoconstrictor responses*

1.4.2.1 *The myogenic response*

The myogenic response describes an endothelium-dependent vasoconstriction in response to increased transmural pressure and vasodilation in response to reduced pressure (Davis & Hill, 1999). This autoregulatory response is considered to be a major determinant of blood flow and vascular tone. Like many other vascular mechanisms, the myogenic response has been suggested to be more prominent in smaller vessels, and to be variable amongst vascular beds (Davis, 1993; Davis & Hill, 1999; Schubert & Mulvany, 1999). It is now well established that the myogenic response is initiated by the depolarization of vascular smooth muscle cells and an increase in the intracellular Ca^{2+} concentration due to

the influx of extracellular Ca^{2+} through VDCCs (Schubert & Mulvany, 1999). Recently, studies have provided evidence that suggests a role for gap junctions in the modulation of myogenic tone, whereby the response in rat cerebral arteries was attenuated in the presence of the putative gap junction inhibitor, 18α-GA (Lagaud et al. 2002b). A role for gap junctions in the myogenic response may be predicted to facilitate and coordinate the spread of vasoconstriction, which may be particularly important in larger vessels containing several layers of smooth muscle cells.

1.4.2.2 Vasomotion

Rhythmical contractions or vasomotion have been demonstrated in many different vascular beds including microcirculatory vessels of the systemic and cerebral circulation both *in vivo* and *in vitro* (Gustafsson, 1993; Hill et al. 1999; Haddock & Hill, 2002). While in some vascular beds vasomotion occurs spontaneously, in others stimulation with agonist is required (Gustafsson, 1993). Vasomotion is thought to be important in the maintenance of vascular resistance and blood flow (Gratton et al. 1998). The mechanisms underlying rhythmical contractions vary between vascular bed and species. However, the underlying mechanism involves oscillations in intracellular Ca^{2+} concentrations that occur through either voltage dependent or voltage independent mechanisms (Hill et al. 2001). Gap junctional coupling between adjacent smooth muscle cells has been suggested to be critical for the coordination of these oscillations. As such, putative gap junction inhibitors have been demonstrated to prevent vasomotion in a number of vascular beds (Chaytor et al. 1997; Hill et al. 1999). The endothelium has also been shown to be involved in vasomotion in several vessels including the rat basilar and mesenteric arteries (Gustafsson, 1993; Haddock & Hill, 2002), in which removal of the endothelium resulted in the loss of synchronized Ca^{2+} oscillations in the smooth muscle, suggesting an important role for electrical coupling of the endothelium and smooth muscle via MEGJs.

1.4.3   Conducted vascular responses

The regulation of tissue perfusion is an essential function of the microcirculation and results from the conduction of vasodilator and vasoconstrictor responses to vessels upstream in order to coordinate blood flow. Conducted vasodilation and vasoconstriction has been demonstrated in a number of vascular beds and relies on the electrotonic spread of current through gap junction channels in the vessel wall (Segal & Duling, 1989; Xia &

Duling, 1995). The morphological arrangement of endothelial cells along the length of arteries, combined with extensive coupling of endothelial cells provides a low resistance pathway for the conduction of hyperpolarization over large distances within a vascular bed (Haas & Duling, 1997; Dora, 2001; Segal *et al.* 2001; Yamamoto *et al.* 2001; Sandow *et al.* 2003d). Stimulation of the endothelium with ACh initiates a bi-directional spread of vasodilatory responses, due to the conduction of hyperpolarization along the endothelium (Segal & Duling, 1989; Xia & Duling, 1995; Welsh & Segal, 1998; Segal *et al.* 1999; Hungerford *et al.* 2000; Emerson *et al.* 2001, 2002; Yamamoto *et al.* 2001; Budel *et al.* 2003; Ujiie *et al.* 2003). In some arterioles it has been shown that conducted vasodilation is mediated by the action of EDHF, while local vasodilatory responses are mediated by NO, prostaglandins and EDHF (Hungerford *et al.* 2000; Hoepfl *et al.* 2002). Thus, MEGJs are considered to play an important role at distal sites, allowing hyperpolarization to be transferred from the endothelium to the smooth muscle in order to effect a relaxation. Furthermore, in cremaster and skeletal muscle arterioles of Cx40 knockout mice, conducted vasodilation was significantly attenuated, further demonstrating the importance of gap junctional coupling for this response (de Wit *et al.* 2000; Figueroa *et al.* 2003).

In contrast to the conduction of vasodilatory responses, vasoconstrictor responses are conducted within the smooth muscle, and not the endothelium in some vessels (Xia & Duling, 1995; Beny, 1997; Bartlett & Segal, 2000; Budel *et al.* 2003), while in other vessels, vasoconstrictor responses are not conducted at all (Segal *et al.* 1999). Such results suggest differences in the extent of coupling within the smooth muscle of different arteries (Segal *et al.* 2001), as well as the modulation of Cxs therein (Sandow *et al.* 2003d). Conducted vasoconstriction results from the conduction of depolarizing current along the blood vessel wall via gap junctions within the media, followed by Ca^{2+} influx through VDCCs and subsequent vasoconstriction (Xia & Duling, 1995). Indeed, within hamster cheek pouch arterioles, vasoconstriction was conducted exclusively along the smooth muscle of the vessel, but was inhibited at sites of smooth muscle cell damage (Bartlett & Segal, 2000). In some vessels, responses arising in the smooth muscle can be conducted into the endothelium (Beny, 1997), further highlighting a role for MEGJs.

1.5   STUDIES IN CONNEXIN DEFICIENT MICE

The deletion of a single Cx protein either globally or in a specific cell type can have significant effects on vascular function, while providing a unique method for determining the functional role of specific Cx isotypes in vascular responses. Cx43 knockout (Cx43$^{-/-}$) mice die shortly after birth from an obstructed right ventricular outflow tract (Reaume *et al.* 1995). However, the ability of the knockout mice to survive to term suggests other Cx isotypes may compensate for the lack of Cx43 in other tissues during development. More recently, knockout mice that are heterozygous for the Cx43 (Cx43$^{+/-}$) gene have been developed and shown to be postnatally viable (Guerrero *et al.* 1997). These mice displayed a 50% reduction of Cx43 in both atrial and ventricular myocardium and a slowing of cardiac conduction in the ventricular myocardium (Guerrero *et al.* 1997; Thomas *et al.* 1998), suggesting that a functional compensation by Cx40, may be present in the atria, to thus prevent conduction abnormalities in the Cx43$^{+/-}$ mice (Thomas *et al.* 1998). Indeed, mice deficient in both Cxs 43 and 40 die postnatally from severe cardiac abnormalities (Kirchhoff *et al.* 2000). In contrast, several studies have demonstrated a lack of significant changes in cardiac conduction parameters in Cx43$^{+/-}$ mouse (Morley *et al.* 1999; Kirchhoff *et al.* 2000), supporting the suggestion of functional compensation by other Cxs, such as Cxs 40 and 45, in the heart. Indeed, it has recently been demonstrated that Cx45 protein, while not upregulated in the heart of the Cx43$^{+/-}$ mouse, is redistributed within the ventricular myocardium (Johnson *et al.* 2002). Neither the expression nor distribution of Cx40 protein was altered in Cx43$^{+/-}$ mouse (Johnson *et al.* 2002). However, it is possible that the lack of effect on cardiac conduction in Cx43$^{+/-}$ mice simply resulted from the over-abundance of Cx43 such that a 50% reduction in expression had little physiological effect. In support of this hypothesis, recent studies by Gutstein *et al.* (2001a) whereby Cx43 was inactivated exclusively in cardiomyocytes, have demonstrated that while heart structure and contractile function was not altered, mice developed ventricular arrhythmia due to reduced ventricular conduction (Gutstein *et al.* 2001a). In addition, chimeric mice engineered to show heterogeneous disruption of Cx43 in the heart (Gutstein *et al.* 2001b), demonstrate reduced ventricular conduction.

The role of Cx43 in vascular endothelial function has been examined in mice where Cx43 has been selectivity deleted in endothelial cells (Liao *et al.* 2001; Theis *et al.* 2001). Endothelial knockout mice were developed using the Cre/loxP mediated deletion of Cx43, and replacement of the coding region by the lacZ reporter gene. This method enabled the specific deletion of Cx43 in endothelial cells. Liao *et al.* (2001) found that endothelial

Cx43 knockout mice were hypotensive and displayed elevated levels of plasma NO and angiotensin. In contrast, endothelial Cx43 knockout mice developed by Theis *et al.* (2001) found no such alteration in blood pressure compared to control mice and concluded that there were no obvious changes in vascular development in these mice.

Cx45 knockout (Cx45$^{-/-}$) mice show widespread abnormalities of the systemic vasculature and die early in embryonic development from impaired formation of the yolk sack vasculature and other major arteries (Kumai *et al.* 2000; Krüger *et al.* 2000; Simon & McWhorter, 2002). Thus, these studies demonstrate that Cx45 is essential for embryonic cardiovascular development.

In contrast to Cx43$^{-/-}$ or 45$^{-/-}$ knockout mice, mice lacking either Cx37 (Cx37$^{-/-}$) or 40 (Cx40$^{-/-}$) are viable into adulthood. However, female Cx37$^{-/-}$ mice are infertile resulting from abnormal oocyte and follicular development (Simon *et al.* 1997), while Cx40$^{-/-}$ mice display abnormal cardiac conduction properties and are predisposed to cardiac arrhythmia (Kirchhoff *et al.* 1998; Simon *et al.* 1998; Tamaddon *et al.* 2000). While the absence of Cx40 does not appear to affect vascular development (Simon & McWhorter, 2002), Cx40$^{-/-}$ mice show reduced conduction of endothelium-dependent vasodilatory responses following application of ACh or bradykinin in the skeletal microcirculation (de Wit *et al.* 2000). The residual dilation present at upstream sites is thought to result from remaining gap junction channels, containing Cxs 37 and 43. Conducted vasoconstriction in skeletal muscle arterioles from Cx40$^{-/-}$ mice was not affected (Figueroa *et al.* 2003).

The above studies demonstrate the essential role for Cxs 43 and 45 in the development of the cardiovascular system, while Cx40 plays an important role in the coordination of vasomotor responses in the vascular endothelium. Mice lacking either Cx40 or Cx37 survive into adulthood, while mice lacking both Cxs 37 and 40 die shortly after birth due to severe vascular abnormalities (Simon & McWhorter, 2002). Further studies in Cx37 and Cx40 knockout mice have shown that optimal expression of endothelial Cxs may be dependent on the activity of a co-expressed Cx (Krüger *et al.* 2002; Simon & McWhorter, 2003). Indeed, expression of Cxs 37 and 40 in aortic endothelial cells is down-regulated in Cx40$^{-/-}$ and Cx37$^{-/-}$ mice, respectively (Simon & McWhorter, 2003) with the deletion of Cx40 having a greater effect on Cx37 expression than vice versa. Reduced Cx expression also corresponds with a reduction in intercellular dye transfer, where again the deletion of Cx40 had a greater effect than deletion of Cx37. Double knockout mice showed complete abolition of intercellular dye transfer. The

expression of Cx43 was not altered in the endothelium of Cx37 and Cx40 double knockout mice (Simon & McWhorter, 2003), however both Cxs 37 and 43 were increased in the aortic media of Cx40$^{-/-}$mice (Krüger *et al.* 2002; Simon & McWhorter, 2003). Furthermore, deletion of Cx40 had greater effects in embryonic Cx40 knockout mice than in adult mice, suggesting an increased role for Cx40 in vascular development.

1.6   CHANGES IN GAP JUNCTIONS DURING DISEASE

If gap junctions are essential for normal vascular function, then alterations in Cx expression and cellular coupling are likely to be implicated in the etiology of vascular diseases such as hypertension, atherosclerosis, diabetes and septic shock.

1.6.1   Hypertension

Little is known regarding Cx expression in muscular arteries during hypertension, with most studies having concentrated on Cx43 expression in the aorta of the rat (Haefliger *et al.* 1997a,b, 2001; Haefliger & Meda, 2000). This is surprising, given that the aorta is a large elastic artery and is thus not directly involved in maintenance of peripheral resistance (Mulvany & Aalkjaer, 1990). Such studies are therefore unlikely to be relevant for elucidating the mechanisms associated with the etiology of diseases such as hypertension. However, the results of such studies do highlight the possibility that changes in Cx expression during hypertension may be related to the underlying cause of the disease. Indeed, it is interesting that variation in Cx expression has been found in the aortic media of different hypertensive rat models. In deoxycorticosterone acetate (DOCA)-salt and renal-clip models of hypertension, Cx43 expression was increased in the thoracic aorta (Haefliger *et al.* 1997b; Watts & Webb, 1996; Haefliger & Meda, 2000), whilst in L-NAME induced hypertensive rats, Cx43 expression was decreased (Haefliger *et al.* 1999; Haefliger & Meda, 2000). Recently, Cx45 has also been examined in vessels from spontaneously hypertensive rats (SHR, Li & Simard, 2002), in which the expression of both Cxs 43 and 45 was increased in the cerebral artery, while expression was unchanged in the aorta and femoral artery. Little is known regarding the cellular location of these changes, however it may be assumed that in the whole vessel preparations used in Western and Northern blotting experiments, smooth muscle is the predominate cell type. In contrast to Li & Simard (2002), recent studies of the SHR by Haefliger *et al.* (2001) have shown a decrease

in Cx43 expression; specifically in endothelial cells of the aorta. As discussed in section 1.5, mice deficient in Cx40 have increased blood pressure and a significant attenuation of the conducted vasodilatory response (de Wit *et al.* 2000). Together these results suggest a role for gap junctions in vascular function and hypertension.

1.6.2 *Atherosclerosis, diabetes and inflammation*

Within vascular cells, changes in Cx expression have been reported to occur in association with other disease states including atherosclerosis, diabetes and inflammatory conditions such as septic shock. Increased Cx43 expression has been reported in atherosclerotic plaques, while *in vitro*, cells cultured in medium containing high glucose levels show reduced Cx43 expression and unaltered expression of Cxs 37 and 40 (Blackburn *et al.* 1995; Sato *et al.* 2002; Kwak *et al.* 2002, 2003). During atherosclerosis, increased Cx43 expression may be required for increased smooth muscle cell proliferation, which occurs during lesion development (Blackburn *et al.* 1995; Polacek *et al.* 1997; Kwak *et al.* 2002), and indeed this situation may reflect the general up-regulation of Cxs in early developmental processes and cellular differentiation. In contrast, hyperglycemia associated with diabetes may increase the phosphorylation of Cx proteins and thereby reduce cellular coupling (Inoguchi *et al.* 2001; Oku *et al.* 2001). In a similar manner, inflammatory mediators lipopolysaccharide and cytokines, such as tumor necrosis factor α (TNF-α), have been shown to modulate Cx phosphorylation, resulting in reduced cellular communication (Ferro *et al.* 1993; Hu & Cotgreave, 1997; Lidington *et al.* 2000, 2002, 2003; Tyml *et al.* 2001). The expression of Cxs 37 and 40, but not Cx43 have also been shown to be down-regulated following exposure to TNF-α (van Rijen *et al.* 1998).

From the above discussion, it is clear that while alterations in Cx expression are evident in some disease states, relatively little is known regarding the expression of the four vascular Cxs in the smooth muscle and endothelium of blood vessels during hypertension.

1.7 EXPERIMENTAL HYPERTENSION

Essential hypertension in humans is characterized by a sustained increase in blood pressure resulting from an increase in peripheral vascular resistance (Staessen *et al.* 2003). Hypertension is multifactorial in nature, with both genetic and environmental influences contributing to the etiology of the disease. Worldwide, essential hypertension affects 25-

35% of the population, with the incidence increasing to 60-70% in the elderly population (Staessen *et al.* 2003). Hypertension is a major risk factor for the development of other cardiovascular diseases such as stroke and heart failure (Staessen *et al.* 2003). The study of hypertension encompasses the use of several genetic animal models, the SHR being most commonly used as a model for human essential hypertension (Stoll & Jacob, 2001). The SHR is an inbred strain developed by Okamoto & Aoki (1963) through the mating of a male and female Wistar Kyoto (WKY) rat, both displaying elevated blood pressure. This was followed by successive inbreeding of hypertensive brother-sister pairs, resulting in a colony of rats with a 100% occurrence of spontaneous hypertension. Okamoto & Aoki (1963) defined hypertension as a systolic blood pressure exceeding 150 mmHg, and it was demonstrated that hypertension progressively developed with age. Studies to date demonstrate that hypertension develops from approximately 4 weeks of age, however, this varies between individual studies, with established hypertension occurring by 10-12 weeks of age (Lais *et al.* 1977; Kihara *et al.* 1993; Dickhout & Lee, 1998). Inbred WKY rats were initially developed as a normotensive control for the SHR (Hansen *et al.* 1973). However, valid questions have arisen as to the validity of the WKY as a genetic control for the SHR (Louis & Howes, 1990). Studies have shown significant genetic diversity between the WKY and the SHR, with the distribution of animals before they were fully inbred contributing to this variation (Kurtz & Morris, 1987; Kurtz *et al.* 1989; Alemayehu *et al.* 2002). Furthermore, differences between WKY and SHR strains occur even between laboratories. Unfortunately, even in light of such differences, the WKY remains the most appropriate normotensive strain for comparative studies with the SHR.

Both human and experimental hypertension are associated with marked alterations in endothelial function and vascular structure, both of which may significantly affect vascular tone and peripheral vascular resistance (Mulvany & Aalkjaer, 1990).

1.7.1 Endothelial dysfunction

As discussed above, the endothelium is essential for the maintenance of vasomotor tone, producing vasodilatory factors such as NO, prostaglandins and EDHF, and contracting factors, which include endothelin-1, thromboxane A_2, prostaglandin H_2 and superoxide anion (Vanhoutte & Boulanger, 1995). Diseases such as hypertension and atherosclerosis are associated with the altered production and action of both endothelial-derived vasodilator and vasoconstrictor substances, a process described as endothelial

26

dysfunction. Furthermore, the sensitivity of smooth muscle cells to these factors is altered. The end result, impaired endothelium-dependent vasodilation, compromises both normal vascular tone and arterial function (Boulanger, 1999; Mombouli & Vanhoutte, 1999; Puddu et al. 2000).

Other factors involved in the regulation of vascular tone include the action of angiotensin-converting enzyme (ACE). ACE plays an important role in the metabolism of vasoconstrictors such as angiotensin II (AngII), endothelin-1 and the vasodilator, bradykinin (Momose et al. 1993; Mombouli & Vanhoutte, 1999; Puddu et al. 2000). While AngII is generally not up-regulated in the SHR, receptor number and responsiveness to AngII is increased in some tissues (Schiffrin et al. 1984; Kost & Jackson, 1993; Campbell et al. 1995).

1.7.1.1 Vasodilator factors

The mechanisms that underlie impaired endothelial function during hypertension vary with animal model and the vascular bed. For example, while reduced production of NO has been reported to underlie endothelial dysfunction in some hypertensive rat models (Rees et al. 1996; Hayakawa & Raij, 1998; Lou et al. 2001), in the SHR, eNOS activity is up-regulated. While the production of NO is increased or unchanged in the SHR, the biological activity of NO is inhibited, probably due to the increased activity of superoxide (Omar et al. 1992; Kerr et al. 1999). Moreover, the sensitivity of the smooth muscle to contractile factors is usually increased (Ge et al. 1995; Hayakawa et al. 1995; Nava et al. 1995; Noris et al. 1995; Noll et al. 1997). Studies in several vascular beds have demonstrated that the endothelium-dependent relaxation attributed to NO and EDHF is reduced in SHR and the SHR-SP (Vanhoutte, 1989; Fujii et al. 1990; Sunano et al. 1999; Vazquez-Perez et al. 2001). In other studies, endothelium-dependent hyperpolarization in the caudal artery of the SHR, was reduced, while EDHF-mediated relaxation was not affected (Sandow et al. 2003b). This apparent discrepancy was suggested to be accounted for by the compensatory increase in the incidence of MEGJs in the SHR, thus contributing to the maintenance of the EDHF-mediated relaxation in this vessel (Sandow et al. 2003b).

Given the role for gap junctions in the coordination of the vascular response, the altered expression of gap junction in the endothelium and media may contribute to the impaired vasodilatory characteristics present endothelial dysfunction.

1.7.1.2 Contracting factors

Endothelin-1 is a potent vasoconstrictor, which is produced in the endothelium in response to various agonists including vasopressin and AngII (Schiffrin, 1998), and which acts on endothelin type A and B receptors found on smooth muscle and endothelial cells (Schiffrin, 1999). Expression of endothelin-1 in the endothelium can be modulated by the vasodilatory factors, NO and EDHF (Nakashima & Vanhoutte, 1993; Schiffrin, 1998), while stimulation of ET_A and ET_B receptors in the smooth muscle initiates vasoconstriction (Schiffrin, 1999). Increased endothelin-1 production has also been demonstrated in a number of models of hypertension including the stroke-prone SHR (SHR-SP), and DOCA-salt hypertensive rats (Schiffrin, 1998, 1999). Thromboxane A_2 is a prostanoid produced in small amounts in the endothelium, which acts to initiate a vasoconstriction following activation of receptors in the smooth muscle (Halushka et al. 1989). The oxygen free radical, superoxide, is produced in endothelial cells in response to stimuli such as ACh, bradykinin and shear stress (Shimizu et al. 1994), and has been shown to inactivate NO and inhibit vasodilation (Tschudi et al. 1996). In the SHR, increased expression of cyclooxygenase-1 results in the increased production of thromboxane A_2 and prostaglandin H_2 (Nakazono et al. 1991; Ge et al. 1995; Dohi et al. 1996; Bouloumie et al. 1997; Vaziri & Oveisi, 1998; Vaziri et al. 2001). In a similar manner, the activity of superoxide is increased during hypertension (Omar et al. 1992; Grunfeld et al. 1995; Rajagopalan et al. 1996; Kerr et al. 1999). Changes in Ca^{2+} sensitivity to the contractile apparatus have also been shown to contribute to the development of hypertension (Suzuki & Ford, 1992; Ungvari & Koller, 2000).

1.7.2 Vascular remodeling during hypertension

During hypertension, the increase in peripheral vascular resistance contributes to the maintenance of increased blood pressure, which is frequently associated with structural remodeling of the blood vessel wall (Mulvany & Aalkjaer, 1990; Intengan & Schiffrin, 2000; Touyz, 2000). Vascular remodeling, which occurs in both elastic and muscular arteries describes changes in the thickness of the media and luminal diameter (Mulvany et al. 1996). Small muscular arteries and arterioles are considered to be the main sites of peripheral vascular resistance and therefore remodeling of these vessels has been implicated in the development of hypertension (Mulvany & Aalkjaer, 1990; Heagerty et al. 1993). The definition of such vessels based on size is an arbitrary measure, as vessels less

than approximately 500 µm in diameter are considered to be the primary sites of peripheral vascular resistance (Mulvany & Aalkjaer, 1990). In contrast, large elastic arteries such as the aorta and the superior mesenteric artery are essentially conduit vessels. The role remodeling of such vessels plays in the development of hypertension is unknown. While there is substantial information regarding remodeling of the vascular smooth muscle, less is known regarding morphological changes that may occur in the vascular endothelium during hypertension.

1.7.2.1 Remodeling of the vascular smooth muscle

Several categories of vascular remodeling have been described, with the type often depending on the vascular bed examined. Hypertrophic remodeling results in a decrease in luminal diameter and hypertrophy of the vascular smooth muscle (Heagerty et al. 1993; Dickhout & Lee, 1999; Dickhout & Lee, 2000; Intengan & Schiffrin, 2000; Touyz, 2000). This type of remodeling is characterised by an increase in the media to lumen ratio and medial cross-sectional area (Intengan & Schiffrin, 2000). The increase in medial volume seen in hypertrophic remodeling may result from either hyperplasia or hypertrophy of smooth muscle cells in combination with an increase in the amount of extracellular protein. The second type of remodeling is termed eutrophic remodeling, and occurs when both the outer diameter and luminal diameter of the blood vessel are decreased (Mulvany et al. 1996). This also results in an increase in the media to lumen ratio, although the medial cross-sectional area is unchanged. In this type of remodeling, changes in the medial layer arise from the rearrangement of existing smooth muscle cells around a smaller lumen (Baumbach & Heistad, 1989; Intengan & Schiffrin, 2000). Increased apoptosis along the adventitial surface or alterations in the extracellular matrix components and cell adhesion molecules may also contribute to the medial changes seen in eutrophic remodeling (Diez et al. 1997; Sharifi & Schiffrin, 1998; Dickhout & Lee, 1999; Intengan et al. 1999; Intengan & Schiffrin, 2000).

Hypertrophic remodeling has been shown in several vascular beds of the SHR and SHR-SP, including in the aorta, mesenteric, carotid, renal, cerebral, interlobular and intramyocardial arteries (Mulvany et al. 1978, 1985; Mulvany & Korsgaard, 1983; Lee et al. 1983; Lee, 1985, 1987; Amann et al. 1995, 1997; Arribas et al. 1997; Mulvany, 1995; Dickhout & Lee, 1997, 2000; Fujii et al. 1999; Rizzoni et al. 1998). However, whether the increase in medial area result from hypertrophy or hyperplasia of smooth muscle cells

varies depending on the particular vascular bed, age and the species examined. Eutrophic remodeling has also been demonstrated in a number of vascular beds from the SHR (Baumbach & Heistad, 1989; Arribas *et al.* 1996; Mulvany *et al.* 1996; Intengan *et al.* 1999). These studies support the heterogeneous nature of medial changes that occur in different regions of the same vascular bed and amongst different vascular beds, with both hypertrophic and eutrophic remodeling having been demonstrated in the SHR.

1.7.2.2 Remodeling of the vascular smooth muscle and the onset of hypertension

In the thoracic aorta, mesenteric and interlobular arteries and the main renal artery of the pre-hypertensive SHR, an increase in the number of smooth muscle cell layers has been observed (Lee, 1985, 1987; Norrelund *et al.* 1994; Mulvany *et al.* 1995; Dickhout & Lee, 1997; Van Gorp *et al.* 2000). Thus, structural changes have been demonstrated in the pre-hypertensive SHR indicating that such changes may contribute to the development of hypertension, in at least some vascular beds. For example, in mesenteric arteries of pre-hypertensive SHR, prior to the increase in blood pressure, thickening of the medial wall results from hyperplasia of smooth muscle cells, while hypertrophy of smooth muscle cells occurs in parallel with increased blood pressure (Mulvany *et al.* 1978, 1985; Lee *et al.* 1983; Lee & Smeda, 1985; Lee, 1985, 1987; Dickhout & Lee, 1997). These secondary vascular changes may contribute to the maintenance of hypertension (Lee & Smeda, 1985).

1.7.2.3 Remodeling of the endothelium

As detailed above, changes in shear stress are known to affect both endothelial cell structure and function, and therefore directly modulate vasomotor tone. Changes in shear stress have been implicated in the progression of atherosclerosis (Davies *et al.* 1992; Davies, 1997), while in hypertension altered vascular responses have been demonstrated in several vascular beds, following increased peripheral resistance and resultant changes in shear stress (see section 1.7.1). Several studies *in vitro* have demonstrated altered endothelial cell morphology and alignment in response to changed flow conditions. In situations of laminar flow, endothelial cells became aligned to the direction of flow, while under turbulent flow endothelial cells maintain a polygonal shape and display increased DNA synthesis (Davies *et al.* 1986; Barbee *et al.* 1994; DePaola *et al.* 1992, 1999).

In vivo, most remodeling data has been derived from the rat thoracic aorta, with several more recent studies also examining the mesenteric artery. The results of these

studies are somewhat conflicting; authors having reported both increased and decreased endothelial cell size and density depending on the model of hypertension examined. Arribas *et al.* (1997) have shown that there were fewer endothelial cells in the mesenteric artery of adult SHR-SP, associated with the decrease in luminal diameter. In rats made hypertensive by ligation of the abdominal aorta, initially, hypertrophy of endothelial cells within the aorta was observed, while several weeks after ligation, endothelial cells were smaller than in controls (Hüttner *et al.* 1979). On the other hand, in renovascular hypertension and mineralocorticoid hypertensive models, an increase in endothelial cell density and replication was observed in the thoracic aorta early after induction of hypertension (Daniel *et al.* 1982; Hüttner *et al.* 1982; De Chastonay *et al.* 1983). Cell replication was reduced to that of control in latter phases of most hypertensive models, while endothelial cell density remained elevated (Daniel *et al.* 1982; De Chastonay *et al.* 1983). The exception were animals made hypertensive by high salt diets in which endothelial cell density returned to control levels (De Chastonay *et al.* 1983). In other experiments involving disruption of blood flow in the rat and rabbit coronary artery, hyperplasia of endothelial cells could be demonstrated (Emanueli *et al.* 2000; Masuda *et al.* 2003; Sho *et al.* 2003). This response was shown to precede remodeling of the vascular smooth muscle and involve AngII mediated proliferation of endothelial cells (Emanueli *et al.* 2000; Sho *et al.* 2003).

It is clear from the above studies that remodeling occurs in both the vascular endothelium and smooth muscle in response to changes in hemodynamic conditions within the blood vessel. In some vessels remodeling has been found to precede the development of hypertension, while in other vascular beds, remodeling occurs as an adaptive process in response to an increase in blood pressure and may be associated with the maintenance of hypertension. These studies further highlight the heterogeneity in the form of both endothelial and smooth muscle cell remodeling in different models of hypertension and within different vascular beds.

1.8   THESIS AIMS AND OUTLINE

1.8.1   *Aims*

The above literature review outlines a clear role for gap junctional coupling within the vascular wall in the coordination and control of a range of vascular responses, which

could impact on, or contribute to, blood flow and peripheral vascular resistance. Furthermore, examination of data concerning Cx expression within the vascular system has uncovered enormous variation in experimental results amongst different vascular beds. In particular, vessels with differing functional properties appear to demonstrate different patterns of Cx expression. While many studies have examined the expression of Cxs within the vascular endothelium and smooth muscle, in some cases results have been conflicting. The lack of specificity of Cx antibodies and poor experimental technique in some studies may account for some of these differing results. Analysis and quantification of cell specific Cx distribution within both the smooth muscle and endothelium of structurally and functionally different vessels has yet to be performed.

Changes in vascular function are recognized to be associated with altered hemodynamic conditions such as the changes in shear stress. Moreover, such changes may underlie the pathogenesis of several disease states including hypertension. Given that cellular communication is essential for vasomotor control, it may by hypothesized that changes in endothelial function can be directly correlated with altered gap junction expression. Indeed, this seems to be the case in several disease states including hypertension. To date, little is known regarding Cx expression during hypertension. Most studies have been concerned with changes to Cx43 in the rat aorta, while there is little or no data regarding the expression of Cxs 37, 40 and 45, or the cellular location of such changes. Indeed, such studies may therefore have little physiological relevance to studies of hypertension, given that the aorta is a large conduit artery and therefore not involved in the maintenance of peripheral vascular resistance. To date, no studies have compared gap junction expression in functionally different vascular beds of hypertensive animals.

The aim of this thesis was to systematically examine Cx expression in the endothelium and smooth muscle of the thoracic aorta in comparison to the caudal artery of the Wistar rat through the quantification of messenger ribonucleic acid (mRNA) and protein expression using real-time polymerase chain reaction (PCR) and immunohistochemistry. Real-time PCR is a highly sensitive technique that allow the absolute quantification of mRNA from intact vessels. Immunohistochemistry was used in order to detect Cx protein specifically within the endothelial and smooth muscle cell layers. The thoracic aorta and caudal artery were chosen to represent two functionally different vascular beds. The thoracic aorta is an example of a large elastic artery, while the caudal artery is an example of a muscular artery and as such is more likely to be involved in the

control of peripheral vascular resistance (Mulvany & Aalkjaer, 1990; Christensen & Mulvany, 2001).

Cx expression has also been examined in a hypertensive animal model, the SHR. Changes in Cx expression have been related to remodeling of the media and endothelium. Whether changes in Cx expression and cellular morphology occurred prior to the onset of hypertension has also been examined. Changes in Cx expression and cell morphology within the endothelium has been compared to those of mesenteric and basilar arteries which have a demonstrated role in determining peripheral resistance.

Finally, the impact that changes in Cx expression and vascular remodeling, within both the endothelium and smooth muscle, may have on blood vessel function has been examined in the caudal and mesenteric arteries of the SHR in comparison to the WKY. Electrophysiological methods were used to record changes in membrane potential and to assess the conduction of endothelium-dependent vasodilatory responses, while tension myography was used to assess the contribution of endothelial-derived factors to vessel relaxation.

1.8.2 Thesis outline

The results presented in this thesis have been divided into the following sections:

- Chapter 2, methods

- Chapter 3, characterization of affinity purified Cx antibodies. Specificity was determined using Western blotting and immunohistochemical examination of cells transfected with the appropriate Cx sequence in tissues known to express each Cx.

- Chapter 4, comparison of the distribution of Cx mRNA and protein in the thoracic aorta and caudal artery of the Wistar rat using real-time PCR and immunohistochemistry.

- Chapter 5, comparison of Cx mRNA and protein distribution and vascular remodeling of the thoracic aorta and caudal artery of the adult hypertensive (SHR) and normotensive (WKY) rats using real-time PCR and immunohistochemistry.

- Chapter 6, investigation of the relationship of vascular changes to the blood pressure increase using SHR and WKY.

- Chapter 7, a comparison of the changes in Cx expression and vascular remodeling in other vascular beds within the hypertensive rat.

- Determination of the impact of changes in Cx expression and vascular remodeling on the functional responses in the caudal and mesenteric arteries of the SHR compared to the WKY, has been included into Chapters 5 and 7.

CHAPTER 2
MATERIALS AND METHODS

2.1 ANIMALS

Experiments were performed on an inbred strain of male WKY rats and age matched SHR at 3 and 12 weeks of age. SHR were obtained from the Flinders University Medical Centre animal facility from stock originally derived from the National Institutes for Health, Bethesda, MD. Experiments in young adult animals were performed on outbred male Wistar rats at 4-6 weeks of age. Animals were killed humanely with an overdose of ether anaesthetic. In experiments where animals were perfused prior to dissection, rats were anaesthetised with an intraperitoneal injection of ketamine and rompun (44 and 8 mg/kg, respectively). All experiments were conducted in line with the *Australian Code of Practice for the Care and Use of Animals for Scientific Purposes*, under a protocol approved by the Animal Experimentation Ethics committee of the Australian National University.

2.2 BLOOD PRESSURE RECORDINGS

Systolic blood pressure was recorded using the non-invasive tail cuff method (HyperRat, SDR Clinical Technology, Australia). SHR (n=4-15 animals) and WKY rats (n=4-8 animals) were acclimatized to the method of restraint over a period of 1 week prior to measuring blood pressure. In this time, animals were handled frequently and were placed on a heated base plate for periods of 30 min. For blood pressure recordings, animals were restrained on a base plate heated to 35-40°C and allowed to acclimatize for approximately 15 min before reading commenced (Mangos *et al.* 1999). Blood pressure measurements were recorded for each animal at weekly intervals beginning at 4 weeks of age until 14 weeks. Each experiment was carried out between 1000 and 1200 h and animals were restrained for maximum periods of 45 min. Blood pressure was not measured at ages less than 4 weeks owing to the variability of readings in very young animals using this technique. For each animal, four readings within 10 mmHg were obtained and used to determine mean systolic blood pressure.

2.3   ARTERIAL PREPARATIONS

Four different arteries were examined, the thoracic aorta, caudal artery, primary mesenteric artery and the basilar artery. The thoracic aorta was dissected from the aortic arch to the diaphragm. The caudal artery was dissected from the base of the tail extending two thirds along its length. Primary mesenteric arteries supplying the upper ileum, were dissected free of the superior mesenteric artery and secondary mesenteric arteries. The basilar artery was dissected from the vertebral arteries to the Circle of Willis.

2.4   mRNA EXPRESSION FOR CONNEXINS IN RAT BLOOD VESSELS

2.4.1   *Extraction of RNA*

Messenger RNA was extracted from intact thoracic aorta and caudal arteries dissected from 4-5 week old Wistar rats and 3 and 12 week old WKY and SHR. Vessels were rapidly dissected into cold phosphate buffered saline (PBS), cleaned of adherent fat and stored in RNAlater (Ambion, USA) before being homogenized in cold RNAzol B (Tel-test Inc., USA) for RNA extraction according to the manufacturer's instructions. RNA was precipitated from the aqueous phase using isopropanol and the pellet washed with 75% ethanol. Any contaminating genomic DNA was removed from the total RNA using the MessageClean Kit (GenHunter Corp., USA) following the manufacturer's instructions. Alternatively, vessels were rapidly frozen in liquid nitrogen and ground into a fine powder. RNA was extracted using the RNeasy RNA extraction kit (QIAGEN, USA), incorporating deoxyribonuclease I (DNase I) treatment for removal of genomic DNA. Four separate RNA extractions were prepared for each arterial type. The amount and purity of RNA was determined by optical density readings at 260, 280 and 320 nm.

2.4.2   *Complementary DNA (cDNA) synthesis*

Messenger RNA was reverse transcribed (42°C for 1h, 50°C for 1h, 90°C for 10 min) in the presence of oligo dT primers (100 ng/µl, Stratagene, USA) and reverse transcriptase (200 U/µl, GIBCO BRL, USA). For each sample, a separate reaction was performed without the presence of reverse transcriptase enzyme to control for any residual genomic DNA contamination.

2.4.3 Cloning of vascular connexins

Fragments of Cxs 37, 40, 43 and 45 cDNA were amplified from 4-6 week old Wistar thoracic aorta samples using a capillary thermal cycler (Corbett Research, Australia). Reactions were performed in triplicate in a total reaction volume of 20 μl, each containing 100 ng of cDNA sample, 1 X PCR reaction buffer containing 1.5 mM $MgCl_2$ (Roche, Germany), 0.2 mM dNTP mix, 1.2 μM of each primer and 1 U of Taq DNA polymerase (Roche, Germany). Primers specific for Cxs 37, 40 and 43 were designed from published rat sequences (see Table 2.1). Since the rat sequence for Cx45 was not known, forward (5'-ACAAGAAGGCAGCTCGGAGCAA-3') and reverse (5'-CAAGGAAGTCTGCTGCACACATA-3') primers were designed to be 100% homologous with published human, mouse and wolf sequences. These primers amplified a product of 321 bp from rat caudal artery (annealing at 63°C for 10 sec, extension at 72°C for 35 sec), and this product was purified and sequenced using the ABI PRISM Dye Terminator Cycle Sequencing Ready Reaction Kit (Applied Biosystems, USA). The rat Cx45 sequence obtained was aligned with the published human, mouse and wolf sequences and found to be 98% homologous to the corresponding mouse sequence and 93% homologous to the consensus sequence for the four species. New primers were designed specifically to the rat Cx45 sequence (see Table 2.1), and these were used to amplify a product of 132 bp. Products were amplified using the following conditions, 2 min at 95°C, 35 cycles of 10 sec at 95°C, primer annealing for 10 sec at temperatures shown in Table 2.2, and primer extension at 72°C for the times shown in Table 2.2. Each experiment included control reactions containing no cDNA. PCR products for each primer set were pooled and run on a 2% agarose gel to confirm a single product of the appropriate size.

PCR products were purified using High Pure PCR Product Purification Kit (Boehringer Mannheim, Germany) according to manufacturer's instructions. PCR products were eluted in 50 μl of Milli Q water and concentration was estimated by running samples on a 2% agarose gel against markers of known concentration. Ligation reactions were performed using the pGEM-T Vector System (Promega, USA) according to manufacturer's instructions. Following ligation, samples were electroporated into TOP 10 F' Cells (Invitrogen, USA) and transformants were plated onto LB plates containing ampicillin (100 μg/ml), isopropylthio-β-D-galactosidase (IPTG, 25 mg/ml) and 5-bromo-4-chloro-3indolyl-β-D-galactoside (X-Gal, 25 mg/ml). Plates were allowed to incubate overnight at 37°C

37

	Forward primer	Reverse primer	Product size
Connexin 37	AGCTCTGCATCCAAGAAGCAGTA	AGTTGTCTCTCAAGTGCCTTTGA	133
Connexin 40	GGAAAGAGGTGAACGGGAAGATT	CACAGCCATCATAAAGACAATGAA	238
Connexin 43	GAGATGCACCTGAAGCAGATTGAA	GATGTTCAAAGCGAGAGACACCAA	308
Connexin 45	AACAGAAGGCAGCTCGGAGCAA	CAAGGAAGTCTGCTGCACACATA	132
18S	CCAGTAGCATATGCTTGTCTCAA	CGACCAAACCAACCATAACTGATT	112
SP6-T7 (no insert)	CATACGATTTAGGTGACACTATAG	TAATACGACTCACTATAGGG	100

Table 2.1 Oligonuclotide primer sequences used in PCR reactions.

	Annealing		Extension	
	temperature	time	temperature	time
Connexin 37	60°C	10 s	72°C	35 sec
Connexin 40	60°C	10 s	72°C	25 sec
Connexin 43	65°C	10 s	72°C	25 sec
Connexin 45	63°C	10 s	72°C	20 sec
18S	61°C	10 s	72°C	15 sec
SP6-T7	50°C	10 s	72°C	45 sec

Table 2.2 PCR thermocycling conditions.

before being screened for successful transformants. Successful insertion of the PCR product into the plasmid disrupts part of the coding region for the β-galactosidase enzyme, resulting in the formation of white colonies, while blue colonies arise from plasmids without the inserted PCR product. Single white colonies were selected and the presence of the plasmid and the inserted PCR product was confirmed with PCR. These clones were then grown overnight at 37°C in Luria-bertani (LB) medium containing ampicillin (100 µg/ml). Plasmid DNA was isolated and purified from cultures using the QIAprep miniprep kit (QIAGEN, USA) according to the manufacturer's instructions, and DNA was quantified using a spectrophotometer. Plasmid DNA was amplified to confirm the presence of only one insert, using primers specific for the SP6 and T7 sequences of the plasmid which flank the plasmid cloning site (see Table 1). Each reaction contained 5 pg/µl plasmid DNA, 1x PCR reaction buffer (Roche, Germany) with 1.5 mM $MgCl_2$, 250 nM of each primer, 0.2 mM dNTP mix and 1U of Taq DNA polymerase (Roche, Germany) in a 20 µl reaction volume. Products were amplified using the following conditions, 2 min at 95°C, followed by 35 cycles of 10 sec at 95°C, 10 sec at 50°C, 45 sec at 72°C.

2.4.4 *Real time - polymerase chain reaction*

Quantitative real time PCR of cDNA samples obtained from thoracic aorta and caudal arteries was performed using the Applied Biosystems ABI Prism 7700 sequence detection system and SYBR green core reagents kit (Applied Biosystems, USA). Reactions were performed in duplicate in a total reaction volume of 25 µl, each containing 50 ng of cDNA sample or 3 fold dilutions of plasmid standards. All samples were diluted in water containing tRNA (Sigma, USA, final concentration of 1 ng / reaction). Reactions contained 1X SYBR green PCR buffer containing Passive Reference 1, 3 mM $MgCl_2$, 1.5 mM dNTP mix and 0.625 U of AmpliTaq Gold DNA polymerase (Applied Biosystems, USA). Primers specific for Cxs 37, 40, 43 and 45 were used at a concentration of 800 nM (see Table 2.1 for primer sequences). Products were amplified using the following conditions, 13 min at 95°C, to activate the AmpliTaq Gold DNA polymerase, followed by 40 cycles of 15 sec at 95°C, primer annealing for 15 sec at temperatures shown in Table 2.3, and primer extension at 72°C for the times shown in Table 2.3. Each experiment included control reactions containing no enzyme or no cDNA, and RNA samples that had not been reverse transcribed, to test for amplification of genomic DNA. Increases in PCR product present in each sample were measured in the real time PCR system as increases in SYBR green

	Annealing temperature	Extension time
Connexin 37	60°C	60 sec
Connexin 40	60°C	60 sec
Connexin 43	65°C	85 sec
Connexin 45	63°C	60 sec
18S	61°C	60 sec

Table 2.3 Real-time PCR thermocycling conditions.

fluorescence. The threshold cycle (Ct) value calculated by the sequence detection software is defined as the cycle number when fluorescence was first detected above background. PCR products for each primer set were run on 2% agarose gels to confirm the presence of a single band.

Quantification of samples was achieved after constructing standard curves using plasmid preparations containing each of the cloned PCR products. Standard curves were constructed in duplicate for each Cx by three-fold serial dilutions of the plasmid cDNA from 10^5 copies. The logarithm of the input plasmid cDNA concentration, as expressed in copy number, was plotted versus the mean Ct value obtained from the duplicate samples. In order to normalise samples for variations in RNA extraction, real-time PCR of tissue samples was performed using primers directed against a short segment of the 5' region of 18S ribosomal RNA (see Tables 1 and 3 for primer sequences and thermocycling conditions respectively) and standard curves were constructed using plasmid preparations containing the cloned PCR product. The number of copies of each Cx was then expressed relative to 18S ribosomal RNA.

2.5 CHARACTERISATION OF CONNEXIN SPECIFIC ANTIBODIES

2.5.1 *Antibodies*

Antibodies were raised in sheep against amino acids 266 to 281 of the C-terminus of rat Cx37 (Cx37/266), amino acids 254 to 270 of the C-terminus of rat Cx40 (Cx40/254) and amino acids 354-367 of human Cx45 (Cx45/354, Coppen *et al.* 1998; Yeh *et al.* 1998; Yeh *et al.* 2000). This last peptide was 93% homologous to the mouse sequence while the rat sequence is unknown. Peptide sequence against which each of the above antibodies were generated are listed in Table 2.4. Antibodies were produced by the Institute of Medical and Veterinary Sciences, Adelaide, SA and affinity purified against the immunogenic peptides (Mimotopes Pty Ltd., Australia). Antibodies against rat Cx43 were commercially raised in rabbits (Cx43/Zy, Zymed, USA) against an unknown peptide within the third cytoplasmic domain, and reactivity is independent of phosphorylation status. Commercial antibodies were raised in rabbits against amino acids 318-333 of mouse Cx37 (Cx37/ADI), amino acids 340-358 of mouse Cx40 (Cx40/ADI). For Cx45, antibodies raised in rabbits against amino acids 285-298 of mouse Cx45 (Cx45/ADI, Alpha Diagnostic

Antibody	Sequence origin	Peptide sequence	Host
Cx37/266	Rat	[266] YLPMGEGPSSPPCPTY [281]	Sheep
Cx40/254	Rat	[256] VQGLTPPPDFNQCLR [270]	Sheep
Cx45/354	Human	[354] QAYSHQNNPHGPRE [367]	Sheep

Table 2.4 Peptide sequence for anti-connexin antibodies.

International, USA), and amino acids 354-367 of human Cx45 (Cx45/Chem, Chemicon) were used.

Specificity of Cx antibodies was subsequently determined in COS-7 cells transfected with DNA for each Cx and in tissues enriched for the expression of each Cx, using Western blotting and immunohistochemistry.

2.5.2 Cell transfection

DNA encoding mouse Cxs 37, 40, 43, and 45 were a kind gift of Dr Klaus Willecke (Willecke *et al.* 1991; Hennemann *et al.* 1992a,b). The regions encoding each Cx gene were individually subcloned into the eucaryotic expression vector pcDEF3 under the control of the human EF-1α promoter as detailed by Goldman *et al.* (1996). Mouse and rat Cx genes share substantial identity and the regions encoding the antigenic determinants against which the antibodies used in this work were raised are wholly conserved between these species.

COS-7 cells were cultured in Dulbecco's Modified Eagle Medium H16 (DMEM) supplemented with 10% fetal bovine serum, penicillin (100 U ml^{-1}) and streptomycin (100 µg ml^{-1}). COS-7 cells were harvested, counted and 1.8 x 10^7 cells were electroporated (960 µF, 0.2 kV) in a 300 µl volume of DMEM using 25 µg plasmid DNA. Transfected cells were cultured at 37°C for 72 h then either prepared for immunohistochemistry or the membranes were harvested for Western blotting.

2.5.3 Western blotting

Transfected COS-7 cells were harvested, freeze-thawed, and centrifuged (600 x g, 10 min, 4°C). The supernatant was transferred into a clean tube and centrifuged (22,130 x g, 30 min, 4°C) and the membrane-enriched pellet was aliquoted and stored at -20°C. Aliquots of transfected COS-7 cell membrane-enriched proteins (15 µg protein) were dissolved in lithium dodecyl sulfate (LDS) sample buffer (2% LDS, 250 mM Tris-Cl, 10% glycerol, 2mM EDTA, pH 8.5) for 1 h at 37°C, then overnight at 4°C. The samples were separated by electrophoresis in bis-Tris polyacrylamide gels using 3-[N-morpholino]propanesulfonic acid (MOPS)-SDS running buffer and blotted onto nitrocellulose membranes according to the manufacturer's recommendations (Invitrogen, USA). Following transfer, blots were washed in PBS, blocked with 3% bovine serum albumin (BSA) and probed with sheep serum containing antibodies against Cx37

(1:100000, Cx37/266), Cx40 (1:100000, Cx40/254) and Cx45 (1:100000, Cx45/354), or rabbit antibodies against Cx43 (1:1000, Cx43/Zy, Zymed, USA). Specific binding was visualized using horseradish peroxidase-conjugated donkey anti-sheep IgG (1:5000, Jackson ImmunoResearch Laboratories, USA) or goat anti-rabbit IgG (1:5000, Sigma, USA,) and ECL chemiluminescence (Amersham Biosciences, UK).

To confirm specificity, each antibody was incubated at 37°C for 1 h, then overnight at 4°C, with a 2-fold molar excess of the peptide against which the antibody was raised. The blocked antibody was then used in Western blotting detection as described above.

Brain, heart, liver, lung, thoracic aorta and caudal arteries were removed from 5-6 week old Wistar rats and snap frozen in liquid nitrogen. Tissues were ground under liquid nitrogen in a mortar and pestle and resuspended in 1ml of lysis buffer (1 mM $NaHCO_3$ pH 7.05, 10 mM EDTA, 10 mM iodoacetamide, 10 mM tetra-sodium pyrophosphate, 1 mM PMSF and 1 µg/ml each of antipain, aprotinin, pepstatin-A, chymostatin and leupeptin). Tissues were further disrupted by grinding in a polytron blender. Unbroken cells and large debris were removed by centrifugation at 1000 g for 5 mins at 4°C, the supernatant was then removed and centrifuged at 3000 g for 5 mins. The pellet was discarded and the supernatant centrifuged at 20000 g for 15 mins at 4°C. The supernatant was discarded and the membrane-enriched pellet was resuspended in lysis buffer. Protein concentration was measured using the Bio-Rad protein assay kit.

Membrane-bound connexins were subsequently solubilized by incubation in 2X SDS sample buffer (5% SDS, 125 mM Tris-Cl (pH 6.8), 20% glycerol, 2 mM β-mercaptoethanol, 0.1% (w/v) bromophenol blue) for 60 mins at 37°C. Aliquots containing 5 µg of protein were separated by SDS-PAGE on 12% polyacrylamide gels, using Rainbow molecular weight markers (Amersham Biosciences, UK), and blotted onto Immobilon-P membranes (Millipore, USA). Blots were probed with sheep antibodies against Cxs 37 (1:1000, Cx37/266), 40 (1:1000, Cx40/254) and 45 (1:500, Cx45/354), rabbit anti-Cx43 (1:1000) and the commercial rabbit anti-Cx37 (1:300, 1:1000) and anti-Cx45 (1:500). Western blots were developed using horse-radish peroxidase-conjugated donkey anti-sheep IgG (1:4000, Jackson ImmunoResearch Laboratories, USA) or goat anti-rabbit IgG (1:10000, Sigma), and ECL chemiluminescence reagents (Amersham Biosciences, UK) according to the manufacturer's instructions. To confirm specificity, antibodies were incubated at 37°C for 1 h, then overnight at 4°C, with a 10-fold excess by weight of the

41

peptide against which the antibody was raised. The blocked antibody was then used in Western blotting detection as described above.

Identification of phosphorylated Cx43 isoforms was performed in samples of thoracic aorta, caudal artery and heart tissue, lysed in RIPA buffer (150mM NaCl, 1% NP40, 0.25% deoxycholic acid, 0.1% SDS, 1mM EDTA containing 1mM PMSF and 20 µg/ml each of leupeptin, aprotinin, pepstatin, antipain and chymostatin according to the method of Nagy *et al.* (1997). The phosphatase inhibitors NaF (10mM) and sodium orthovanadate (10mM) were added to several samples of each tissue in order to compare the level of phosphorylation between samples. For dephosphorylation, samples were treated with calf intestinal alkaline phosphatase (CIP, Boehringer Mannheim, Germany) at a concentration of 1 U/µg tissue. Samples containing CIP were incubated at 37°C for 30 mins prior to solubilisation of all proteins in 2X SDS sample buffer. Samples (10 µg protein) were separated by SDS-PAGE on 8% polyacrylamide gels and blotted onto Immobilon-P membranes (Millipore, USA). Protein was detected using rabbit anti-Cx43 antibodies (Zymed, USA) at a concentration of 1:1000. Blots were developed using an ECL kit (Amersham Biosciences, UK) as describe above.

2.5.4 *Immunohistochemistry*

The specificity of Cx37/266 and Cx45/354 antibodies was determined in rat lung and ventricular endocardium respectively, tissues known to express each Cx. Tissues were removed and impregnated with 30% sucrose in phosphate buffered saline (PBS) before freezing in Cryo-M-Bed (Bright Instrument Company Ltd., England). 10 µm thick cryosections were cut for each tissue and mounted on slides coated with either 2% gelatin or 2% silane (3-aminopropyltrithoxysilane). Tissues were pre-incubated for 30 mins in a blocking solution of 2% (w/v) BSA, 0.2% (v/v) Triton-X in PBS, followed by incubation for 1 h at room temperature in Cx37/266 (1:250) for lung sections or Cx45/354 (1:500) for ventricle sections, diluted in blocking buffer. After washing in PBS, tissues were incubated for 1 h at room temperature with Cy3-conjugated anti-goat immunoglobulins (1:100, Jackson ImmunoResearch Laboratories, USA) in 0.01% (v/v) Triton-X in PBS. Lung sections were subsequently incubated for 1 h at room temperature with rabbit anti-human von Willebrand factor polycolonal antiserum (anti-vWF, 1:300, Dako, Denmark) to specifically detect endothelial cells, followed by washes in PBS and then incubation in swine anti-rabbit fluorescein iso-thiocyanate (FITC) (1:40, Dako, Denmark), for 1 h at

room temperature. All sections were washed in PBS prior to mounting in buffered glycerol.

2.6 PROTEIN EXPRESSION FOR CONNEXINS IN RAT BLOOD VESSELS

2.6.1 *Tissue preparation*

The thoracic aorta and caudal arteries from 4-5 week old Wistar rats, and 3 and 12 week old WKY and SHR rats were prepared for immunohistochemical examination of the smooth muscle and the endothelium as tissue sections or as whole mount preparations respectively. Primary mesenteric and basilar arteries were also prepared from 3 and 12 week old WKY and SHR rats for whole-mount examination of the endothelium.

Tissue sections. To obtain tissue for cryosectioning, animals were anaesthetised with ether and killed by cervical dislocation. The thoracic aorta and caudal arteries were removed and impregnated with 30% sucrose in PBS before freezing in Cryo-M-Bed (Bright Instrument Company Ltd., England). 10 μm thick cryosections were cut transversely or longitudinally for each vessel and mounted on slides coated with 2% silane (Sigma, USA).

Whole mount preparations. To obtain tissue for *en face* examination of the endothelium, animals were anesthetized by intraperitoneal injection of ketamine / rompun (44 and 8 mg/kg respectively) and perfused via the left ventricle at a pressure of 60 mmHg, with 0.9% (w/v) NaCl containing 0.1% (w/v) $NaNO_3$, 0.1% (w/v) BSA and 5 U/ml heparin at $25°C$. The right atrium was cut in order to allow an outflow of perfusate. Once cleared of blood, animals were perfused with 2% (w/v) paraformaldehyde in 0.1 M sodium phosphate buffer. The thoracic aorta, caudal artery, primary mesenteric artery and basilar artery were removed into PBS, cut into 5 mm long segments, cut open longitudinally and pinned flat on Sylgard (Dow Corning, USA).

2.6.2 *Immunohistochemistry*

Cryosections and whole-mount tissues were pre-incubated for 30 mins in a blocking solution of 2% (w/v) BSA, 0.2% (v/v) Triton-X in PBS, followed by incubation in Cx37, Cx40, Cx43 or Cx45 antibodies, diluted in blocking buffer. Cryosections were incubated in primary antibody solution (1:250 for Cx37/266, Cx37/ADI, Cx40/254, Cx40/ADI and Cx43, 1:500 for Cx45/354) for 1 h at room temperature, while whole-mount tissues were incubated in primary antibody solution (1:100) for 2 hs at $37°C$. After washing in PBS,

tissues were incubated for 1 h at room temperature with Cy3-conjugated anti rabbit or anti-goat immunoglobulins (1:100, Jackson ImmunoResearch Laboratories, USA) in 0.01% (v/v) Triton-X in PBS. Some tissue samples were subsequently incubated for 1 h at room temperature with rabbit anti-human von Willebrand factor polycolonal antiserum (anti-vWF, 1:300, Dako, Denmark) to specifically detect endothelial cells. Other samples were labelled with rabbit anti-chicken gizzard smooth muscle myosin (1:100, kindly supplied by U. Groschel-Stewart), at room temperature for 1 h, to specifically label smooth muscle cells. After washing in PBS, tissues were incubated in swine anti-rabbit FITC (1:40, Dako, Denmark), for 1 h at room temperature, washed and mounted in buffered glycerol.

To test the specificity of each antibody, tissues were incubated either without primary antibody or with primary antibody that had previously been pre-incubated for 1 h at room temperature with a 10-fold excess by weight of the peptide against which the antibody was raised.

2.6.3   Confocal microscopy

All immunolabeled tissues were viewed using a Leica confocal laser scanning microscope (TCS 4D, Leica Instruments, Austria), equipped with an argon/krypton laser and fitted with the appropriate filters for the detection of Cy3 and FITC fluorescence. Optical sections of smooth muscle and endothelial cell layers were simultaneously obtained for both Cy3 (Cx staining) and FITC (anti-vWF staining or α-smooth muscle myosin) labels. For tissue sections, optical sections were collected at 1 μm intervals throughout the section thickness, while for whole mount tissue optical sections were collected at 1 μm intervals throughout the endothelial cell layer as determined by the extent of the anti-vWF labelling. Care was taken to maintain similar gain settings for comparisons of antibody staining between vessels. Each series of images was recombined to create a single image incorporating all smooth muscle or all endothelial cell labelling. For each vessel, images from 3 different fields were obtained for analysis and samples taken from 4 different animals. Cx labeling in the media was visualized using a higher zoom factor than that was required to view Cx labelling in the endothelium.

2.6.4   Morphometric analysis

Morphometric measurements of endothelial cell parameters and Cx expression within the endothelium and smooth muscle were made using the AIS imaging system

(Analytical imaging station, version 1.0, Imaging Research, Canada). Endothelial cells labelled for Cx37 were used to determine cell length, width, area and perimeter. Cx expression was quantified by first measuring the average size of the smallest labelled structures in each preparation and defining these as individual gap junctional plaques. The size of individual plaques was used in the grain counting function to determine the number of Cx plaques per square micrometer of smooth muscle or endothelium. Using this method, underestimation of plaque number in areas containing closely adjacent plaques is minimized. However, the method would overestimate the number of plaques if plaque size actually did vary significantly. By use of the endothelial cell parameters, counts were adjusted to give the number of plaques per endothelial cell and subsequently the number of plaques per 100 μm of endothelial cell perimeter. In the case of the smooth muscle cells, Cx expression was defined as the number of plaques per square micrometer of transverse or longitudinal medial area, because identification of individual cells in the multilayered media was not possible. For Cx expression in the smooth muscle, sections double labelled with vWF were used to ensure endothelial staining was not included. All analyses were performed on the recombined images of the endothelial and smooth muscle cells. In immunofluorescent studies, it should be noted that a number of different factors preclude comparisons of expression levels of proteins labelled with different antibodies. These factors include the affinity of primary antibody, saturation of the antibody signal and the effects of steric hindrance in cases where proteins are co-expressed (Severs *et al.* 2001), all of which may affect the intensity of the fluorescent signal. Therefore throughout this thesis, comparisons of immunofluorescent signals have been made predominately between vessels labelled with a particular Cx antibody rather than comparing the intensity of each antibody in one tissue.

2.7   STRUCTURAL CHARACTERISTICS OF RAT BLOOD VESSELS

2.7.1   Electron microscopy

12 week old male WKY and SHR rats were anaesthetized with an intraperitoneal injection of ketamine and rompun (44 and 8 mg/kg, respectively) and perfused at a pressure of 60 mmHg with 0.9% NaCl containing 0.1% $NaNO_3$, 0.1% BSA and 5 units/ml heparin at 25°C, and then with 3% glutaraldehyde and 1% paraformaldehyde in 0.1 M sodium cacodylate buffer for 10 min at room temperature. A portion of the thoracic aorta, caudal,

primary mesenteric and basilar arteries were removed and further immersion fixed at 4°C for 1.5 h. Vessels were subsequently cut into 2 mm longitudinal segments, postfixed in 2% osmium tetroxide in 0.1 M sodium cacodylate buffer for 2 h, stained with saturated aqueous uranyl acetate for 2 h and embedded in Araldite 502 according to conventional procedures. Random sections were collected on Formvar (ProSciTech, Australia) and ~10 nm carbon coated slot grids. Montages of electron micrographs taken on a Hitachi 7000 electron microscope (X2,500) were digitized and analysed for lumen diameter, the number of smooth muscle cell layers and medial cross-sectional area using methods similar to those previously described by Sandow *et al.* (2002). Vessel circumference was estimated as the length of the internal elastic lamina (IEL). Vessels circumference was then used to determine diameter at the level of the IEL. The number of medial smooth muscle cell layers was determined by averaging the number of smooth muscle cells from the outer edge of the IEL to the inner edge of the external elastic lamina along four linear plots 90° apart. The medial-cross sectional area was determined using the MCID imaging system (Imaging Research, Canada).

In control experiments, SHR caudal arteries were perfused at high pressure (160 mmHg) and vessel morphology was examined to determine the effect of different perfusion pressures on morphological data in the SHR. Results of these experiments showed no change in the number of medial smooth muscle cell layers, the luminal diameter or the area of endothelial cells when compared to vessels prepared by perfusion at 60 mmHg (data not shown). These results are similar to those obtained in mesenteric arteries from WKY and SHR rats perfused at different pressures (Owen *et al.* 1988).

2.8   FUNCTIONAL CHARACTERISTICS OF RAT BLOOD VESSELS

2.8.1   Wire myography

Endothelium-dependent relaxation was assessed in caudal arteries of the WKY and SHR at 12 weeks of age, using a Mulvany-Halpern type myograph (Mulvany & Halpern, 1977; Sandow *et al.* 2003b). Ring segments, 1 mm in length, were mounted on two 40 μm diameter tungsten wires, secured between two supports, attached to either a micrometer screw or a force transducer. Vessels were continuously superfused with Krebs' solution (in mM, NaCl, 120; KCl, 5.0; $NaHCO_3$, 25.0; NaH_2PO_4, 1.0; $CaCl_2$, 2.5; $MgCl_2$, 2.0; glucose, 22.0) gassed with 95% O_2, 5% CO_2 and maintained at 33-34°C (Hill *et al.* 1999).

Following an equilibration period of 30 min, vessels were stretched in increments until their tension was equivalent to 80 mmHg (Mulvany & Halpern, 1977). Following a further 10 min equilibration period, vessels were pre-constricted with phenylephrine (2.5 to 6 μM) to achieve a constriction of approximately 60% of maximal constriction, equivalent to 0.85 g of tension. A single concentration of ACh (1 μM) was added to the superfusate to assess endothelial integrity. Vessels displaying relaxations of 40% or greater of the maximal constriction to phenylephrine were used for subsequent experiments. Data was recorded using a MacLab chart recorder (ADInstruments, USA) and results were expressed as % relaxation of phenylephrine-induced constriction. Cumulative dose-response curves to ACh were performed in the presence and absence of N_w-nitro-L-arginine methyl ester hydrochloride (L-NAME, 100 μM) and indomethacin (10 μM), inhibitors of nitric oxide synthase and prostaglandins respectively. Basal nitric oxide was inhibited using the nitric oxide scavengers, hydroxocobalamin (100 μM) and carboxy-PTIO (100 μM). The role of B/I and S conductance K_{Ca} channels was examined using specific inhibitors, charybdotoxin (60 nM) and apamin (0.5 μM) respectively. In other experiments, gap junction antagonists 18β-GA (20 μM) and Cx-mimetic peptides ([43]Gap26, [40]Gap27 and [37,43]Gap 27, 100 μM each in combination; purity >95%) were dissolved in the superfusate before addition of a single dose of ACh (1 μM). Cx-mimetic peptides were dissolved in the physiological saline and recirculated for 60 min before addition of ACh. Recirculation for a period of 60 min was found to have no effect on endothelium-dependent responses to a single concentration of ACh. In control experiments, responses to ACh were examined in the presence of indomethacin and Cx-mimetic peptides, before and after the addition of L-NAME. All other experiments were performed in the presence of L-NAME and indomethacin.

2.8.2 Electrophysiology

Intracellular recordings of membrane potential were examined in caudal arteries obtained from 12 week old WKY and SHR. Arterial segments were pinned flat in a Sylgard coated recording chamber and superfused with Krebs' solution, gassed with 95% O_2, 5% CO_2. Membrane potential of smooth muscle cells was measured using fine glass microelectrodes (120-220 MΩ) (Flaming Brown micropipette puller, Sutter Instrument Co. USA) filled with 0.5 M KCl as previously described (Hill *et al.* 1999). Membrane potential was recorded using an Axoclamp 2B (Axon Instruments, USA). A sharp decrease in

47

membrane potential of 20 to 40 mV indicated a successful impalement. Identification of impaled cells was determined using electrodes filled with 10% FITC conjugated-dextran (FITC-dextran, 3000 MW) or 3% Lucifer yellow, backfilled with 0.5 M KCl or LiCl (Sandow *et al.* 2002; Coleman *et al.* 2001). At the conclusion of each experiment, vessels were fixed in 4% paraformaldehyde in PBS, mounted in buffered glycerol and photographed with a Nikon Coolpix 950 digital camera on a compound microscope.

In experiments examining smooth muscle cell coupling, bipolar electrodes placed on either side of the vessel were used to stimulate perivascular nerves. Smooth muscle cells were impaled at the adventitial border of the blood vessel, the surface closest to the perivascular nerve terminals, or immediately below the luminal surface, several cells away from the nerve terminals. Recordings at the luminal surface were obtained by the removal of side branches from the surface of the artery allowing the electrode to be advanced through the hole in the vessel wall through the exposed endothelium. Excitatory junction potentials (EJPs) were recorded following a single neural stimulus of 0.1 ms pulse width, delivered by a DS2 isolated stimulator (Axon Instruments, UK). Stimulus strength was increased until a maximal response was achieved. In each experiment, amplitude, rise time (10 to 90 % of the peak amplitude) and time constant of decay of EJPs were measured.

Endothelium-dependent smooth muscle cell hyperpolarization was determined by impaling cells at the adventitial border of the caudal artery. Cumulative dose-response curves to ACh were performed in the presence and absence of L-NAME (100 μM) and indomethacin (10 μM). Vessels were incubated in the presence of L-NAME and indomethacin for 30 min prior to the addition of ACh. In other experiments ACh (1 M) was applied iontophoretically (200 nA, 10 s) in the presence of charybdotoxin (60 nM) and apamin (0.5 μM) or following the removal of the endothelium. Responses were also examined using iberiotoxin (100 nM), 18β-GA and hydroxocobalamin (100 μM), inhibitors of BK_{Ca} channels, gap junctions and basal NO, respectively.

2.8.3 *Conducted hyperpolarization and vasodilation*

The conduction of EDHF-mediated smooth muscle cell hyperpolarisation was determined in the mesenteric artery of the 12 week WKY and SHR. Following an equilibration period, smooth muscle cells were impaled at the adventitial border of the blood vessel and ACh (1 M) was applied iontophoretically (500 nA, 0.5 s) at the local site (0 mm), and at sites 0.5, 1, 1.5, 2 and 2.5 mm downstream. ACh induced hyperpolarization

was recorded in smooth muscle cells impaled at the local site. In some experiments, vessels were incubated in barium (Ba^{2+}, 30 μm) for 15 minutes, prior to recording ACh induced hyperpolarization in order to examine the role of inwardly rectifying potassium channels (K_{IR}) in the conducted response. In all experiments, vessels were incubated in the presence of L-NAME (100 μM) and indomethacin (10 μM) for 40 min prior to the addition of ACh. Identification of impaled cells was determined using electrodes filled with 0.2% propridium iodide.

In separate experiments, arterial segments were pinned flat using the outer connective tissue layer in a Sylgard coated recording chamber and superfused with Krebs' solution, gassed with 95% O_2, 5% CO_2. Following an equilibration period, vessels were pre-constricted with phenylephrine (10^{-6} M), to achieve a standardised constriction of approximately 60% of maximal constriction in all vessels, and ACh (1 M), was iontophoreticlly applied at the local site and at sites 0.5, 1, 1.5 and 2 mm downstream. Changes in vessel diameter in response to ACh were recorded at the local site, using the edge-tracking program, DIAMTRAK (T.O. Neild, Flinders University, Australia). ACh induced relaxation was also recorded in the presence and absence of Ba^{2+}. Data was expressed as % change in relaxation. In control experiments, responses to ACh were examined as the iontophoretic pipette was moved away from the surface of the vessel in 0.1 mm steps, to as distance of 0.5 mm. These experiments were performed to ensure that responses were not due to diffusion of ACh from the iontophoretic pipette to the recording site. The flow of superfusate along the vessel was in the opposite direction to the recording electrode. All experiments were performed in the presence of L-NAME (100 μM) and indomethacin (10 μM).

2.9   STATISTICAL ANALYSIS

Results are expressed as the mean ± the standard error of the mean (SEM). For immunohistochemical experiments, data from the individual fields was used to calculate a mean for each animal. Statistical significance was tested using one way analysis of variance followed by t-tests using Bonferroni correction for multiple groups. A P value of <0.05 was taken as significant.

2.10   DRUGS, CHEMICALS AND SOLUTIONS

All drugs and chemicals used are listed below. ACh, apamin, ampicillin, carboxy-PTIO, charybdotoxin, hydroxocobalamin, iberiotoxin, indomethacin, Lucifer yellow, phenylephrine and 18β-GA were purchased from Sigma, USA. Cx-mimetic peptides, [43]Gap26 (VCYDKSFPISHVR), [40]Gap27 (SRPTEKNVFIV), [37,43]Gap27 (SRPTEKTIFII) (Chaytor et al. 2001) were synthesised and purified by the Biomolecular Resource Facility, John Curtin School of Medical Research. L-NAME was purchased from Sapphire Bioscience Pty Ltd., (Australia). IPTG was purchased from Astral Scientific (Australia), X-Gal was obtained from Progen Industries Pty Ltd., (USA). FITC-dextran was purchased from Molecular Probes Inc., (USA). All other reagents used were of standard analytical grade.

CHAPTER 3
CHARACTERISATION OF CONNEXIN ANTIBODIES

3.1 INTRODUCTION

As discussed in a recent review by Severs *et al.* (2001), the use of improperly characterised antibodies can lead to the misinterpretation of immunohistochemical data. For example, previous studies using a commercially available Cx45 antibody (Kanter *et al.* 1992; Davis *et al.* 1995; Verheule *et al.* 1997), described extensive expression of Cx45 throughout the ventricular myocardium in a pattern similar to Cx43. In contrast, using a fully characterised Cx45 antibody directed against amino acids 354-367 of human Cx45, Coppen *et al.* (1998) demonstrated highly localized expression of Cx45 in the sinoatrial node (SA) of the rat and mouse heart. This area was also Cx40 positive (Bastide *et al.* 1993; Coppen *et al.* 1998), while Cx43 was restricted to cells located at the periphery of the SA node and in surrounding atrial myocytes (Coppen *et al.* 1998, 1999; Honjo *et al.* 2002). Cx45 was also detected in the atrioventricular node and His bundle of the rodent heart (Coppen *et al.* 1999), but was absent from ventricular myocytes (Coppen et al. 1998; Vozzi *et al.* 1999), where Cx43 was expressed extensively (Coppen *et al.* 1998, 1999; Vozzi *et al.* 1999). Coppen *et al.* (1998) further demonstrated that the commercial Cx45 antibody used in the earlier studies cross-reacted with Cx43 and thus resulted in the apparent widespread distribution of Cx45 in the ventricular myocardium. It was subsequently shown that an identical 4 amino acid sequence motif was present in the epitopes that were recognised by both the commercial Cx45 and Cx43 antibodies. Furthermore, when the commercial Cx45 antibody was pre-incubated with an immunogenic peptide encompassing the Cx43 peptide sequence, Cx45 staining was completely abolished (Coppen *et al.* 1998). These data therefore highlight the problems associated with incompletely characterised antibodies.

Since immunohistochemical analysis forms the basis for the protein studies carried out in this thesis, the antibodies used here have been specifically characterised to avoid the problems alluded to above. Once specificity was demonstrated, Cx antibodies have been used to assess Cx distribution within rat blood vessels, results of which will be presented in subsequent Chapters. For Cxs 37, 40 and 45, purified antibodies were obtained by affinity

chromatography of the serum of sheep that had been immunized with synthetic peptides specific for each Cx. Previous researchers have used these peptide sequences to develop Cx isotype specific antibodies (Coppen *et al.* 1998; Yeh *et al.* 1998; Severs, 1999; Yeh *et al.* 2000). Affinity-purified antibodies are denoted as Cx37/266, Cx40/254 and Cx45/354 corresponding to anti-Cx37, 40 and 45, respectively. Commercially available antibodies for Cxs 37 (Cx37/ADI), 40 (Cx40/ADI), 43 (Cx43/Zy) and 45 (Cx45/ADI and Cx45/Chem) were also tested.

Western blotting and immunohistochemical studies were carried out using these antibodies to examine cells that had been transfected with plasmid DNA expressing each Cx isotype and in a range of rat tissues known to specifically express each Cx. The tissues chosen were rat heart, brain, lung, liver and thoracic aorta. Cx37 has previously been identified in rat heart, brain, lung and liver (Haefliger *et al.* 1992; Reed *et al.* 1993; Nakamura *et al.* 1999), Cx40 has been identified in the rat heart and lungs (Haefliger *et al.* 1992; Beyer *et al.* 1992; Bastide *et al.* 1993), Cx43 in rat heart, brain and thoracic aorta (el Aoumari *et al.* 1991; Kadle *et al.* 1991; Dupont *et al.* 1991) and Cx45 in rat heart, brain and lung (Coppen *et al.* 1998; Jacob & Beyer, 2001).

3.2   RESULTS

3.2.1   *Transfected cells*

Immunohistochemistry. Immunolabelling was also performed on COS-7 cells that had been transiently transfected with plasmid DNA expressing either Cxs 37 (COS-Cx37, Figure 3.1A,F,K,P), 40 (COS-Cx40, Figure 3.1B,G,L,Q), 43 (COS-Cx43, Figure 3.1C,H,M,R) or 45 (COS-Cx45, Figure 3.1D,I,N,S) and in untransfected cells (Figure 3.2 E,J,O,T) using Cx37/266, Cx40/254, Cx43/Zy and Cx45/354. Only transfectants expressing the Cx to which the antibody was directed were positively labelled (Figure 3.1A-S). Cx labelling was found predominatly within the cytoplasm of each cell. Specificity of each antibody was confirmed by the absence of labelling in transfectants expressing the other Cx types. No labelling was detected for any Cx antibody in the untransfected cells (Figure 3.1E,J,O,T). Similarly, Cx37/ADI and Cx45/Chem labelled only transfected cells expressing Cx37 or Cx45, respectively (Sandow *et al.* 2003d).

Western blotting. Western blotting analysis was performed on membranes of COS-7 cells that had been transiently transfected with plasmid DNA expressing either, Cx37, 40,
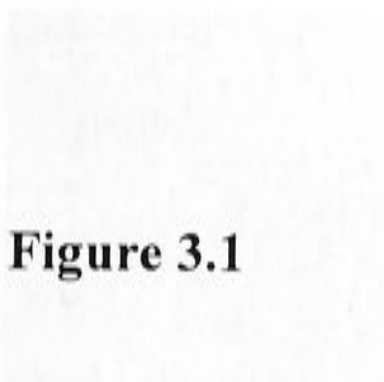
Figure 3.1

Figure 3.1.

Characterisation of affinity-purified connexin (Cx) antibodies. COS-7 cells that had been transfected with plasmid expressing DNA for Cxs 37 (COS-Cx37, A,F,K,P) , 40 (COS-Cx40, B,G,L,Q), 43 (COS-Cx43, C,H,M,R), and 45 (COS-Cx45, D,I,N,S), were labelled with antibodies specific for each Cx (Cx37/266, A-D; Cx40/254, F-I; Cx43/Zy, K-N; Cx45/354, P-S). Only transfectants expressing the Cx to which the antibody was directed were positively labelled (COS-Cx37, A; COS-Cx40, G, COS-Cx43, M; COS-Cx45, S). Specificity of each antibody was confirmed by absence of labelling in transfectants expressing the other Cx types, and by the absence of labelling in untransfected cells (E,J,O,T). Calibration bar represents 20 μm.

Cx37/266   Cx40/254   Cx43/Zy   Cx45/354

COS-Cx37   COS-Cx37   COS-Cx37   COS-Cx37
A   F   K   P

COS-Cx40   COS-Cx40   COS-Cx40   COS-Cx40
B   G   L   Q

COS-Cx43   COS-Cx43   COS-Cx43   COS-Cx43
C   H   M   R

COS-Cx45   COS-Cx45   COS-Cx45   COS-Cx45
D   I   N   S

Untransfected   Untransfected   Untransfected   Untransfected
E   J   O   T
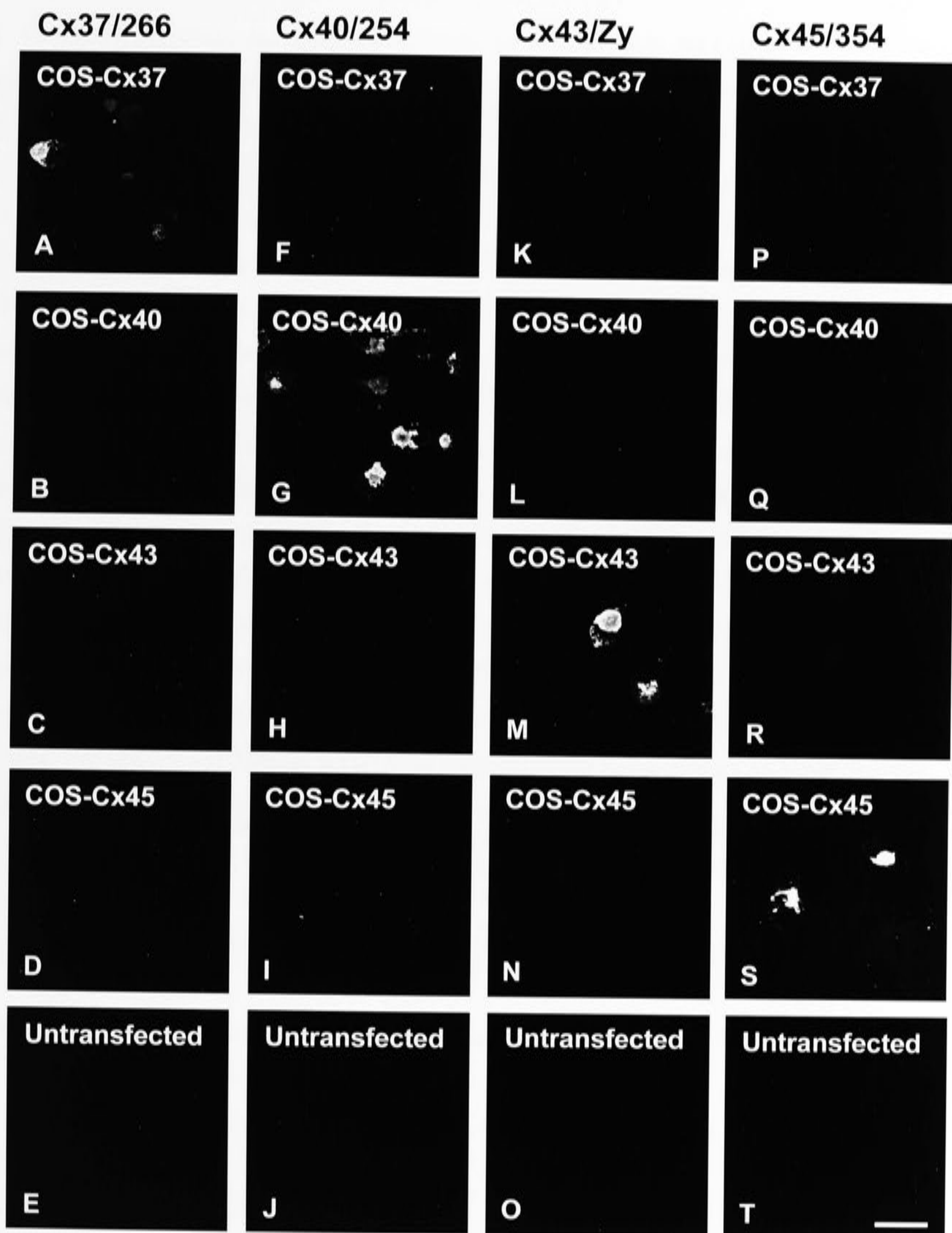
43 or 45 (COS-Cx37, COS-Cx40, COS-Cx43 and COS-Cx45, respectively, Figure 3.2A-D). Cx37/266-antiserum recognised two bands, corresponding to the expected sizes of the phosphorylated and non-phosphorylated forms of the protein, in COS-Cx37 cells (Figure 3.2A, -control peptide). No specific bands were found in transfected cells expressing other Cx isotypes, nor following incubation of the antibodies with the appropriate immunogenic peptide (Figure 3.2A, -/+control peptide). Similarly, Cx37/ADI recognised two bands of the appropriate molecular weight, specifically in COS-Cx37 cells, which were blocked following incubation with the appropriate immunogenic peptide (Figure 3.2B, -/+ control peptide). Cx40/254-antiserum (Figure 3.2C, -control peptide) recognised two specific bands at the appropriate molecular weight exclusively in transfected COS-7 cells expressing Cx40. Cx43/Zy revealed the presence of multiple isoforms of Cx43 in transfected cells expressing Cx43 (Figure 3.2D, -peptide). Cx45/354-antiserum (Figure 3.2E, -control peptide) recognised one band at the appropriate molecular weight, in transfected cells expression Cx45. Labelling of these bands was abolished following incubation of the antibodies with the appropriate immunogenic peptide (Figures 3.2C, D, E, +control peptide). On Western blots, no bands specific for Cx45 were detected using Cx45/Chem to probe extracts of transfected cells expressing Cx45 (Figure 3.2F, -/+control peptide). No specific bands were detected in transfected cells expressing Cxs other than the isotype against which antisera were raised (Figure 3.2C,D,E, -peptide).

3.2.2 Connexin specific tissues

Immunohistochemistry. When tested on sections of rat lung, Cx37/266 showed that Cx37 was abundantly expressed within the endothelium of blood vessels throughout the lung, and within the smooth muscle layers of the bronchioles (Figure 3.3A). Staining was completely blocked by peptide (Figure 3.3B). Using Cx40/ADI, punctate labelling was observed in the media of the rat thoracic aorta. Staining of the rat ventricle with Cx45/ADI and Cx45/354, revealed differences in the extent of labelling. Cx45/ADI stained cardiac myocytes throughout the ventricular myocardium (Figure 3.3C), while Cx45/354 only stained myocytes along the endocardial border (Figure 3.3D).

Western blotting. Cx43/Zy revealed the presence of multiple isoforms of Cx43 in extracts of brain, heart and lung, but not in the liver. Higher molecular weight isoforms appeared to predominate in the heart (Figure 3.4A, -peptide). All isoforms were blocked by pre-incubation of Cx43/Zy with immunogenic peptide (Figure 3.4A, +peptide). When

Figure 3.2

Figure 3.2.

Characterisation of Cx antisera by Western blotting. COS-7 cells transfected with plasmid DNA expressing Cxs 37, 40, 43 and 45, were labelled with antibodies specific for each Cx (Cx37/266-antiserum, A; Cx37/ADI, B; Cx40/254-antiserum, C; Cx43/Zy, D; Cx45/354-antiserum, E; Cx45/Chem, F). Arrows show the position of expected Cx bands. The left panel represents incubation with Cx antibody whereas the right panel represents pre-incubation of the antibody with the appropriate immunogenic peptide. Only transfectants expressing the Cx to which the antibody was directed showed a band of the correct molecular weight, as indicated by arrows in the –peptide panels. Specificity of each antibody was confirmed by the absence of specific bands in transfectants expressing the other Cx types, or in the presence of the appropriate control peptide (+peptide).

A Cx37/266-antiserum

COS-Cx37 40 43 45   37 40 43 45

—97—

—52—

—33—

—21—

- control peptide   + control peptide

B Cx37/ADI

COS-Cx37 40 43 45   37 40 43 45

—97—

—52—

—33—

—21—

- control peptide   + control peptide

C Cx40/254-antiserum

COS-Cx37 40 43 45   37 40 43 45

—97—

—52—

—33—

—21—

- control peptide   + control peptide

D Cx43/Zy

COS-Cx37 40 43 45   37 40 43 45

—97—

—52—

—33—

—21—

- control peptide   + control peptide

E Cx45/354-antiserum

COS- Cx37 40 43 45   37 40 43 45

—97—

—52—

—33—

—21—

- control peptide   + control peptide

F Cx45/Chem

COS-Cx37 40 43 45   37 40 43 45

—97—

—52—

—33—

—21—

- control peptide   + control peptide
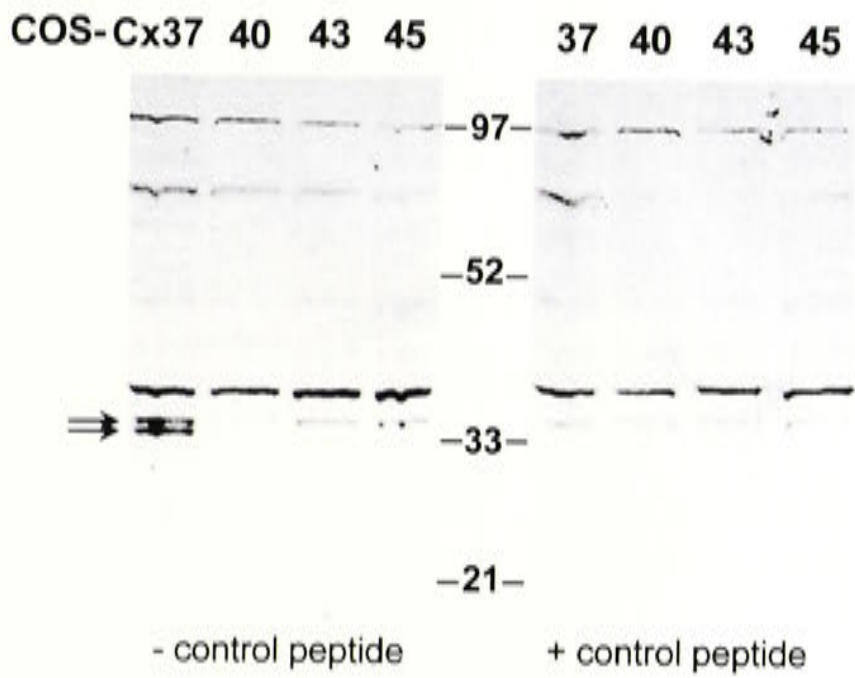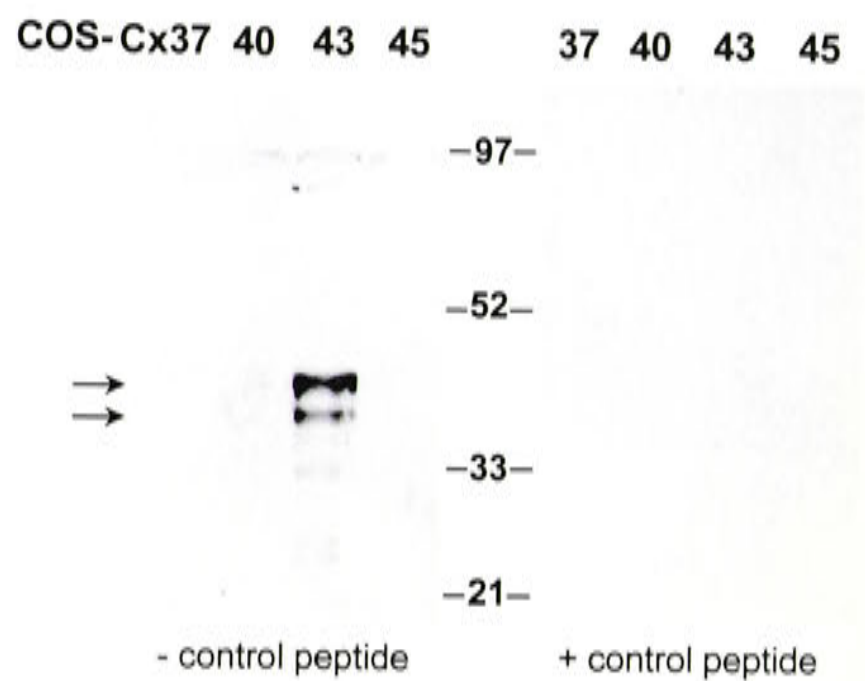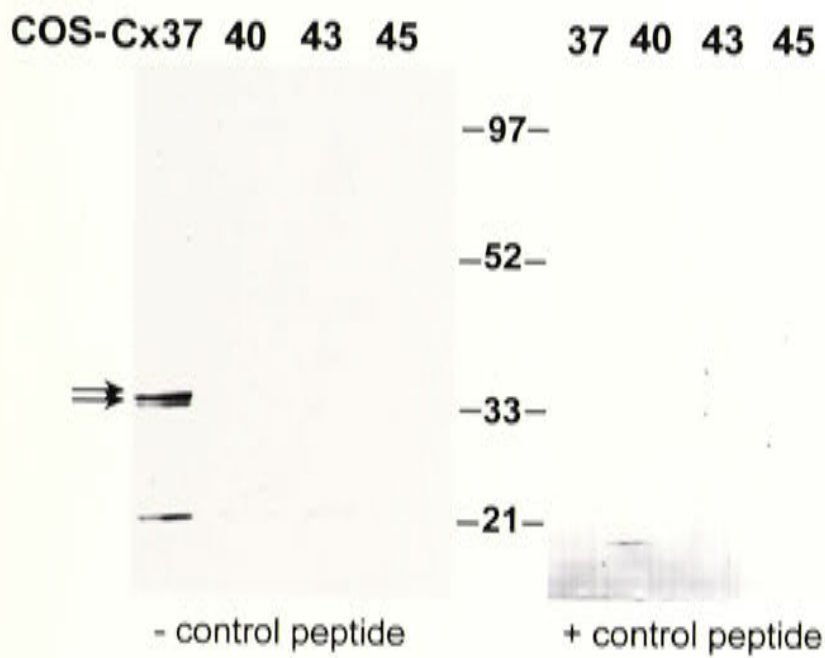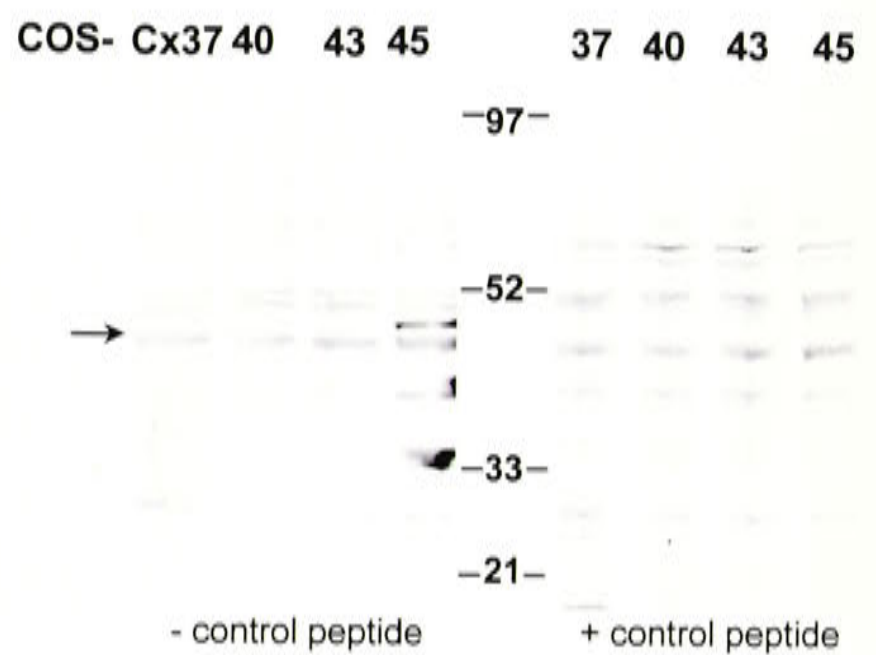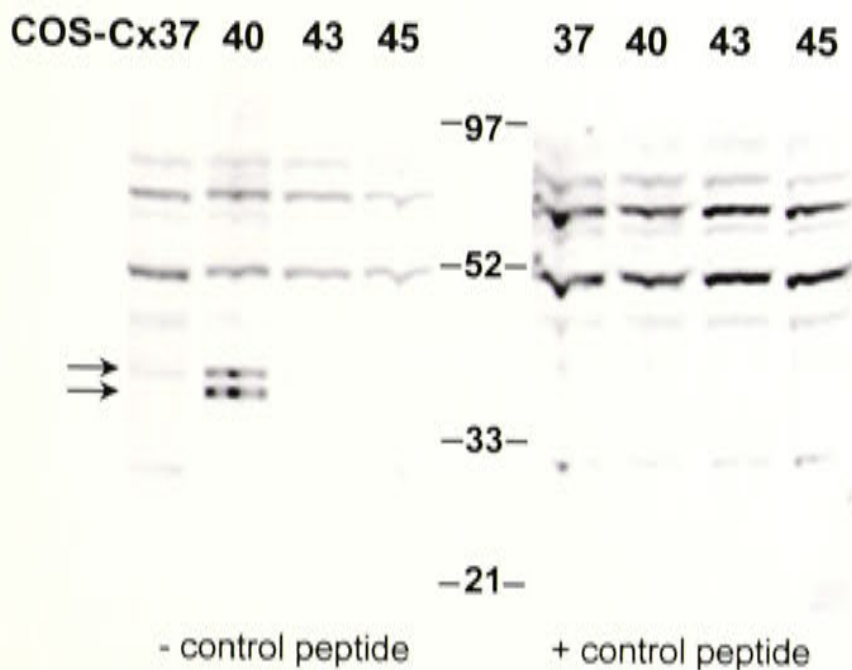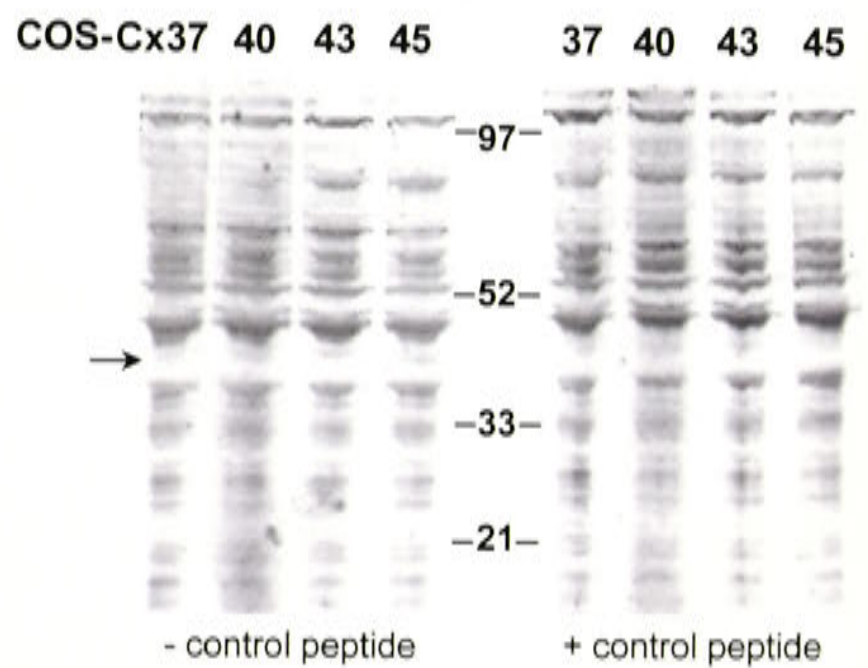
Figure 3.3

Figure 3.3.

Cx37 expression in the lung and Cx45 expression in the heart of 4 week old Wistar rat. (A) Sections of the rat lung were stained with Cx37/266. Cx37 labelling is seen in the endothelium of blood vessels (bv) within the lung and in smooth muscle cells (arrows) of the bronchiole (br). (B) Cx37 labelling was abolished when the antibody is incubated in antigenic peptide prior to incubating with tissue. (C-D) Heart sections were incubated with Cx45/ADI (C) and Cx45/354 (D). Punctate staining with Cx45/ADI was detected along the edges of cardiac myocytes throughout the ventricle (C), while Cx45/354 labelled Cx45 only along the endocardial border (D). Calibration bars represent 10 μm.
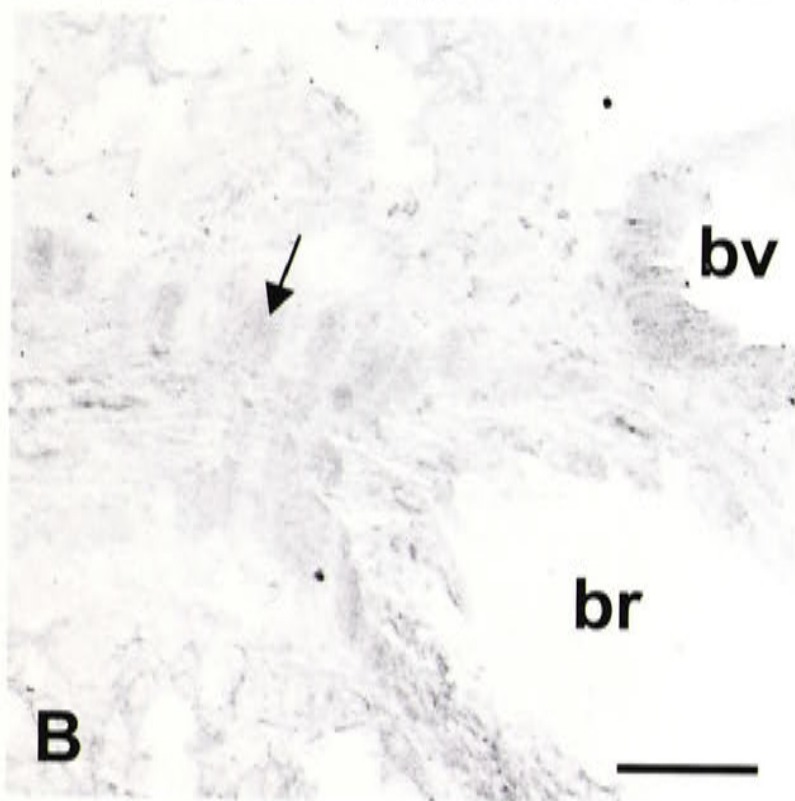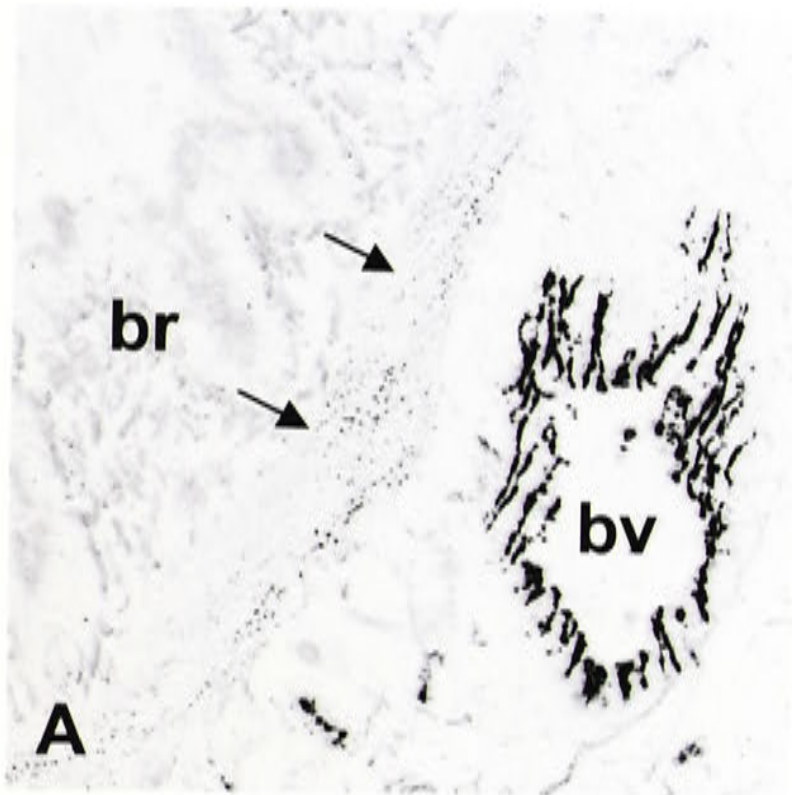
Figure 3.4

Figure 3.4.

Tissue specific expression of Cx43. (A) Tissue extracts (5 μg) from rat brain, heart, lung, liver, caudal artery (CA) and thoracic aorta (ThA) were separated on 12% SDS PAGE gels and probed with Cx43/Zy. Unphosphorylated and phosphorylated (*) forms are indicated by arrows (- control peptide). All forms disappeared when the antibody was pre-incubated with the immunogenic peptide (+ control peptide). (B) Tissue extracts (10 μg) from rat heart, CA and ThA were separated on 8% SDS PAGE gels and probed with Cx43/Zy. Extracts were prepared in buffer either containing (first panel) or not containing (second panel) the phosphatase inhibitors sodium fluoride and sodium orthovanadate (NaF/PhI) or were incubated with alkaline phosphatase (AlkPhos, second panel). Higher molecular weight forms of Cx43 were removed by treatment of all three tissues with alkaline phosphatase. Prot Inh, protease inhibitor.

A

Brain Heart Lung Liver   Brain Heart Lung Liver

—97—

—66—

**
Cx43 *
                                          —45—

—30—

- peptide   + peptide
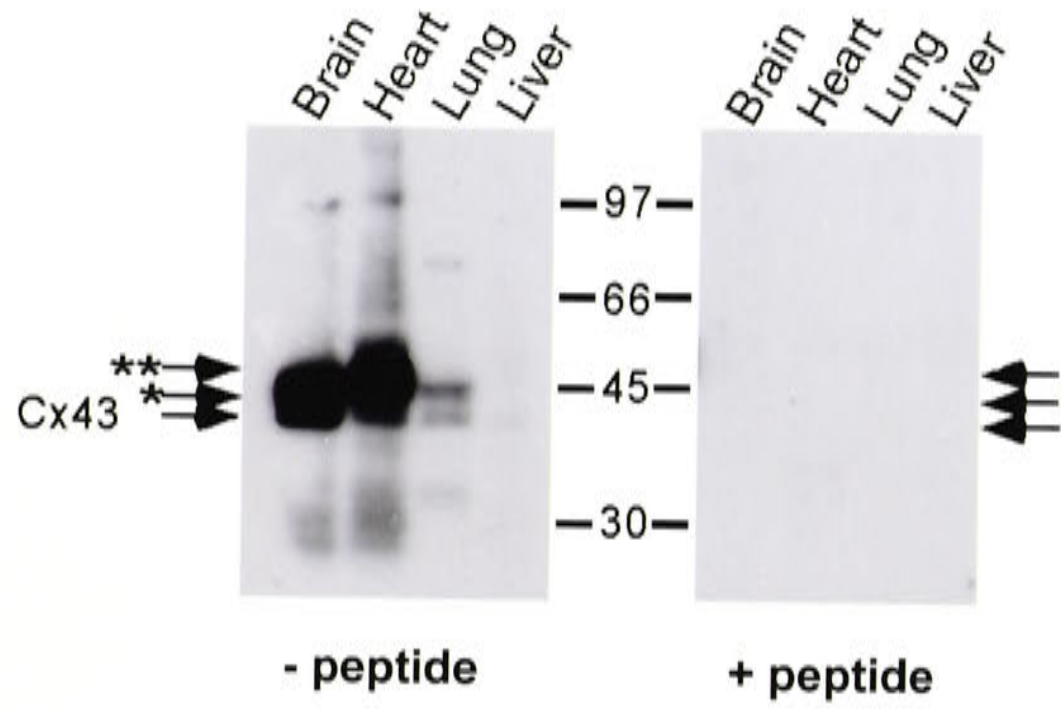
B

Prot Inh	+	+	+		+	+	+		+	+	+
NaF/ Phl	+	+	+		-	-	-		-	-	-
Alk Phos	-	-	-		-	-	-		+	+	+
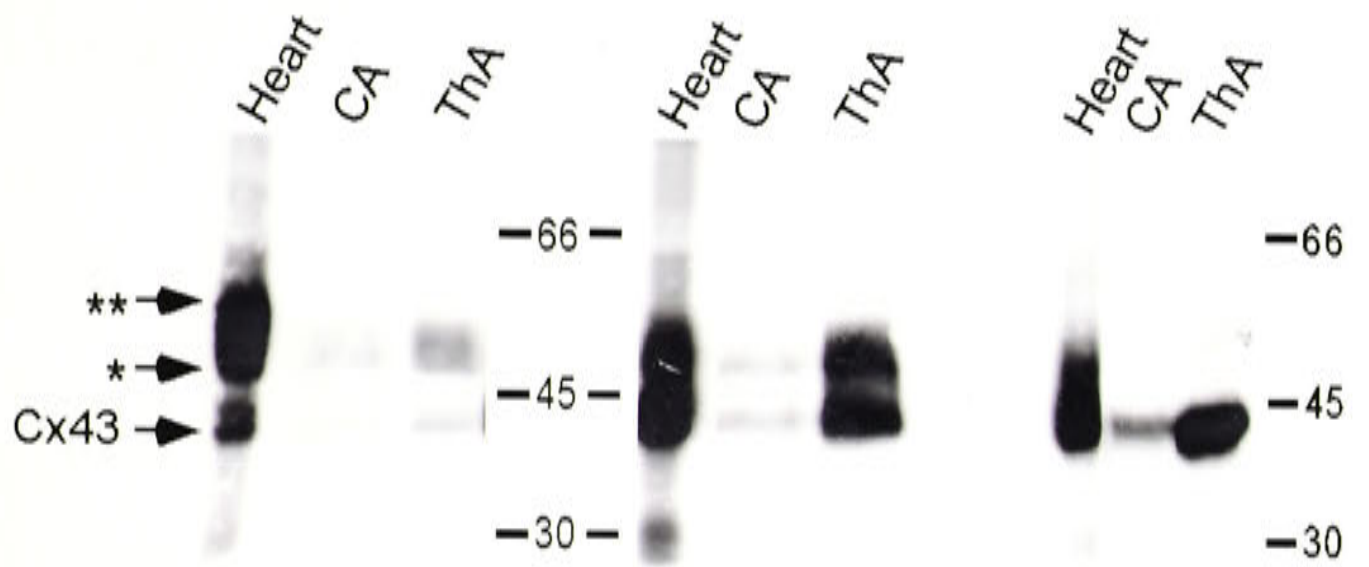
Heart CA ThA   Heart CA ThA   Heart CA ThA

—66—   —66—

**→

*→

Cx43→
                    —45—   —45—

                    —30—   —30—

Figure 3.5

Figure 3.5.

Western blotting of tissue extracts from rat brain, heart, lung and liver using Cx40/254 (A), Cx45/354 (B) and Cx45/ADI (C). Arrows show the position of the expected Cx bands. The left panels represent incubation with Cx antibody whereas right panels represent pre-incubation of the antibody with immunogenic peptide. Lower molecular weight proteins that cross-react with the commercial Cx45 antibody are marked (*).

A

Lung Liver   Lung Liver

— 66 —

— 45 —

Cx40 →

— 30 —

- peptide   + peptide

B

Brain Heart Lung   Brain Heart Lung

— 66 —

Cx45 →   — 45 —   →

— 30 —

- peptide   + peptide

C

Brain Heart Lung   Brain Heart Lung

— 66 —

Cx45 →   — 45 —   →
* →   → *

— 30 —

- peptide   + peptide
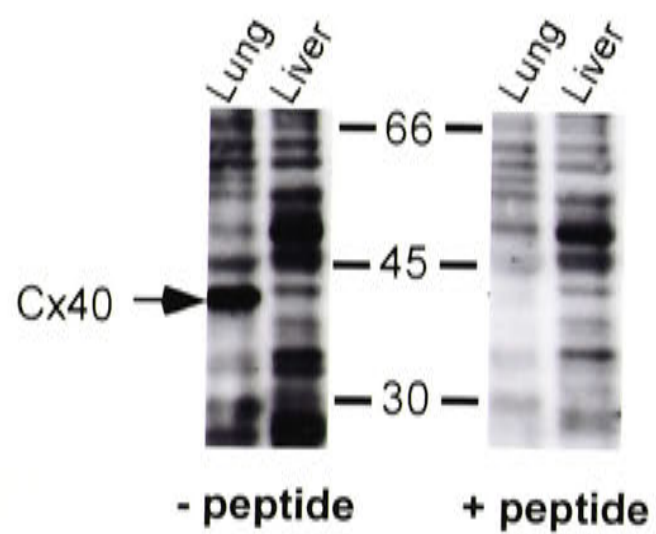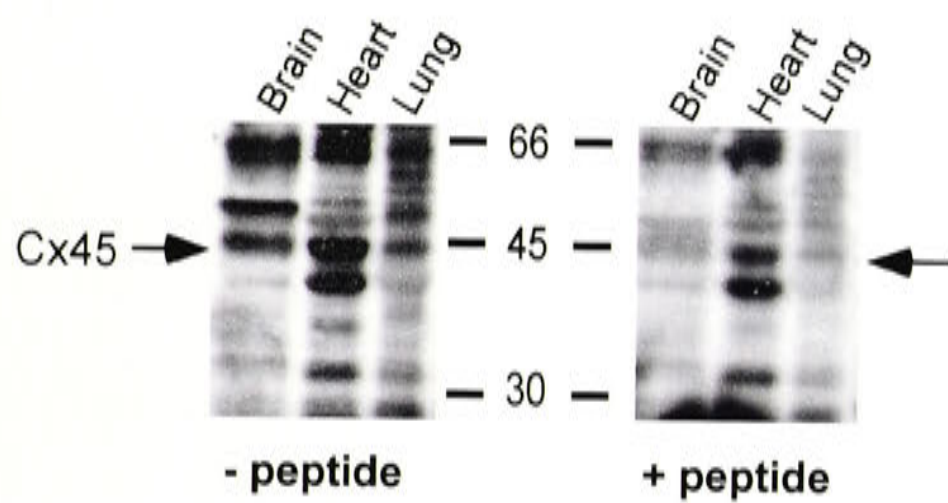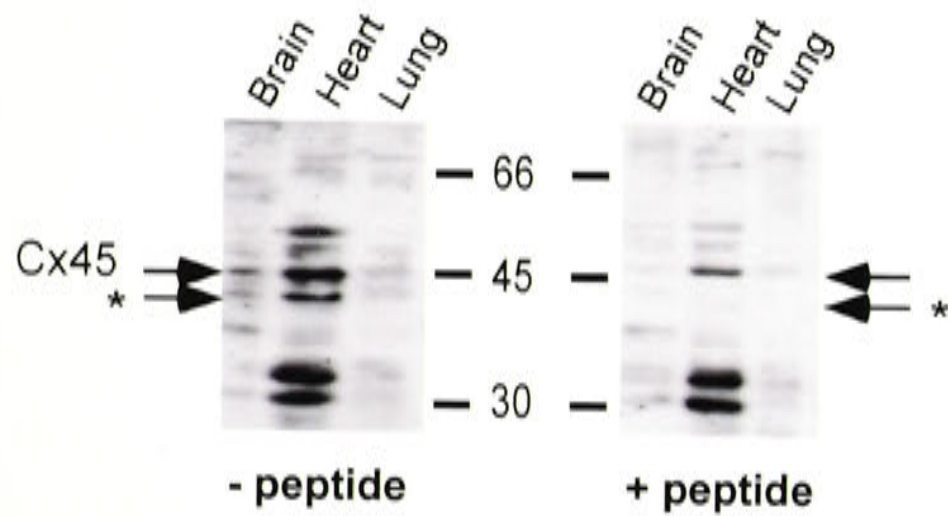
samples of heart, thoracic aorta and caudal artery were not treated with phosphatase inhibitor (Figure 3.4B, - NaF/PhI) or were treated with phosphates (Figure 3.4B, + Alk Phos), a shift in mobility towards the lower molecular weight form was found, confirming that the high molecular weight forms were phosphorylated Cx43.

Although Cx37/266 and Cx37/ADI worked well in immunohistochemistry, numerous bands were stained on Western blots of rat tissues, and the staining of these bands was unaffected when blots were probed with peptide-blocked antibody (data not shown). Cx40/254 and Cx40/ADI also stained numerous bands on Western blots of rat lung and liver extracts, as did Cx45/354 and Cx45/ADI in Western blots of brain, heart and lung extracts. In each case only a small number of bands disappeared when the antibodies were pre-incubated with immunogenic peptide (Figure 3.5A-C). Thus, Cx40/254 specifically recognised a band of 40 kDa that was present in tissue from the lung, but not the liver (Figure 3.5A, -/+peptide). In addition, the staining intensity of a 45 kDa band in extracts of lung tissue was reduced on blots probed with peptide blocked antibody. On the other hand, Cx40/ADI cross reacted with Cx43 as evidenced by the appearance of bands on Western blots of brain tissue, that were equivalent in size to those stained with antibodies against Cx43 (data not shown). Cx45/354 revealed the presence of a specific 45 kDa band in all tissues tested. A higher molecular weight band, which was blocked by peptide, was also present in brain extracts (Figure 3.5B, -/+peptide). In contrast, Cx45/ADI labelled a 45 kDa band and also a lower molecular weight species in brain and heart extracts (Figure 3.5C, asterisk).

3.3   DISCUSSION

COS-7 cells that had been transfected with plasmid DNA expressing either Cxs 37, 40, 43 or 45 confirmed the specificity of Cx37/266, Cx40/254, Cx45/354 affinity-purified antibodies and the commercially available antibodies Cx43/Zy, Cx37/ADI and Cx45/Chem. Antibodies to each Cx only labelled those cells that had been transfected with DNA expressing the corresponding Cx, and this specific staining was blocked by pre-incubation of antibodies with the appropriate immunogenic peptide. The affinity-purified antibodies that were used in this study were raised against short synthetic peptides that were derived from the published sequences for each Cx. Antibodies against the same sequences have

been shown previously to be subtype selective using Western blotting and immunohistochemistry of transfected cells (Coppen *et al.* 1998; Yeh *et al.* 1998; Yeh *et al.* 2000), as well as immunoelectron microscopy (Yeh *et al.* 1998).

For Cxs 37, 40 and 45, two different antibodies directed against distinct epitopes within each Cx were used to examine expression of each of the Cxs in transfected cells as well as rat tissues. Immunohistochemical studies using Cx37/266 specifically labelled transfected cells expressing Cx37 and also extensively stained the blood vessels and bronchioles of the lung, as previously described by Nakamura *et al.* (1999). However, while both antibodies labelled appropriate bands in Western blots of transfected cells, neither labelled any specific bands in Western blots of Cx37 enriched rat tissues. This may be due to the higher concentration of Cx37 protein in transfected cell extracts as compared to rat tissues.

Cx40/254 detected a 40 kDa protein in Western blots of tissue samples, as well as in transfected cells expressing Cx40, in parallel to results previously published for an antibody directed to a similar amino acid sequence (Yeh *et al.* 1998). Cx40/ADI however, appeared to cross-react with Cx43 on Western blots of rat brain extracts and in immunohistochemical studies of the rat aorta, so its use was discontinued.

Cx45/354 labelled a restricted area within the ventricular endocardium, which is consistent with the studies of Coppen *et al.* (1998) who developed an antibody against the same epitope. Cx45/ADI however, cross-reacted with Cx43, in the same pattern as that described by Coppen *et al.* (1998) using another commercial antibody directed against a similar epitope. Coppen *et al.* (1998) have elegantly identified the cross reacting peptide as residues 283 to 286 of Cx43. In contrast to Cx45/ADI, Cx45/Chem is directed to the same amino acid sequence as Cx45/354. Using this antibody, specific immunohistochemical labelling was obtained in cells transfected with Cx45, but not in cells transfected with other Cx isotypes. However, this antibody did not detect specific bands for Cx45 on Western blots of transfected cell extracts. The reason for this discrepancy is unknown.

Cx43/Zy stained a number of molecular weight bands which were confirmed here to represent unphosphorylated and phosphorylated Cx43 (see van Veen *et al.* 2001). Using a similar antibody, Hossain *et al.* (1994) found no differences in immunohistochemical staining of brain tissues in which different relative amounts of these phosphorylated forms existed. Similarly, Western blotting and immunohistochemistry of transfected cells

expressing Cx43 showed specific labelling when probed with Cx43/Zy. Tissue specific distribution of the unphosphorylated and phosphorylated forms of Cx43 has been previously reported (Kadle *et al.* 1991). In the present study, the higher molecular weight phosphorylated forms predominated in extracts of the heart and thoracic aorta, while the lower molecular weight forms were more prevalent in extracts of the brain and caudal artery. Hossain *et al.* (1994) demonstrated that the predominance of the lower molecular weight forms in the brain was due to rapid dephosphorylation of Cx43. Since Cx43 in the caudal artery is restricted to the endothelium, while Cx43 in the thoracic aorta was predominantly expressed in the smooth muscle (see Chapter 4), differences in specific kinases or phosphatases may exist between these two tissues.

In conclusion, the results of this Chapter have shown that Cx37/266, Cx40/254, and Cx45/354 antibodies and the commercially available Cx43/Zy, Cx37/ADI and Cx45/Chem antibodies are isotype specific in both transfected cells and rat tissues. While working well in Western blots of transfected cells and for the immunohistochemistry of transfected cells and rat tissues, these antibodies, with the exception of Cx43/Zy did not work efficiently on Western blots of rat tissues. Consequently, Cx37/266, Cx40/254 and Cx45/354 affinity purified antibodies and the Cx43/Zy antibody were chosen for subsequent immunohistochemical examination of Cx protein expression in rat blood vessels, the results of which are presented in the following Chapters.

CHAPTER 4

EXPRESSION OF CONNEXINS IN THE MEDIA AND ENDOTHELIUM OF THE WISTAR RAT THORACIC AORTA AND CAUDAL ARTERY

4.1   INTRODUCTION

As discussed in Chapter 1, four Cx proteins, Cxs 37, 40, 43 and 45 have been identified in vascular tissue (see Severs, 1999; Krüger *et al.* 2000; Kumai *et al.* 2000). While three of the four vascular Cxs have been shown to be expressed by endothelial cells of most vessels (see Hill *et al.* 2001), the identity of the Cxs connecting adjacent smooth muscle cells in arteries is less clear.

In large elastic arteries, such as the aorta, Cx43 is thought to be the major gap junctional protein expressed in the smooth muscle (Hong & Hill, 1998; Yeh *et al.* 1998; Nakamura *et al.* 1999; van Kempen & Jongsma, 1999). More recently, some studies have shown expression of other Cxs in addition to Cx43 in the media of elastic arteries, although some of these differences may be attributed to heterogeneity amongst animal species, in addition to questionable specificity of the antibodies used (Hill *et al.* 2001). For example, Cx40 has been shown in the aorta of the cow and pig but not the rat (van Kempen & Jongsma, 1999), while Cx37 has been reported in the pulmonary artery and aorta of the rat in some studies (Nakamura *et al.* 1999), but not in other studies (van Kempen & Jongsma, 1999).

In muscular arteries, identification of the major Cx isoform has been more difficult. Cx43 has not been found in the media of a number of large muscular arteries including the caudal, basilar, mesenteric and coronary arteries (Hong & Hill, 1998; Bastide *et al.* 1993; Bruzzone *et al.* 1993; Gros *et al.* 1994; Yeh *et al.* 1997b), although it has been reported in pial and cremaster arterioles in rats and cheek pouch arterioles in hamsters (Little *et al.* 1995). On the other hand, Cx40 appears to be a potential candidate in the media, having been identified in the coronary artery in a number of species (van Kempen & Jongsma, 1999), in the basilar artery (Li & Simard, 1999), and in a number of different arterioles of rats and hamsters (Little *et al.* 1995; Arensbak *et al.* 2001; Haefliger *et al.* 2001). Recent data from our laboratory have, however, failed to confirm the results in hamster arterioles

(Sandow *et al.* 2003d). Cx45 is also receiving some attention (Ko *et al.* 2001; Li & Simard, 2001), since its identification in arterial smooth muscle in embryonic and adult mice (Alcoléa *et al.* 1999; Krüger *et al.* 2000; Kumai *et al.* 2000). On the other hand, Cx37 is generally considered to be an endothelial Cx, although it has been described in the media of the larger coronary arteries of the rat (van Kempen & Jongsma, 1999) and in the media of collateral vessels during coronary arteriogenesis in dogs (Cai *et al.* 2001).

Considering the absence of a clearly identifiable Cx in the media of muscular arteries and the potential for some confusion due to non specificity of antibodies (see Chapter 3), in this Chapter, we chose to compare Cx expression at both mRNA and protein levels in a large muscular artery with expression in an elastic artery. For this purpose we have chosen the caudal artery and thoracic aorta, respectively. By using real time PCR, we have quantified mRNA expression in the two vessels and related this to protein expression using both immunohistochemistry and Western blotting.

4.2   RESULTS

4.2.1   *Expression of mRNA for vascular connexins*

Quantification of mRNA expression of the vascular Cxs using real time PCR was achieved by constructing standard curves from the plasmid clones of the four Cxs and of 18S RNA (see Figure 4.1 for Cx40). mRNA in the arterial samples was therefore expressed as Cx copy number and normalized to the number of copies of 18S RNA. Data showed that in the thoracic aorta, expression of mRNA for Cx43 was significantly greater than mRNA expression for Cxs 37, 40 and 45 ($P<0.05$, Figure 4.2). In the caudal artery, expression of mRNA for Cx37 was significantly greater than expression of mRNA for Cxs 40, 43, and 45 ($P<0.05$, Figure 4.2). Expression of Cx37 mRNA was also significantly greater in the caudal artery than in the thoracic aorta ($P<0.05$, Figure 4.2), while mRNA for Cx43 was significantly greater in the thoracic aorta than in the caudal artery ($P<0.05$, Figure 4.2). Expression of mRNA for Cx37 in the caudal artery was not significantly different from mRNA expression for Cx43 in the thoracic aorta. Expression of mRNA for Cxs 40 and 45 were not significantly different between the two arteries (Figure 4.2).

Figure 4.1
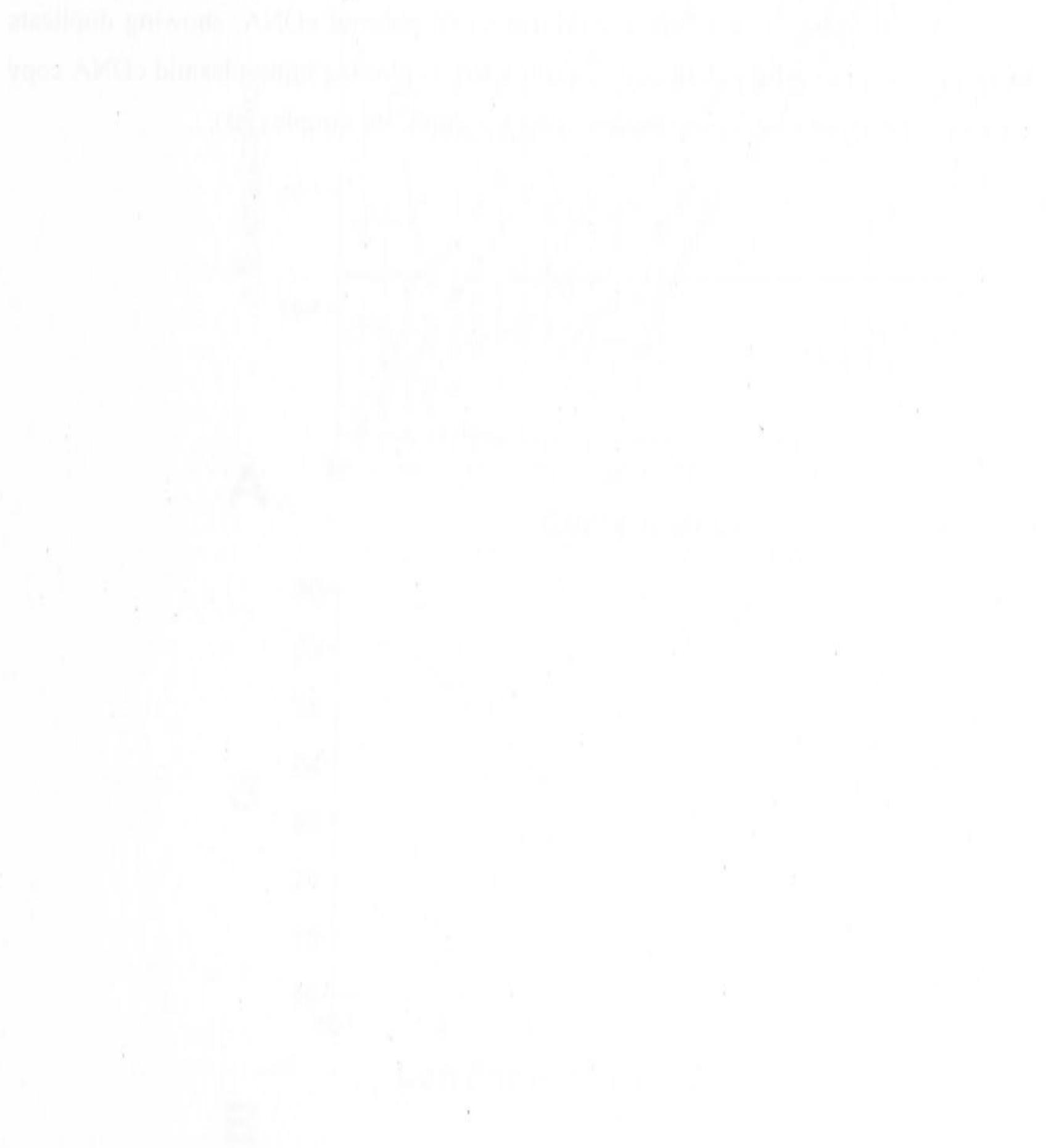
Figure 4.1.

Amplification plot of serially diluted Cx40 plasmid cDNA, showing duplicate samples (A). Plasmid standard curve constructed by plotting input plasmid cDNA copy number versus mean Ct value obtained from the duplicate samples (B).

A

B
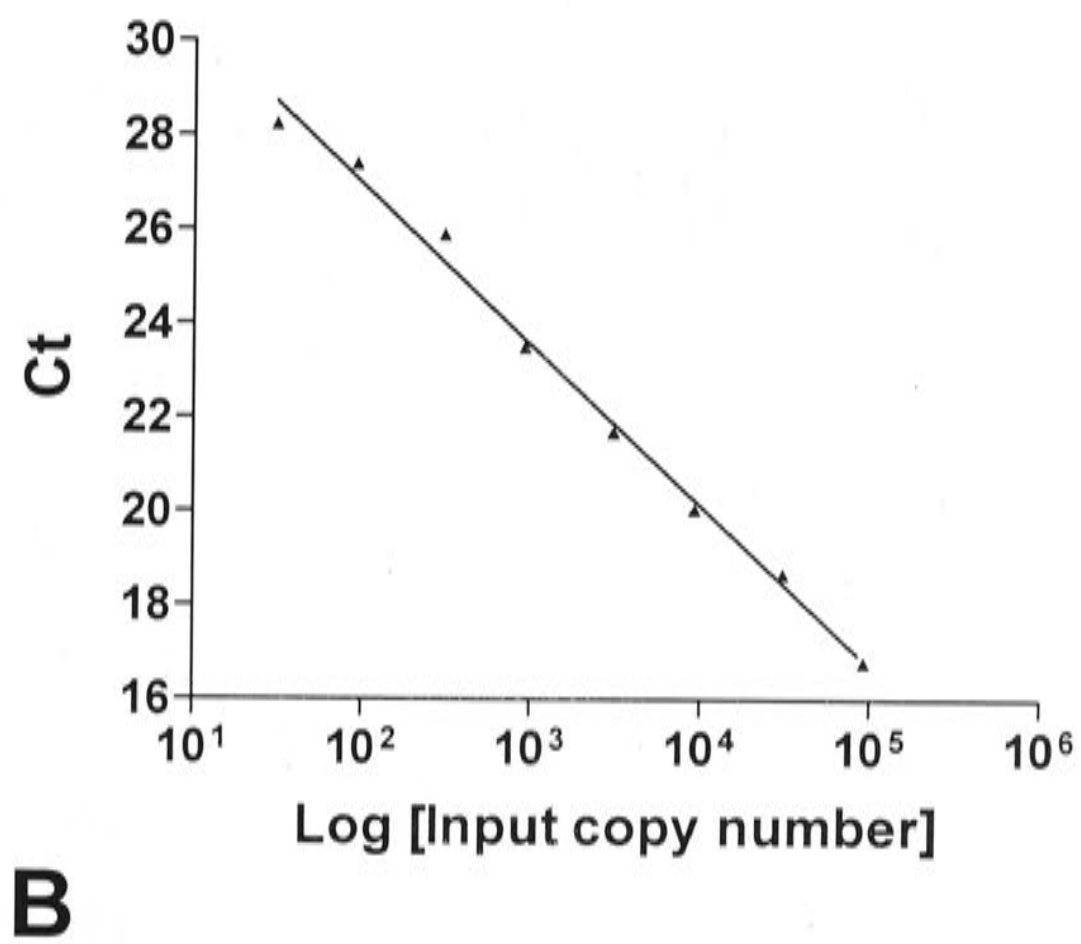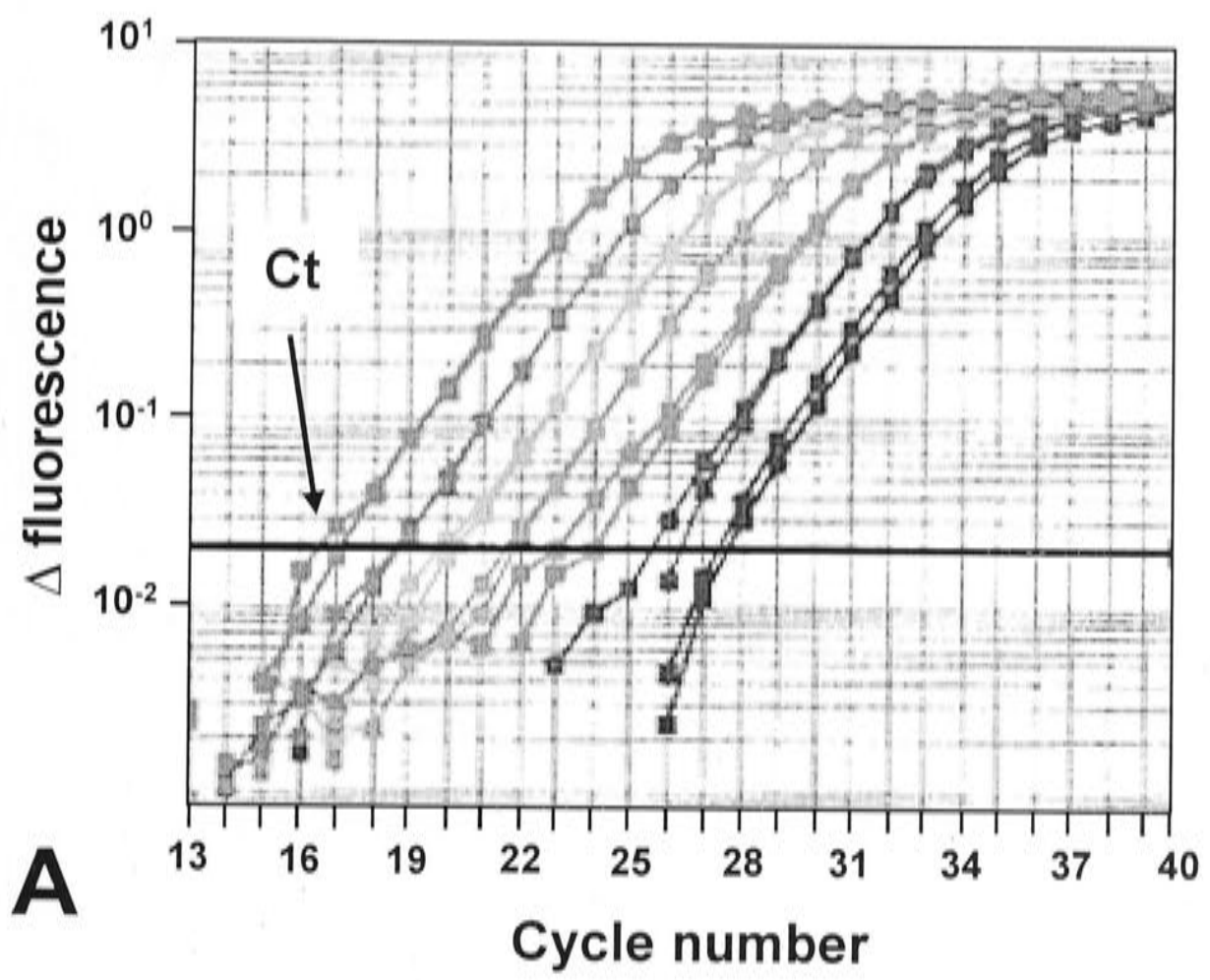
Figure 4.2

Figure 4.2.

mRNA expression of Cxs 37, 40, 43 and 45 in the Wistar rat thoracic aorta and caudal artery. Copy numbers for each Cx are expressed per copy of 18S ribosomal RNA using plasmid standard curves. Values are mean ± SEM. [*]$P<0.05$, significantly different from the caudal artery. [†]$P<0.05$, significantly different from Cxs 37, 40 and 45 in the thoracic aorta. [‡]$P<0.05$, significantly different from Cxs 40, 43 and 45 in the caudal artery. $n=4$ separate RNA preparations.
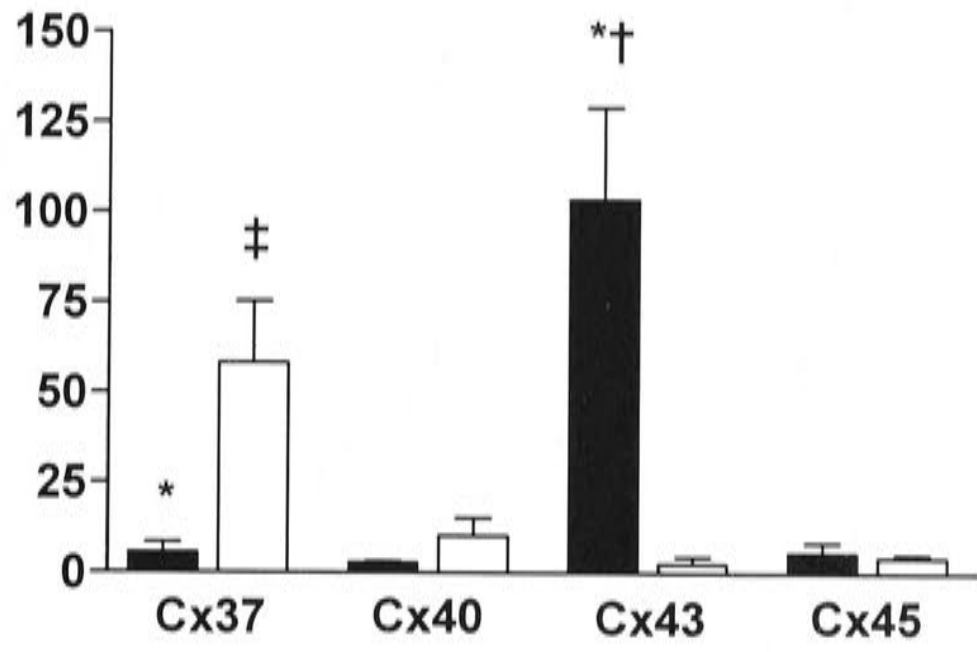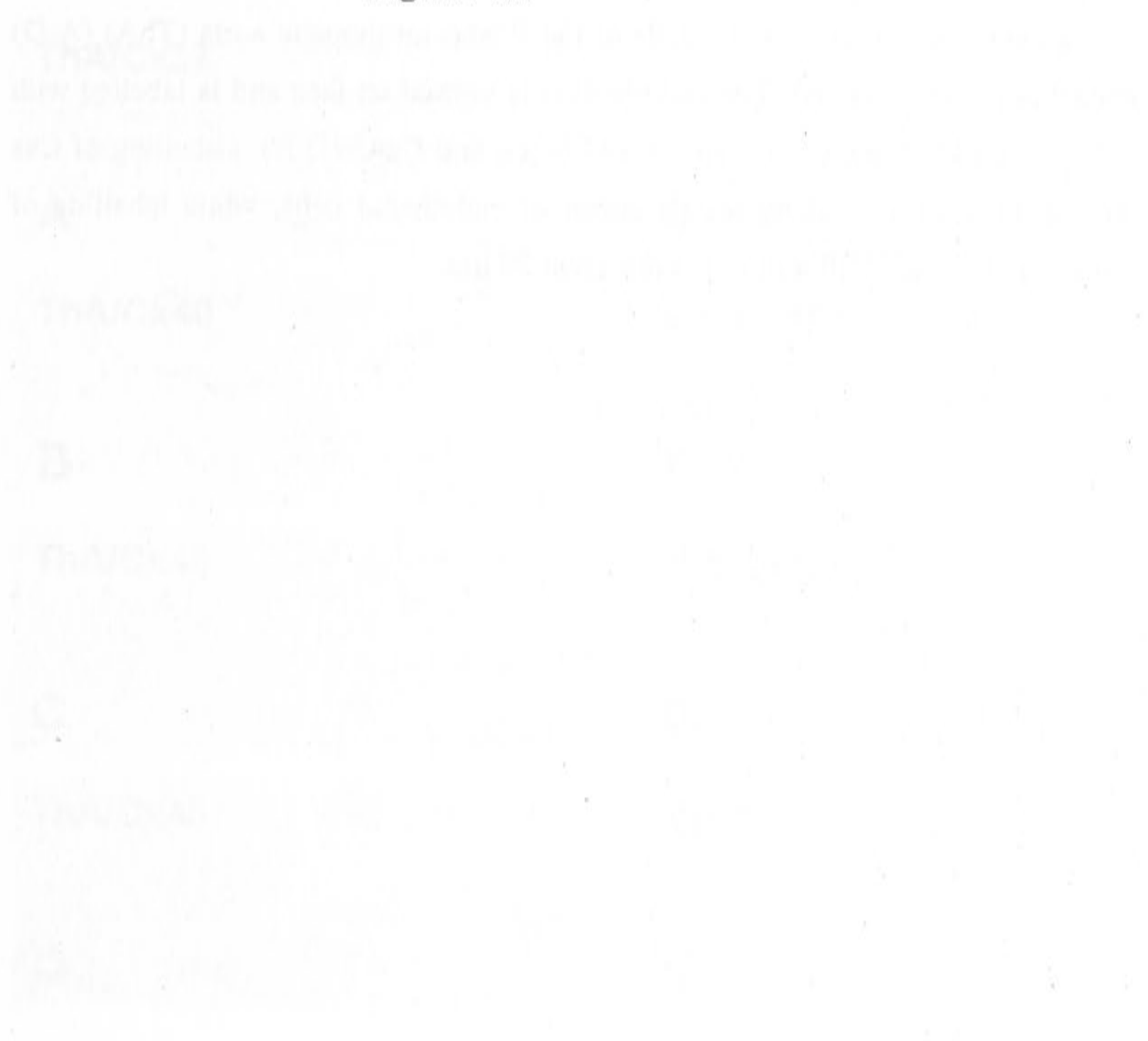
Figure 4.3

Figure 4.3.

Cx expression in endothelial cells of the Wistar rat thoracic aorta (ThA) (A-D) and caudal artery (CA) (E-H). The endothelium is viewed en face and is labelled with antibodies to Cx37 (A,E), Cx40 (B,F), Cx43 (C,G) and Cx45 (D,H). Labelling of Cxs 37, 40 and 43 is evident along the perimeter of endothelial cells, while labelling of Cx45 was not detected. Calibration bar represent 20 μm.

ThA/Cx37

A

ThA/Cx40

B

ThA/Cx43

C

ThA/Cx45

D

CA/Cx37

E

CA/Cx40

F

CA/Cx43

G

CA/Cx45

H
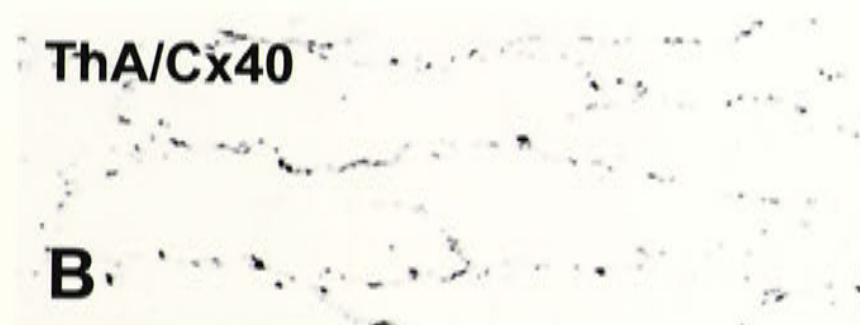
Figure 4.4

Figure 4.4.

Length (A), surface area (B), width (C) and perimeter (D) of endothelial cells from the Wistar rat thoracic aorta (ThA) and caudal artery (CA). Values are mean ± SEM. $^*P<0.05$, significantly different from the ThA. n=4 animals.
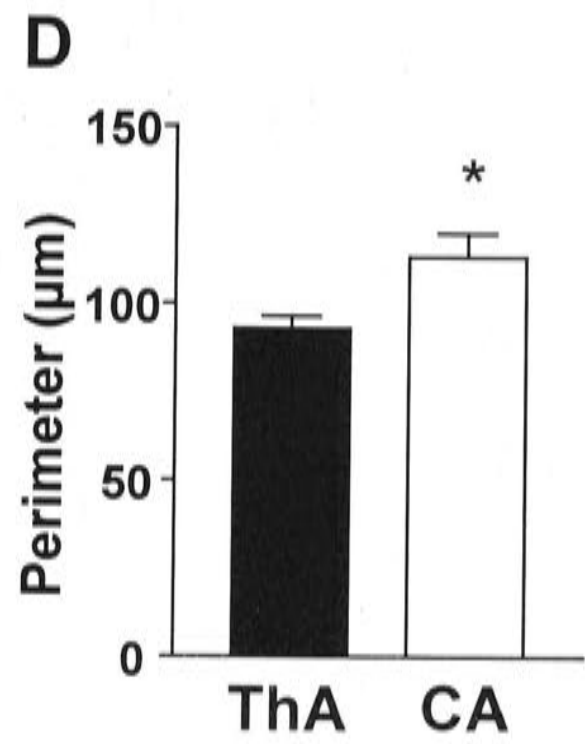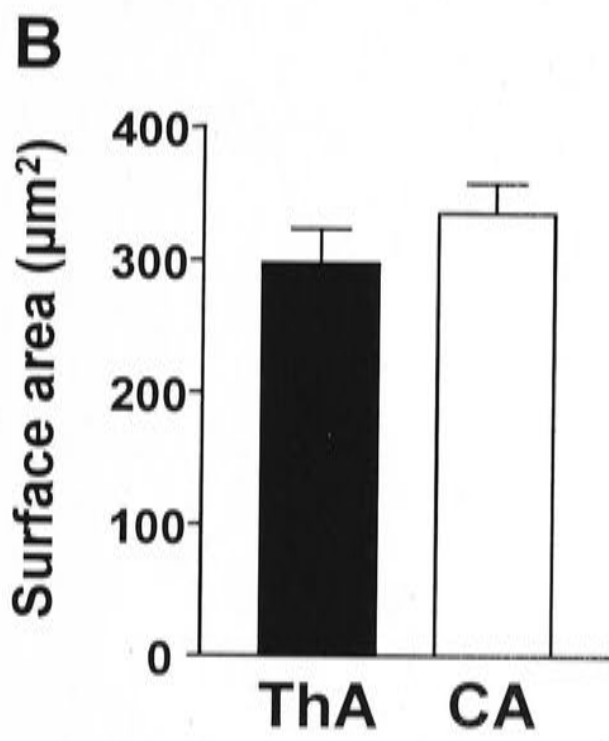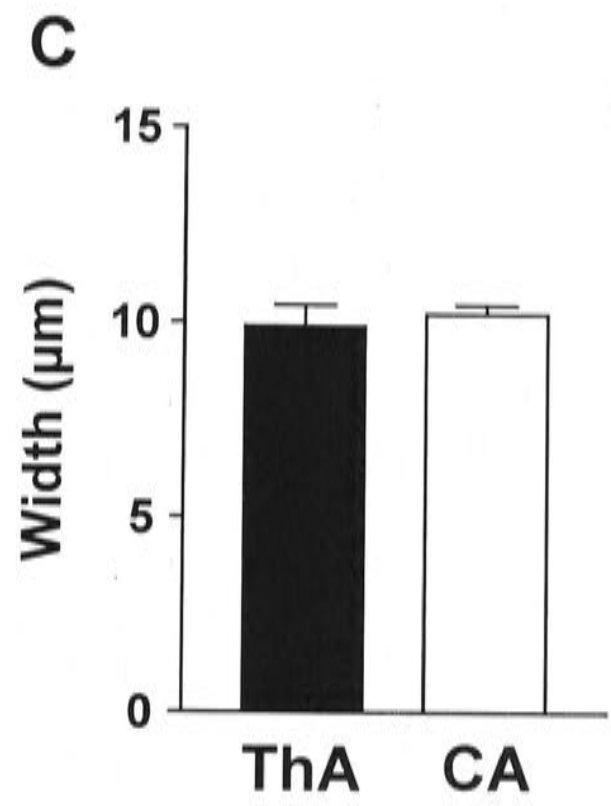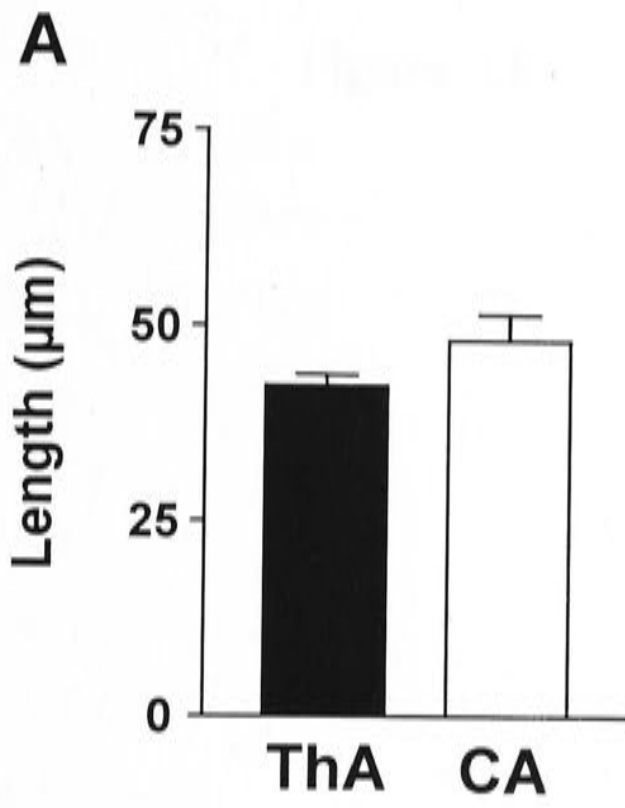
Figure 4.5

Figure 4.5.

Protein expression for Cxs 37, 40, 43 and 45 in the endothelium of the Wistar rat thoracic aorta and caudal artery. Values are expressed as Cx plaques per endothelial cell (A) and as the density of Cx plaques per 100 µm of endothelial cell perimeter (B). Values are mean ± SEM. *$P<0.05$, significantly different from Cx expression in the caudal artery. n=4 animals.

A

Cx plaques per endothelial cell

(Y-axis: 0, 20, 40, 60, 80, 100)

Cx37   Cx40   Cx43   Cx45

*

B

Cx plaques per 100 µm of cell perimeter

(Y-axis: 0, 20, 40, 60, 80, 100)

Cx37   Cx40   Cx43   Cx45

*
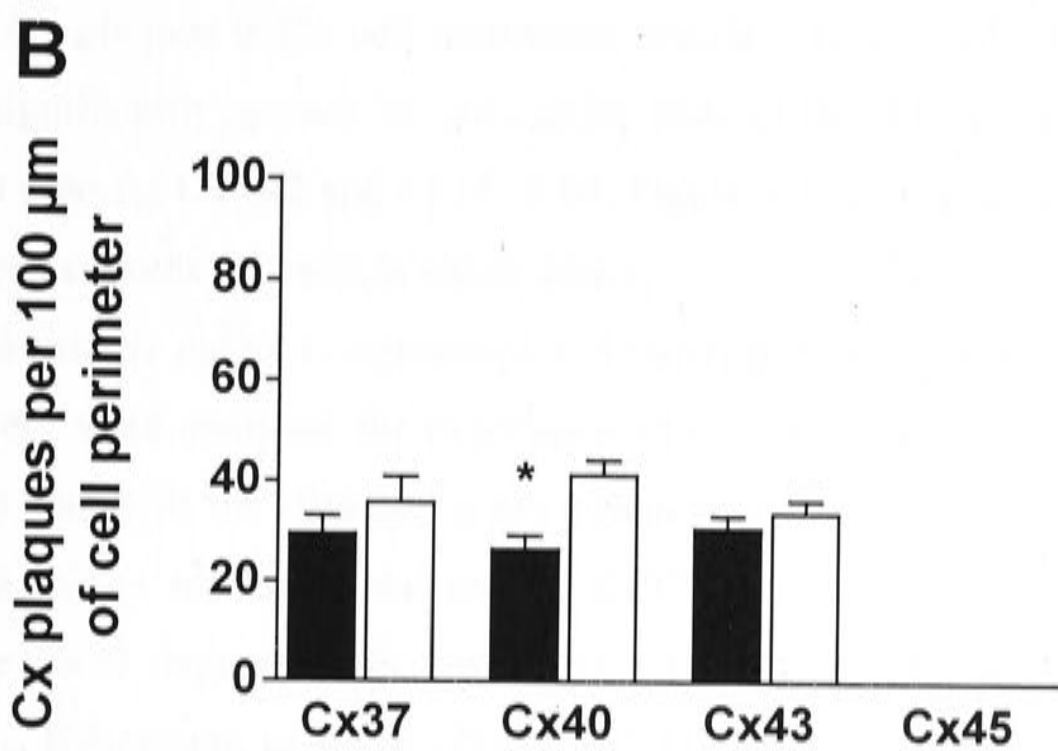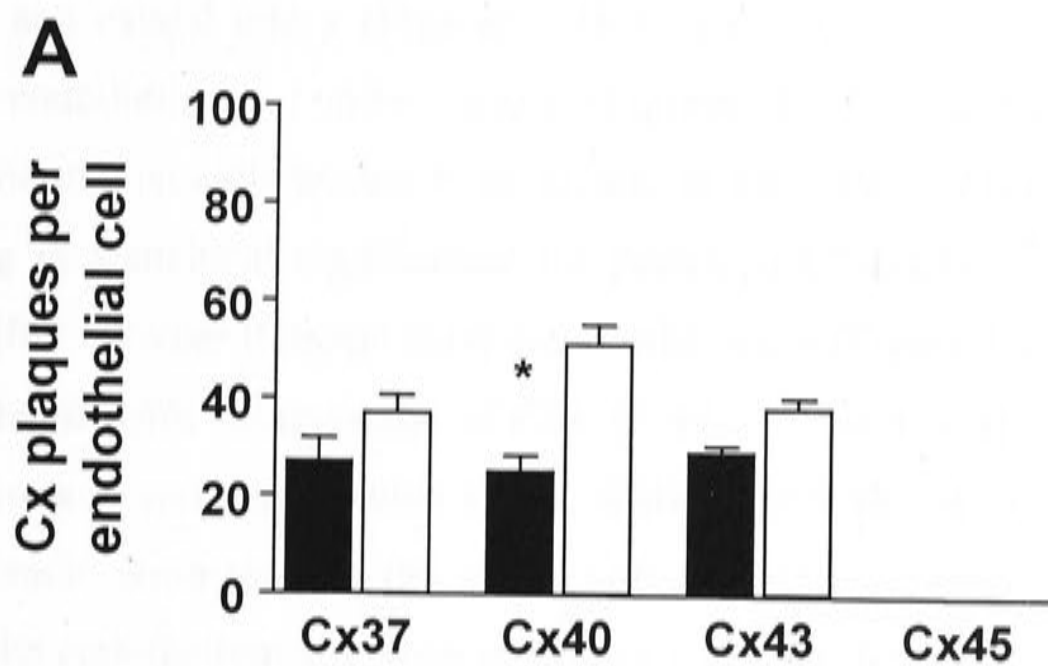
■ Thoracic aorta
□ Caudal artery

4.2.2 *Immunohistochemistry of vascular connexins*

For each of the Cx antisera used here, no staining at all was observed in the absence of the primary antibody or when the primary antibody was pre-incubated with the appropriate antigenic peptide

Morphology of endothelial cells. *En face* views of the luminal surface showed punctate staining for Cxs 37, 40 and 43 along the periphery of endothelial cells in both thoracic aorta and caudal artery (Figures 4.3A-C and E-G respectively). Cx45 was not found in the endothelium of either artery (Figures 4.3D). Surface area, length and perimeter of endothelial cells tended to be greater in the caudal artery than in the thoracic aorta, resulting in statisitical significance for perimeter ($P<0.05$). Width of endothelial cells did not differ between thoracic aorta and caudal artery (Figure 4.4).

Endothelial cells. Expression of Cxs 37 and 43 per endothelial cell was similar between the thoracic aorta and caudal artery, while expression of Cx40 was significantly less in the thoracic aorta than in the caudal artery ($P<0.05$, Figure 4.3, 4.5A). As Cx expression in the endothelium was seen exclusively around the cell periphery (Figure 4.3), the density of Cx plaques in the cell membrane was also calculated. The density of Cx40 plaques was significantly greater in the caudal than in the thoracic aorta while no such difference was seen for Cxs 37 and 43 ($P<0.05$, Figure 4.5B). Plaque sizes for each Cx did not vary between endothelial cells in either artery.

Smooth muscle cells. Longitudinal and transverse sections of the rat thoracic aorta and caudal artery were analysed for expression of Cxs 37, 40, 43 and 45. No significant difference was found in the data for either orientation for any of the four Cxs in either artery. In the media of the caudal artery, Cx37 was highly expressed (Figures 4.6E, 4.7A,B), while Cx37 expression in the thoracic aorta was very sparse ($P<0.05$, Figures 4.6A, 4.7A,B). Expression of Cx40 was absent from the media of both arteries (Figures 4.6B,F, 4.7A,B). Cx43 was abundantly expressed in the media of the thoracic aorta (Figures 4.6, 4.7A,B), but was absent from the media of the caudal artery (Figures 4.6G, 4.7A,B). Cx45 could be detected sparsely in the media of both caudal artery and thoracic aorta (Figures 4.6D,H, 4.7A,B). Double labelling experiments confirmed that Cx45 expression was located between adjacent smooth muscle cells (Figure 4.8).

Plaques of Cxs 37 and 45 in the media of the caudal artery and Cx45 in the thoracic aorta were significantly smaller than Cx43 plaques in the thoracic aorta ($P<0.001$, caudal artery: Cx37, 0.08 ± 0.003 μm; Cx45, 0.06 ± 0.001 μm; thoracic aorta: Cx43, 0.11 ± 0.01

59

Figure 4.6

Figure 4.6.

Cx expression in transverse sections of the Wistar rat thoracic aorta (ThA) (A-D) and caudal artery (CA) (E-H), incubated with antibodies against Cxs 37 (A, E), 40 (B, F), 43 (C, G) and Cx45 (D, H). e, endothelium, sm, smooth muscle. Calibration bar represents 10 μm.
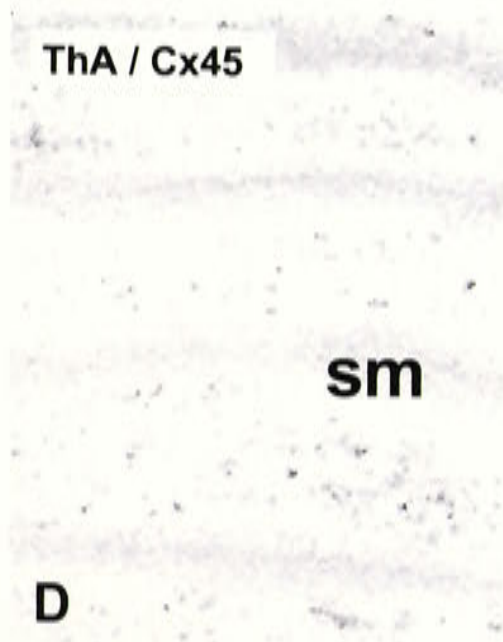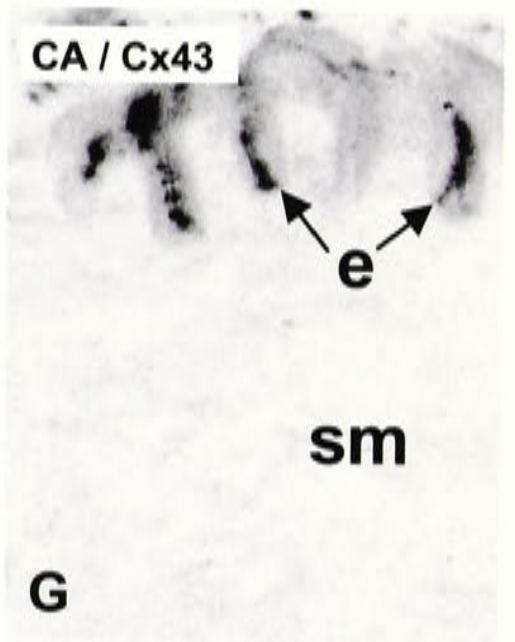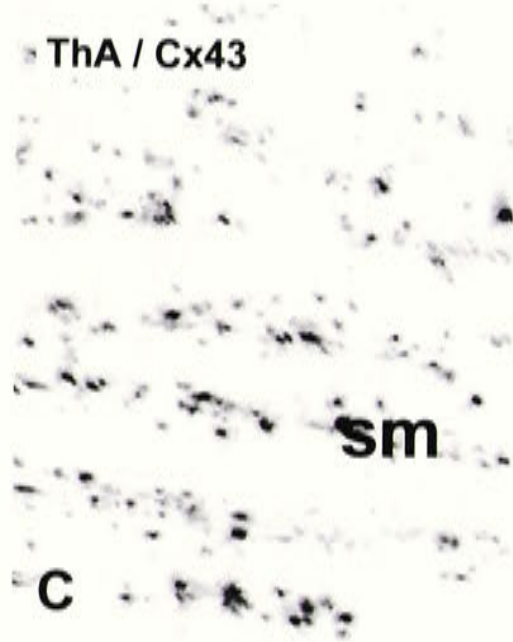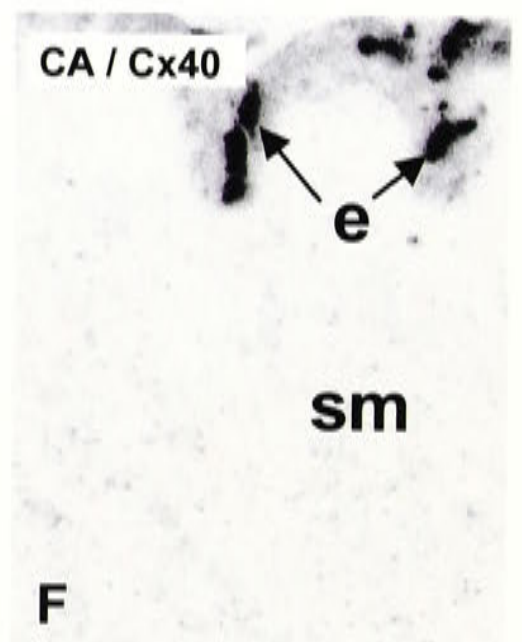
ThA / Cx37

e

sm

A

CA / Cx37

e

sm

E

ThA / Cx40

e

sm

B

CA / Cx40

e

sm

F

ThA / Cx43

sm

C

CA / Cx43

e

sm

G

ThA / Cx45

sm

D

CA / Cx45

sm

H
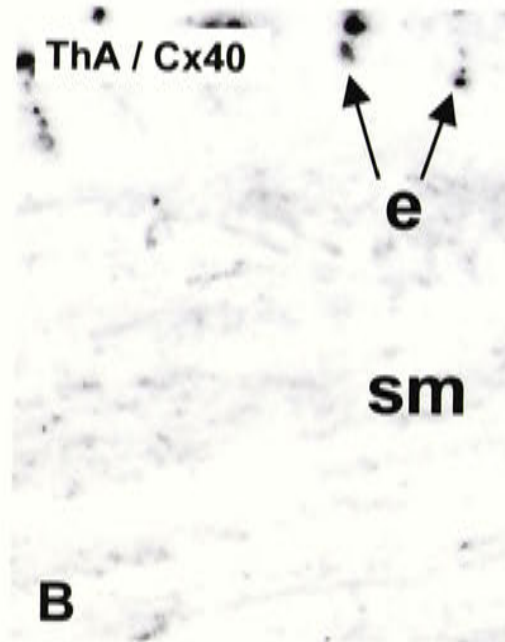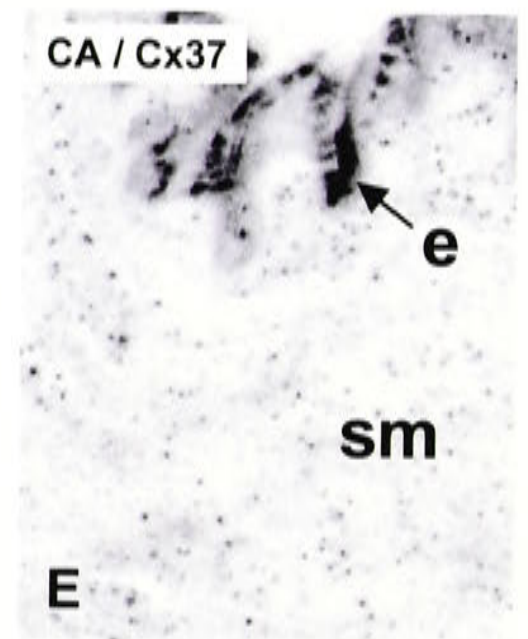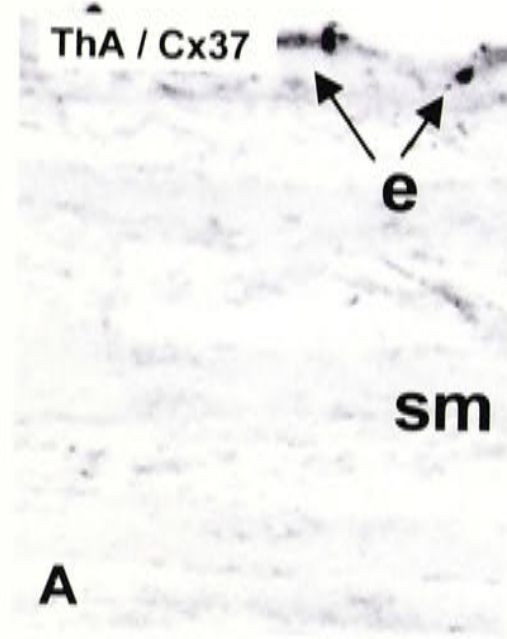
Figure 4.7

Figure 4.7.

Protein expression for Cxs 37, 40, 43 and 45 in the smooth muscle of the Wistar rat thoracic aorta and caudal artery. Values are expressed as plaques per μm^2 in longitudinal sections (A) and transverse sections (B). Values are mean ± SEM. [*]$P<0.05$, significantly different from Cx expression in the caudal artery. $n=4$ animals.

A

Plaques per μm²
Longitudinal sections

0.35
0.30
0.25
0.20
0.15
0.10
0.05
0.00

* *

Cx37   Cx40   Cx43   Cx45

B

Plaques per μm²
Transverse sections

0.35
0.30
0.25
0.20
0.15
0.10
0.05
0.00

* *

Cx37   Cx40   Cx43   Cx45
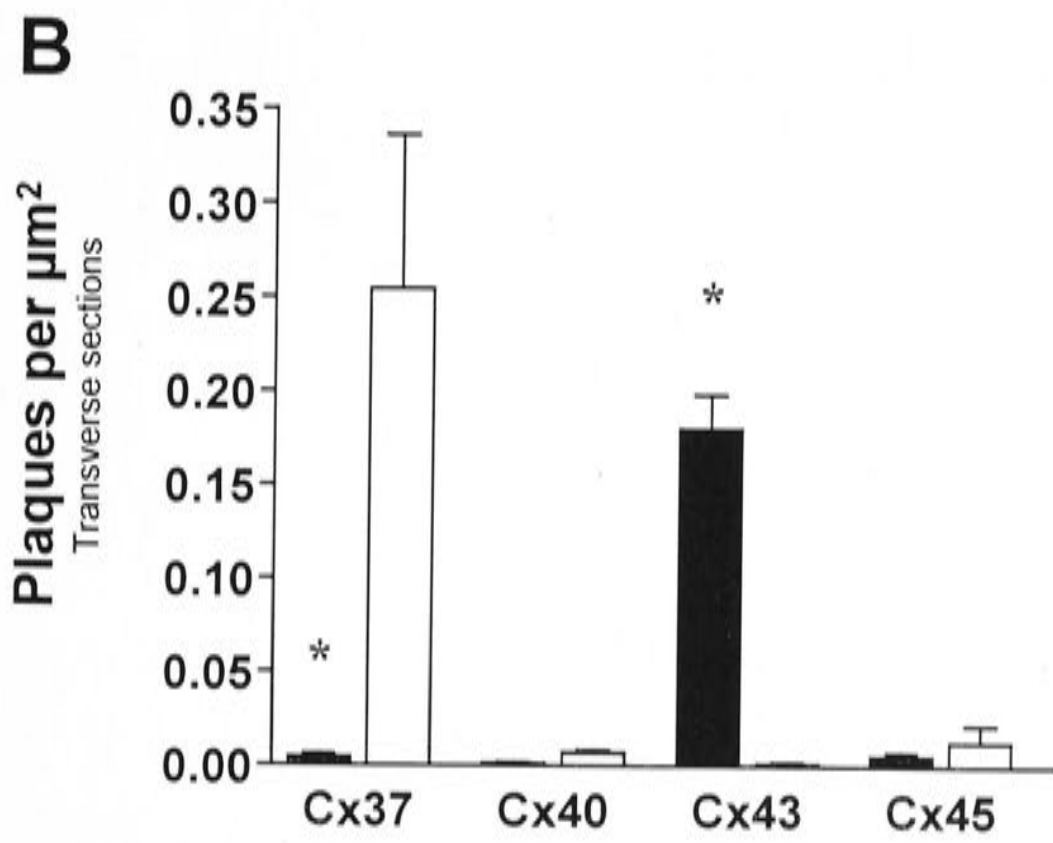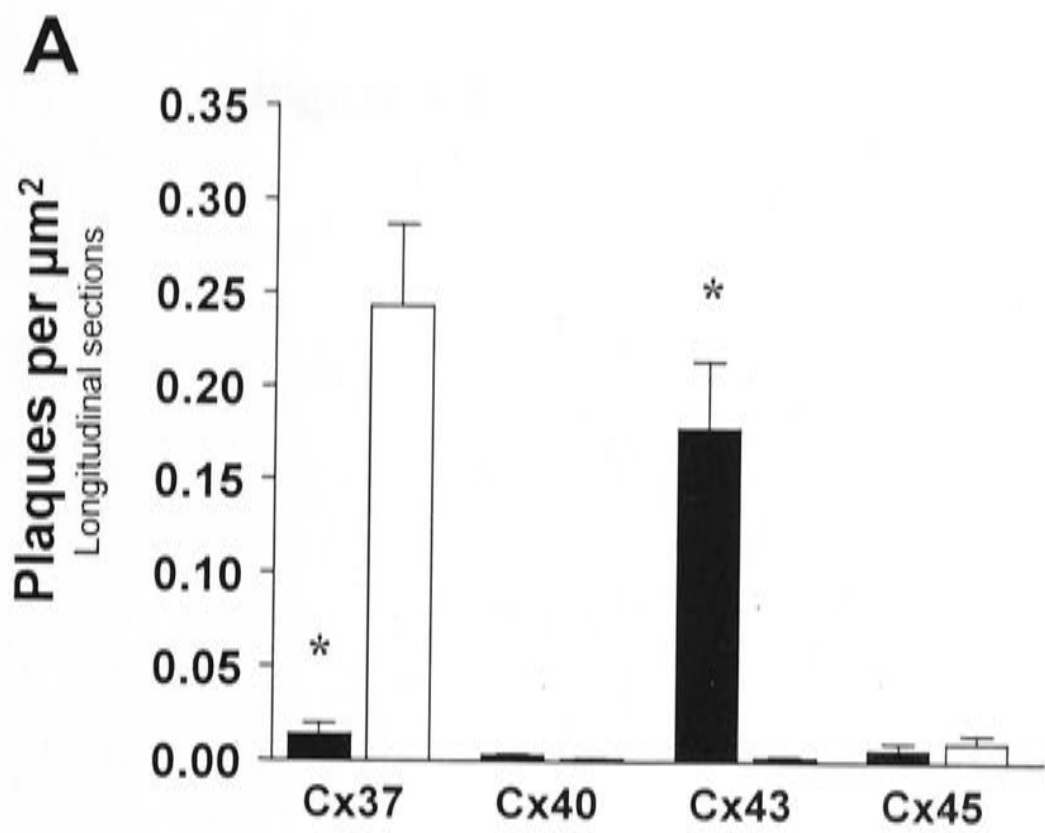
■ Thoracic aorta
□ Caudal artery

Figure 4.8

Figure 4.8.

Expression of Cx45 (green) and smooth muscle myosin (red) in the Wistar rat caudal artery. Smooth muscle myosin specifically labels smooth muscle cells, while Cx45 labelling appears between adjacent smooth muscle cells. Calibration bar represents 10 μm.
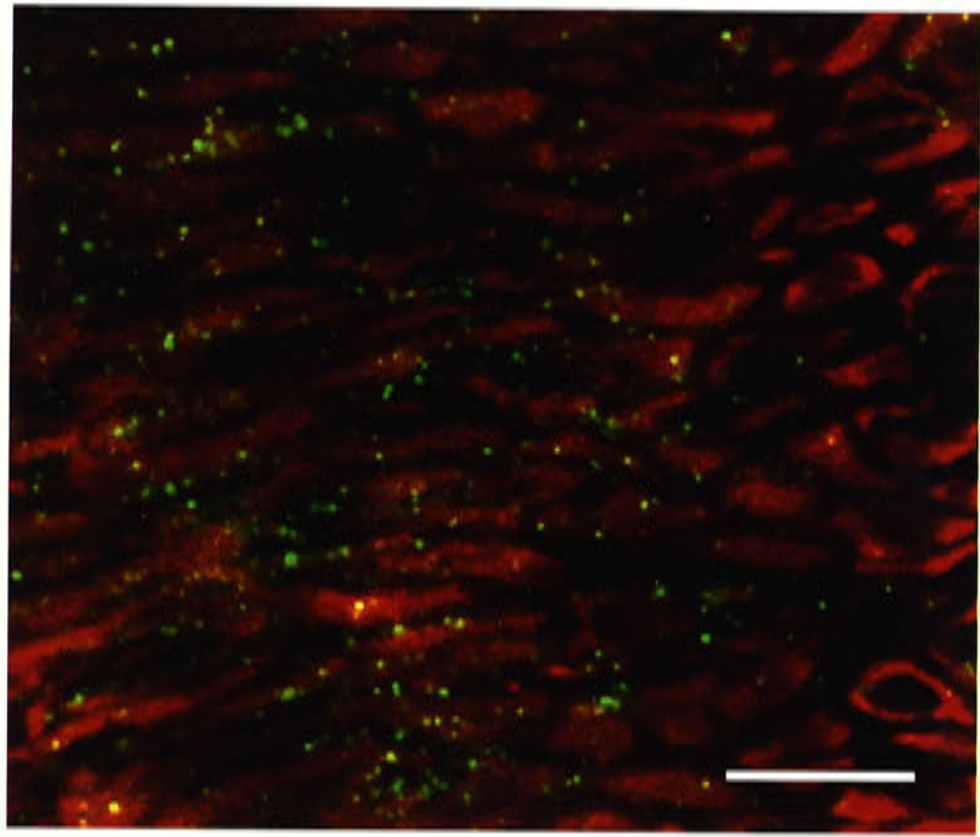
μm; Cx45, 0.06 ± 0.004 μm). Similarly, in the caudal artery, Cx37 plaques between endothelial cells were significantly larger than plaques between smooth muscle cells ($P<0.0001$, endothelial cells: 0.15 ± 0.01 μm, smooth muscle cells: 0.08 ± 0.003 μm), while in the thoracic aorta, plaques for Cx43 were greater in the endothelium than in the smooth muscle ($P<0.001$, endothelial cells: 0.14 ± 0.01 μm, smooth muscle cells: 0.11 ± 0.01 μm).

4.2.3   *Western blotting of vascular connexins*

Rabbit Cx43 antibodies revealed the presence of multiple isoforms of Cx43 in Western blots of extracts of caudal artery and ThA (Figure 4.9A,B), with the higher molecular weight isoforms appearing to predominate in the ThA (Figure 4.9B). All isoforms were blocked by pre-incubation of the Cx43 antibody with immunogenic peptide (Figure 4.9A, +peptide). Cx43 was only detectable in extracts of CA when 10 μg of protein was loaded on the gel (Figure 4.9B), but not when 5 μg was used (Figure 4.9A). Quantification of Cx43 by phosphoimaging revealed that ThA contained at least nine times more Cx43 than the CA (data not shown). When samples of ThA and CA were treated with phosphatase, a shift in mobility towards the lower molecular weight form was found (see Figure 3.4B), confirming that the high molecular weight forms were phosphorylated Cx43.

4.3   DISCUSSION

Significant differences have been found in the Cx make-up of the media, but not the endothelium of an elastic and a muscular artery of the rat using real time PCR and immunohistochemistry. In the caudal artery, mRNA for Cx37 was the most prevalent of the four Cxs and immunohistochemically demonstrable staining was found in the media of that artery but not to any great extent in the thoracic aorta. Using high-resolution confocal microscopy, a single fluorescent spot was defined as a gap junctional plaque, as validated previously (Green *et al.* 1993; Yeh *et al.* 1997b). On the other hand, mRNA for Cx43 was the most prevalent Cx in the thoracic aorta and greatly exceeded expression of Cx43 in the caudal artery. In similar fashion, the specific activity of Cx43 protein on Western blots was significantly greater in the aorta than in the caudal artery, in agreement with the extensive punctate staining in the aortic media and absence in the caudal artery as described previously (Hong & Hill, 1998). In the endothelium, protein for Cxs 37, 40 and 43 was detected in both vessels, as was Cx45 in the media of the two vessels. These data strongly

Figure 4.9

Figure 4.9.

Expression of Cx43 in tissue extracts from the Wistar rat thoracic aorta (ThA) and caudal artery (CA). 5 µg (A) and 10 µg (B) were run on 8% SDS PAGE gels and probed with antibodies to Cx43. Unphosphorylated and phosphorylated forms are indicated by arrows (- peptide). All forms disappeared when the antibody was pre-incubated with the immunogenic peptide (+ peptide).

A

CA ThA   CA ThA

Cx43 * ⇒   —66—

—45—

—30—

- peptide   + peptide

B

CA ThA

—66

Cx43 ** ⇛   —45

*

—30

- peptide

suggest that the predominant Cx connecting smooth muscle cells in the caudal artery is Cx37, in contrast to the aorta where the predominant Cx is confirmed to be Cx43, Cx45 playing a minor role in both arteries.

Although the mRNA preparations of both arteries included smooth muscle cells and endothelial cells, the predominant cell type was the smooth muscle cell as our ultrastructural studies have demonstrated that there are seven or more layers of smooth muscle cells surrounding the single layer of endothelial cells in the two vessels (see Chapter 5). Thus when protein expression for each of the Cx subtypes in the media of the two arteries was compared with the mRNA expression in the vessels, a good correlation was found for all four Cxs in both arteries. In contrast, in cultured smooth muscle cells from preglomerular arterioles of the rat, only Cx40 protein was detected in spite of mRNA expression for Cxs 37, 40 and 43 (Arensbak et al. 2001). While Cx40 protein was also found in sections of preglomerular arterioles in vivo, no mRNA analyses of this and other Cxs were performed (Arensbak et al. 2001). In preliminary experiments for the present study, attempts were made to rub off the endothelium in order to attribute mRNA for specific Cx isoforms to specific cellular layers. Unfortunately, these experiments were not entirely successful, as real time PCR showed that expression of mRNA for the endothelial cell marker von Willebrand factor could still be detected in these "endothelium–denuded" preparations.

While Cx37 was extensively expressed in the media of the caudal artery, it was effectively absent from the media of the thoracic aorta. These results are in agreement with van Kempen et al. (1999) who failed to find any Cx37 labelling in the aorta of several species but in contrast to studies by Nakamura et al. (1999) who described the presence of Cx37 in the smooth muscle of the rat aorta and pulmonary artery. However, the authors did not define which region of the aorta was used and since expression of other Cxs has been shown to vary along the length of the aorta (Hong & Hill, 1998; Ko et al. 2001), it may be difficult to directly compare the results. In the caudal artery, expression of mRNA for Cx37 was 10 fold greater than in the thoracic aorta, in line with the observed staining within the muscle layers. In the same species, Cx37 has also been identified in the media of large coronary arteries (van Kempen & Jongsma, 1999), perhaps suggesting a more widespread role for Cx37 in cell coupling in the media of large muscular arteries of the rat.

In the present study, Cx40 was not detected in the media of either the aorta or caudal arteries or in rat mesenteric arterioles as described by Gustafsson et al. (2003).

These results are in contrast to several previous studies, which have described Cx40 in the media of blood vessels from several species, including preglomerular and pial arterioles of the rat (Little *et al.* 1995; Arensbak *et al.* 2001), hamster cremaster muscle arterioles (Little *et al.* 1995), and coronary arteries from the cow, pig and rat (van Kempen & Jongsma, 1999). Taken together, these results may suggest a greater role for Cx40 in smaller vessels, supporting the idea that heterogeneity exists in the expression of Cxs within different parts of the vascular tree.

In the thoracic aorta, Cx45 was relatively sparsely expressed in contrast to the dense expression of Cx43. A reciprocal relationship between these two Cxs was found throughout the aortic vessels to the iliac artery (Ko *et al.* 2001). In the caudal artery, double labelling with antibodies against smooth muscle myosin showed Cx45 between smooth muscle cells, and using real time PCR, expression was similar to that in the thoracic aorta. The greater expression of Cx37 than of Cx45 in the caudal artery suggests that Cx37 may share a similar inverse relationship to Cx45 in the media of the caudal artery. Alternatively, expression of the two Cxs may have implications for radial versus longitudinal coupling of smooth muscle cells. Recent dye coupling studies in the caudal artery from our lab (Sandow *et al.* 2002) have shown selective spread of lucifer yellow dye between smooth muscle cells in the radial, but not the longitudinal direction. However, in the present study, in the media of both arteries, protein expression of Cxs 37 and 45 did not differ between longitudinal and transverse orientations.

As previously demonstrated, protein for Cxs 37, 40 and 43 was expressed in the endothelium of both the thoracic aorta and caudal artery (Yeh *et al.* 1997a), while expression of Cx45 was not detected in the endothelium of either artery (Krüger *et al.* 2000; Ko *et al.* 2001). Staining was essentially confined to the intercellular borders. In the endothelium of the caudal artery, expression of Cx40 was significantly greater than in the thoracic aorta, while expression of Cxs 37 and 43 was not significantly different between the two arteries. Studies by Gabriels & Paul (1998) have shown that Cx43 expression within the endothelium of the rat thoracic aorta is heterogeneous in distribution, with staining particularly restricted to areas of aortic bifurcation and to small clumps of cells away from bifurcations. In contrast, in the present study the distribution of Cx43 expression was found to be homogenous. This discrepancy is likely to result from the area of aorta examined or the affinity of the antibodies used. Morphological measurements demonstrated some differences in the shape of endothelial cells between the two arteries,

resulting in an increase in cell perimeter in the caudal artery relative to that in the thoracic aorta. In spite of this increase in cell perimeter, the density of Cx40 plaques was still significantly greater in the caudal artery than in the thoracic aorta.

As discussed by Severs *et al.* (2001), the definitive identification of Cx protein localized at a gap junction requires electron microscopy, as gap junction channels are too small to be viewed at the light microscope level. Thus, while clear evidence demonstrating the expression pattern of each Cx has been presented, future experiments involving immunogold electron microscopy would confirm the result presented in this here.

The data presented in this Chapter have demonstrated that Cx37 is the major Cx expressed in the media of the caudal artery, while Cx43 predominates in the thoracic aorta. The sparse expression of Cx45 suggests that it plays a minor role in the media of both arteries, while Cx40 is not expressed in the muscle of either vessel. In contrast, three Cxs are expressed in the endothelium of both vessels and, of these Cx40 is more prevalent in the caudal artery than in the thoracic aorta.

CHAPTER 5

CONNEXIN EXPRESSION AND VASCULAR REMODELING IN THE RAT THORACIC AORTA AND CAUDAL ARTERY DURING HYPERTENSION

5.1   INTRODUCTION

In hypertension, an increase in total peripheral resistance gives rise to the increase in blood pressure that is characteristic of the disease (Mulvany & Aalkjaer, 1990). Increased peripheral resistance is accompanied by structural remodeling of the blood vessel wall, of which several categories have been described. Hypertrophic remodeling results in a decrease in luminal diameter and hypertrophy of the vascular smooth muscle, which may arise from changes in the morphology or number of smooth muscle number cells (Mulvany *et al.* 1996; Dickhout & Lee, 1999, 2000; Intengan & Schiffrin, 2000; Touyz, 2000). Eutrophic remodeling occurs when both the outer and luminal diameters of the blood vessel are decreased. In this type of remodeling, changes in the medial layer arise from the rearrangement of existing smooth muscle cells around the smaller lumen (Baumbach & Heistad, 1989; Intengan & Schiffrin, 2000). In the SHR, blood vessels have been shown to undergo both hypertrophic (Sandow *et al.* 2003b) and eutrophic remodeling (Mulvany *et al.* 1996), fuelling suggestions that the type of remodeling may vary according to the vascular bed examined. In contrast, little is known regarding the morphological changes that may occur in vascular endothelial cells during hypertension. Most data has been confined to the thoracic aorta. As reviewed in Chapter 1, the results of these studies show that both increases and decreases in endothelial cell size and density can occur depending on the vascular bed and the model of hypertension examined (Gabbiani *et al.* 1979; Hüttner *et al.* 1979, 1982; De Chastonay *et al.* 1983; Kowala *et al.* 1988; Arribas *et al.* 1997).

Gap junctional coupling of adjacent cells in the endothelial and smooth muscle cell layers is essential for the coordination of vasomotor responses. However, despite the extensive literature demonstrating cellular remodeling within hypertensive vessels, little is known regarding Cx expression in the blood vessels of hypertensive rat models. As discussed in Chapter 1, most studies have concentrated on Cx43 expression in the aorta of

the rat where increased or decreased Cx expression have been described, depending on the model of hypertension examined (Watts & Webb, 1996; Haefliger *et al.* 1997a,b, 1999, 2001; Haefliger & Meda, 2000). This is surprising given that the aorta is a large elastic artery and is thus not directly involved in the maintenance of peripheral resistance (Mulvany & Aalkjaer, 1990). Such studies are therefore unlikely to be relevant to elucidating the mechanisms associated with the etiology of diseases such as hypertension. Recent studies by Li & Simard (2002) have examined Cxs 43 and 45 in cerebral and systemic vessels of SHR and L-NAME induced hypertensive rats and suggest that changes in Cx expression during hypertension may vary depending on the specific Cx, the vascular bed, the particular model of hypertension and the method employed for analysis. Whether the changes observed in their study were confined to one cell layer or involved both smooth muscle and endothelial cells is not known. Indeed, no studies have focused on Cx expression in endothelial cells during hypertension.

Together with structural changes in the blood vessel wall, hypertension is also associated with endothelial dysfunction, characterised by the altered production and action of vasoactive factors, which include vasodilators such as NO, prostaglandins and EDHF (Mombouli & Vanhoutte, 1999; Shimokawa, 1999). Indeed, several studies have shown a reduction in both NO and EDHF-mediated hyperpolarization in the coronary and mesenteric arteries of the SHR and SHR-SP (Fujii *et al.* 1992; Sunano *et al.* 1999; Vazquez-Perez *et al.* 2001). In contrast, studies in mesenteric arteries of rats made hypertensive with a high salt diet, demonstrate an up-regulation of EDHF-mediated relaxation, while vasodilation to ACh is not altered, thus suggesting the loss of NO activity in this model of hypertension (Sofola *et al.* 2002). Given these results, it is apparent that the ability of an endothelial-derived factor to effect a smooth muscle cell response may be influenced by changes in the number of smooth muscle cell layers, the size of smooth muscle cells and cellular coupling within the media of hypertensive vessels. Indeed, this is of particular relevance for the effect of EDHF, whose action is dependent on gap junctions in many vascular beds (McGuire *et al.* 2001; Sandow *et al.* 2002). In a similar manner, altered morphology and coupling within the endothelial cell layer may further impact on the normal function of vasoactive factors within the blood vessel wall and thus contribute to the hypertension associated endothelial dysfunction.

Given the heterogeneous nature of vascular remodeling during hypertension and the nature of cellular coupling in different vascular beds as described in Chapter 4, the aim of

65

this Chapter is to investigate alterations in cell morphology and expression of the four vascular Cxs in the smooth muscle and endothelial layers of functionally different vessels in an individual model of hypertension. The thoracic aorta and the caudal artery were chosen as examples of elastic and muscular arteries, respectively as described in the previous Chapter. Structural changes observed here in the caudal artery have also been correlated with electrophysiological studies of cell coupling in the media and the action of the vasodilatory factors NO and EDHF during hypertension.

5.2 RESULTS

5.2.1 Blood pressure

A significant increase in systolic blood pressure in the SHR (n=4-15) compared with WKY (n=4-8) was first seen at 9 weeks of age ($P<0.05$, WKY, 121 ± 3.8; SHR, 162 ± 6.7 mmHg) and blood pressure continued to rise until approximately 11-12 weeks of age after which time blood pressure values reached a plateau ($P<0.05$, WKY, 125 ± 3.8; SHR, 193 ± 7.5 mmHg at 12 weeks; Figure 5.1). 12-week old rats were therefore chosen for the subsequent studies.

5.2.2 Vessel morphology

There was no significant difference in luminal diameter, the number of smooth muscle cell layers, or the medial cross-sectional area between the thoracic aorta of WKY and SHR ($P>0.05$, Table 5.1). In the caudal artery, the luminal diameter was significantly smaller in the SHR compared to the WKY, while the number of smooth muscle cell layers and the medial cross sectional area were significantly larger (29% and 26%, respectively), in the SHR compared to the WKY ($P<0.05$, Table 5.1).

Smooth muscle cell morphology was determined in the caudal artery by measuring the surface area, length and width of cells following intracellular labelling with microelectrodes filled with FITC-dextran. The surface area of smooth muscle cells was not significantly different between WKY and SHR ($P>0.05$; WKY, 757 ± 41 μm^2; SHR, 782 ± 56 μm^2), however the length and width of smooth muscle cells differed significantly between the two strains ($P<0.05$, Figure 5.2A,B; length, 138 ± 4.4 μm for WKY, 171 ± 6.7 μm for SHR; width, 9.8 ± 0.5 μm for WKY, 8.1 ± 0.4 μm for SHR).

66

Figure 5.1

Figure 5.1.

Systolic blood pressure of SHR and WKY measured weekly from 4 weeks of age. Values are mean ± SEM. $^*P<0.05$, significantly greater than age-matched WKY. n=4-15 animals.
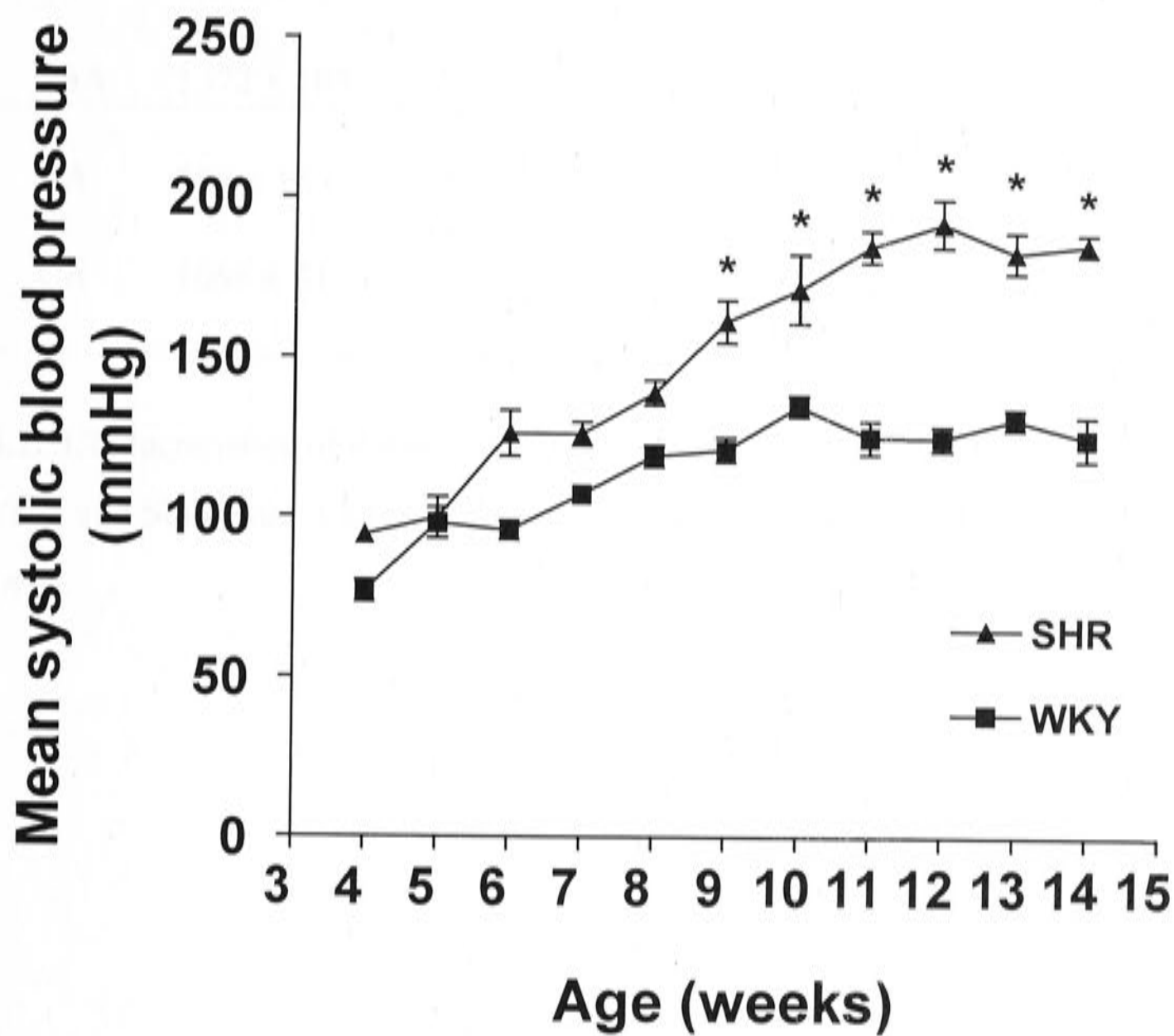
strain	vessel	luminal diameter (μm)	smooth muscle layers	medial cross-sectional area (μm^2)
SHR	ThA	1503 ± 73	7.9 ± 0.1	375,323 ± 18,525
WKY	ThA	1372 ± 105	7.7 ± 0.3	274,186 ± 42,032
SHR	CA	889 ± 18*	8.8 ± 0.5*	51,943 ± 3,533*
WKY	CA	1088 ± 51	7.0 ± 0.3	41,035 ± 3,310

Table 5.1. Characteristics of the thoracic aorta (ThA) and caudal artery (CA) from 12 week WKY and SHR rats. Values are mean ± SEM. $^*P<0.05$, significantly different to WKY. $n=3$.

Figure 5.2
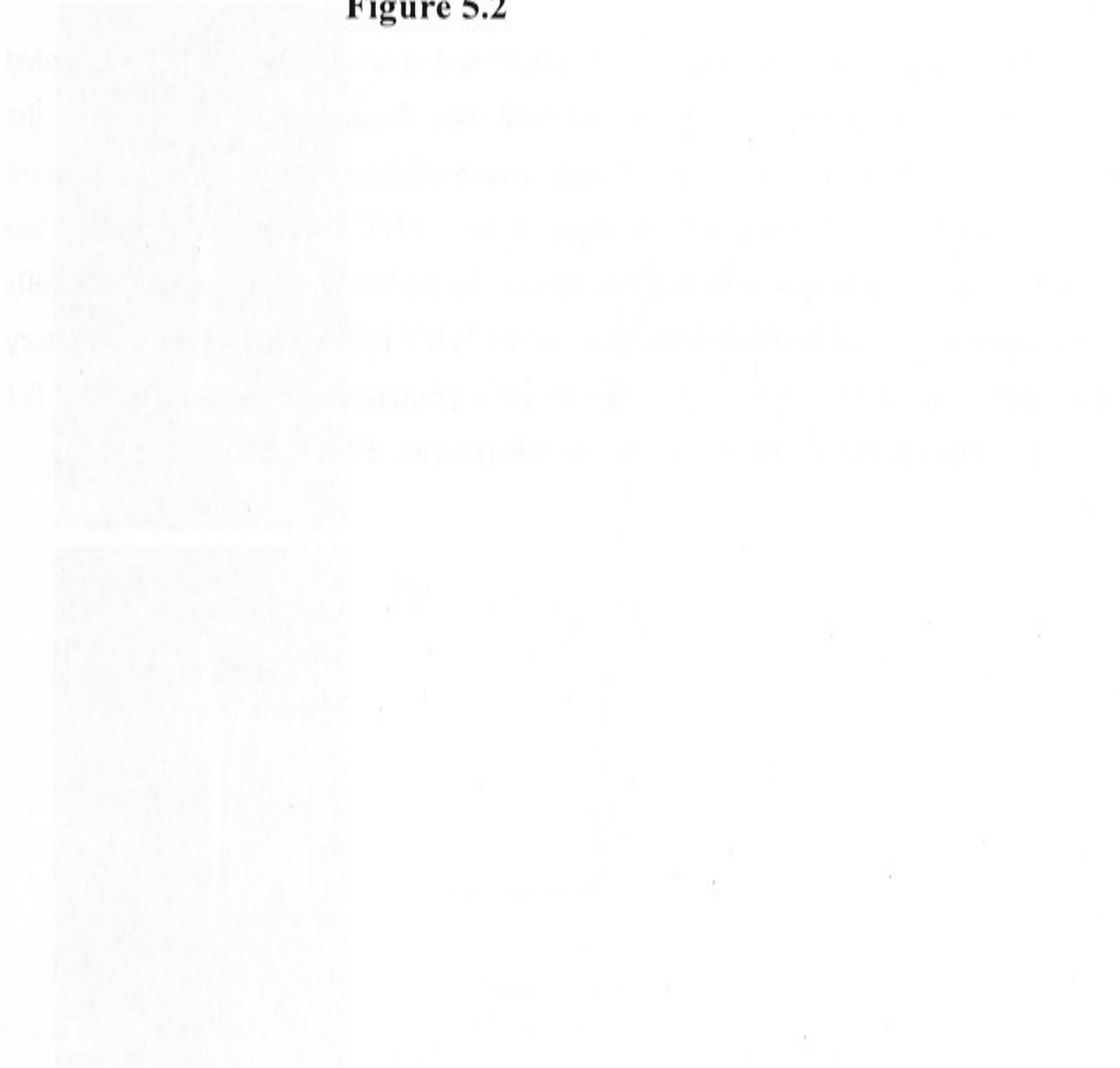
Figure 5.2.

Morphology of smooth muscle cells (A,B) and characteristics of EJPs recorded (C,D) from the caudal artery of WKY and SHR rats. Smooth muscle cells from the WKY (A) and SHR (B) impaled during electrophysiological experiments were positively identified following the injection of 10% FITC-dextran. Calibration bar represents 50 μm. Membrane potential recordings were taken from smooth muscle cells at the adventitial (a) and luminal (b) borders of the WKY (C) and SHR (D). Excitatory junction potentials (EJPs) were evoked by a single supramaximal stimulus (100 mA, 0.1 ms; arrow). Resting membrane potential, -60 mV (C) and -57 mV (D).

C WKY

a

b

D SHR

a

b

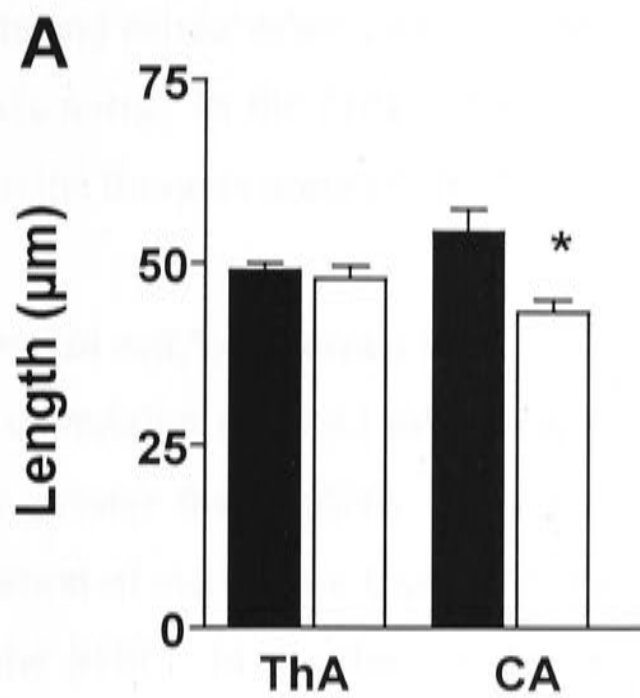5 mV

100 ms

Neural stimulus
(100 mA, 0.1 ms)
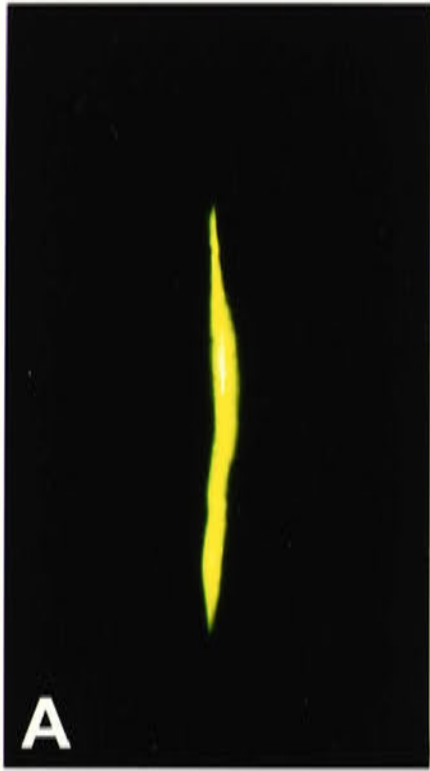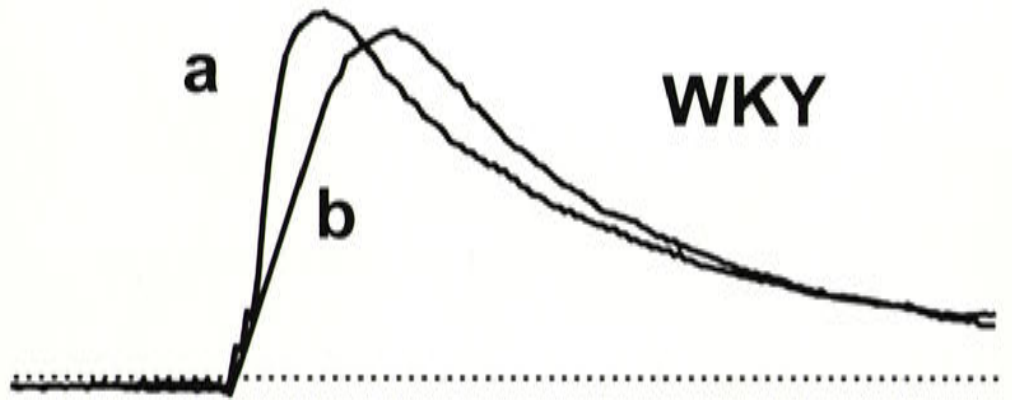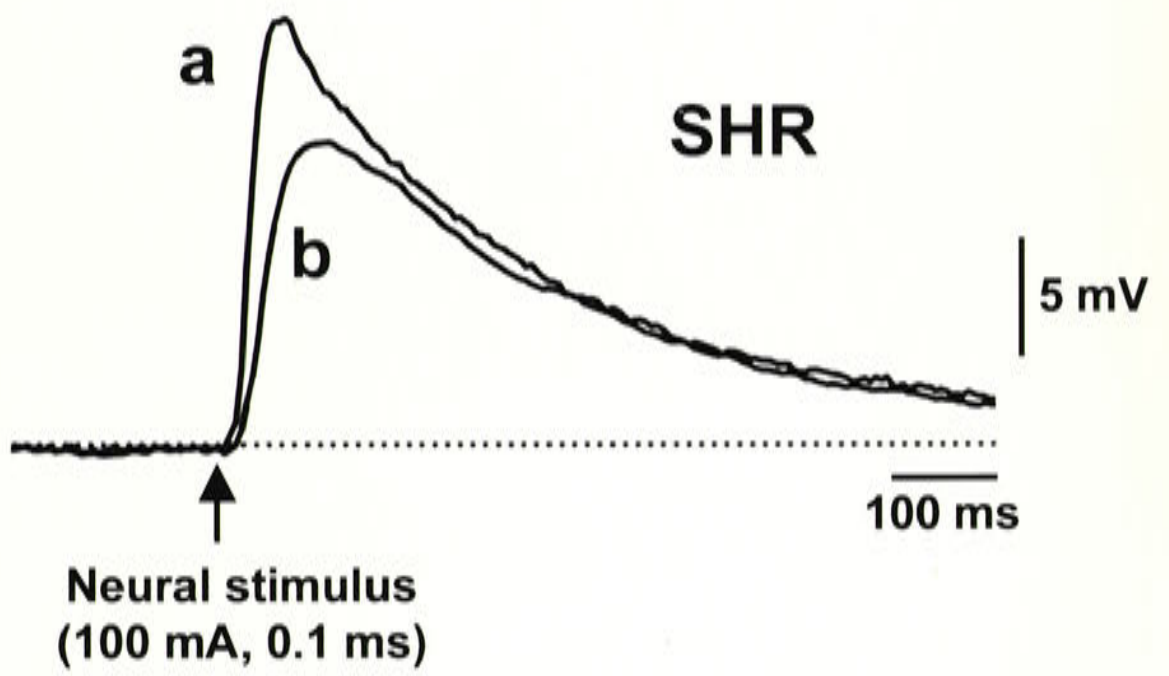
Figure 5.3

Figure 5.3.

Length (A), surface area (B), width (C) and perimeter (D) of endothelial cells from the WKY and SHR thoracic aorta (ThA) and caudal artery (CA). Values are mean ± SEM. *$P<0.05$, significantly different from WKY. n=4-5 animals
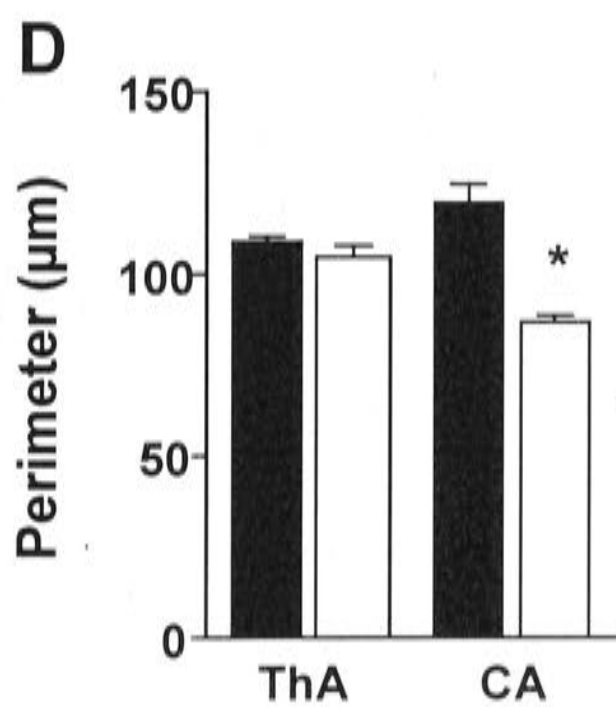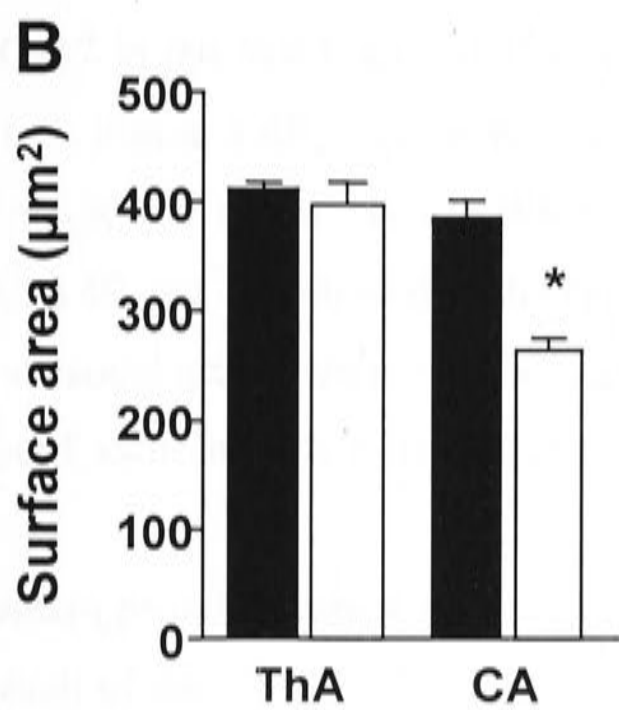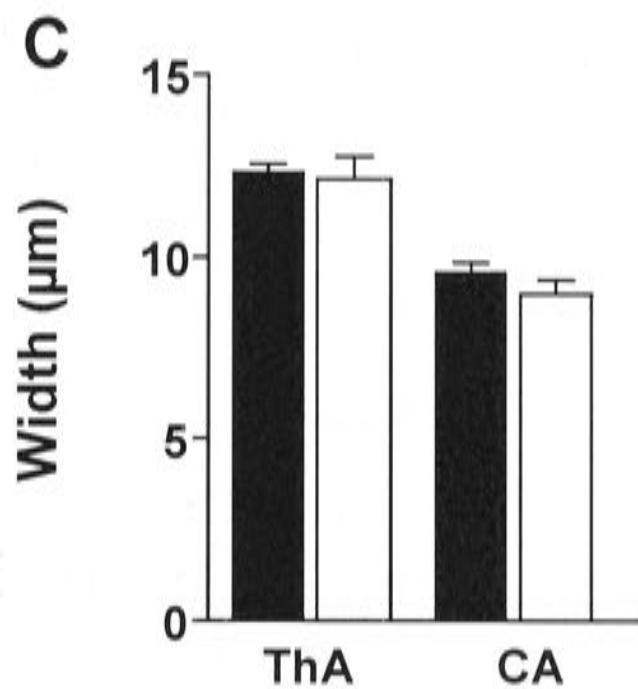
Endothelial cell morphology, as measured by surface area, length, width and perimeter, was not significantly different between WKY and SHR in the thoracic aorta (Figure 5.3). However, in the caudal artery of the SHR, surface area, perimeter and length of endothelial cells were significantly less than in the WKY ($P<0.05$, Figure 5.3). In the WKY, surface area, length and perimeter of endothelial cells was similar in both the thoracic aorta and caudal artery, while width was significantly less in the caudal artery than in the thoracic aorta. In the SHR, all four parameters were significantly less in the caudal artery than in the thoracic aorta ($P<0.05$, Figure 5.3).

5.2.3   Connexin mRNA expression

The expression of Cx43 mRNA in the thoracic aorta in both WKY and SHR was significantly greater than mRNA expression for Cxs 40 and 45 ($P<0.05$, Figure 5.4A), while expression of mRNA for Cx43 was also significantly greater than Cx37 in the WKY, but not in the SHR. In the thoracic aorta, mRNA expression for Cxs 43 and 45 were significantly less in the SHR compared to the WKY ($P<0.05$, Figure 5.4A), while mRNAs for Cxs 37 and 40 were similar in both WKY and SHR. In the caudal artery, expression of mRNA for Cx37 in the WKY and SHR was significantly greater than mRNA for Cxs 40 and 43 ($P<0.05$, Figure 5.4B). There was no significant difference between the expression of mRNA for Cxs 37 and 45 in the WKY or the SHR (Figure 5.4B). There was little mRNA for Cxs 40 and 43 detected in the caudal artery of either the WKY or SHR (Figure 5.4B). In the caudal artery, there was no significant difference between the expressions of any of the four Cxs in the WKY compared to the SHR (Figure 5.4B).

5.2.4   Connexin protein expression

For each of the Cx antisera used here, no staining was observed in the absence of the primary antibody or when the primary antibody was pre-incubated with the appropriate antigenic peptide.

Endothelial cells. *En face* views of the luminal surface of the thoracic aorta and caudal artery showed punctate staining for Cxs 37, 40 and 43 along the periphery of endothelial cells of both the WKY and SHR (Figure 5.5A-C, D-F and 5.6A-C, D-F, for thoracic aorta and caudal artery, respectively), while Cx45 was not detected in the endothelium of either artery (data not shown).

Figure 5.4

Figure 5.4.

    mRNA expression of Cxs 37, 40, 43 and 45 in the WKY and SHR thoracic aorta (A) and caudal artery (B). Copy numbers are expressed per copy of 18S ribosomal RNA by using plasmid standard curves. $^*P<0.05$, significantly less than WKY. $^\dagger P<0.05$, significantly less than the thoracic aorta. n=4-6 animals.
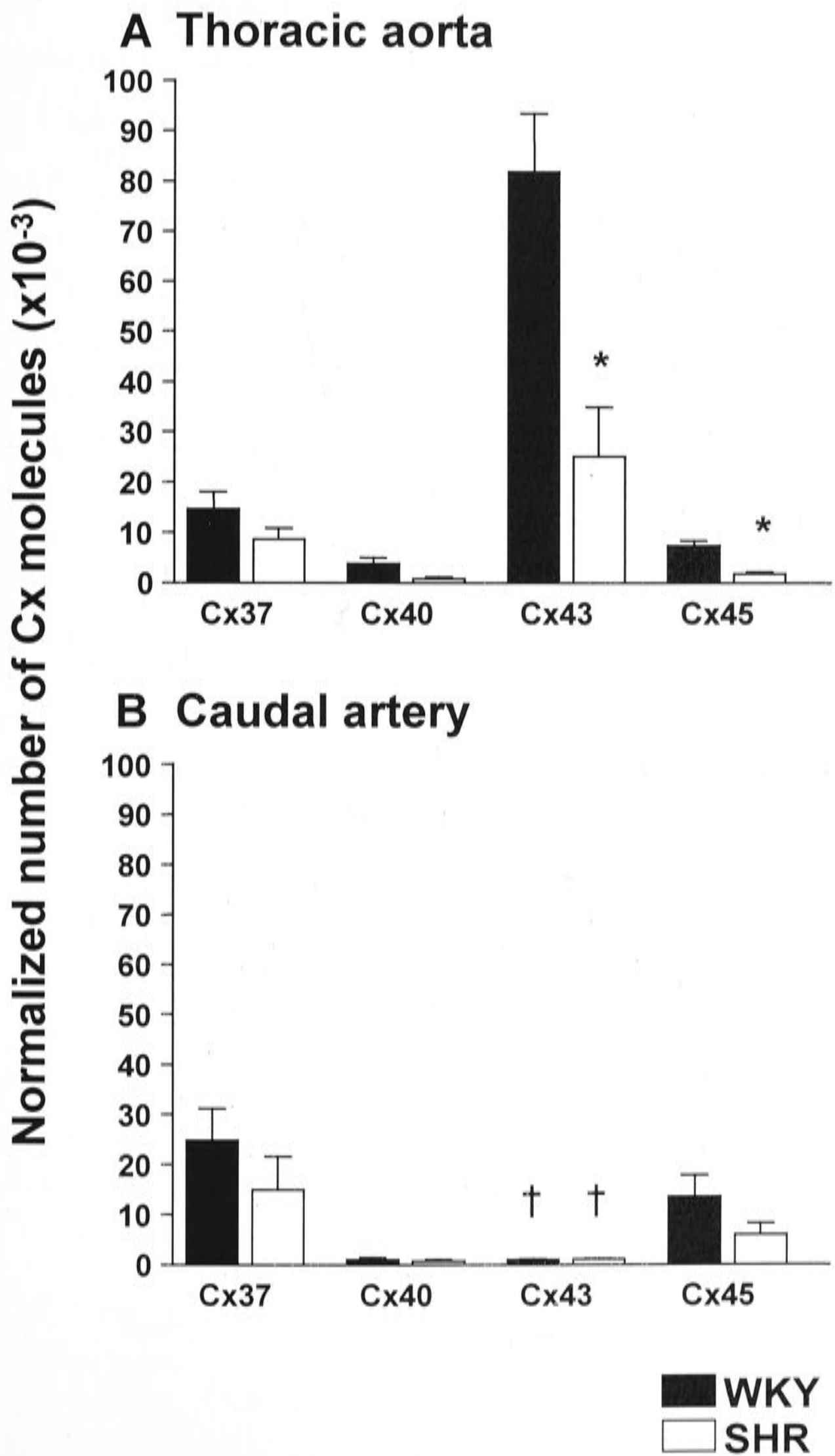
A Thoracic aorta

B Caudal artery

Normalized number of Cx molecules (x10^{-3})

WKY
SHR

Figure 5.5

Figure 5.5.

Cx expression in the endothelium of the thoracic aorta of the 12 week old WKY and SHR. The endothelium is viewed *en face* and is labelled with antibodies to Cx37 (A,D), Cx40 (B,E) and Cx43 (C,F). Labelling of Cxs 37, 40 and 43 is evident along the perimeter of endothelial cells. Calibration bar represents 20 µm.

WKY/Cx37　　　　　SHR/Cx37

A　　　　　　　　　D

WKY/Cx40　　　　　SHR/Cx40

B　　　　　　　　　E

WKY/Cx43　　　　　SHR/Cx43

C　　　　　　　　　F

Figure 5.6

Figure 5.6.

Cx expression in the endothelium of the caudal artery of the 12 week old WKY and SHR. The endothelium is viewed *en face* and is labelled with antibodies to Cx37 (A,D), Cx40 (B,E) and Cx43 (C,F). Labelling of Cxs 37, 40 and 43 is evident along the perimeter of endothelial cells. Calibration bar represents 20 μm.

WKY/Cx37   SHR/Cx37

A   D

WKY/Cx40   SHR/Cx40

B   E

WKY/Cx43   SHR/Cx43

C   F
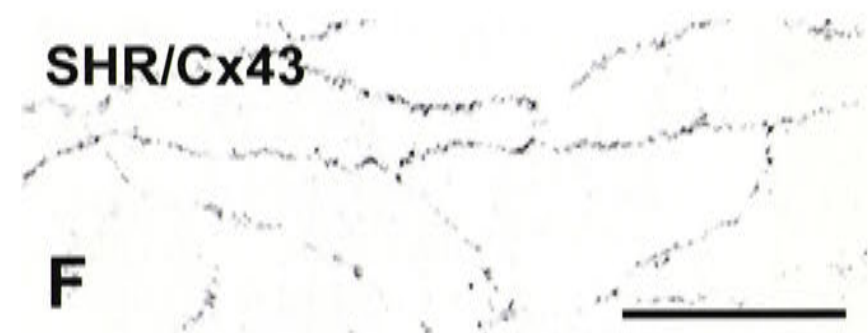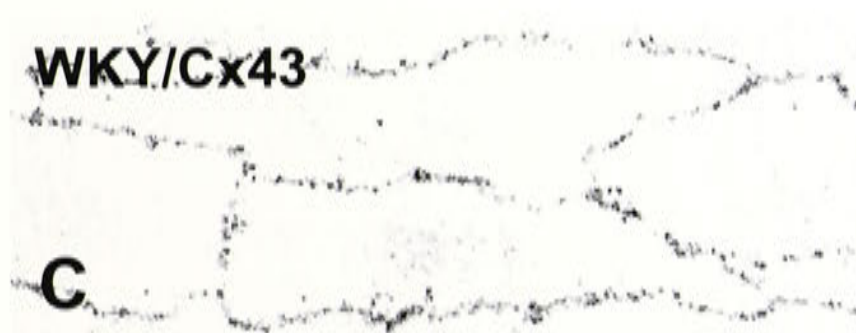
Figure 5.7

Figure 5.7.

   Expression of protein for Cxs 37, 40, 43 and 45 in the endothelium of the WKY and SHR thoracic aorta (A, C) and caudal artery (B, D). Cx plaques expressed per endothelial cell in the thoracic aorta (A) and caudal artery (B), and the density of Cx plaques per 100 μm of endothelial cell perimeter in the thoracic aorta (C) and caudal artery (D). Values are mean $\pm$ SEM. *$P<0.05$, significantly different from Cx expression in the WKY. n=4-5 animals.

A Thoracic aorta

B Caudal artery

C Thoracic aorta

D Caudal artery

Cx plaques per endothelial cell

Cx plaques per 100 µm of cell perimeter

Cx37 Cx40 Cx43
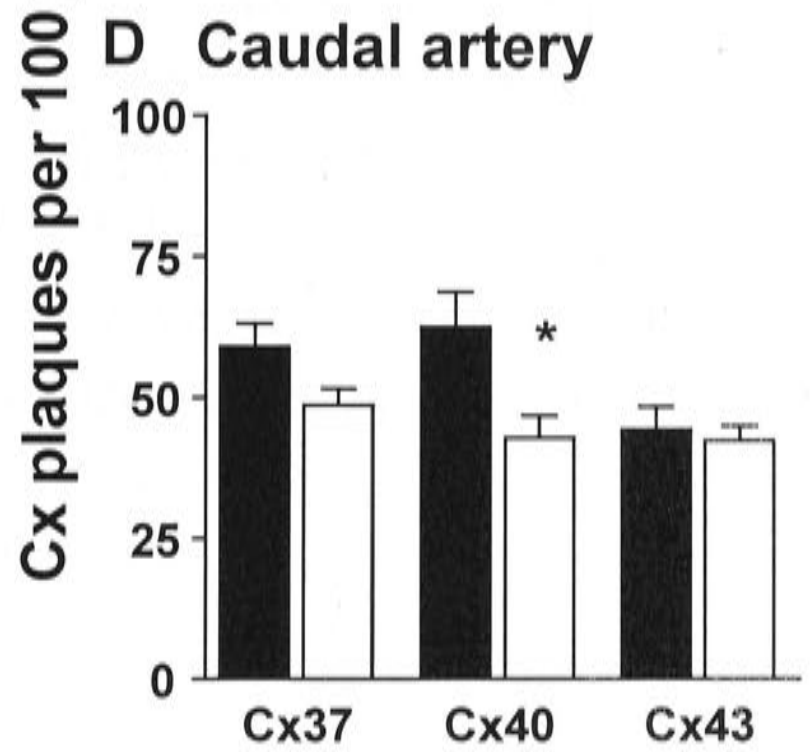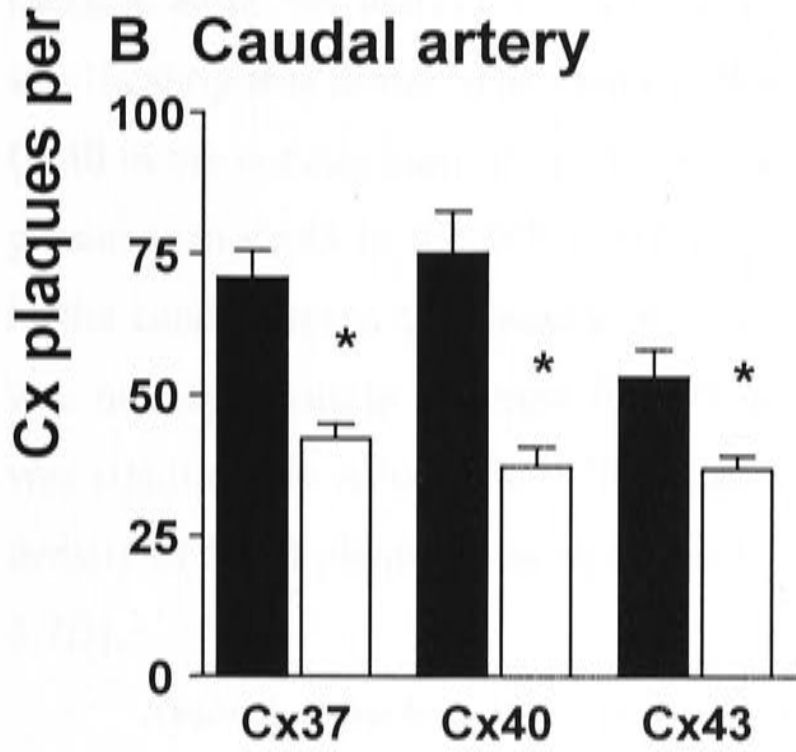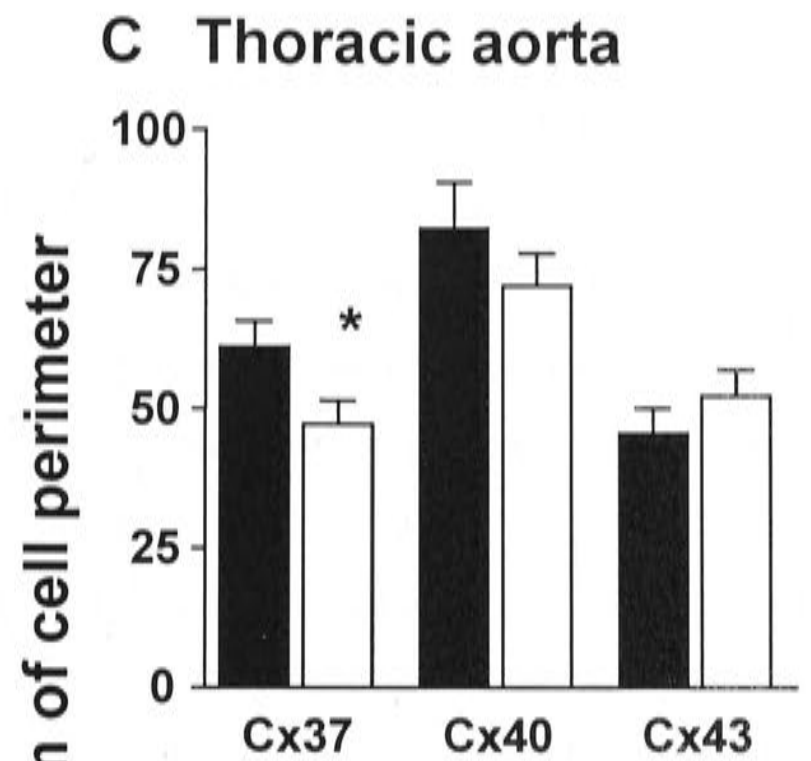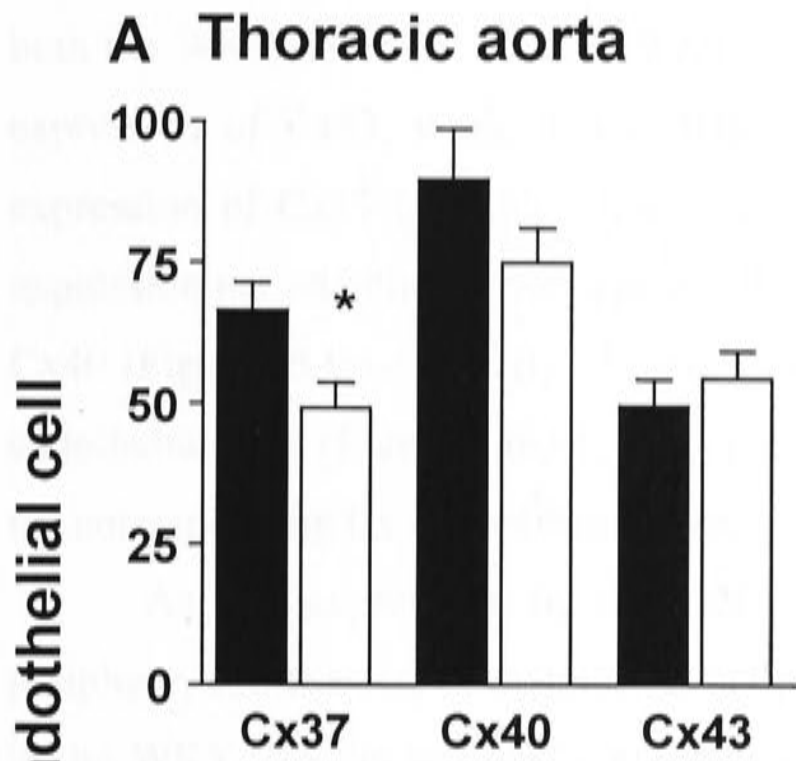
WKY
SHR

In the thoracic aorta, expression of Cx37 per endothelial cell, but not Cx40 or Cx43, was significantly less in the SHR compared to the WKY ($P<0.05$, Figures 5.5A,D, 5.7A). Cx40 was the most abundantly expressed Cx in the endothelium of the thoracic aorta of both the WKY and SHR. In the WKY, expression of Cx40 was significantly greater than expression of Cx43, while in the SHR, Cx40 expression was significantly greater than expression of Cx37 ($P<0.05$, Figures 5.5B,C, D-E, 5.7A,C). In the caudal artery, Cx43 expression per endothelial cell was significantly lower in WKY rats than that of Cx37 or of Cx40 (Figures 5.6A-C, 5.7B). In the SHR, Cxs 37, 40 and 43 were equally expressed in endothelial cells (Figure 5.6D-F, 5.7B,D), and this expression was significantly lower than the corresponding Cx expression in WKY rats ($P<0.05$, Figure 5.7B,D).

As Cx expression in the endothelium was seen exclusively around the cell periphery, and the size of endothelial cells in the caudal artery are smaller in the SHR than in the WKY, the density of Cx plaques in the cell membrane was also calculated. In the thoracic aorta, the density of Cx37 staining per 100 μm of endothelial cell perimeter was significantly less in the SHR than the WKY ($P<0.05$, Figures 5.7C). Again, the density of Cx40 in the endothelium of the thoracic aorta of both the WKY and SHR was significantly greater than Cx43 in the WKY and Cx37 in the SHR respectively ($P<0.05$, Figure 5.7C). In the caudal artery, the density of Cxs 37 and 43 plaques per 100 μm of cell membrane was not significantly different in SHR and WKY, however, the density of Cx40 plaques was significantly reduced in SHR compared to WKY ($P<0.05$, Figure 5.7D). In WKY the density of Cx43 plaques was significantly lower than that of Cxs 37 or 40 ($P<0.05$, Figure 5.7D).

Smooth muscle cells. Longitudinal and transverse sections of the rat thoracic aorta and caudal artery taken from the WKY and SHR were analysed for the expression of Cxs 37, 40, 43 and 45 (Figures 5.8, 5.9). Expression of Cx37 in longitudinal and transverse sections of both the thoracic aorta and caudal artery did not differ between WKY and SHR rats ($P>0.05$, thoracic aorta, Figure 5.8A,E; caudal artery, Figure 5.9A,E; Figure 5.10). Cx40 could not be detected in the media of the thoracic aorta or caudal artery from either strain (thoracic aorta, Figure 5.8B,F; caudal artery, Figure 5.9B,F; Figure 5.10).

Cx43 was abundantly expressed in the media of the thoracic aorta of both the WKY and SHR, but was not detected in the media of the caudal artery of either strain (thoracic aorta, Figures 5.8C,G; caudal artery, Figures 5.9C,G). Expression of Cx43 in longtitudinal sections of the thoracic aorta did not differ in WKY and SHR rats ($P>0.05$, Figure 5.10A),

Figure 5.8

Figure 5.8.

Expression of Cxs 37 (A,E), 40 (B,F), 43 (C,G) and 45 (D,H) in the media of the thoracic aorta from the WKY (A-D) and SHR (E-H) (transverse sections).   e, endothelium. sm, smooth muscle. Calibration bar represents 10 μm.
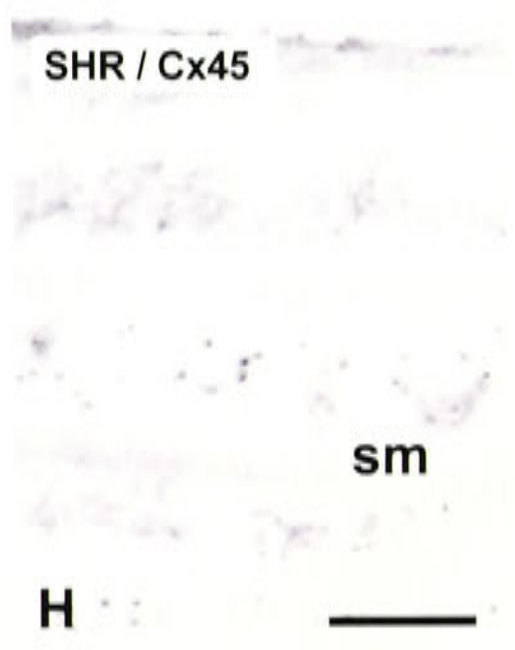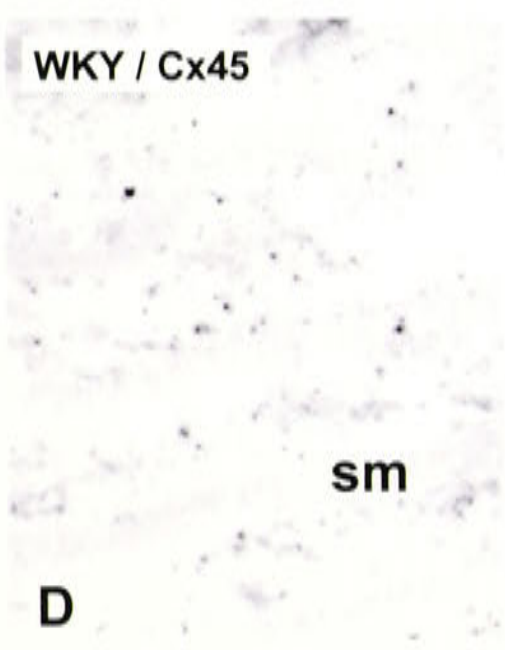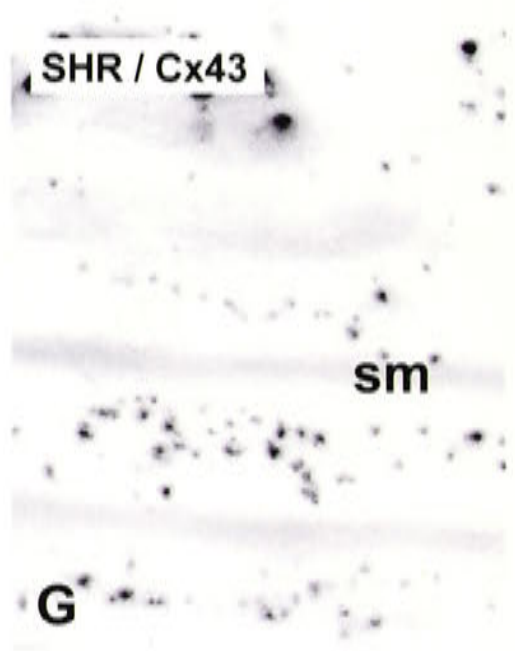
WKY / Cx37   SHR / Cx37
e   e
sm   sm
A   E

WKY / Cx40   SHR / Cx40
e   e
sm   sm
B   F

WKY / Cx43   SHR / Cx43
sm   sm
C   G

WKY / Cx45   SHR / Cx45
sm   sm
D   H

Figure 5.9

Figure 5.9.

Expression of Cxs 37 (A,E), 40 (B,F), 43 (C,G) and 45 (D,H) in the media of the caudal artery from the WKY (A-D) and SHR (E-H) (transverse sections). e, endothelium, sm, smooth muscle. Calibration bar represents 10 μm .
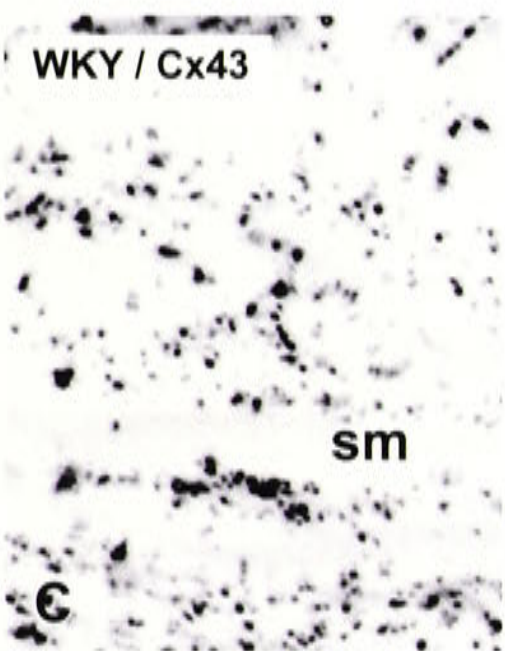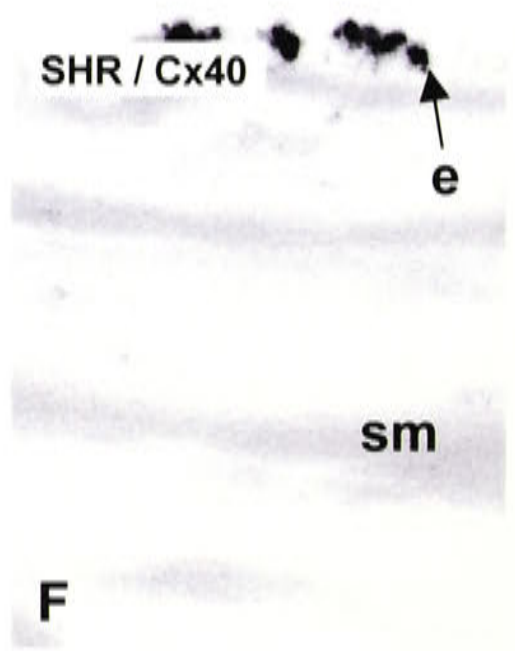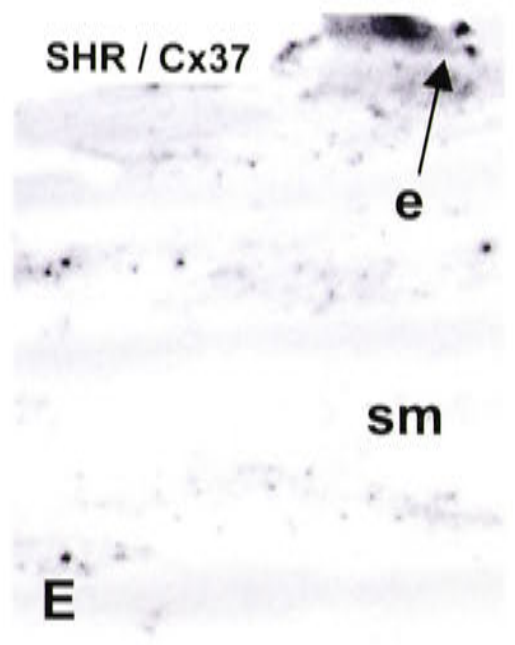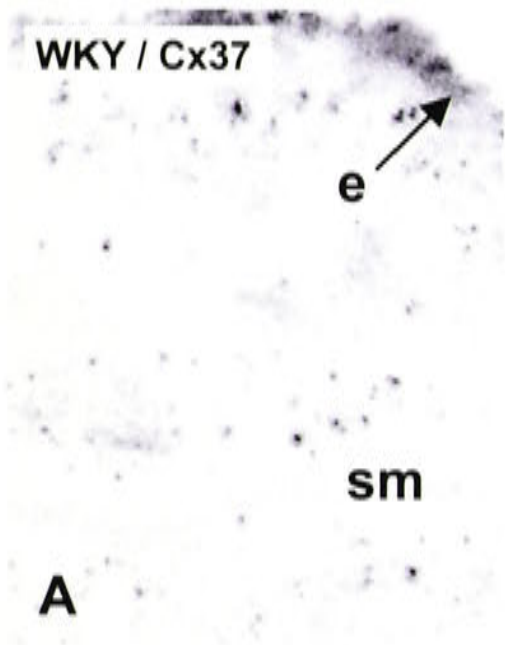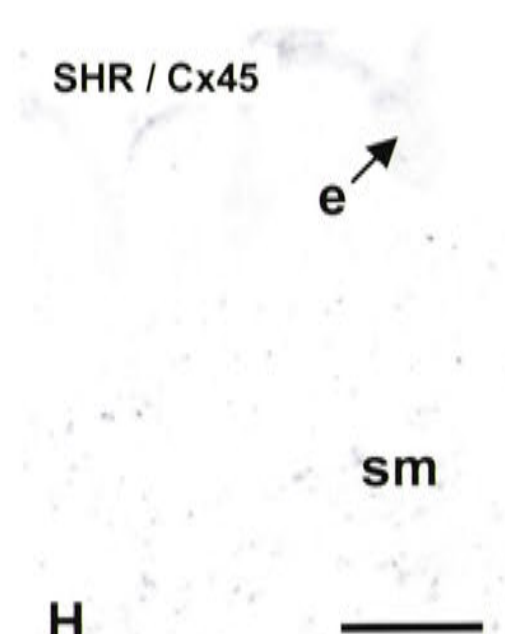
WKY / Cx37   e   sm   A

SHR / Cx37   e   sm   E

WKY / Cx40   e   sm   B

SHR / Cx40   e   sm   F

WKY / Cx43   e   sm   C

SHR / Cx43   e   sm   G

WKY / Cx45   e   sm   D

SHR / Cx45   e   sm   H
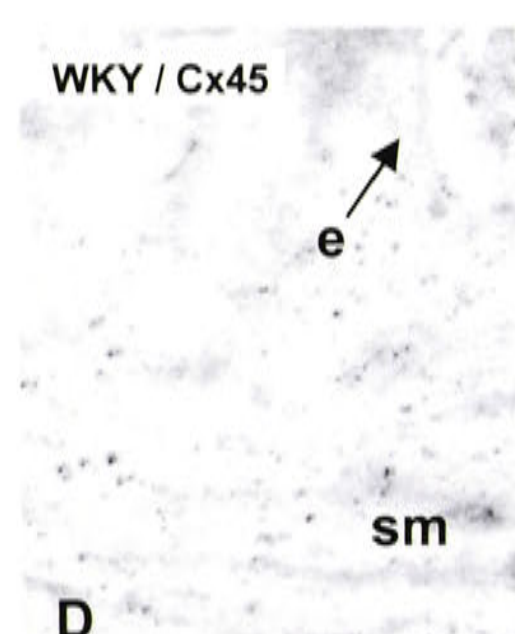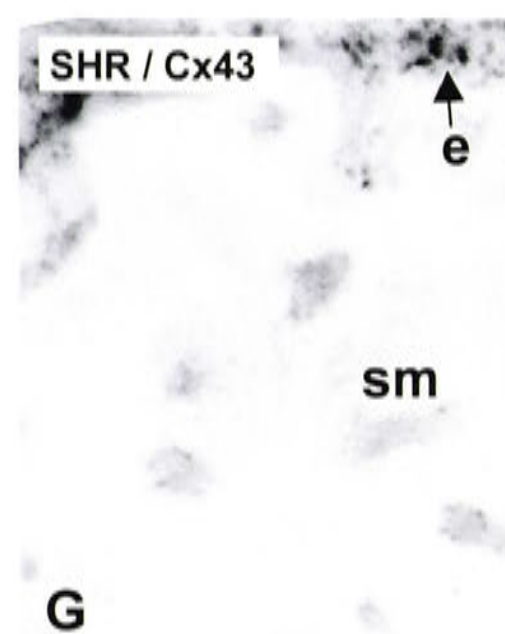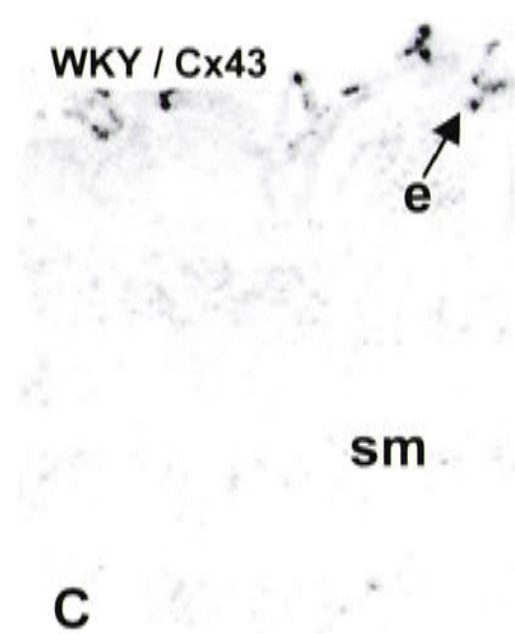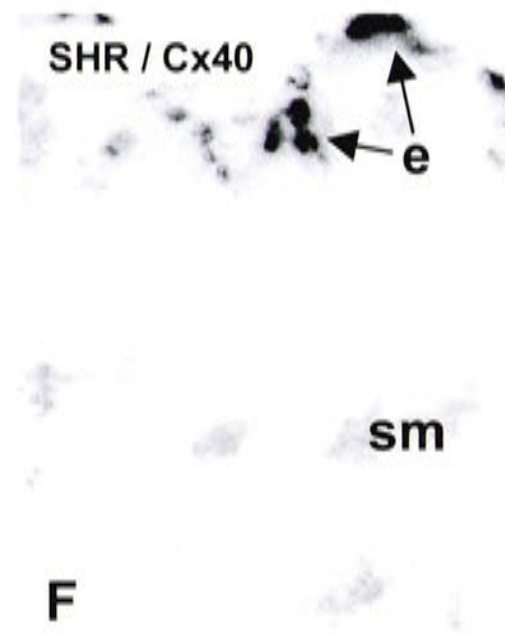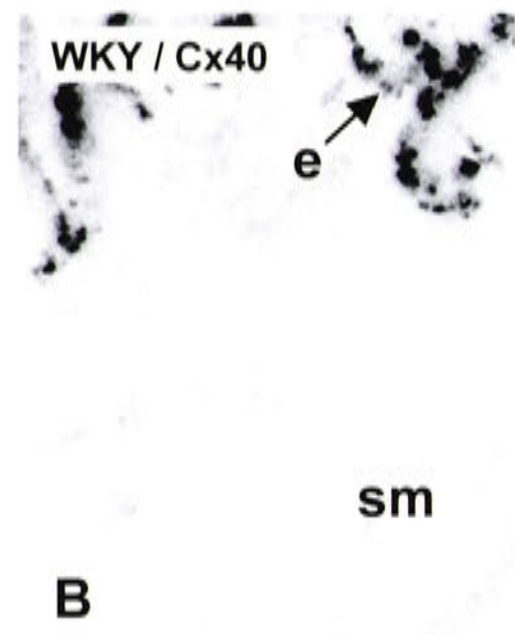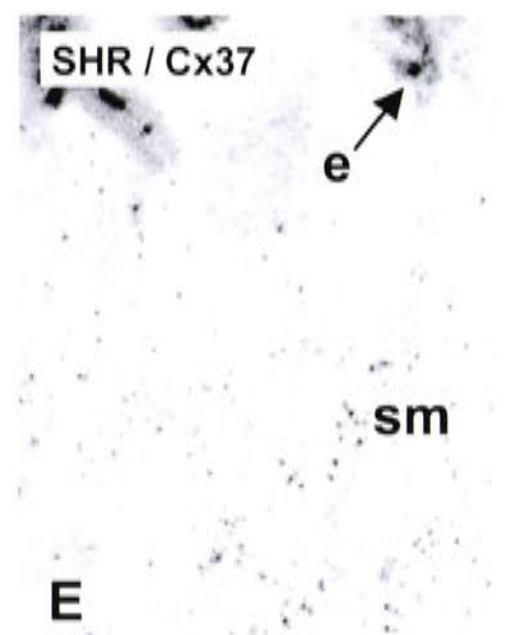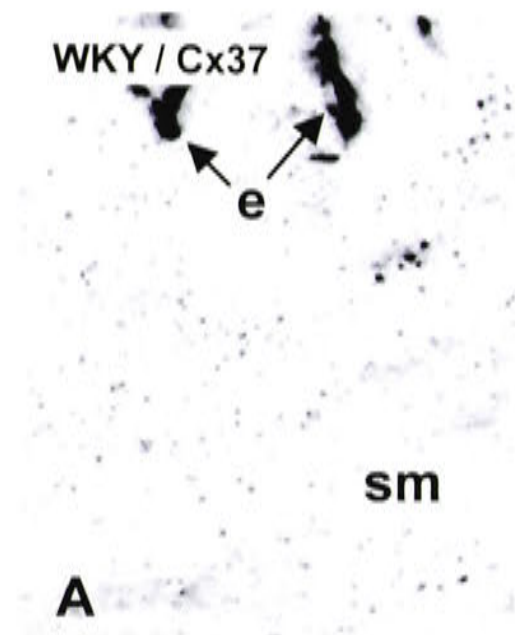
Figure 5.10

Figure 5.10.

Protein expression for Cxs 37, 40, 43 and 45 in the smooth muscle of the WKY and SHR thoracic aorta (A,C) and caudal artery (B,D) at 12 weeks. Values are expressed as plaques per μm^2 in longitudinal (A,B) and transverse (C,D) sections. Values are mean ± SEM. $^{*}P<0.05$, significantly less than WKY. $^{\dagger}P<0.05$, significantly less than the thoracic aorta. $n=4$ animals.

A **Thoracic aorta**

Plaques per µm² (Longitudinal sections)

Cx37 Cx40 Cx43 Cx45

C **Thoracic aorta**

Plaques per µm² (Transverse sections)

Cx37 Cx40 Cx43* Cx45*

B **Caudal artery**

Plaques per µm² (Longitudinal sections)

Cx37 Cx40 Cx43 † Cx45

D **Caudal artery**

Plaques per µm² (Transverse sections)

Cx37 Cx40 Cx43 † Cx45*
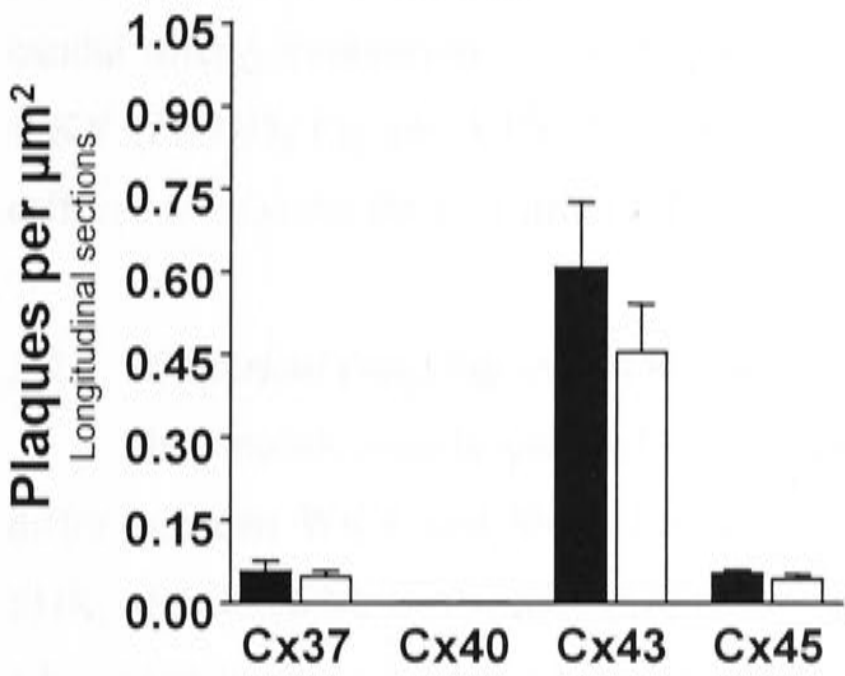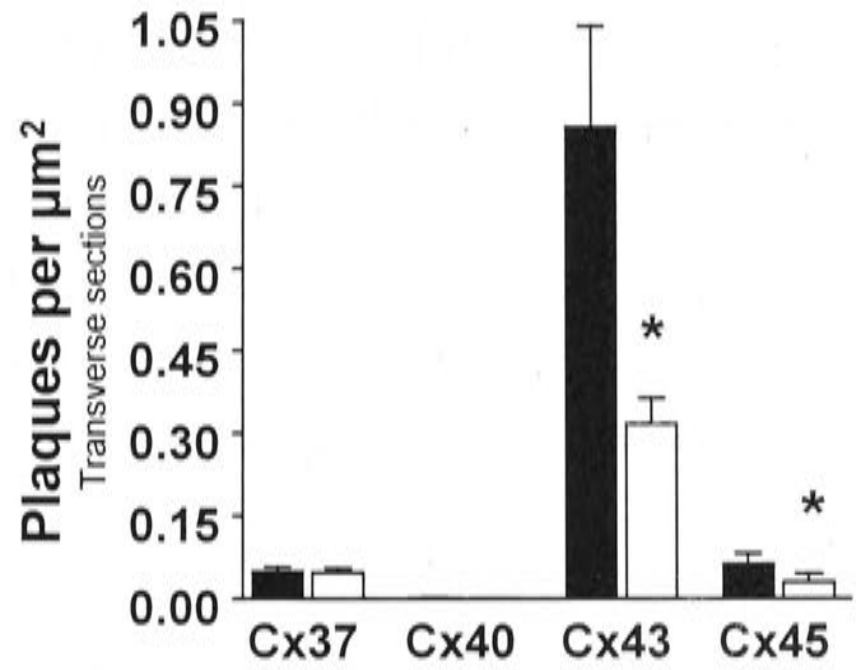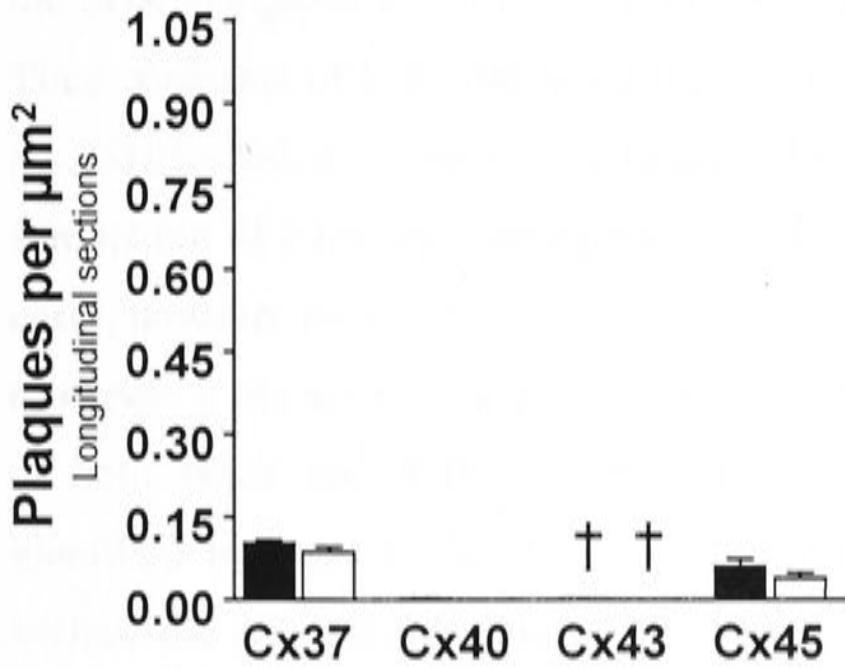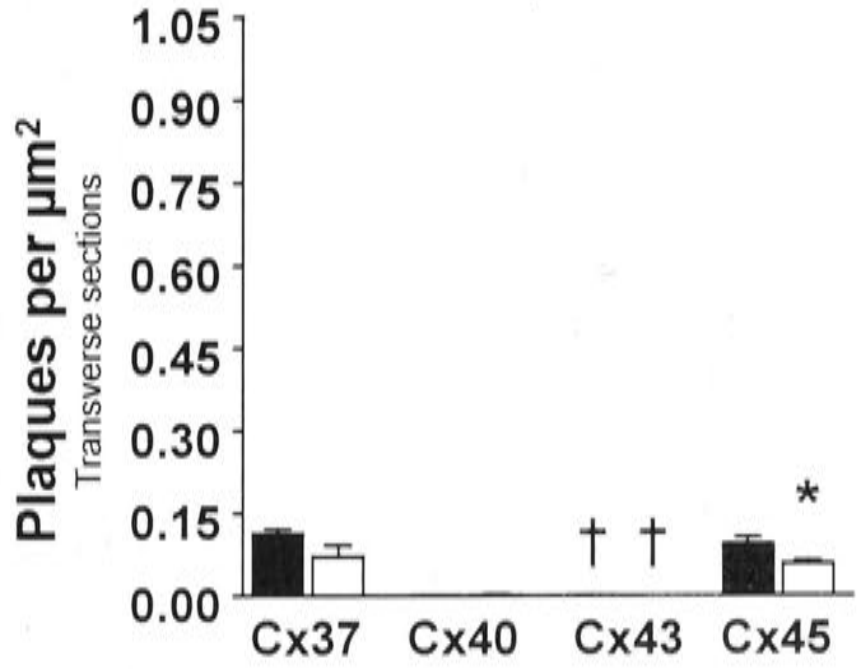
■ WKY
□ SHR

while in transverse sections Cx43 was significantly lower in the SHR compared to the WKY ($P<0.05$, Figures 5.10C). The expression of Cx43 in the thoracic aorta of both the WKY and SHR was significantly greater than expression of any other Cx ($P<0.05$, Figure 5.10A,C).

Cx45 was detected in the media of both arteries studied (thoracic aorta, Figures 5.8D,H; caudal artery, Figures, 5.9D,H). In transverse sections of the thoracic aorta and caudal artery, expression of Cx45 was significantly lower in the SHR compared to the WKY ($P<0.05$, Figures 5.10C,D), while in longitudinal sections, there was no significant difference between the two strains ($P>0.05$, Figures 5.10A,B).

5.2.5 *Electrical coupling within the media of the caudal artery*

In smooth muscle cells of the caudal artery, resting membrane potential did not differ between WKY and SHR ($P>0.05$; WKY -59 ± 1 mV, $n=23$ cells from 7 animals; SHR, -59 ± 1mV, $n=19$ cells from 7 animals). Stimulation of nerves located at the adventitial border of the media evoked excitatory junction potentials (EJPs), which were significantly larger in smooth muscle cells at the adventitial border in the caudal artery of the SHR compared to similar recordings in the WKY ($P<0.05$, Figure 5.2C,D, Table 5.2). Time constants of EJPs did not differ between WKY and SHR ($P>0.05$; WKY, 278 ± 18 ms; SHR, 239 ± 15 ms). Repetitive stimulation (2-10 impulses at 10 Hz) produced summation of EJPs and subsequent contraction. Action potentials were recorded in some cases, however the incidence of these did not differ between WKY and SHR. Stimulation of nerves at the adventitial border evoked EJPs in smooth muscle cells at the luminal border of both WKY and SHR. Cells from which intracellular recordings were made were identified by intracellular dye labelling (Figure 5.2A,B). EJPs recorded at the luminal surface did not differ in amplitude or rise time between WKY and SHR ($P>0.05$, Table 5.2B). However, between the adventitial and luminal borders there was a significant increase in the rise time of EJPs in both WKY and SHR ($P<0.05$, Table 5.2). In the WKY, the amplitude of EJPs recorded in smooth muscle cells did not differ between the adventitial and luminal borders ($P>0.05$). However, in the SHR, the amplitude of EJPs was significantly reduced by 52% in smooth muscle cells at the luminal border compared to the adventitial border ($P<0.05$, Table 5.2B). EJPs recorded in both WKY and SHR were followed by a small, slow membrane depolarization consistent with the action of noradrenaline as described previously (Jobling & McLachlan, 1992).

5.2.6 Activity of endothelium-derived hyperpolarizing factor in the caudal artery

In the caudal artery, in the presence of L-NAME and indomethacin, dose dependent ACh induced relaxation, did not differ between WKY and SHR ($P<0.05$, Figure 5.11A). This relaxation can be attributed to EDHF, since the addition of charybdotoxin (60 nM) and apamin (0.5 μM) abolished the relaxation in both the WKY and SHR. In addition, in the presence of charybdotoxin and apamin, a contraction was uncovered, although the magnitude of this did not differ between WKY and SHR ($P>0.05$, Table 5.3). The addition of 18β-GA significantly reduced the EDHF-mediated relaxation by 100% in the WKY and 73% in the SHR (Table 5.3). Recirculation of Krebs' solution containing the Cx-mimetic peptide combination ([43]Gap26, [40]Gap27, and [37,43]Gap27), L-NAME and indomethacin significantly reduced the EDHF-mediated relaxation in the WKY by 78% and in the SHR by 95% (Table 5.3). The EDHF-mediated relaxation was not altered following recirculation of control Krebs' soloution for 60 min.

In order to examine the specificity of the Cx-mimetic peptide combination for EDHF, a number of control studies were performed in vessels from WKY rats (Figure 5.12). In the presence of L-NAME and indomethacin, an EDHF-mediated relaxation was present (Figure 5.12A,B). Addition of Cx-mimetic peptide combination abolished the EDHF-mediated relaxation but had no effect on the NO-mediated relaxation (Figure 5.12A-D). In the presence of L-NAME, indomethacin and either hydroxocobalamin or carboxy-PTIO, the EDHF mediated relaxation was not different from control in either WKY or SHR ($P>0.05$, Table 5.3).

In the caudal artery, concentration-dependent hyperpolarization induced by ACh, in the presence of L-NAME and indomethacin, was 28% less in the SHR than in the WKY ($P<0.05$, WKY, -18 mV; SHR, -13 mV; Figure 5.11B). L-NAME had no effect on resting membrane potential in either WKY or SHR, although indomethacin depolarised membrane potentials by 5-10 mV. Cumulative addition of ACh did not result in desensitisation of responses, since application of single concentrations of ACh produced similar results.

In both WKY and SHR, the addition of charybdotoxin and apamin significantly attenuated the EDHF-mediated hyperpolarization induced by ACh (Table 5.4). However, in all SHRs and in 4 out of 8 WKY animals, a depolarization was uncovered (Figure 5.11C, Table 5.4). Removal of the endothelium abolished both hyperpolarization and depolarizations in both strains. The addition of iberiotoxin had no effect on ACh induced

strain	location	number of animals	number of cells	amplitude (mV)	rise time (ms)
A.					
SHR	adventitial	7	19	$19 \pm 1^{*}$	24 ± 3
WKY	adventitial	7	23	14 ± 1	34 ± 3
B.					
SHR	adventitial	6	17	$21 \pm 3^{\dagger\ddagger}$	$20 \pm 5^{\dagger}$
SHR	luminal	6	6	10 ± 3	50 ± 6
WKY	adventitial	6	20	15 ± 1	32 ± 6
WKY	luminal	6	6	13 ± 3	50 ± 5

Table 5.2. Characteristics of EJPs recorded from smooth muscle cells of the caudal artery from WKY and SHR. (A) Data for all adventitial smooth muscle cells impaled, (B) preparations in which both adventitial and luminal smooth muscle cells were impaled. Values are mean ± SEM. $^{*}P<0.05$, significantly greater than WKY in A. $^{\dagger}P<0.05$, significantly different from corresponding luminal impalements in B. $^{\ddagger}P<0.05$, significantly greater than WKY adventitial impalements in B.

Figure 5.11

Figure 5.11.

Endothelium-dependent relaxation and hyperpolarization in response to ACh in caudal arteries of SHR and WKY rats. (A) Vasodilation, expressed as % of phenylephrine (PE)-induced constriction, to cumulative application of ACh. (B) Membrane hyperpolarizations in smooth muscle cells induced by cumulative application of ACh. (C) Hyperpolarizations recorded in adventitial smooth muscle cells in SHR following the iontophoretic application of ACh (1 M, 200 nA, 10 s), in the absence (a) and presence (b) of charybdotoxin (ChTx, 60 nM) and apamin (0.5 μM). (D) Hyperpolarizations recorded in smooth muscle cells in SHR following the iontophoretic application of ACh (1 M, 200 nA, 10 s), in the absence (a) and presence (b) of iberiotoxin (100 nM). All experiments were performed in the presence of L-NAME (100 μm) and indomethacin (10 μm). Values in (A) and (B) are expressed as mean ± SEM.

A

Relaxation (% of PE-induced constriction) vs Log_{10} [ACh]

- WKY (●)
- SHR (○)

B

Hyperpolarization (mV) vs Log_{10} [ACh]

C

a

b

ChTx + Apamin   5 mV

ACh (200 nA, 10s)

D

a

b

10 mV

Iberiotoxin

ACh (200 nA, 10s)   5s
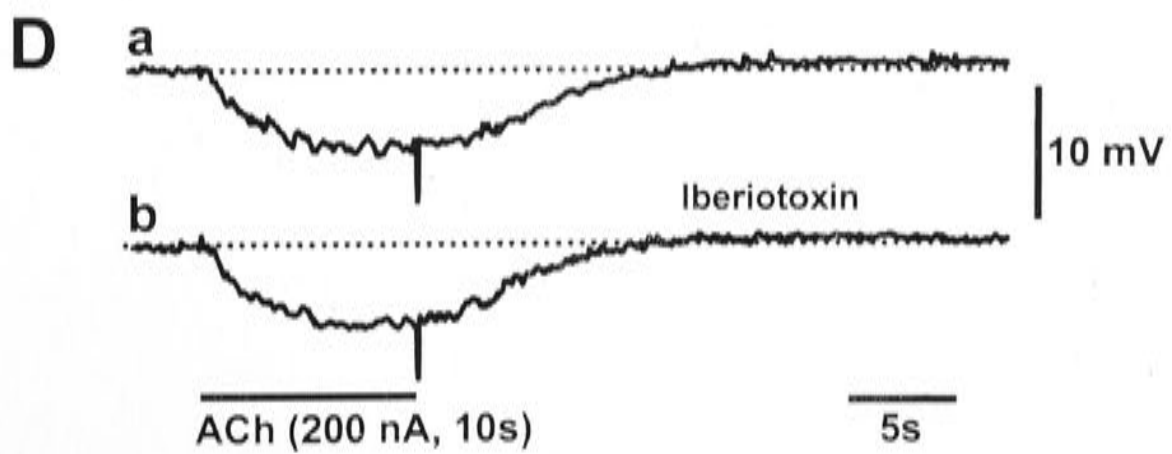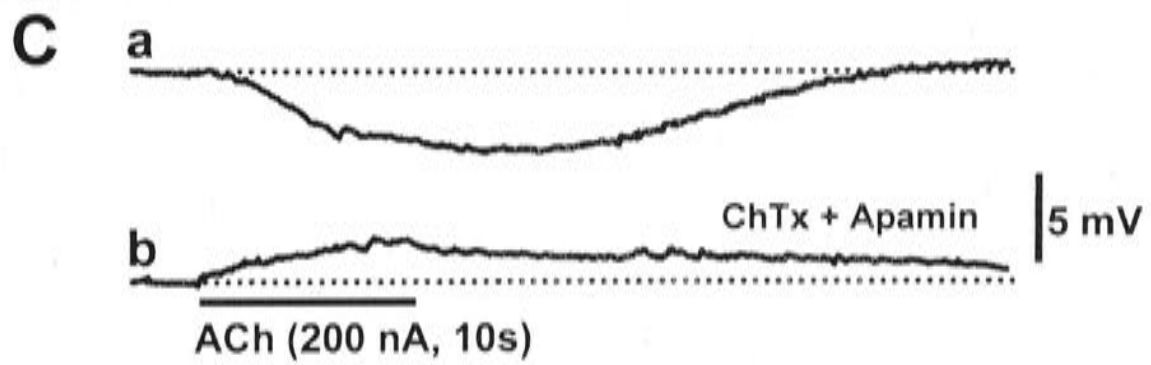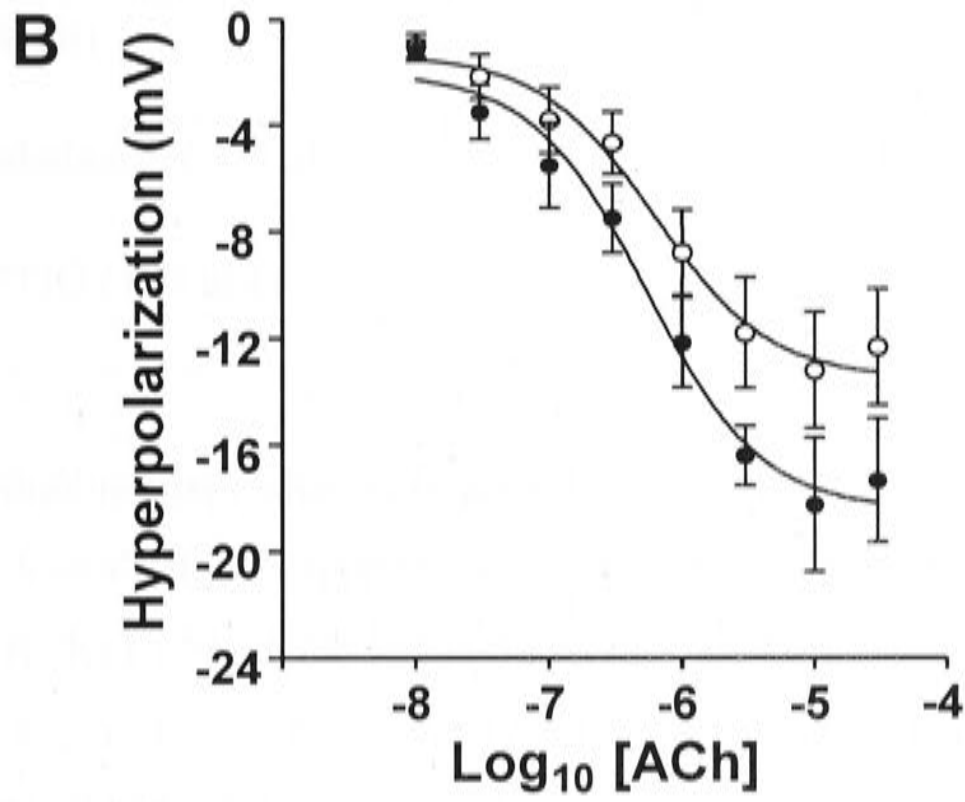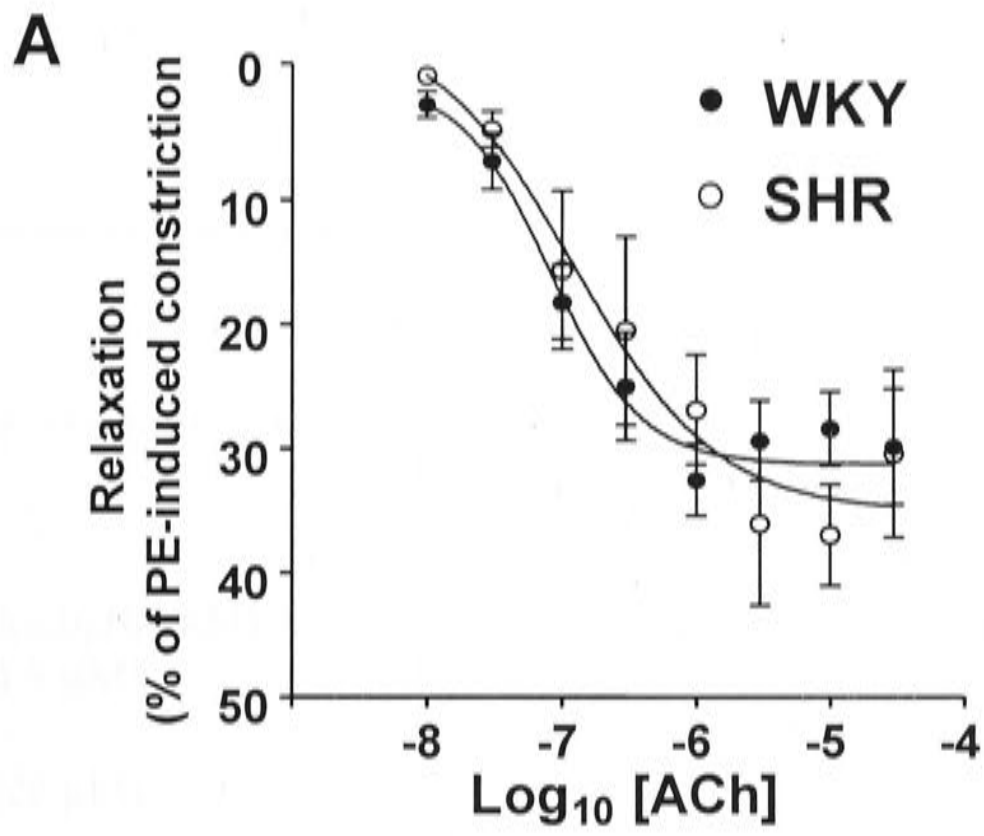
	Relaxation (% of phenylephrine-induced constriction)	
	WKY	SHR
ACh	32 ± 2.9	37 ± 6
ACh + charybdotoxin (60 nM) + apamin (0.5 μM)	$-39 \pm 11^*$	$-25 \pm 5^*$
ACh + 18β-GA (20 μM)	$0 \pm 0^*$	$10 \pm 5^*$
ACh + Gap peptide combination (100 μM each)	$7 \pm 3^*$	$2 \pm 2^*$
ACh + hydroxocobalamin (100 μM)	38 ± 10	52 ± 8
ACh + carboxy-PTIO (100 μM)	35 ± 5	27 ± 5

Table 5.3. Endothelium-dependent relaxation in response to ACh in caudal arteries of WKY and SHR. Vasodilation, expressed as % of phenylephrine-induced constriction, to application of ACh (1 μM) in the WKY and SHR. Negative values indicate constriction. All experiments were performed in the presence of L-NAME (100 μM) and indomethacin (10 μM). Values are mean ± SEM. $^*P<0.05$, significantly different from corresponding control. n=3-5.

Figure 5.12

Figure 5.12.

Endothelium-dependent relaxation in response to ACh (1 μM) in caudal arteries of SHR and WKY rats (expressed as % of phenylephrine (PE)-induced constriction). (A) EDHF, but not NO mediated relaxation was abolished by the addition of the Cx-mimetic peptide combination, [43]Gap26, [40]Gap27 and [37,43]Gap27 (100 μM each), while NO mediated vasodilation was abolished by L-NAME (100 μM). Values are expressed as mean $\pm$ SEM. n=4-7. EDHF mediated vasodilation, before (B) and after (C) the addition of the gap mimetic peptide combination. (D) NO mediated relaxation was unaffected by the addition of indomethacin (10μm) and the Gap mimetic peptide combination.

A

B EDHF
ACh
PE
L-NAME+Indo

C EDHF+Gap peptides
ACh
PE
L-NAME+Indo+Gap peptides

D NO+Gap peptides
ACh
0.5g
PE
Indo+Gap peptides
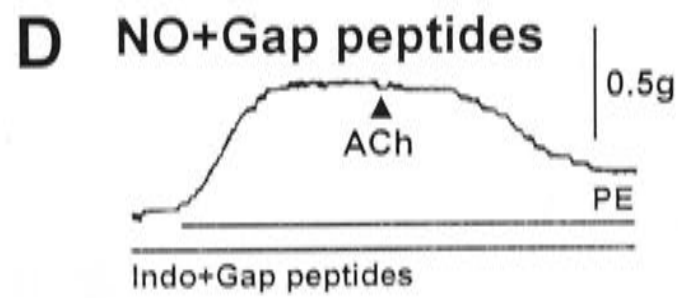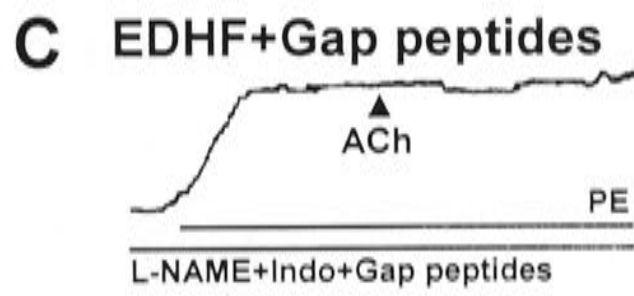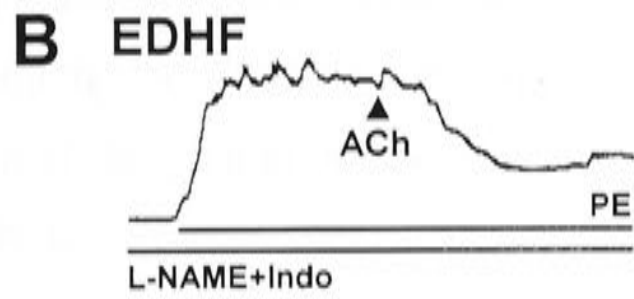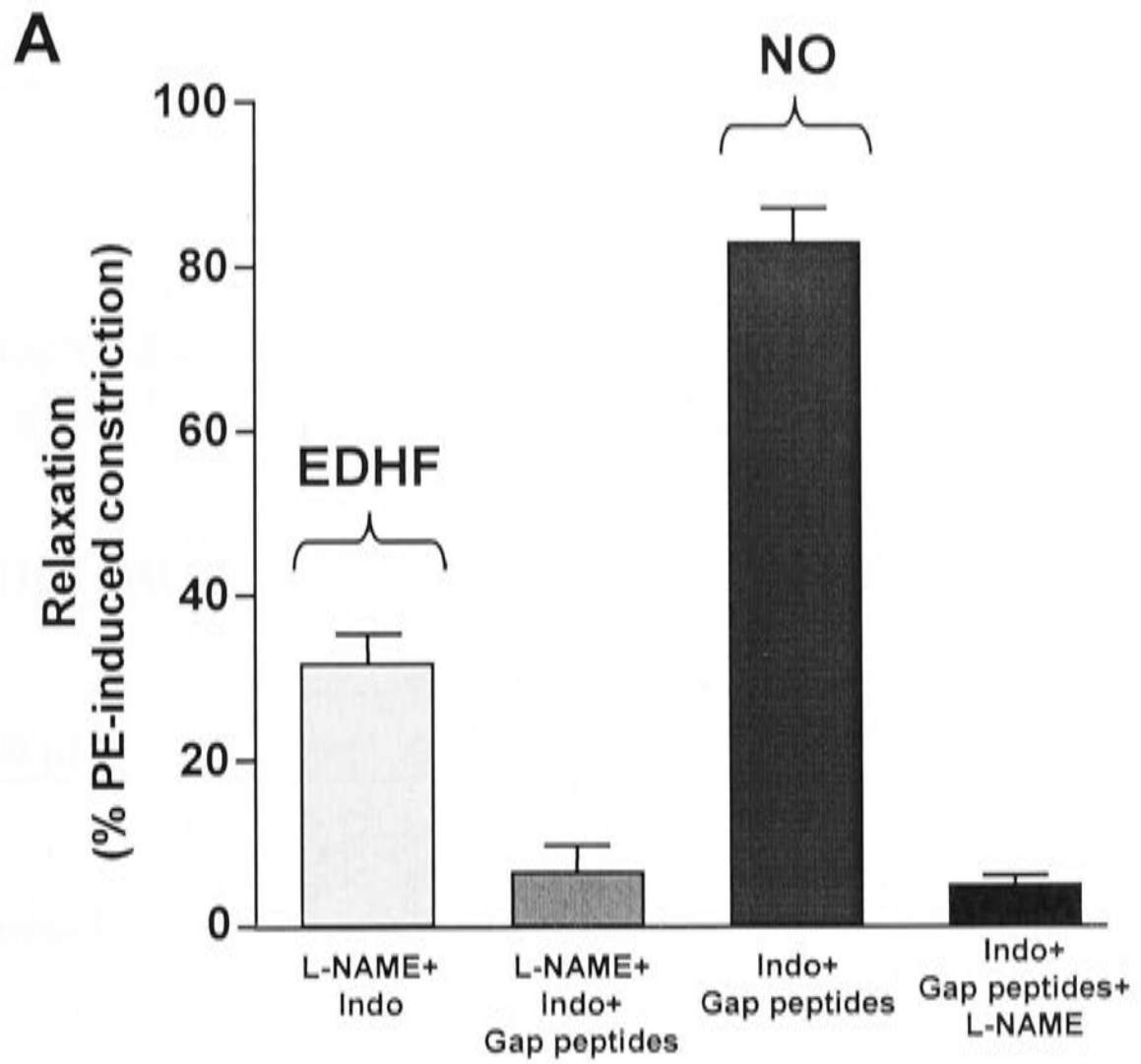
	Hyperpolarization (mV)	
	WKY	SHR
ACh	-10 ± 2	-7 ± 1
ACh + charybdotoxin (60 nM) + apamin (0.5 µM)	+2 ± 1	+3 ± 1
ACh	-13 ± 3	-4 ± 2
ACh + iberiotoxin (100 nM)	-13 ± 4	-4 ± 1
ACh	-12 ± 2	-5 ± 1
ACh + 18β-GA (100 µM)	0 ± 0	0 ± 0*
ACh	-9 ± 2	-8 ± 1
ACh + hydroxocobalamin (100 µM)	-8 ± 3	-8 ± 2

Table 5.4. EDHF-mediated hyperpolarization recorded in smooth muscle cells in the caudal artery of WKY and SHR rats. Hyperpolarizations were recorded in smooth muscle cells following the ionophoretic application of ACh (1 M, 200 nA, 10s), before and after the addition of charybdotoxin and apamin, iberiotoxin, 18β-GA and hydoxocobalamin. Positive values indicate depolarization. All experiments were performed in the presence of L-NAME and indomethacin. Values are expressed as mean ± SEM. $^*P<0.05$, significantly different from corresponding control. n=3-8.

hyperpolarization in either strain (Figure 5.11D, Table 5.4), while, 18β-GA abolished the ACh-induced hyperpolarization in both strains (Table 5.4). In the presence of L-NAME and indomethacin, the addition of hydroxocobalamin had no effect on the hyperpolarization to ACh in either strain (Table 5.4).

5.3   DISCUSSION

Differences between normotensive WKY and hypertensive SHR rats have been identified in the morphology and coupling of cells in the endothelium and media of the thoracic aorta and caudal artery. Furthermore, changes in cellular coupling that involve distinct Cxs within the two cellular layers have been identified in both vessels. In the thoracic aorta, which is an example of a large conduit artery, anatomical remodeling of vascular smooth muscle and endothelial cells was not evident in the SHR, although there was a significant decrease in mRNA expression for Cxs 43 and 45 in intact vessels. In addition, protein expression for Cx37 was decreased in the endothelium while protein for Cxs 43 and 45 was decreased in the smooth muscle. In contrast, in the caudal artery, which is an example of a muscular artery, anatomical remodeling of both the vascular smooth muscle (Sandow *et al.* 2003b) and endothelial cells occurred in the hypertensive rats. This was accompanied by a decrease in the expression of mRNA for Cx45 in intact vessels, and by a decrease in Cx40 protein in the endothelium and Cx45 protein in the smooth muscle, relative to the vessels from normotensive animals. In the caudal artery, decreased Cx expression in the media was accompanied by a decrease in cell coupling.

In the caudal artery of SHR, the remodeling of the arterial wall comprised a decrease in lumen diameter and an increase in the number of smooth muscle cell layers; changes that are characteristic of hypertrophic remodeling. In addition, endothelial cells were found to be smaller in surface area, perimeter and cell length. In contrast, no remodeling of either the smooth muscle or endothelial cell layers was found in the thoracic aorta of SHR. Previous studies in the thoracic aorta of 4 and 15 month old SHR have demonstrated an increase in the medial cross-sectional area and media to lumen ratio (Otsuka *et al.* 1998; Fujii *et al.* 1999; Giummelly *et al.* 1999; Saleh & Jurjus, 2001), although other studies found no difference in the media to lumen ratio at 4 months, or during ageing (Marque *et al.* 1999). Together, the data suggest that within the thoracic aorta, medial remodeling may be limited or may only occur in response to a prolonged

71

increase in blood pressure. On the other hand, the presence of vascular remodeling in a muscular artery at an early stage suggests a role for such changes in the development of hypertension.

The distribution of Cxs in the media and endothelium of the thoracic aorta and caudal artery of both WKY and SHR followed a similar pattern of expression to that described in young adult Wistar rats (Chapter 4). Thus, Cx43 was the most abundantly expressed Cx in the media of the thoracic aorta, while Cx37 was sparsely detected. In contrast, Cx37 was the most abundantly expressed Cx in the smooth muscle of the caudal artery, while Cx43 was detected only in the endothelium. Cx45 was detected in the smooth muscle of both vessels, while Cx40 was not detected in the media of either vessel. In the endothelium of both arteries, Cxs 37, 40 and 43, but not Cx45, were expressed in a punctate manner, delineating the endothelial cell borders. In general, there was a good correlation between mRNA and protein expression given that the smooth muscle significantly outweighed the contribution of the endothelium in both vessels.

The present study is the first to correlate anatomical remodeling of the vascular wall with functional changes in cellular coupling during hypertension. In the caudal artery, results demonstrate a reduction in electrical coupling within the media of the SHR compared to the WKY in line with the decrease in Cx expression. In WKY rats, the rise time of EJPs evoked by neural stimulation and the release of ATP (Hirst *et al.* 1996) in smooth muscle cells at the adventitial border, was faster than that recorded at the luminal border, while there was no change in amplitude. On the other hand, in the SHR, both amplitude and rise time of EJPs recorded at the luminal border, were significantly different to those recorded at the adventitial border. The decrease in amplitude of EJPs (52%) was greater than that which would be expected to result simply from hypertrophy of the media (29%). Concomitant with these changes, we found a significant decrease in Cx45 protein expression, which provides an explanation for the decrease in electrical coupling between smooth muscle cells within the media of the caudal artery of SHR compared to WKY. Other differences were apparent in the nerve-mediated response within the caudal artery of SHR in that of the amplitude of the EJPs recorded in smooth muscle cells at the adventitial border were larger than those recorded in the WKY. These results are similar to those observed in mesenteric arteries of the SHR (Brock & van Helden, 1995) and are thought to result from the increased sympathetic innervation of the caudal artery in the SHR (Cassis *et al.* 1985). As a consequence of the differential attenuation of EJPs in the media, EJPs

recorded in smooth muscle cells at the luminal border of the caudal artery were not different between WKY and SHR. It is interesting to note that expression of protein for Cx45 was reduced in transverse, but not longitudinal sections of the SHR compared to the WKY, suggesting a greater role for radial rather than longitudinal coupling within the media. Furthermore, in the rat caudal artery, smooth muscle cells filled with Lucifer Yellow dye, show movement of the dye in the radial but not the longitudinal direction (Sandow *et al.* 2002).

In contrast to the caudal artery, in the thoracic aorta of the SHR, both Cxs 43 and 45 were reduced in the vascular smooth muscle in the absence of other signs of anatomical remodeling. A similar decrease in the expression of mRNA and protein for Cx43 has been reported in rats made hypertensive by L-NAME treatment, but not in 2 kidney, 1 clip and DOCA-salt hypertensive rats, where increased Cx43 has been described (Watts & Webb, 1996; Haefliger *et al.* 1999, 2000). Together, the results suggest that changes in cellular coupling in any particular artery may vary depending on the aetiology of the model of hypertension and may arise independently of any anatomical reorganisation of the smooth muscle layers. In contrast to the results presented here, Li & Simard (2002), found no change in the expression of protein for Cx45 in Western blots of intact thoracic aortae from SHR. At present the reasons for this discrepancy are unknown.

In the aortic endothelium, despite the lack of morphological remodeling, the staining of protein for Cx37 was significantly reduced during hypertension. On the other hand, in the caudal artery, significantly reduced Cx40 expression accompanied a significant decrease in endothelial cell length. Longitudinal conduction of vasodilatory responses is known to occur in the vascular endothelium, and is thought to be dependent on gap junctions for the coupling of adjacent cells (Segal *et al.* 1999; Emerson & Segal, 2001; Sandow *et al.* 2003d). It can be hypothesised that a reduction in Cx expression and therefore cellular coupling, in addition to changes in cell size in the endothelium, would result in reduced conducted vasodilation. Indeed, studies examining mice lacking Cx40 showed a reduction in the propagation of vasodilatory signals in cremaster muscle arterioles, along with an increase in systemic blood pressure (de Wit *et al.* 2000). It is interesting that Simon & McWhorter (2003) found that endothelial cell dye transfer was reduced to a greater extent in Cx40$^{-/-}$ compared to Cx37$^{-/-}$ mice. Taken together, the results suggest a greater role for Cx40 rather than Cx37 within the endothelium of blood vessels and that decreased Cx40 expression, but not Cx37, may be involved in the development of

hypertension. Whether similar differential reductions in propagation can be demonstrated in the endothelium of the thoracic aorta and caudal artery in the SHR remains to be determined.

Reduction in the coupling of cells within both the media and endothelium of the caudal artery in the SHR were not correlated with a reduction in EDHF-mediated relaxation in the SHR. While relaxation was not significantly different in WKY and SHR, the ACh induced EDHF-mediated hyperpolarization in SHR was 28% less than that in WKY. This reduction is likely to be due to the presence of a depolarization and contraction in the SHR, which was uncovered following the blockade of EDHF with charybdotoxin and apamin. In the WKY, a similar contraction was found following the blockade of EDHF however, this was not consistently associated with a depolarization (4 out of 8 animals). Furthermore, the EDHF-mediated response, but not the NO-mediated response, in the caudal artery of the WKY and SHR, is dependent on gap junctional coupling within the vascular wall since it was blocked by the Cx mimetic peptides. Indeed, these results concur with other studies which demonstrate that a blockade of gap junctions with 18β-GA and / or Cx-mimetic peptides is associated with a significant attenuation of EDHF relaxation (Chaytor et al. 2001; Griffith et al. 2002; Sandow et al. 2002), but not the relaxation attributed to NO. The maintenance of the EDHF response in the face of reduced coupling in the media and endothelium of the SHR thus appears to be due to the up-regulation of MEGJs in the SHR (Sandow et al. 2003b). No role was found for the involvement of an epoxyeicosatrienoic acid- mediated activation of BK_{Ca} channels, or for L-NAME insensitive NO in the EDHF mediated response in the caudal artery. This is in contrast to other vessels such as the mesenteric artery, where an L-NAME insensitive NO component has been described (Chauhan et al. 2003).

In conclusion, the results presented in this Chapter demonstrate that heterogeneity in anatomical remodeling and electrical coupling of the smooth muscle and endothelium occurs between different vascular beds in a single model of hypertension. Alterations in Cx expression were found in the media and endothelium of both vessels, although the specific isoform of Cx involved was different in the two vessels and within the two cellular layers. The presence of vascular remodeling in a muscular artery, but not in conduit vessels, supports a role for such changes in the development of hypertension. In the aorta, significant changes could be identified in cellular coupling even in the absence of gross anatomical remodeling, suggesting that such changes may not be associated with

hypertension. Changes in Cx expression in the caudal artery of hypertensive rats corresponded with changes in cellular coupling in the media, and thus could have important implications for vascular disease.

CHAPTER 6

VASCULAR CHANGES AND CONNEXIN EXPRESSION IN THE THORACIC AORTA AND CAUDAL ARTERY IN RELATION TO THE ONSET OF HYPERTENSION

6.1   INTRODUCTION

As discussed in Chapter 5, Cx expression and cellular morphology are altered in both vascular layers of arteries from adult hypertensive rats, with the type and nature of the remodeling observed during hypertension depending on the vessel examined. However, whether vascular remodeling is a cause or a consequence of increased blood pressure is controversial. Early studies examining vascular remodeling in the SHR have shown that morphological changes can be characterized as either primary or secondary. It has generally been noted that in large elastic arteries such as the superior mesenteric artery and the aorta, vascular remodeling is a secondary adaptive response, developing after the increase in blood pressure has become evident. In contrast, in large and small muscular arteries, including the peripheral mesenteric arterial bed, structural changes have been observed in the pre-hypertensive SHR. These primary changes usually involve an increase in the medial cross-sectional area and an increase in the number of smooth muscle cell layers. The exact nature underlying the vascular remodeling varies with the blood vessel being examined and the specific stages in the development of hypertension (Lee, 1985; 1987; Norrelund et al. 1994; Dickhout & Lee, 1997; Van Gorp et al. 2000). Thus, there is evidence to suggest that vascular remodeling can occur prior to increased blood pressure, or as an adaptive response, whereby remodeling may contribute to the maintenance of elevated blood pressure.

As discussed in Chapter 5, changes in vascular morphology occur in parallel with altered cellular coupling in the caudal artery, but not in the thoracic aorta. In this Chapter, Cx expression within the endothelial and smooth muscle cell layers of the aorta and caudal artery from pre-hypertensive animals is investigated. Changes in endothelial cell morphology were also examined in parallel with changes in Cx expression. In the SHR, a significant increase in blood pressure does not occur until 9 weeks of age (Chapter 5), although blood pressure shows a trend to increase from 4 weeks of age. Consequently, 3-

76

week old animals were defined to be pre-hypertensive in the present study, as blood pressure at this age was not different from normotensive age-matched animals. Endothelial cell morphology and vascular Cx expression at 3 weeks in WKY and SHR was compared with that of 12 week old normotensive and hypertensive animals, as examined in Chapter 5. The data from the 12 week rats is included in some of the Figures to facilitate comparisons.

Little is known regarding the changes that occur in Cx expression in the cardiovascular system during development and aging. Recently, the pattern of Cx expression in rat aortic endothelium has been shown to vary during development (Yeh *et al.* 2000). Within the endothelium, Cxs 37, 40 and 43 were shown to have distinct patterns of expression. All were highly expressed at birth; however, expression was immediately down-regulated within the first weeks following birth. Following this period, Cxs 37 and 43 continued to be down-regulated in a Cx specific pattern, while Cx40 expression was maintained at a constant level throughout development and into adulthood (Yeh *et al.* 2000). Changes in Cx expression were also accompanied by increases in endothelial cell size in the aorta (Yeh *et al.* 2000).

In the vascular smooth muscle, changes in Cx expression have been shown to occur in parallel with changes in cell function in the aorta. During postnatal development, smooth muscle cells of the synthetic phenotype predominate in the aortic wall where they undergo mitosis and synthesize large amounts of extracellular matrix to result in a thickening of the media and the formation of elastic laminae (Nakamura, 1988; Blackburn *et al.* 1997). In fully developed vessels, smooth muscle cells of the contractile phenotype predominate. In the prenatal rat aorta, smooth muscle cells show increased levels of Cx43, in parallel with rapid growth of the aortic media and the presence of the synthetic smooth muscle cell phenotype. Cx43 expression was at its highest 1 week postnatal, with expression decreasing to be maintained a constant level into adulthood (Blackburn *et al.* 1997). Therefore in the vascular media, an increase in Cx43 expression may act to maintain smooth muscle cells in the synthetically active phenotype that is required for the rapid growth of the media. Interestingly, the peak in Cx43 expression at 1 week corresponded with a transient increase in blood pressure (Blackburn *et al.* 1997). In contrast to these studies, results of the previous Chapter suggest that Cx expression is decreased in the aorta of hypertensive rats, although it is not known what happens during the pre-hypertensive phase. No studies have yet examined the expression of all 4 vascular Cxs in other blood vessels during development.

6.2 RESULTS

6.2.1 Expression of mRNA for vascular connexins in 3 week old rats

Expression of mRNA for all four Cxs was similar in the thoracic aorta, and did not differ between WKY and SHR ($P>0.05$, Figure 6.1A). In the caudal artery the expression of mRNA for Cx37 was significantly greater than mRNA expression of Cxs 40, 43 and 45 in both the WKY and SHR. Expression of Cxs 37 and 45 in the SHR was significantly greater than in the WKY ($P<0.05$, Figure 6.1B). Cxs 40 and 43 were also detected in small amounts in the caudal artery, however expression did not differ between WKY and SHR (Figure 6.1B).

During development between 3 and 12 weeks of age, expression of mRNA for Cxs 43 and 45 in the thoracic aorta increased in the WKY at 12 compared to 3 weeks of age ($P<0.05$, Figure 6.1A,C), while in the SHR expression did not differ ($P>0.05$). The expression of mRNA for Cxs 37 and 40 did not differ between 3 and 12 weeks in either the WKY or SHR ($P>0.05$, Figure 6.1A,C). In the caudal artery, mRNA for Cxs 37, 40 and 43 were decreased at 12 weeks compared to 3 weeks of age in both WKY and SHR ($P<0.05$, Figure 6.1B,D). In a similar manner, expression of mRNA for Cx45 was decreased in the caudal artery of the SHR at 12 weeks ($P<0.05$), while there was no change in Cx45 mRNA in the WKY between 3 and 12 weeks of age ($P>0.05$, Figure 6.1B,D).

6.2.2 Endothelial cell morphology

En face views of the luminal surface showed a typical pattern of Cx expression, with punctate staining along the periphery of endothelial cells (Figure 6.3). No areas devoid of endothelial cells were found.

At 3 weeks of age, endothelial cell surface area, length, width and perimeter were not significantly different between SHR and WKY in either the thoracic aorta or caudal artery ($P>0.05$, Figure 6.2).

In the thoracic aorta of WKY rats, between 3 and 12 weeks of age, surface area, length, width and perimeter of endothelial cells was significantly greater at 12 weeks than at 3 weeks of age ($P<0.05$, Figure 6.2A). In SHR rats between 3 and 12 weeks, surface area, width and perimeter of endothelial cells was significantly greater at 12 weeks than at 3 weeks ($P<0.05$), however, length of endothelial cells did not differ ($P>0.05$, Figure 6.2A).
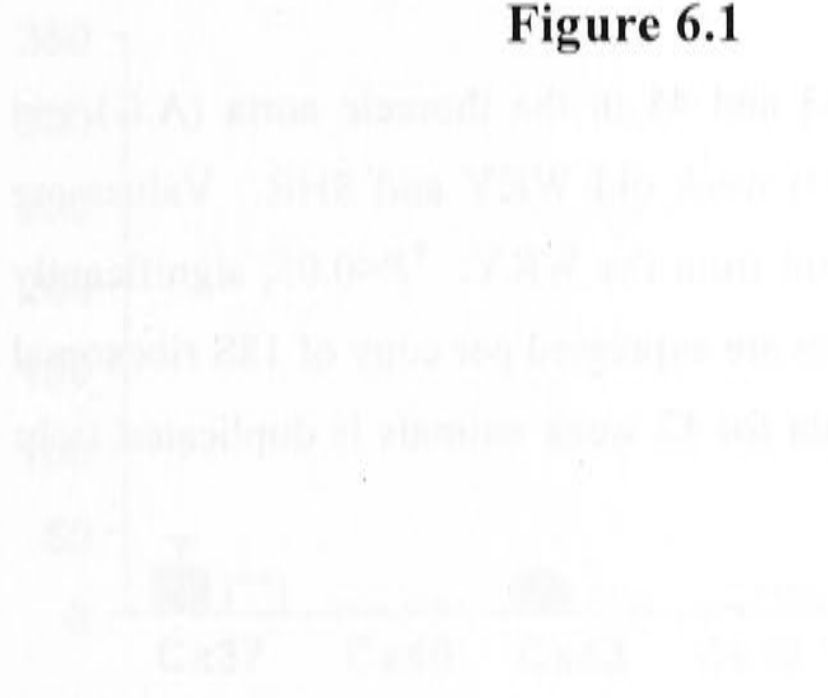
Figure 6.1

Figure 6.1.

mRNA expression of Cxs 37, 40, 43 and 45 in the thoracic aorta (A,C) and caudal artery (B,D) of 3 (A,B) and 12 (C,D) week old WKY and SHR. Values are mean ± SEM. [*]$P<0.05$, significantly different from the WKY. [†]$P<0.05$, significantly different from 3 week animals. Copy numbers are expressed per copy of 18S ribosomal RNA by using plasmid standard curves. Data for 12 week animals is duplicated from Chapter 5 for comparison.

3 weeks

A Thoracic aorta

B Caudal artery

12 weeks

C Thoracic aorta

D Caudal artery

normalized number of Cx molecules (10^{-3})
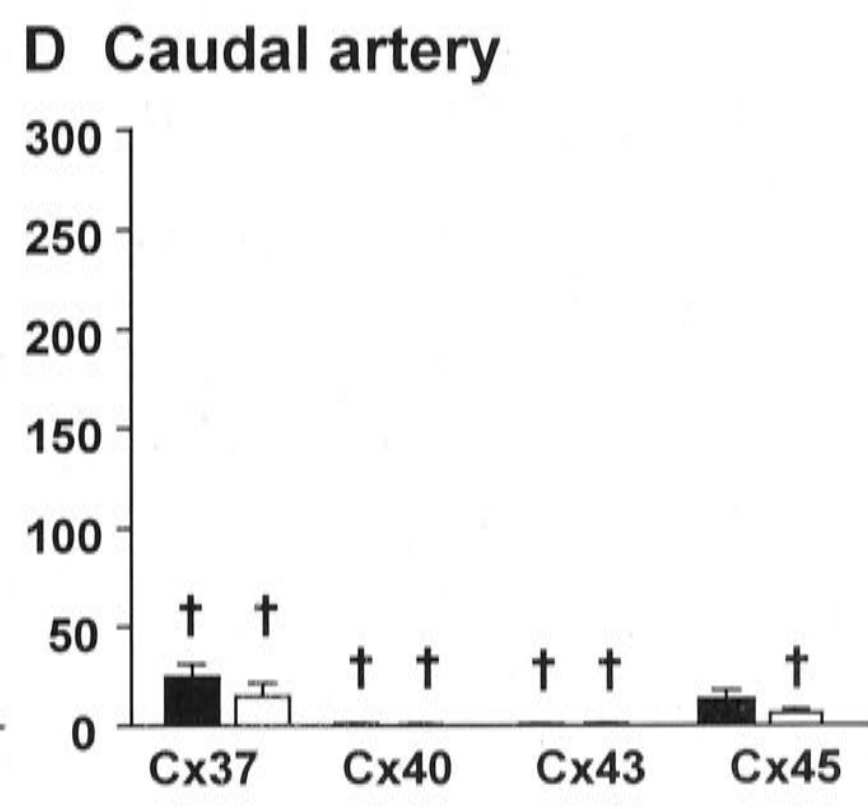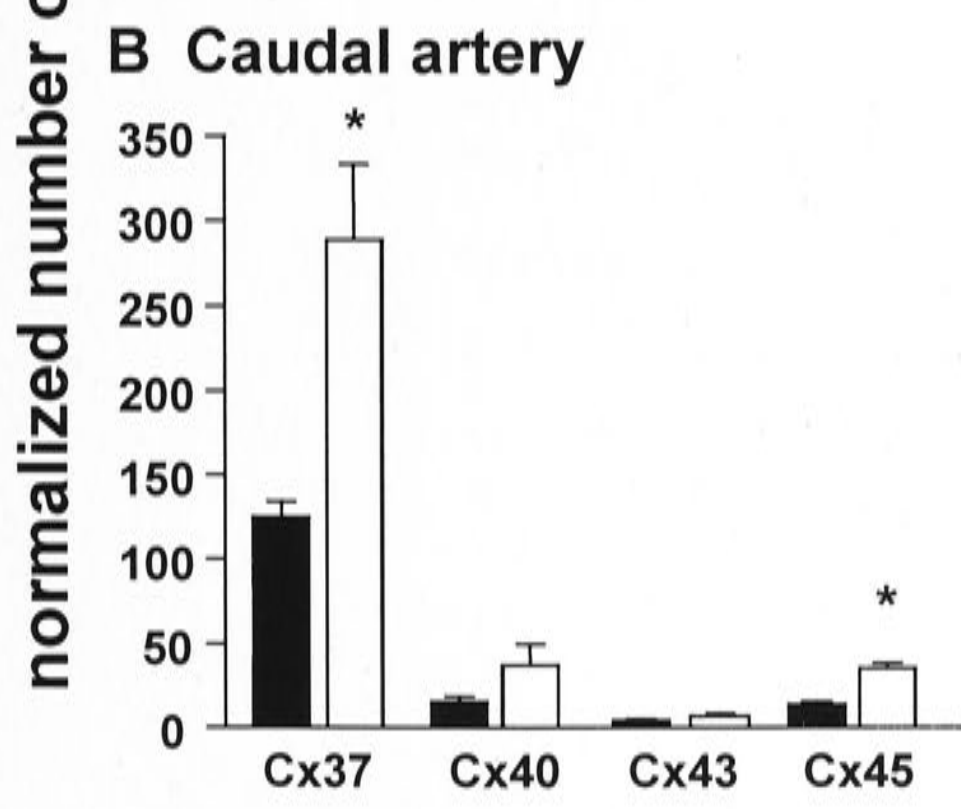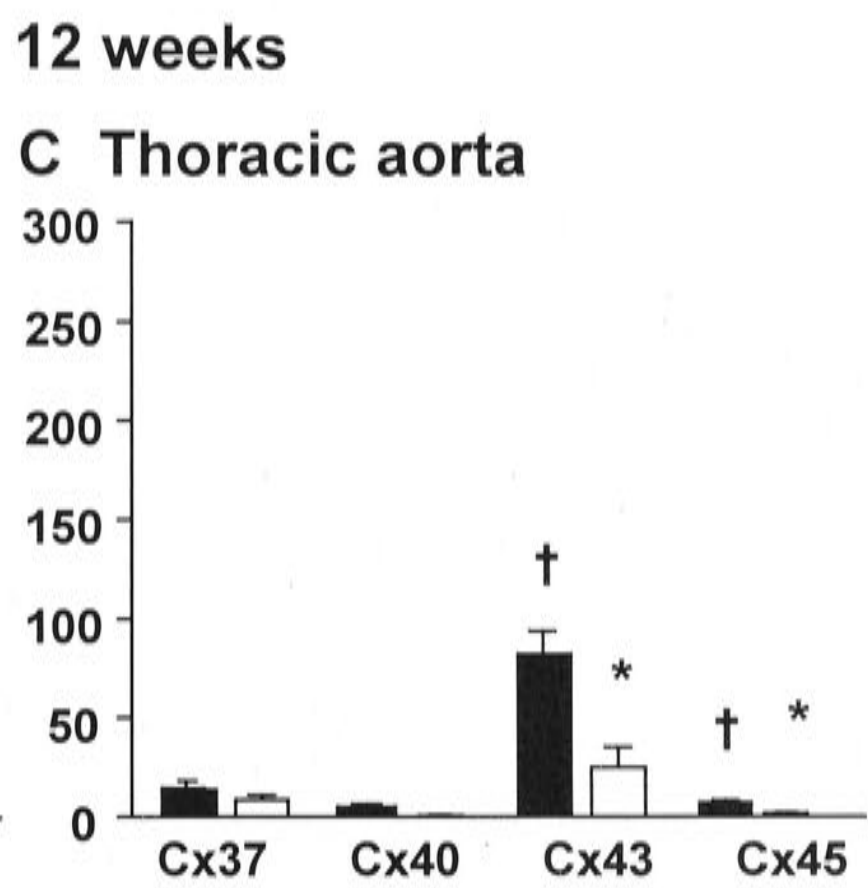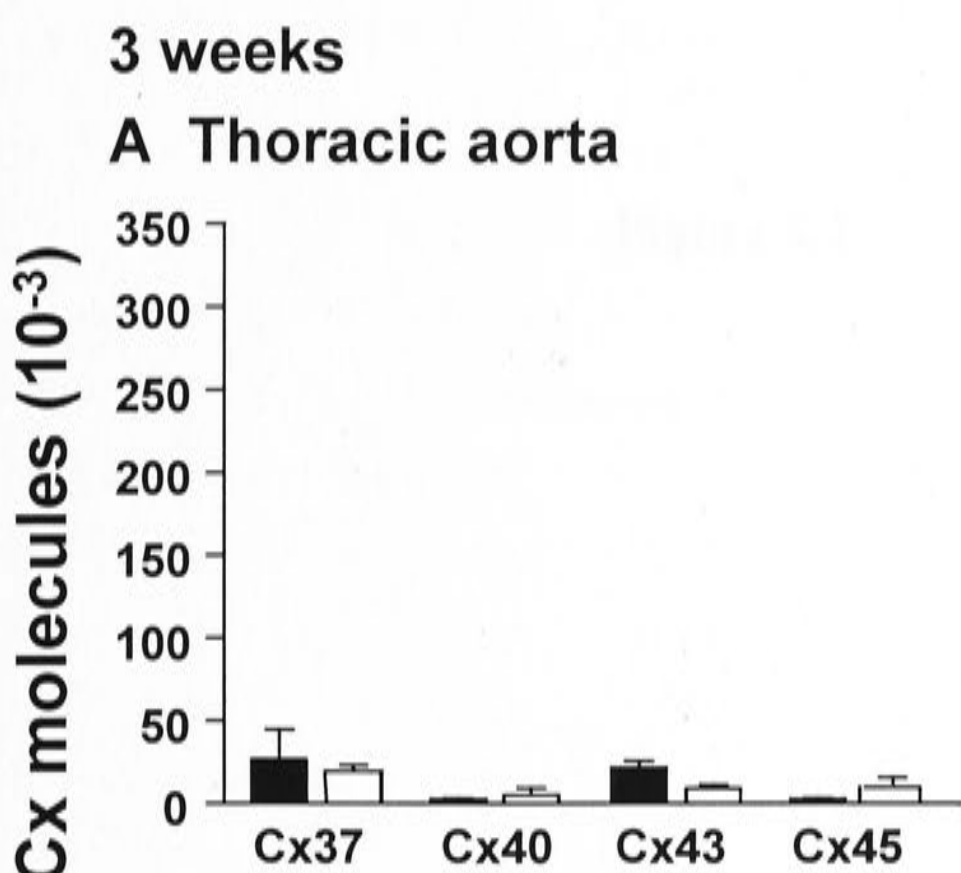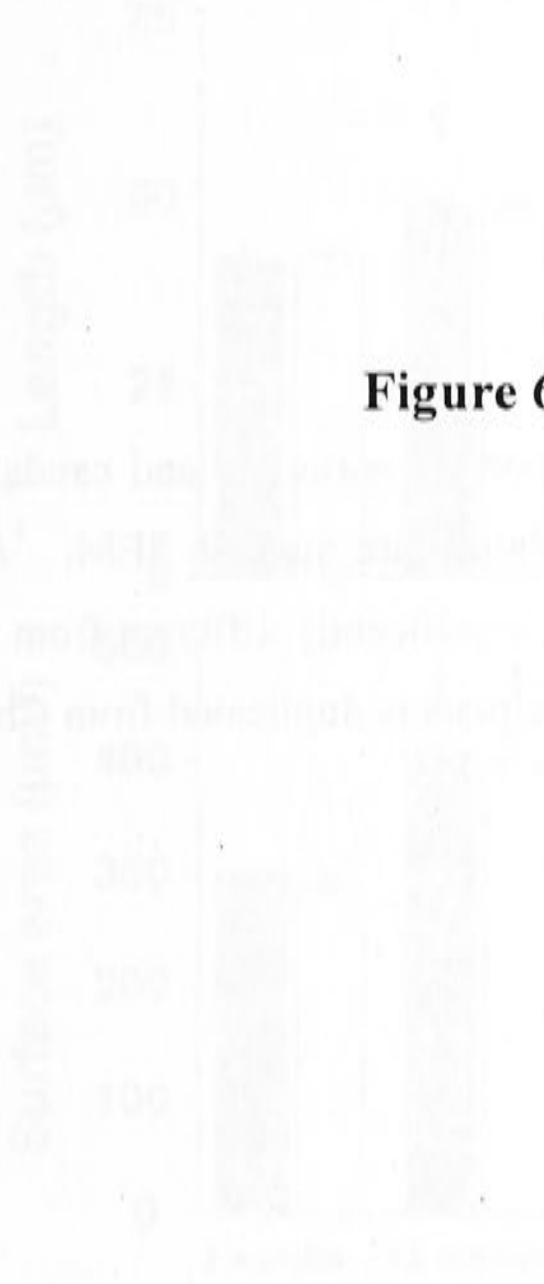
Figure 6.2

Figure 6.2.

Morphology of endothelial cells from the thoracic aorta (A) and caudal artery (B) of 3 and 12 week old WKY and SHR rats. Values are mean ± SEM. *$P<0.05$, significantly less than age matched WKY. †$P<0.05$, significantly different from 3 week old strain matched rats. n=3-4. Data for 12 week animals is duplicated from Chapter 5 for comparison.

A Thoracic aorta

B Caudal artery

WKY
SHR

In the caudal artery of WKY rats, between 3 and 12 weeks of age, there was no significant change in the surface area, length, width or perimeter of endothelial cells ($P>0.05$, Figure 6.2B). In SHR rats over the same developmental period, endothelial cell surface area, length and perimeter decreased significantly ($P<0.05$), while width did not change during development ($P>0.05$, Figure 6.2B).
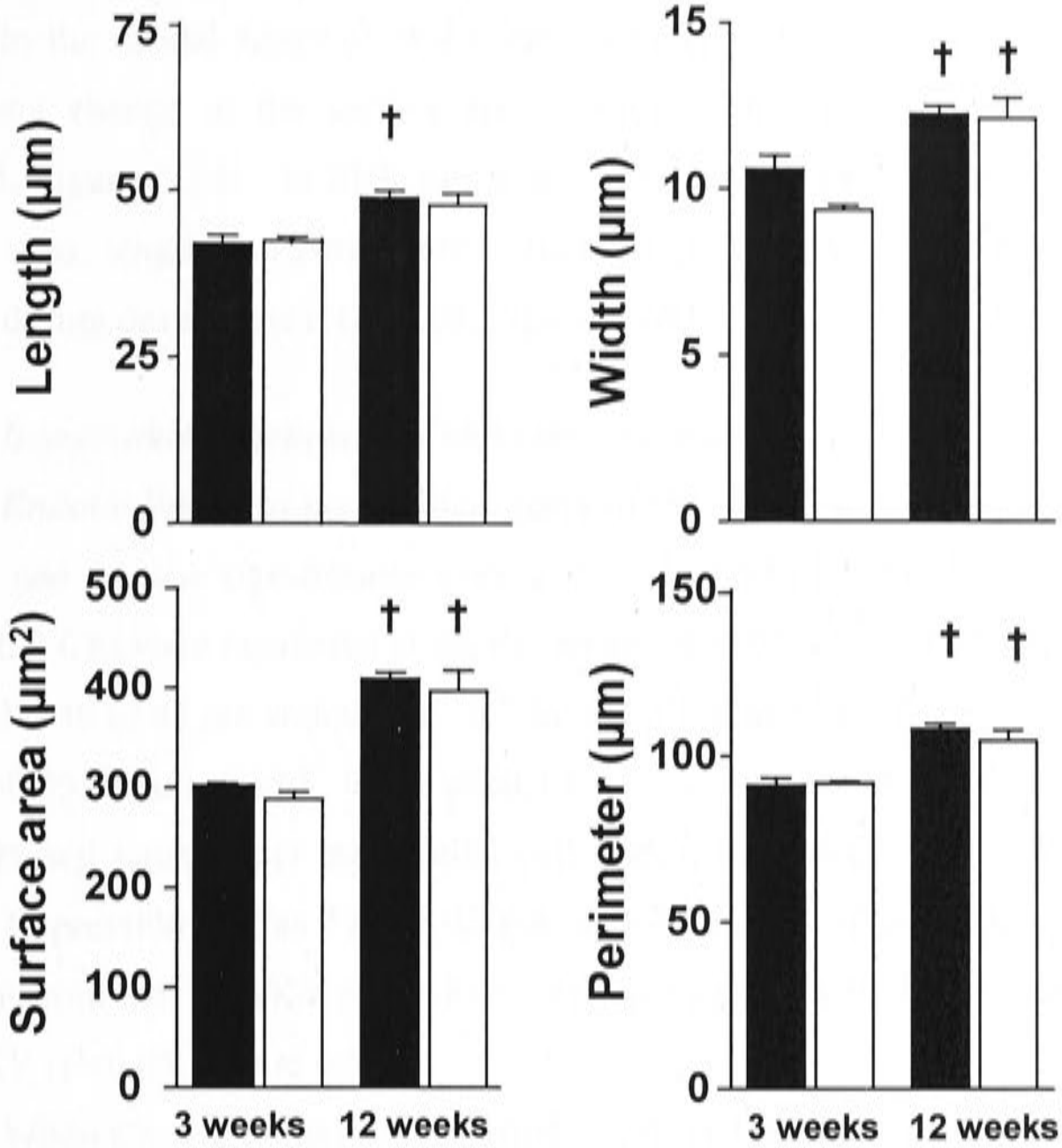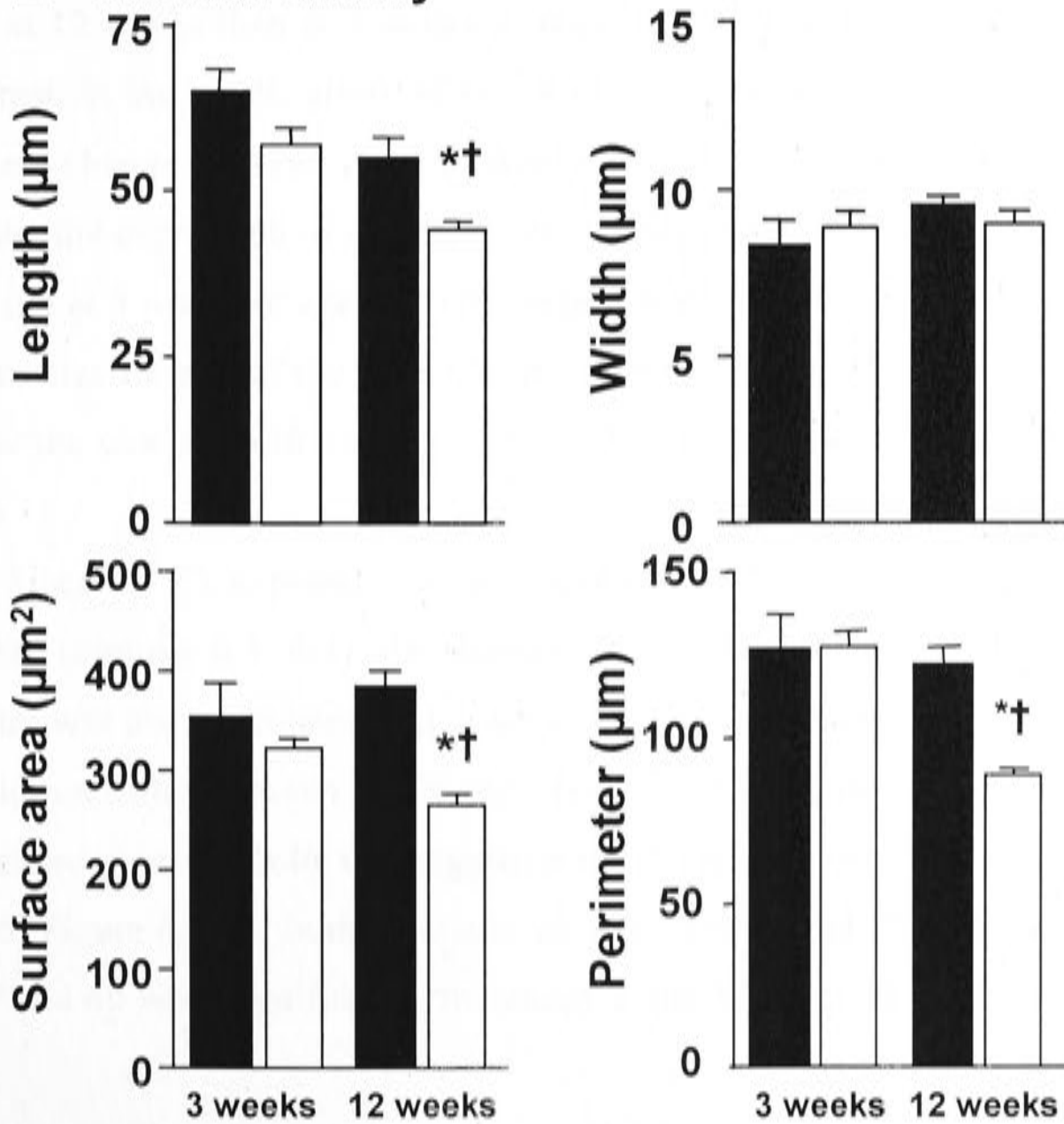
6.2.3 *Immunohistochemistry of vascular connexins*

Endothelium. In the thoracic aorta of the WKY at 3 weeks of age, expression of Cxs 37 and 40 was significantly greater than for Cx43 ($P<0.05$, Figure 6.3A-D). In the SHR, all 3 Cxs were expressed at similar levels ($P>0.05$, Figure 6.3E-H, 6.5A). Expression of Cxs 37, 40 or 43 per endothelial cell did not differ between WKY and SHR at 3 weeks of age ($P>0.05$, Figure 6.5A). In the caudal artery, at 3 weeks of age, Cxs 37, 40 and 43 were all expressed equally per endothelial cell within both WKY and SHR rats (Figure 6.4, 6.5B). Expression of Cxs 37 and 43 per endothelial cell in the SHR was not significantly different from that in WKY rats, while Cx40 was significantly lower than expression within the WKY ($P<0.05$, Figure 6.5B).

When Cx expression per endothelial cell at 3 weeks was compared to 12 weeks of age (see Chapter 5) in the thoracic aorta, expression of all three Cxs was significantly greater at 12 weeks than at 3 weeks in both the WKY and SHR ($P<0.05$, Figure 6.5A,E). In contrast, in the caudal artery of the WKY, expression of Cxs 37, 40 and 43 showed no significant change between 3 and 12 weeks ($P>0.05$, Figure 6.5B,F). On the other hand, in SHR rats, the expression of all three Cxs was significantly lower at 12 weeks compared to expression at 3 weeks of age ($P<0.05$, Figure 6.5B,F). There was no significant difference in plaque size for any of the three Cxs between WKY and SHR rats at either age ($P>0.05$), however the size of Cx40 plaques increased between 3 and 12 weeks in the SHR ($P<0.05$, Table 6.1).

Since the Cx expression in the endothelium was almost exclusively around the cell perimeter (Figures 6.3, 6.4), the density of Cx plaques per 100 μm of endothelial cell perimeter was also calculated. At 3 weeks of age, the density of Cx plaques in the thoracic aorta did not differ between WKY and SHR ($P>0.05$, Figure 6.5C); however, in the caudal artery expression of Cx40 was significantly reduced in the SHR compared to the WKY ($P<0.05$, Figure 6.5D). In the thoracic aorta between 3 and 12 weeks of age, the density of Cxs 37 and 40 were significantly increased in the WKY at 12 weeks compared to 3 weeks

79

Figure 6.3

Figure 6.3.

Cx expression in endothelial cells from the thoracic aorta of WKY (A-D) and SHR (E-H) rats at 3 weeks of age. The endothelium is viewed *en face* following incubation in antibodies against Cxs 37 (B,F), 40 (A,C,E,G) and 43 (D,H). Typical punctate Cx expression delineates the borders of endothelial cells. Panels B-D and F-H are magnified images illustrating Cx plaques outlining the perimeter of endothelial cells. Calibration bars represent 20 μm.
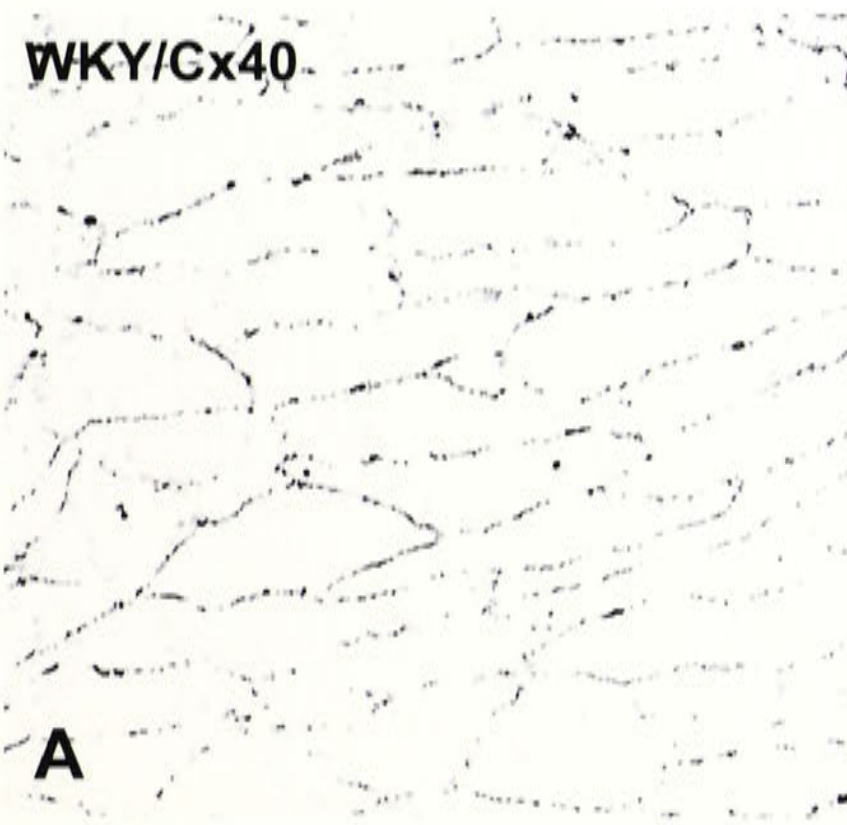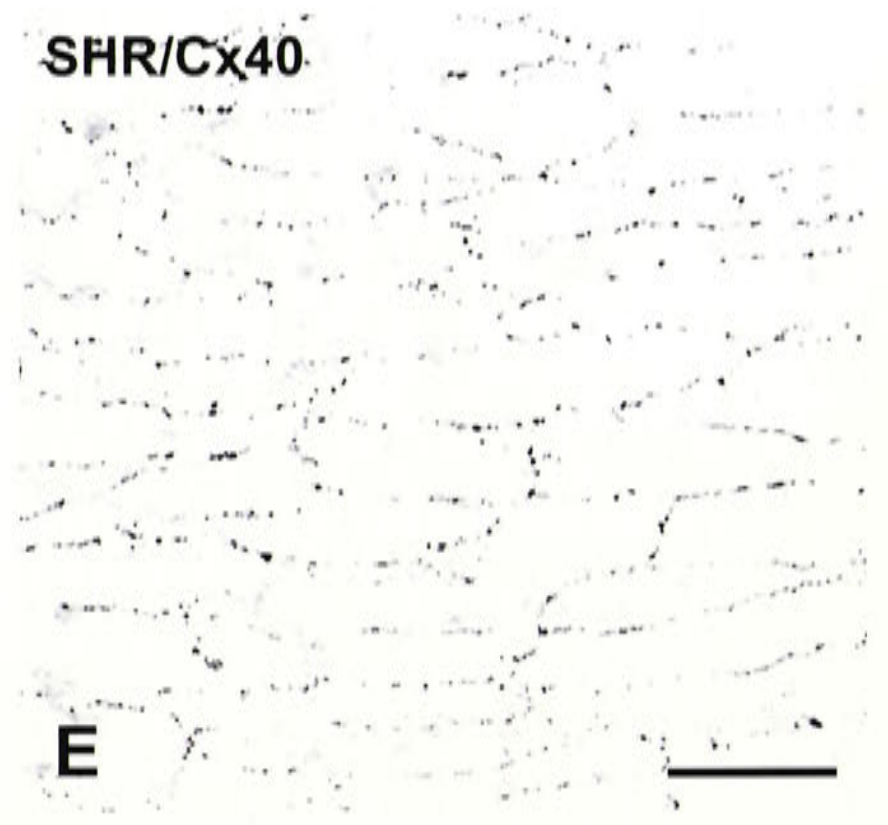
WKY/Cx40   A   SHR/Cx40   E
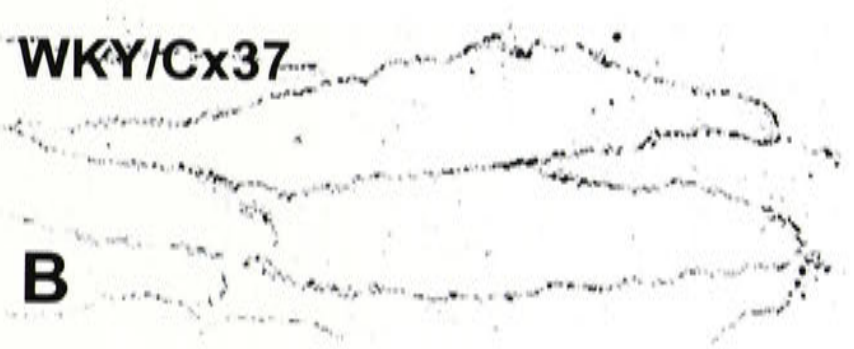
WKY/Cx37   B   SHR/Cx37   F
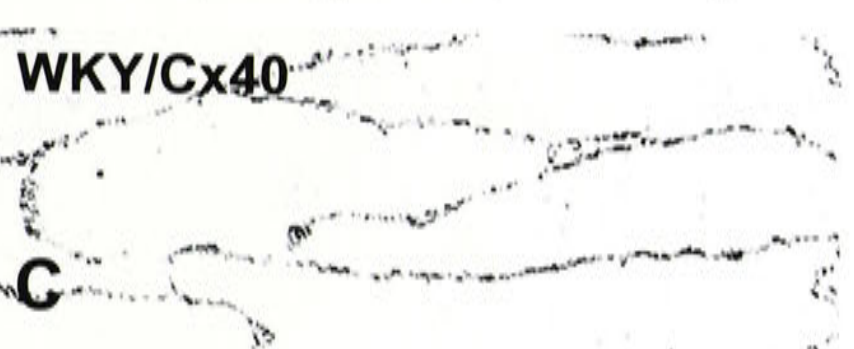
WKY/Cx40   C   SHR/Cx40   G

WKY/Cx43   D   SHR/Cx43   H

Figure 6.4

Figure 6.4.

Cx expression in endothelial cells from the caudal artery of WKY (A-D) and SHR (E-H) rats at 3 weeks of age. The endothelium is viewed *en face* following incubation in antibodies against Cxs 37 (B,F), 40 (A,C,E,G) and 43 (D,H). Typical punctate Cx expression delineates the borders of endothelial cells. Panels B-D and F-H are magnified images illustrating Cx plaques outlining the perimeter of endothelial cells. Calibration bars represent 20 μm.

WKY/Cx40

SHR/Cx40

A

E

WKY/Cx37

SHR/Cx37

B

F

WKY/Cx40

SHR/Cx40

C

G

WKY/Cx43

SHR/Cx43

D

H

Figure 6.5

Figure 6.5.

Expression of protein for Cxs 37, 40 and 43 in the endothelium of the thoracic aorta (A,C,E,G) and caudal artery (B,D,F,H) of 3 (A-D) and 12 (E-H) week old WKY and SHR rats. Cx plaques are expressed per endothelial cell (A,B,E,F) and as the density of Cx plaques per 100 μm of endothelial cell perimeter (C,D,G,H). Values are mean ± SEM. *$P<0.05$, significantly different from Cx expression in the WKY. †$P<0.05$, significantly greater than 3 week animals. $n=3-4$ animals. Data for 12 week animals is duplicated from Chapter 5 for comparison.
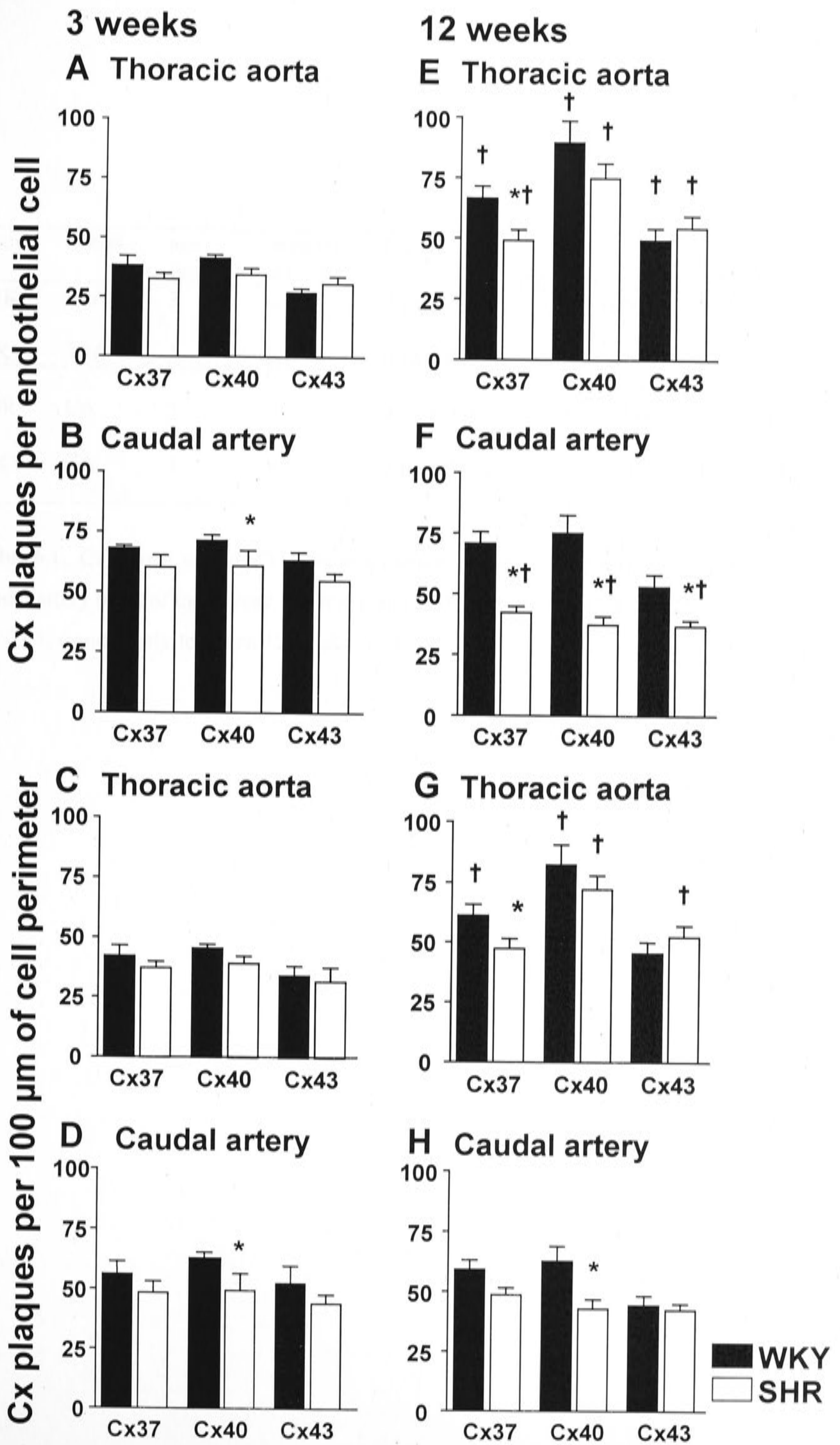
strain	vessel	age (weeks)	number of animals	Cx37	Cx40 plaque size (μm^2)	Cx43
SHR	ThA	3	3	0.13 ± 0.001	$0.13 \pm 0.001^{*}$	$0.13 \pm 0.004^{*}$
WKY	ThA	3	3	0.13 ± 0.003	0.13 ± 0.002	0.14 ± 0.004
SHR	CA	3	4	0.15 ± 0.003	0.15 ± 0.003	0.15 ± 0.01
WKY	CA	3	4	0.15 ± 0.002	0.14 ± 0.002	0.16 ± 0.003

Table 6.1. Cx plaque size (μm^2) in the endothelium of the thoracic aorta (ThA) and caudal artery (CA) of the 3 week old WKY and SHR. Values are mean $\pm$ SEM. [*]$P<0.05$, significantly less then 12 weeks. $n=4$.

of age, while Cxs 40 and 43 were increased in the SHR at 12 weeks ($P<0.05$, Figure 6.5C,G). In the caudal artery between 3 and 12 weeks of age, the density of Cx plaques did not differ in either the WKY or SHR ($P>0.05$, Figure 6.5D,H).

In each case, no Cx labeling was observed in the absence of primary antibody, or following pre-incubation of primary antibody with its antigenic peptide.

Smooth muscle. Longitudinal and transverse sections of the 3-week old thoracic aorta and caudal artery taken from the WKY and SHR were analyzed for the medial expression of Cxs 37, 40, 43 and 45. Cx37 was sparsely expressed in the thoracic aorta in both strains (Figures 6.6A,E). In the caudal artery Cx37 expression was more abundant, but did not differ between WKY and SHR rats ($P>0.05$, Figures 6.7A,E, 6.8B,D). Cx40 could not be detected in the media of the thoracic aorta or caudal artery from either strain (Figures 6.6B,F, 6.7B,F). Cx43 was abundantly expressed in the media of the thoracic aorta and did not differ between WKY and SHR ($P>0.05$, Figures 6.6C,G, 6.8A,C), but was not detected in the media of the caudal artery of either strain (Figures 6.7C,G). The expression of Cx43 in the thoracic aorta of both the WKY and SHR was significantly greater than expression of any other Cx ($P<0.05$, Figure 6.6, 6.7, 6.8A,C). Cx45 was sparsely detected in the media of both arteries studied and did not differ between longitudinal and transverse sections ($P<0.05$, Figure 6.6D,H, 6.7D,H, 6.8). In the thoracic aorta, Cx45 expression did not differ between WKY and SHR. However, in the caudal artery, Cx45 expression was significantly greater in transverse sections in the SHR compared to the WKY ($P<0.05$, Figures 6.8A-D).

In transverse sections of the thoracic aorta, between 3 and 12 weeks of age (see Chapter 5), expression of Cx37 was increased in both the WKY and SHR at 12 weeks compared to 3 weeks of age ($P<0.05$, Figure 6.8C,G). Cx43 was increased in transverse sections of the WKY thoracic aorta at 12 weeks of age ($P<0.05$, Figure 6.8C,G), while expression was not altered in the SHR during development. The expression of Cx45 in the thoracic aorta was increased during development in the WKY (Figure 6.8C,G). In transverse sections of the caudal artery, between 3 and 12 weeks, expression of Cx37 did not differ in either the WKY or the SHR. Expression of Cx45 was greater at 12 weeks compared to 3 weeks of age in transverse sections of both the WKY and SHR ($P<0.05$, Figure 6.8D,H). Cx expression did not differ in longitudinal sections of either the thoracic aorta or caudal artery between 3 and 12 weeks.

Figure 6.6

Figure 6.6.

Expression of Cxs 37 (A,E), 40 (B,F), 43 (C,G) and 45 (D,H) in the media of the thoracic aorta from 3 week old WKY (A-D) and SHR (E-H) (transverse sections). e, endothelium, sm, smooth muscle. Calibration bar represents 10 μm.

WKY / Cx37 — e — sm — A

SHR / Cx37 — e — sm — E

WKY / Cx40 — e — sm — B

SHR / Cx40 — e — sm — F

WKY / Cx43 — e — sm — C

SHR / Cx43 — e — sm — G

WKY / Cx45 — sm — D

SHR / Cx45 — e — sm — H
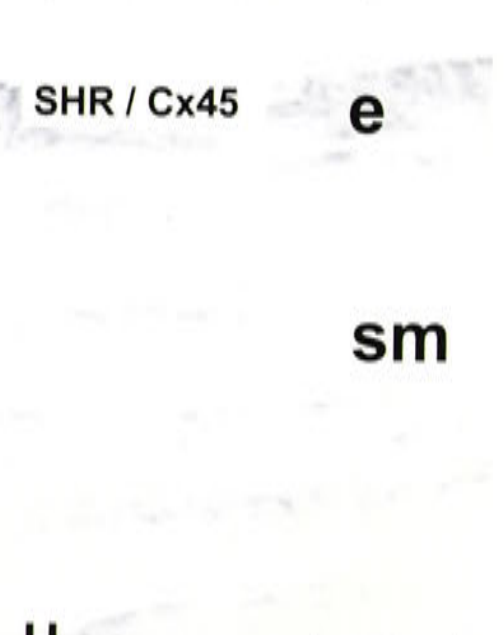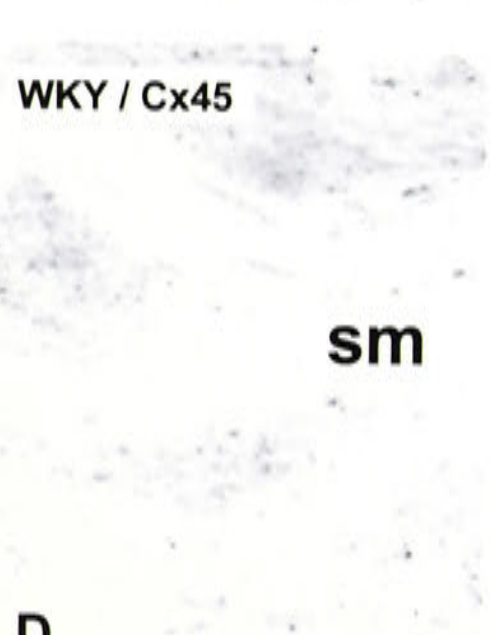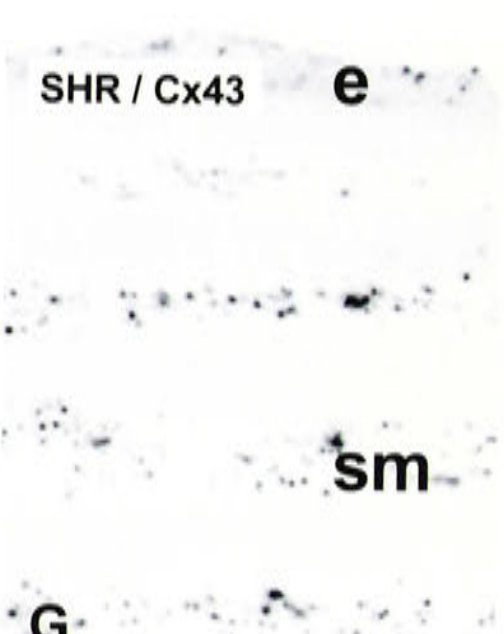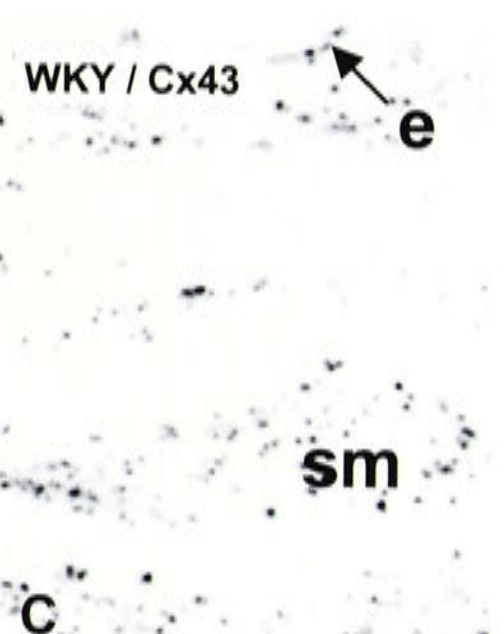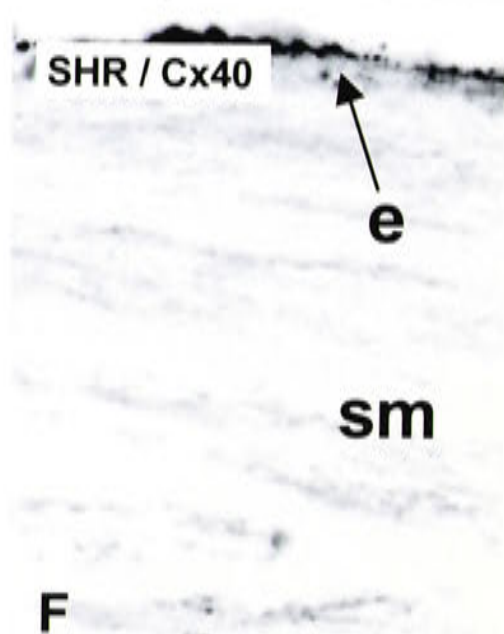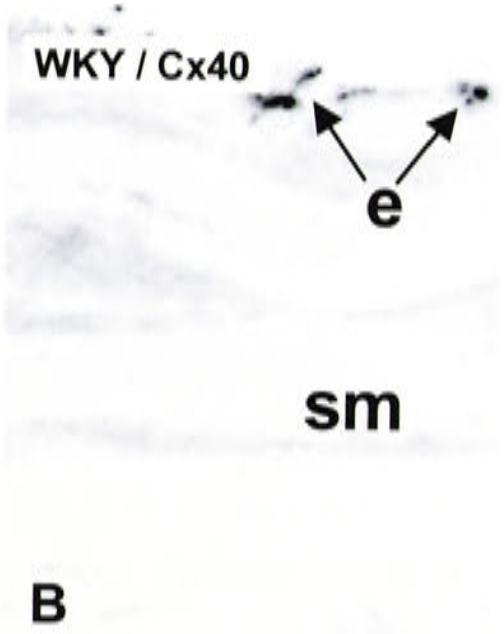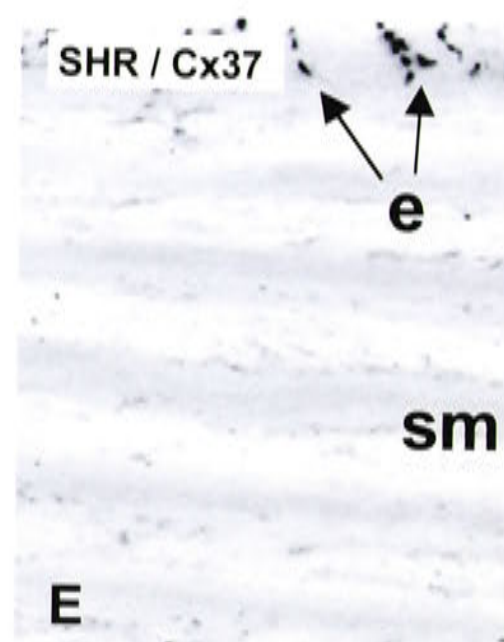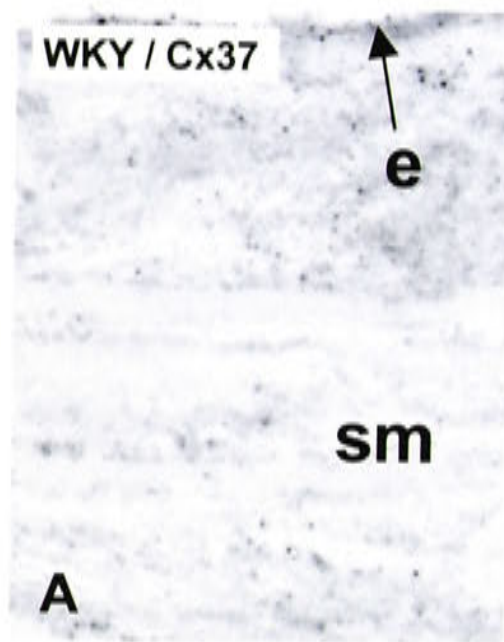
Figure 6.7

Figure 6.7.

Expression of Cxs 37 (A,E), 40 (B,F), 43 (C,G) and 45 (D,H) in the media of the caudal artery from 3 week old WKY (A-D) and SHR (E-H) (transverse sections). e, endothelium, sm, smooth muscle. Calibration bar represents 10 μm.

WKY / Cx37 — e sm — A

SHR / Cx37 — e sm — E

WKY / Cx40 — e sm — B

SHR / Cx40 — e sm — F

WKY / Cx43 — e sm — C

SHR / Cx43 — e sm — G

WKY / Cx45 — e sm — D

SHR / Cx45 — e sm — H
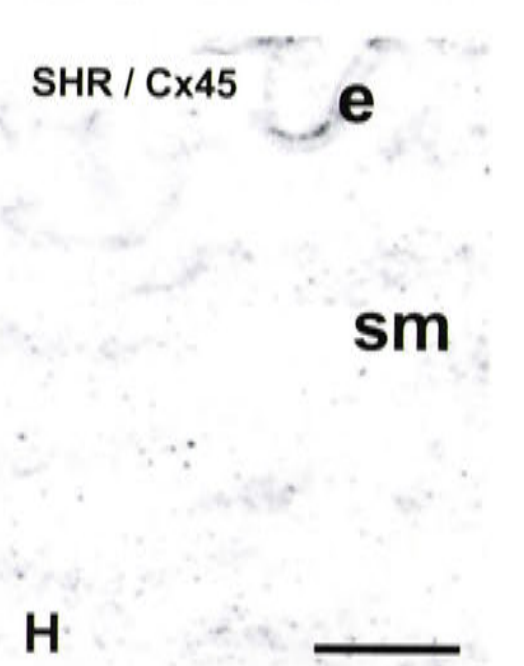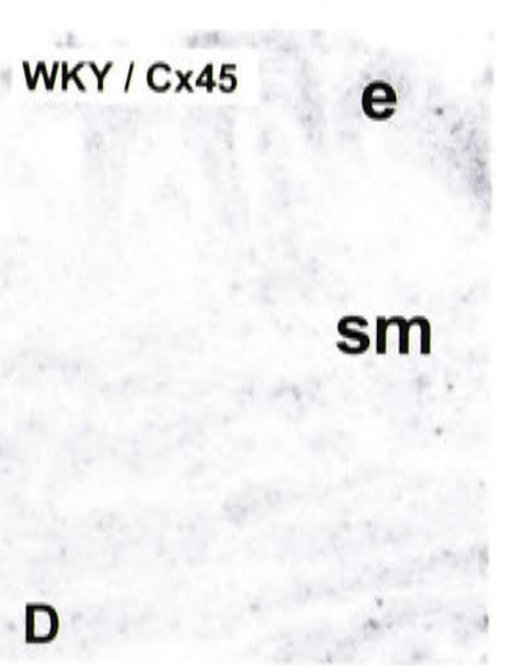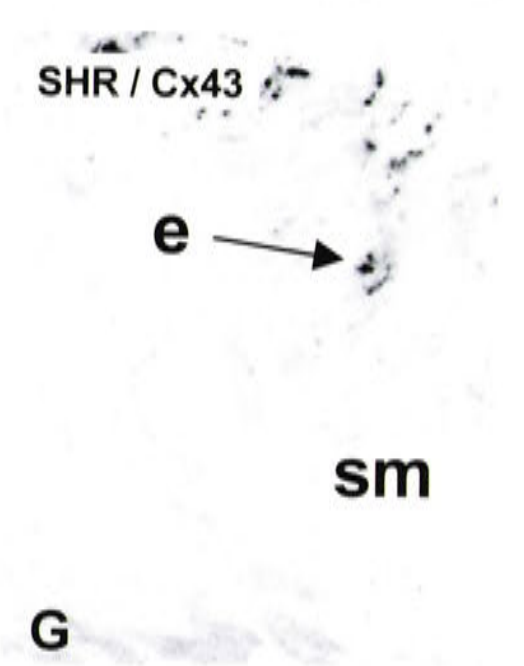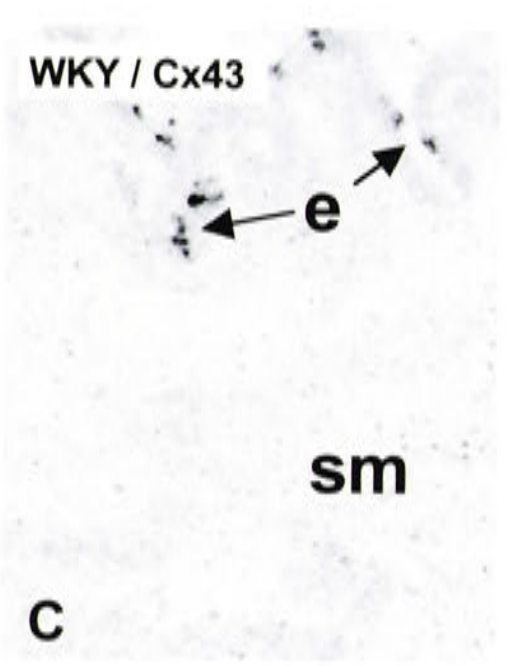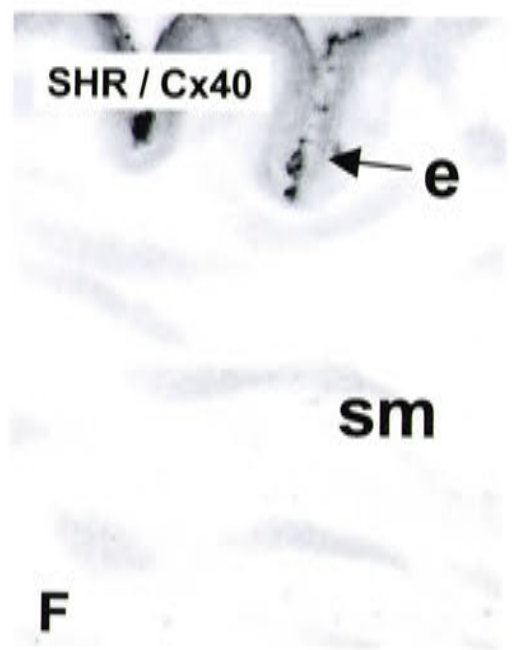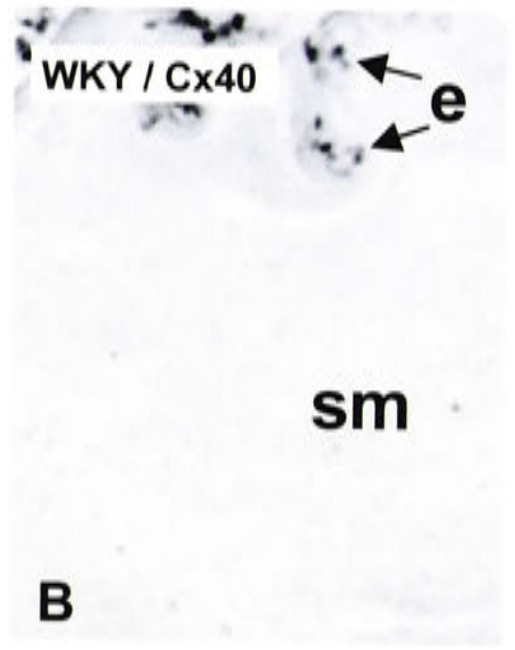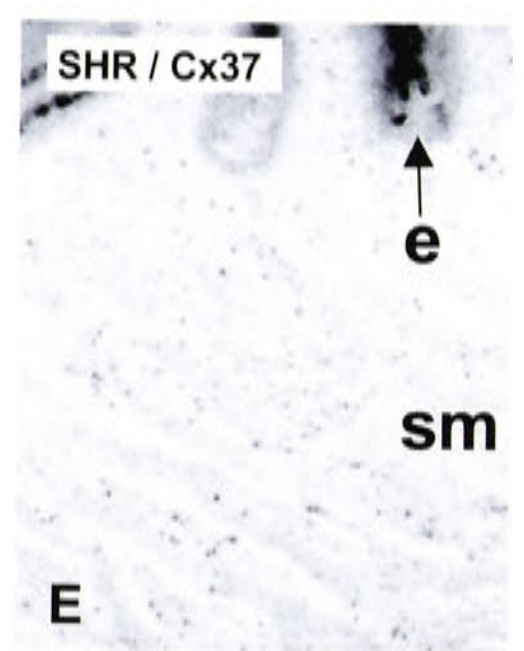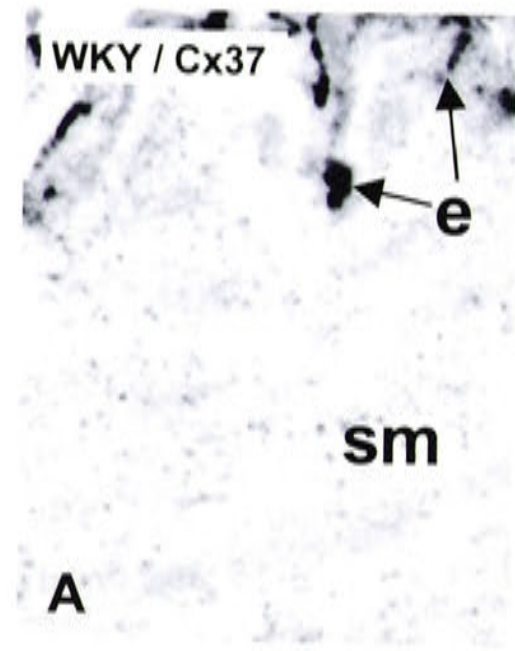
Figure 6.8

Figure 6.8.

Protein expression for Cxs 37, 40, 43 and 45 in the smooth muscle of the thoracic aorta (A,C,E,G) and caudal artery (B,D,F,H) of 3 (A-D) and 12 (E-F) week old WKY and SHR rats. Values are expressed as plaques per μm^2 in longitudinal (A,B,E,F) and transverse (C,D,G,H) sections. Values are mean $\pm$ SEM. $^*P<0.05$, significantly different to WKY. $^\dagger P<0.05$, significantly different to 3 week animals. $n=4$ animals. Data for 12 week animals is duplicated from Chapter 5 for comparison.

3 weeks

A Thoracic aorta

Plaques per µm²
Longitudinal sections

Cx37 Cx40 Cx43 Cx45

B Caudal artery

Plaques per µm²
Longitudinal sections

Cx37 Cx40 Cx43 Cx45

C Thoracic aorta

Plaques per µm²
Transverse sections

Cx37 Cx40 Cx43 Cx45

D Caudal artery

Plaques per µm²
Transverse sections

Cx37 Cx40 Cx43 Cx45
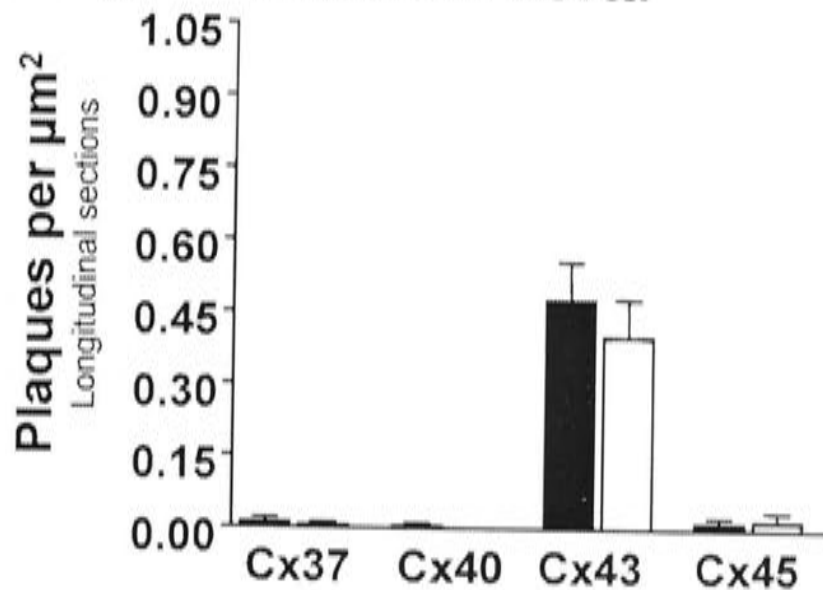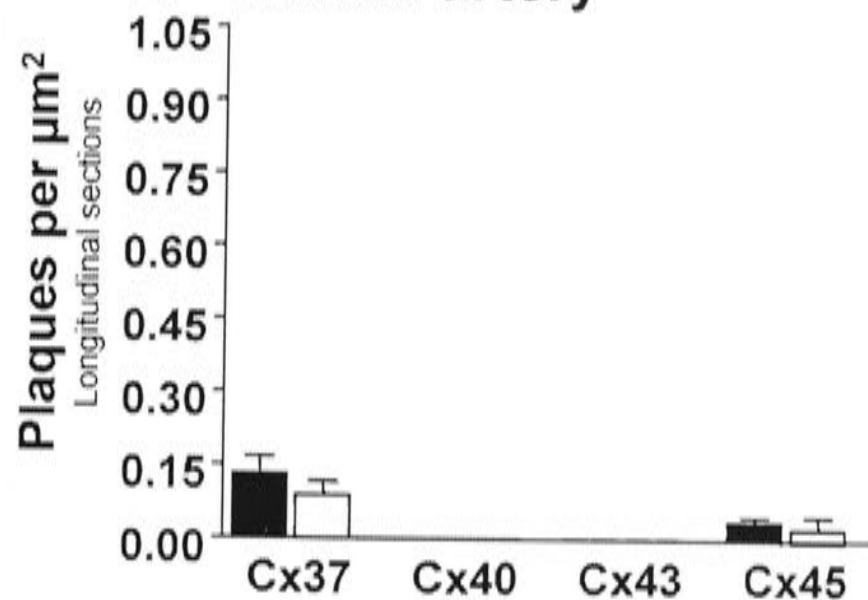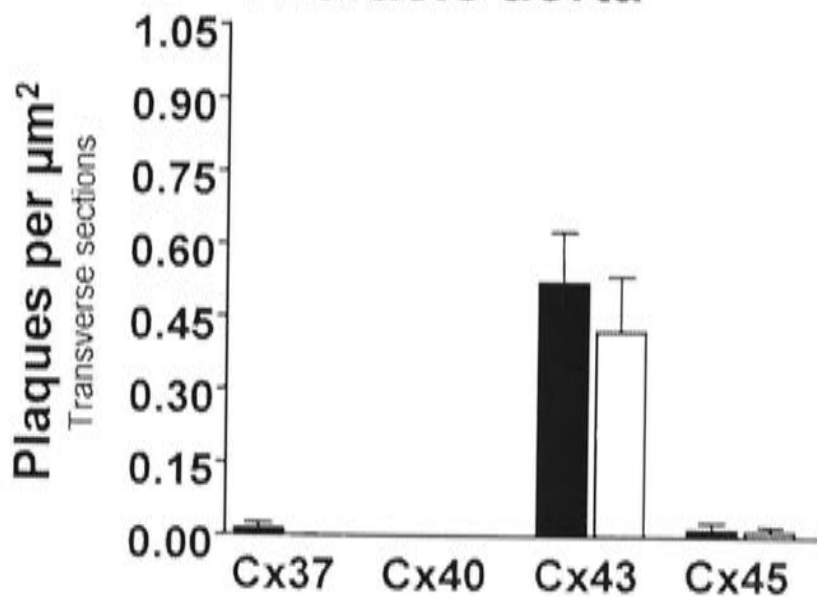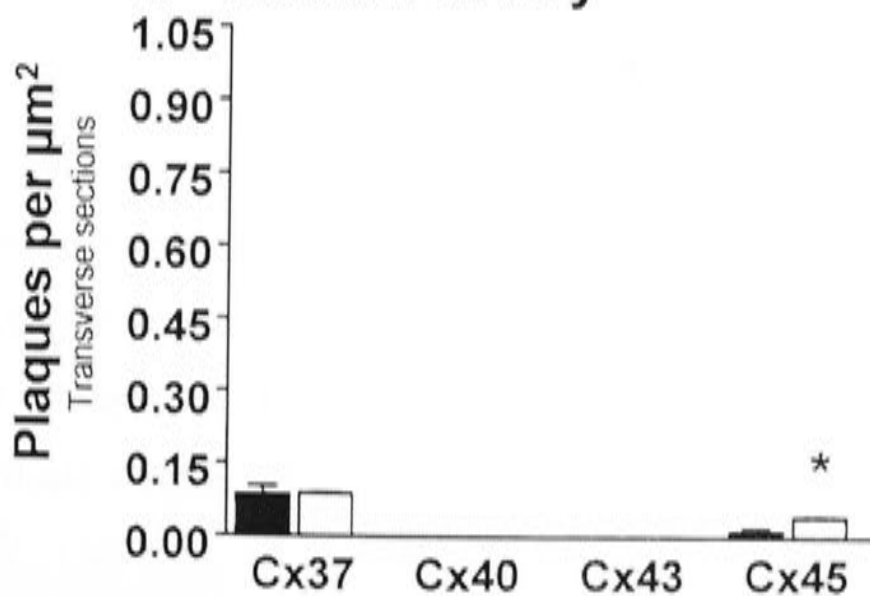
12 weeks

E Thoracic aorta

Cx37 Cx40 Cx43 Cx45

F Caudal artery

Cx37 Cx40 Cx43 Cx45

G Thoracic aorta

Cx37 Cx40 Cx43 Cx45
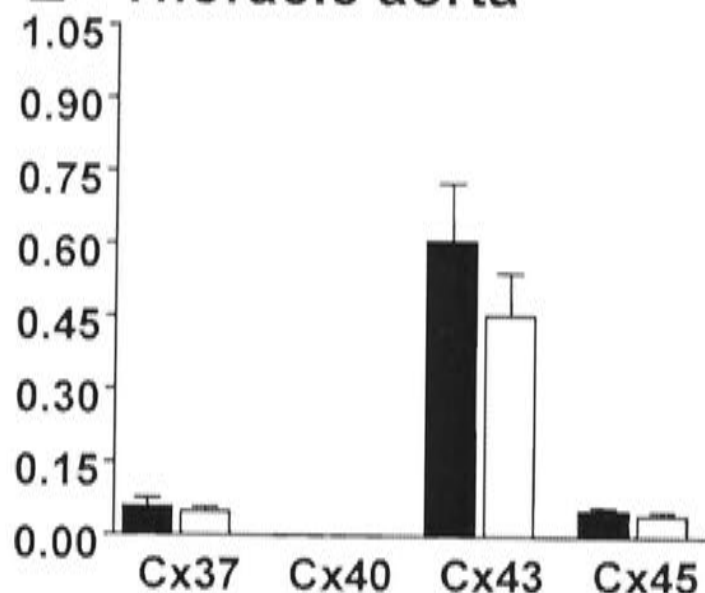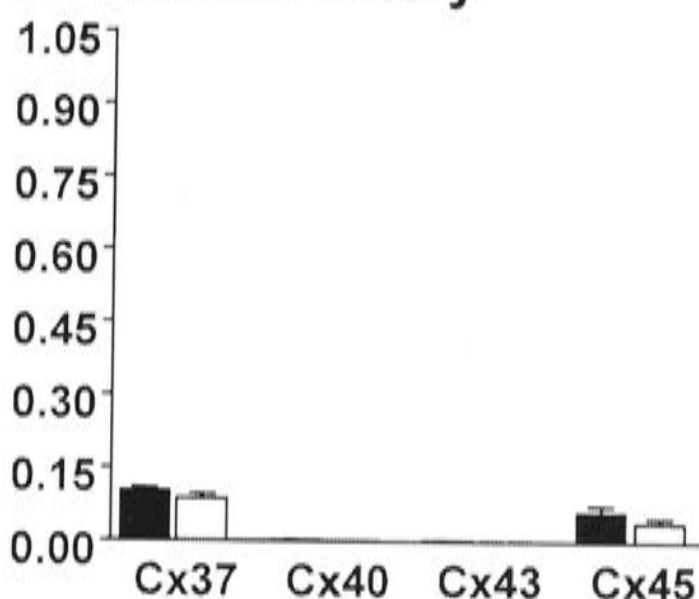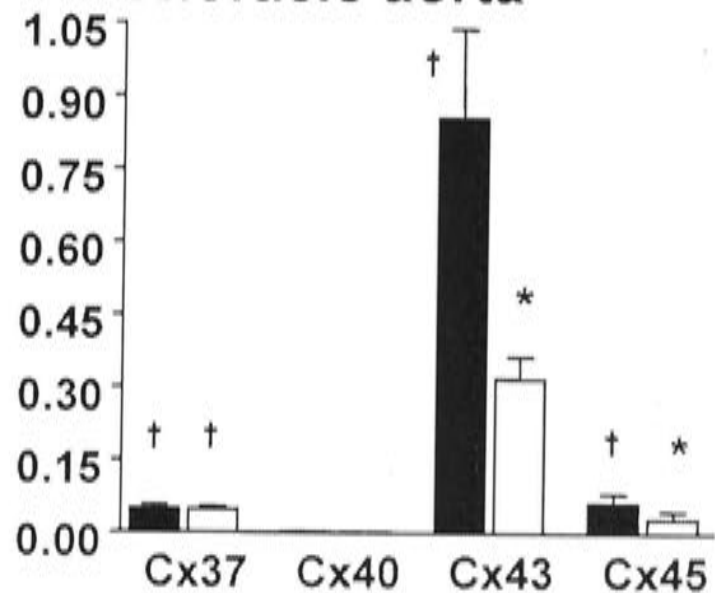
H Caudal artery

■ WKY
□ SHR

Cx37 Cx40 Cx43 Cx45
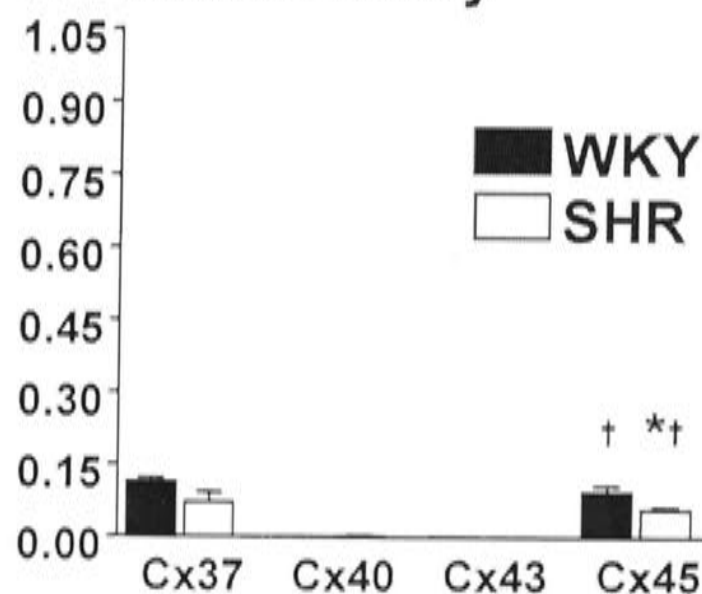
6.3 DISCUSSION

The results of the current Chapter have demonstrated several differences in the time course of the morphological development and Cx expression in the thoracic aorta and the caudal artery of WKY and SHR. While the caudal artery appeared to be developmentally mature at 3 weeks, the thoracic aorta was still relatively immature, in that changes in Cx expression and cell size continued to occur in the latter vessel. Thus, the morphological differences and alterations in Cx expression observed in the 3 month hypertensive rats compared to the normotensive rats represented a failure of the normal developmental increase in Cx expression in the aorta, but a selective decrease in cell size and Cx expression in the caudal artery. Furthermore, in the caudal artery of the SHR, a decrease in the expression of Cx40 within the endothelium and an increase in Cx45 within the smooth muscle precede the increase in blood pressure, thus suggesting a causative role for these Cxs in the development of hypertension. In contrast, in the thoracic aorta, Cx expression was similar in both the WKY and SHR in the pre-hypertensive period, suggesting no role in the development of hypertension.

During normal vascular development of the thoracic aorta in the WKY rat, endothelial cell size increased with age in a similar pattern to that previously reported (Yeh *et al.* 2000). In parallel, expression of protein for all 3 Cxs per endothelial cell was significantly increased during development. However, when expressed as the density of Cx plaques per length of cell membrane, the increase in Cx43 expression per endothelial cell resulted simply from the increase in cell size, while the density of Cxs 37 and 40 increased during development. In contrast to these results Yeh *et al.* (2000), reported that the expression of Cx43 was reduced in the thoracic aorta during development, while Cx40 remained highly expressed throughout development and into old age, and expression of Cx37 fluctuated. The reason for this discrepancy in results may reflect the time points examined in each study. While Yeh *et al.* (2000), studied expression between 4 weeks and 16 months, no intermediate time points were examined. In contrast to the thoracic aorta, endothelial cell size and Cx protein expression in the caudal artery of the WKY were maximal at 3 weeks of age with no further increase seen at 12 weeks, suggesting that development of the caudal artery may occur more rapidly than that for the thoracic aorta. Furthermore, the differing results may reflect the functional differences between the two blood vessels. The thoracic aorta is a large conduit vessel and as such has little role in the

control of peripheral resistance and therefore blood pressure. On the contrary, control of peripheral resistance occurs within muscular arteries (Folkow, 1982; Christensen & Mulvany, 2001). Therefore it is likely that development of these latter vessels may be more advanced at a younger age to ensure the maintenance of vascular haemodynamics and efficient tissue perfusion.

In the thoracic aorta of the SHR, endothelial cell size increased in a similar pattern during development to that observed in the WKY, suggesting that endothelial cell development is not affected by, or contributes to increased blood pressure. However, in other studies a transient increase in cell size has been described in the thoracic aorta of animals made hypertensive by aortic ligation, although such a possibility cannot be excluded in the present study (Hüttner et al. 1979). In parallel with the increase in cell size, expression of Cxs 37, 40 and 43 within the endothelium of the thoracic aorta also increased during development. The reduced expression of Cx37 in the SHR compared to the WKY at 12 weeks is likely to result from a failure of the developmental increase in Cx37 as seen in the WKY. The reduced Cx37 expression was apparently due to a smaller number of plaques per endothelial cell and not changes in individual plaque size. A lack of change in gap junctional area has also been reported in the thoracic aorta of various hypertensive models (Hüttner et al. 1982; McGuire & Twietmeyer, 1985), although transient increases in gap junctional area have been reported during the period prior to blood pressure reaching maximal levels (McGuire & Twietmeyer, 1985). In contrast to the thoracic aorta, in the caudal artery of the SHR, endothelial cell size and Cx expression are decreased during development, since endothelial cells at 12 weeks of age were significantly smaller (30%) than those in 3 week old, pre-hypertensive SHR. As the effect on cell size was due to a reduction in cell length rather than cell width, any increase in the total number of endothelial cells in the SHR would be manifest in the longitudinal, rather than in the radial direction. However since the smaller luminal circumference (18%) in the SHR compared to the WKY would result in a 33% reduction in endothelial surface area per unit length of artery then it is possible that the reduction in endothelial cell size occurs secondarily to alterations in vascular geometry. In parallel with reduced endothelial cell size, expression of protein for Cxs 37, 40 and 43 within the endothelium of the caudal artery decreased significantly during development, due to a reduction in the number of gap junctional plaques per cell, rather than a reduction in individual plaque size.

As described in Chapter 4, mRNA preparations of arteries included smooth muscle cells and endothelial cells, however, in these preparations, smooth muscle cells predominate. In the thoracic aorta of WKY during development, expression of mRNA and protein for Cxs 43 and 45 in the smooth muscle increased, while expression of Cxs 37 and 40 was maximal at 3 weeks of age. A transient peak in Cx43 expression has been reported in smooth muscle cells of the thoracic aorta of 7-day old normotensive rats (Blackburn *et al.* 1997), which occurred in association with a developmental rise in blood pressure and a period when smooth muscle cells were undergoing proliferation, before differentiating into the contractile phenotype (Nakamura, 1988). Similarly, in the present study, an increase in both Cxs 43 and 45 occurred in parallel with the normal developmental rise in blood pressure. While there was abundant expression of protein for Cx43 in the thoracic aorta at 3 weeks, this was not reflected in mRNA expression. This may reflect the differential turnover of Cxs in young animals. In the caudal artery of the WKY, expression of mRNA for Cxs 37, 40 and 43 was maximal at 3 weeks of age, mRNA expression decreasing between 3 and 12 weeks. In contrast, the expression of protein for Cx45 increased in the smooth muscle during development. Together these results suggest that within the thoracic aorta, Cxs 43 and 45 are required for normal development, while in the caudal artery Cx45 may be more important. In the caudal artery at 3 weeks of age, expression of Cx45 was significantly greater in transverse but not in longitudinal sections of the SHR. As detailed in Chapter 5, the difference between longitudinal and transverse sections may reflect an increased role for radial rather than longitudinal coupling of smooth muscle cells in the caudal artery.

In the aorta of the SHR, the expression of mRNA and protein for all 4 Cxs was maximal at 3 weeks of age. During development, unlike in the WKY, there was no change in the expression of either Cxs 43 or 45. Together, these results suggest a role for Cx43 and to a lesser extent, Cx45 during development of smooth muscle cells within normotensive rats, while such a role may be altered in the SHR. In the caudal artery, expression of mRNA for Cxs 37 and 45, the 2 major Cxs expressed in the caudal artery (Chapter 4), were increased in the SHR at 3 weeks and expression was down regulated during development. While expression of protein for Cx45 was also increased at 3 weeks of age in the SHR, no such change was seen for Cx37. The increase in Cx45 may be associated with early medial remodeling, which occurs in the SHR.

At 3 weeks of age, before a significant increase in blood pressure could be recorded in SHR animals, there was a trend for the expression of Cxs 37, 40 and 43 to be less in the endothelium of the caudal artery compared to the WKY, and this reached significance for Cx40. In contrast, in the media of the caudal artery, expression of Cx45 was greater in the SHR compared to the WKY at 3 weeks. The observed trend to a decrease in Cx expression in the endothelium and an increase in expression in the media at 3 weeks may suggest a causative role for these changes in the development of the hypertension. Alternatively, these differences may reflect inherent differences between the two strains. In terms of cause and effect, treatment of the SHR with anti-hypertensive drugs such as ACE inhibitors, will be necessary to differentiate between these two hypotheses. Other changes, which are associated with hypertension, have been reported in the blood vessels of pre-hypertensive rats, such as an up-regulation of Rho-kinase, which is thought to precede the development of hypertension (Mukai *et al.* 2001). In contrast to the caudal artery, there was no significant difference in Cx expression within the endothelium or in the medial layers of the thoracic aorta between WKY and SHR at 3 weeks of age.

In conclusion, the results presented in this Chapter have demonstrated that the reductions in the expression of Cx40 in the endothelium of the caudal artery at 12 weeks of age (Chapter 5) are also present in pre-hypertensive rats. In a similar manner, there was an increase in the expression of Cx45 in the media, suggesting that such changes may contribute to the development of hypertension. In contrast, no changes in cellular morphology or Cx expression were found in the thoracic aorta before the onset of hypertension. These results indicate that remodeling of the endothelium in both the thoracic aorta and caudal artery, and the changes observed in Cx expression in the smooth muscle and endothelium of the thoracic aorta at 12 weeks of age, as demonstrated in Chapter 5, may occur in response to elevated blood pressure rather than contributing to the development of hypertension.

CHAPTER 7

CONNEXIN EXPRESSION AND VASCULAR REMODELING IN RESISTANCE ARTERIES DURING HYPERTENSION

7.1   INTRODUCTION

Blood vessels contributing significantly to peripheral vascular resistance are termed resistance arteries and include arterioles and small arteries with diameters less than 500 μm (Johnson & Hanson, 1962). Resistance arteries are thought to play a major role in the development and or maintenance of diseases such as hypertension (Folkow, 1982; Christensen & Mulvany, 2001). Unlike the systemic circulation where small arteries and arterioles are the main sites of peripheral vascular resistance, in the cerebral circulation, the major site of resistance to blood flow occurs in larger arteries such as the basilar artery (Faraci & Heistad, 1990).

During hypertension, alterations in vascular function have been reported in both the systemic and cerebral circulation. For example, reduced endothelium-dependent and flow-mediated relaxation has been reported in mesenteric arteries of the SHR and SHR-SP (Fujii *et al.* 1990; Sunano *et al.* 1999). Similarly, in the basilar and middle cerebral arteries and in cerebral arterioles of the SHR and SHR-SP, agonist induced endothelium-dependent vasodilation is impaired (Faraci, 1992; Faraci & Heistad, 1998). Other functional properties including vasomotion are also altered in many vascular beds during hypertension (Lefer *et al.* 1990; Shimamura *et al.* 1999). Cell communication via gap junctions is known to play an important role in many functional properties including the conduction of endothelial responses and vasomotion (Chaytor *et al.* 1997; Segal *et al.* 1999; Shimamura *et al.* 1999; Emerson & Segal, 2001). Thus the altered expression of gap junctions may contribute to the alteration of many these functional responses during hypertension (Shimamura *et al.* 1999).

Concomitant with the functional changes observed during hypertension, vascular remodeling has been reported in both the mesenteric and cerebral arteries of the hypertensive rat. Within cerebral vessels, eutrophic remodeling has predominantly been described. For example, in the basilar artery and branches of the posterior cerebral artery of the adult SHR-SP, a reduction in both the external and luminal diameter has been

demonstrated, in combination with an increased medial to lumen ratio, all characteristics of eutrophic remodeling (Baumbach & Heistad, 1989; Hajdu & Baumbach, 1994; Arribas *et al.* 1996). Within the mesenteric arteries, hypertrophic remodeling has been consistently reported in the SHR and SHR-SP, however, whether such remodeling involves hypertrophy or hyperplasia of smooth muscle cells varies depending on factors such as the stage of hypertension and the region of vessel examined (Mulvany *et al.* 1978, 1985; Lee *et al.* 1983; Lee & Smeda, 1985; Lee, 1985, 1987; Dickhout & Lee, 1997). Thus these studies clearly indicate the heterogeneous nature of medial changes amongst different blood vessels, with both hypertrophic and eutrophic remodeling having been demonstrated in vessels of the SHR. In contrast to studies within the smooth muscle, data regarding morphological changes within the endothelium during hypertension is limited, previous studies having focused on the thoracic aorta, as detailed in Chapter 1.

In Chapter 5, Cx expression was shown to be differentially altered in the endothelium and smooth muscle of functionally different blood vessels during hypertension. These changes were accompanied by altered cellular morphology in the caudal artery but not in the thoracic aorta during hypertension. In this Chapter, we have examined the morphology of endothelial and smooth muscle cell layers and the distribution of Cxs within the primary mesenteric and basilar arteries during hypertension. These arteries were chosen as they represent resistance arteries of the systemic and cerebral circulation respectively (Faraci & Heistad, 1998). The results presented in this Chapter, in parallel with Chapter 5, provide a systematic examination of vascular changes occurring in several different blood vessels within a single model of hypertension. As a functional correlate of endothelial cell changes, we have examined the conduction of vasodilatory responses within the endothelial layer of the mesenteric artery in normotensive and hypertensive rats.

7.2   RESULTS

7.2.1   *Vessel morphology*

Morphological characteristics of the vascular media were determined from electron micrographs of the mesenteric and basilar arteries of 12 week old WKY and SHR. The number of smooth muscle cell layers and the medial cross-sectional area were significantly greater in the mesenteric artery of the SHR compared to the WKY ($P<0.05$, Table 7.1). In

strain	vessel	luminal diameter (μm)	smooth muscle layers	medial cross-sectional area (μm^2)
SHR	MA	205 ± 99	$9.4 \pm 1.4^*$	$37,248 \pm 201^*$
WKY	MA	198 ± 12	4.3 ± 0.3	7510 ± 616
SHR	BA	212 ± 14	5.1 ± 0.5	9154 ± 1065
WKY	BA	234 ± 1.2	5.3 ± 0.6	9257 ± 260

Table 7.1. Characteristics of mesenteric (MA) and basilar arteries (BA) from 12 week WKY and SHR rats. Values are mean ± SEM. $^*P<0.05$, significantly different to WKY. n=3.

the mesenteric artery, the luminal diameter was similar in both the WKY and SHR (Table 7.1). In the basilar artery, there was no change in luminal diameter, the number of smooth muscle cell layers or the medial cross-sectional area between the WKY and SHR (Table 7.1).

7.2.2 Endothelial cell morphology

En face views of the luminal surface showed a typical pattern of Cx expression, delineating the periphery of endothelial cells in both the mesenteric and basilar arteries (Figures 7.2 and 7.3 respectively). No areas devoid of endothelial cells were found.

In the mesenteric artery, surface area and length of endothelial cells were significantly less in the SHR compared to the WKY ($P<0.05$, Figures 7.1, 7.2), while perimeter and width of endothelial cells were not significantly different. In the basilar artery there was no significant difference in surface area, length, perimeter or width of endothelial cells between the WKY and SHR (Figure 7.1). Endothelial cell morphology was not significantly different between the two vessels in WKY (Figure 7.1).

7.2.3 Connexin protein expression in the vascular endothelium

For each of the Cx antisera used here, no staining was observed in the absence of the primary antibody or when the primary antibody was pre-incubated with the appropriate antigenic peptide.

En face views of the luminal surface showed punctate staining for Cxs 37, 40 and 43 along the periphery of endothelial cells in the mesenteric artery (Figure 7.2A-C, E-G), while in the basilar artery, Cx staining was arranged continuously along the periphery of endothelial cells rather than in a punctate fashion (Figure 7.3A-C, E-G). Cx45 was not found in the endothelium of either artery (Figures 7.2D,H, 7.3D,H).

As Cx labelling in the basilar artery did not appear in clearly defined plaques, Cx labelling was expressed as the area occupied by Cx staining per endothelial cell. In the mesenteric artery of the SHR, expression of both Cxs 37 and 40 were significantly reduced ($P<0.05$, Figures 7.2, 7.4A). In the basilar artery, expression of Cx37 per endothelial cell was significantly less in the SHR compared to the WKY ($P<0.05$, Figures 7.3A,E, 7.4B).

As Cx expression in the endothelium was seen exclusively around the cell periphery and the surface area of endothelial cells was less in mesenteric arteries of the SHR, the density of Cx plaques in the cell membrane was also calculated. Area of Cx37 staining per

Figure 7.1

Figure 7.1.

Morphology of endothelial cells from 12 week old WKY and SHR mesenteric (MA) and basilar arteries (BA). Values are mean ± SEM. *$P<0.05$, significantly different from the WKY. n=4 animals.
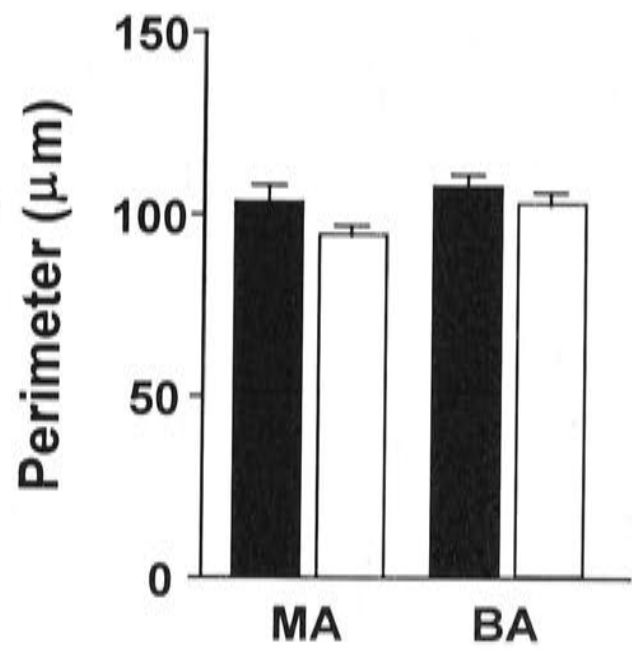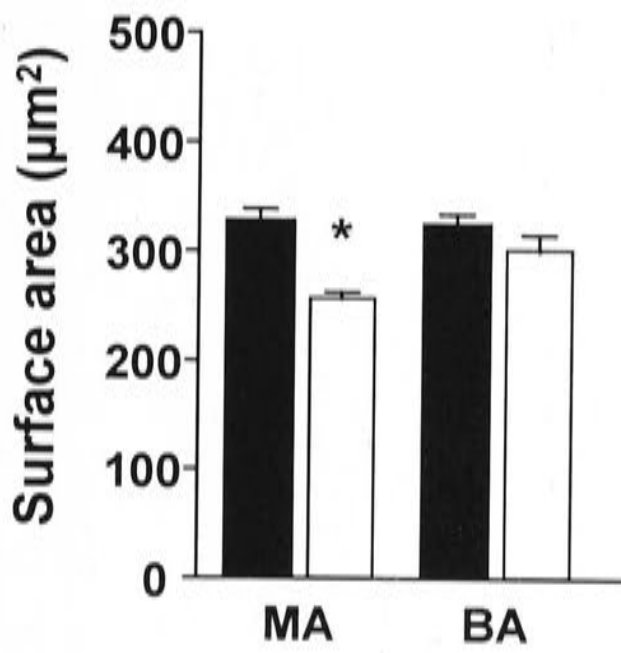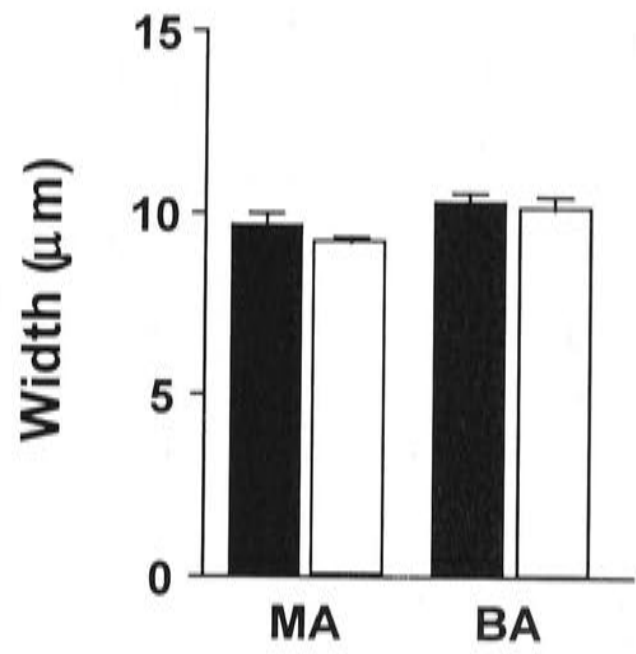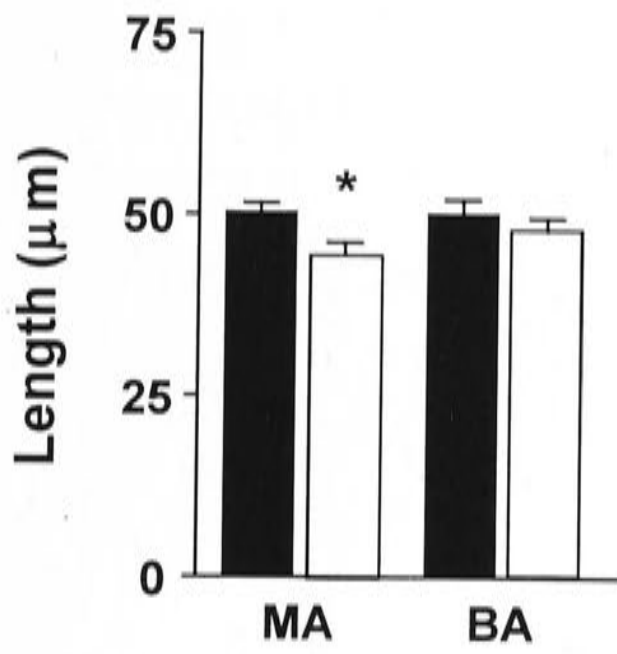
Figure 7.2

Figure 7.2.

Cx protein expression in the mesenteric artery of 12 week old WKY and SHR. The endothelium is viewed *en face* and is labelled with antibodies to Cx37 (A,E), Cx40 (B,F), Cx43 (C,G) and Cx45 (D,H). Labelling of Cxs 37, 40 and 43 is evident along the perimeter of endothelial cells, while labelling of Cx45 was not detected. Calibration bar represents 20 μm.

WKY/Cx37

SHR/Cx37

A

E

WKY/Cx40

SHR/Cx40

B

F

WKY/Cx43

SHR/Cx43

C

G

WKY/Cx45

SHR/Cx45

D

H

Figure 7.3

Figure 7.3.

Cx protein expression in the basilar artery of 12 week old WKY and SHR. The endothelium is viewed *en face* and is labelled with antibodies to Cx37 (A,E), Cx40 (B,F), Cx43 (C,G) and Cx45 (D,H). Labelling of Cxs 37, 40 and 43 is evident along the perimeter of endothelial cells, while labelling of Cx45 was not detected. Calibration bar represents 20 μm.

WKY/Cx37

SHR/Cx37

A

E

WKY/Cx40

SHR/Cx40

B

F

WKY/Cx43

SHR/Cx43

C

G

WKY/Cx45

SHR/Cx45

D

H

Figure 7.4

Figure 7.4.

Protein expression for Cxs 37, 40, 43 and 45 in the endothelium of the 12 week old WKY and SHR mesenteric (A,C) and basilar arteries (B,D). Values are expressed as the area of Cx staining per endothelial cell (A,B) and area of Cx staining per 100 μm of endothelial cell perimeter (C,D). Values are mean ± SEM. *$P<0.05$, significantly different from Cx expression in the WKY. $n=4$ animals.

A   Mesenteric Artery

Area of Cx staining per endothelial cell

Cx37   Cx40   Cx43

B   Basilar Artery

Cx37   Cx40   Cx43

C   Mesenteric Artery

Area of Cx staining per 100 µm of cell perimeter

Cx37   Cx40   Cx43

D   Basilar Artery

Cx37   Cx40   Cx43

WKY
SHR
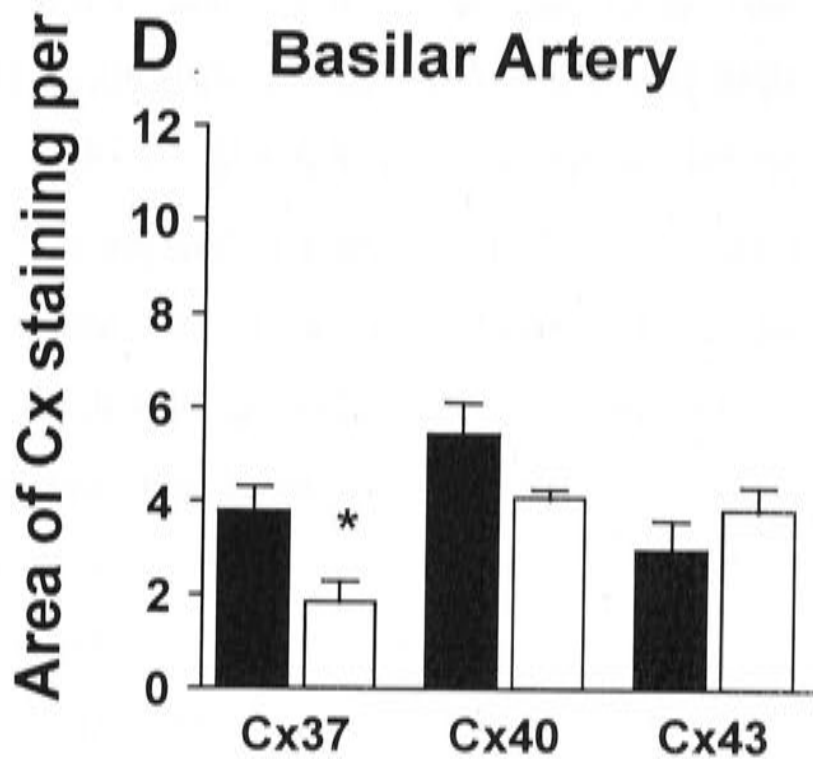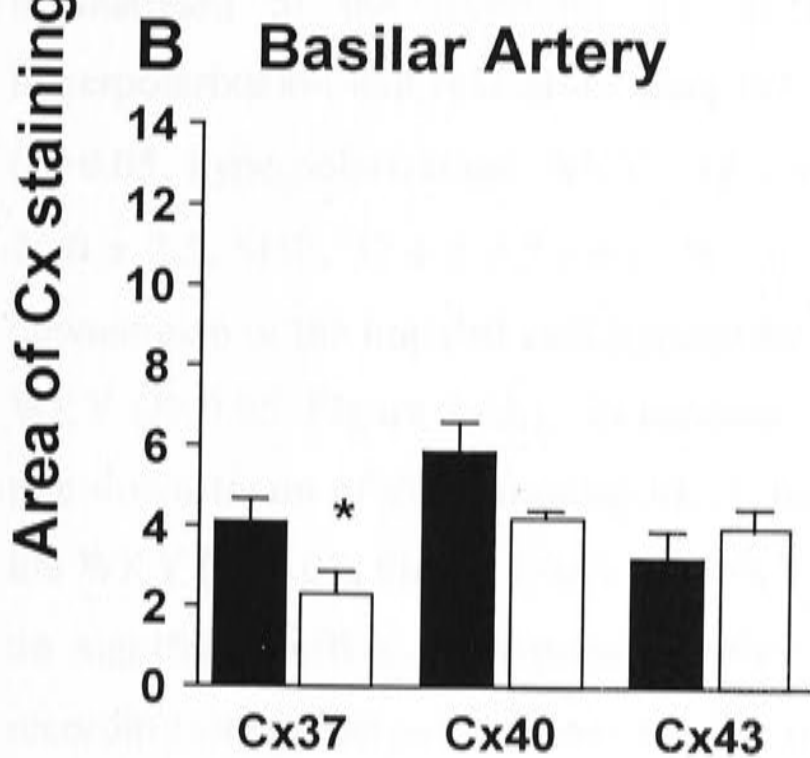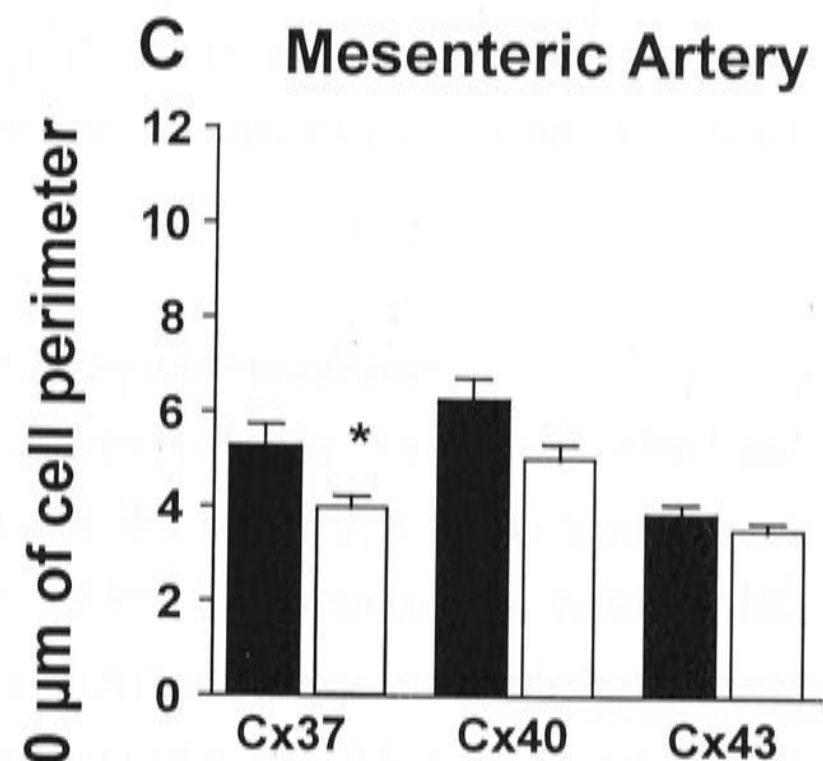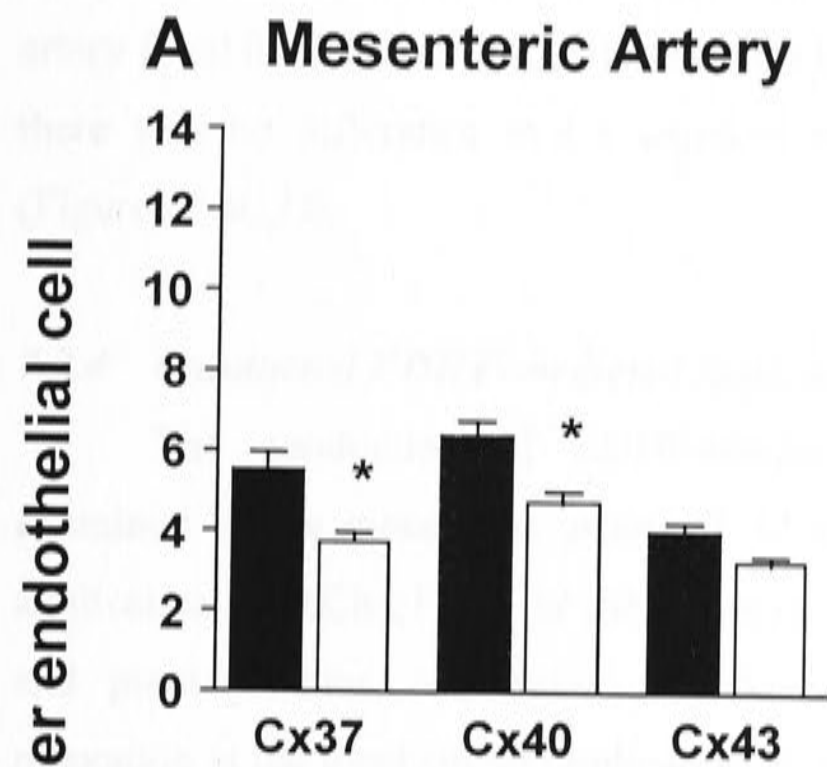
100 µm of endothelial cell perimeter in the mesenteric and basilar arteries was significantly less in the SHR than the WKY ($P<0.05$, Figures 7.4C,D). In the SHR, the density of Cxs 37 and 40 expression in the mesenteric artery was significantly greater than in the basilar artery ($P<0.05$, Figures 7.4C,D), while Cx43 was not significantly different. In the WKY, there was no difference in Cx expression between the mesenteric and basilar arteries (Figures 7.4C,D).

7.2.4 *Conducted EDHF-mediated hyperpolarization and vasodilation*

The conduction of EDHF-mediated hyperpolarization and vasodilation was examined in the mesenteric artery of 12 week old WKY and SHR. The iontophoretic application of ACh (1 M), in the presence of L-NAME and indomethacin, to inhibit NO and prostaglandins respectively, produced an EDHF-mediated hyperpolarization and relaxation at the local site of application and when applied to sites 0.5, 1, 1.5, 2 and 2.5 mm downstream of the recording site in both WKY and SHR. At the local site, hyperpolarization and relaxation were not significantly different between WKY and SHR ($P>0.05$, hyperpolarization: WKY, -18.3 ± 0.7, SHR, -15.8 ± 0.8 mV; relaxation: WKY, 26.0 ± 2.5, SHR, 32.4 ± 3.7 µm). When ACh was applied at sites 0.5, 1, 1.5 and 2 mm downstream of the impaled cell, hyperpolarization was reduced in the SHR compared to the WKY ($P<0.05$, Figure 7.5A). In contrast, when ACh was applied at sites 0.5 mm and 1.5 mm downstream of the recording site, relaxation was significantly less in the SHR than in the WKY ($P<0.05$, Figure 7.6A). In WKY rats, incubation of vessels in Ba^{2+} (30 µM) had no significant effect on hyperpolarization or relaxation when ACh was applied at the recording site (hyperpolarization: $+Ba^{2+}$, -16.8 ± 0.7 mV; relaxation: $+Ba^{2+}$, 29.3 ± 1.5 µm). However, hyperpolarization was reduced when ACh was applied at sites 0.5 and 1 mm downstream of the recording site, while the local relaxation was reduced when ACh was applied 1 and 1.5 mm downstream ($P<0.05$, Figures 7.5B, 7.6B). In the SHR, hyperpolarization and relaxation in response to ACh at the local site was not altered by the incubation of Ba^{2+} ($P>0.05$, hyperpolarization: $+Ba^{2+}$, -14.2 ± 0.7 mV; relaxation: $+Ba^{2+}$, 31.1 ± 3.8 µm), nor was the conducted response to ACh altered (Figures 7.5C, 7.6C). When conducted hyperpolarization and relaxation responses in the presence of Ba^{2+} were compared in the WKY and SHR, there was no significant difference between the two

Figure 7.5
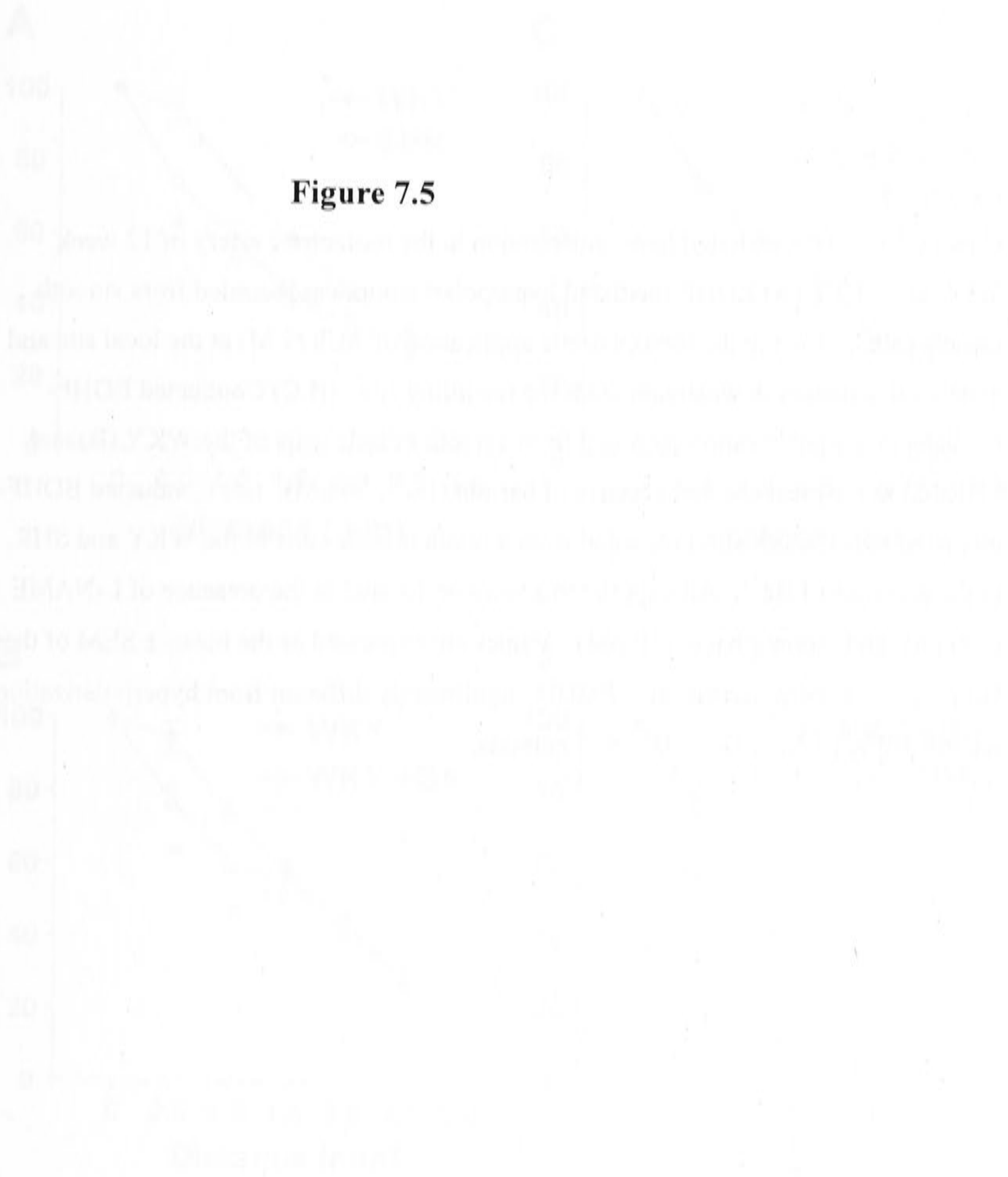
Figure 7.5.

Conducted EDHF-mediated hyperpolarization in the mesenteric artery of 12 week WKY and SHR. (A) EDHF-mediated hyperpolarization was recorded from smooth muscle cells following the iontophoretic application of ACh (1 M) at the local site and at defined distances downstream from the recording site. (B,C) Conducted EDHF-mediated hyperpolarization recorded from smooth muscle cells of the WKY (B) and SHR (C) in the presence and absence of barium (Ba^{2+}, 30 μM). (D) Conducted EDHF-mediated hyperpolarization recorded from smooth muscle cells in the WKY and SHR, in the presence of Ba^{2+}. All experiments were performed in the presence of L-NAME (100 μM) and indomethacin (10 μM). Values are expressed as the mean $\pm$ SEM of the % change in hyperpolarization. *$P<0.05$, significantly different from hyperpolarization recorded WKY (A) or Ba^{2+} (B). n=7 animals.
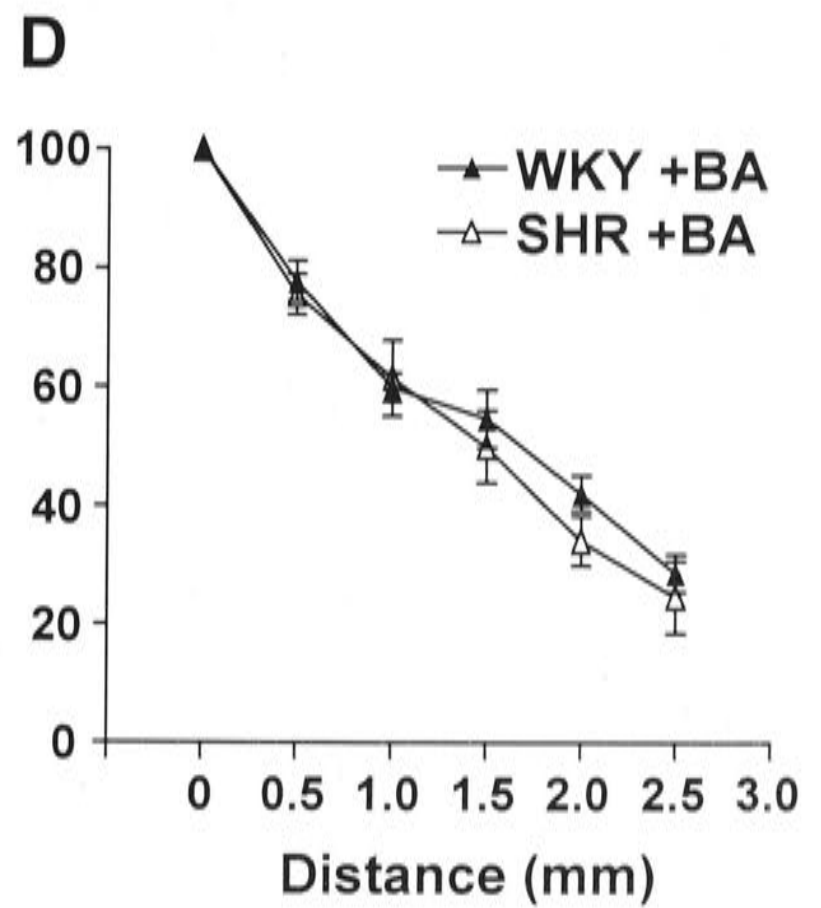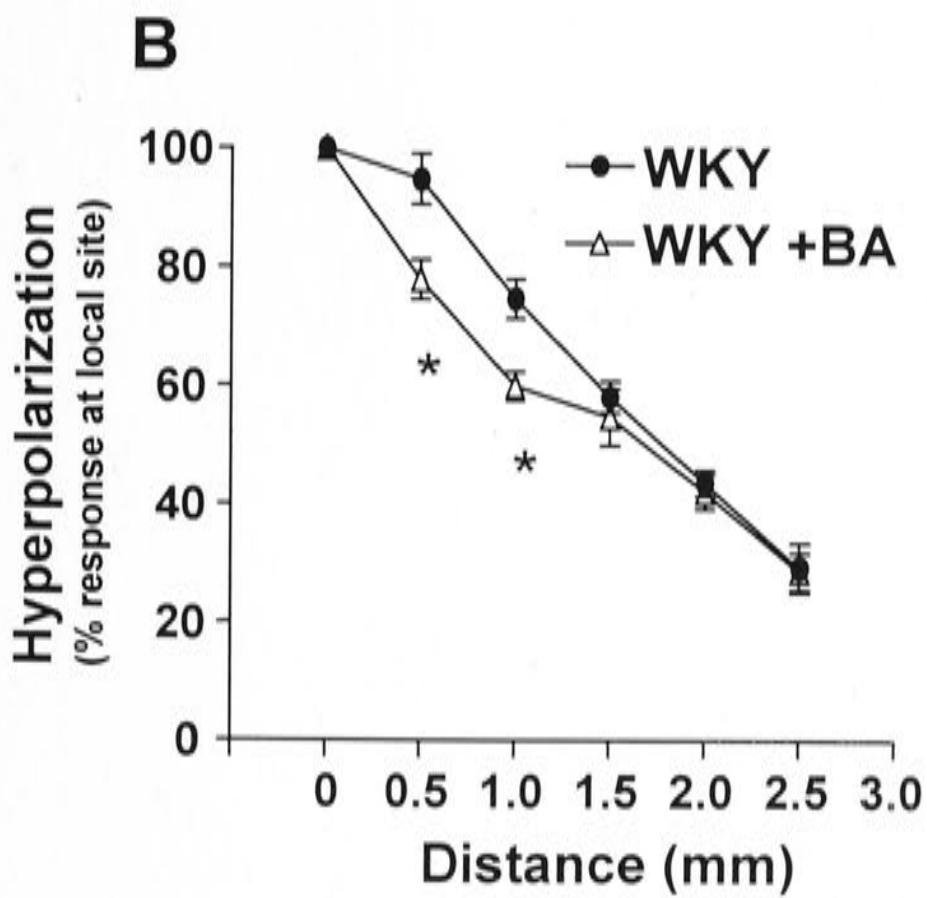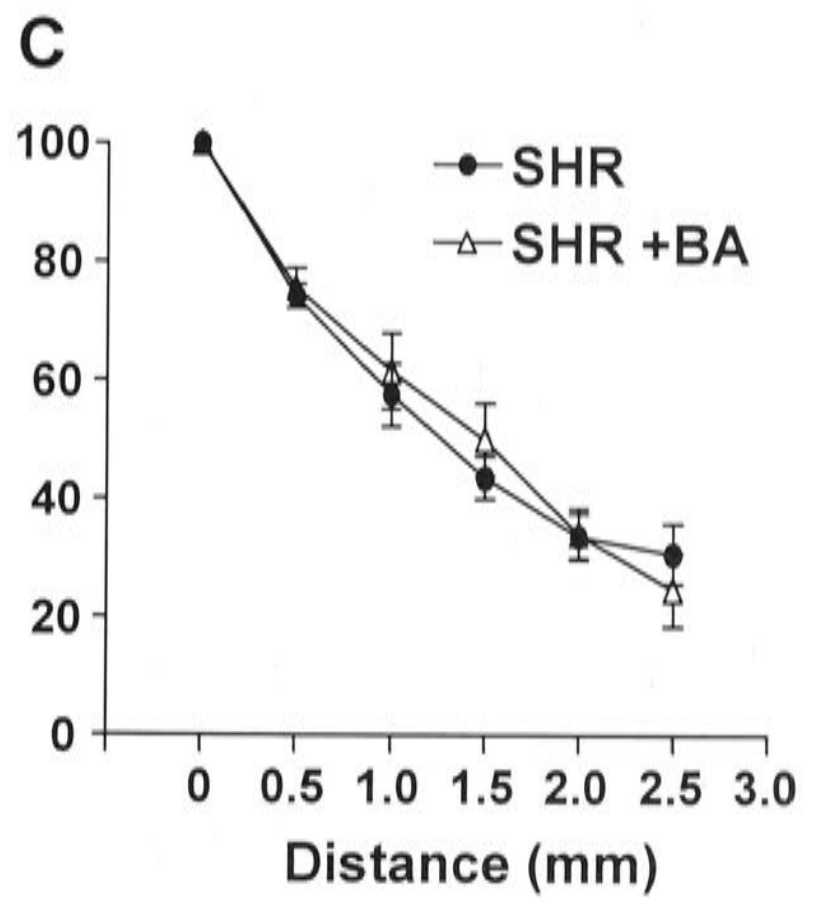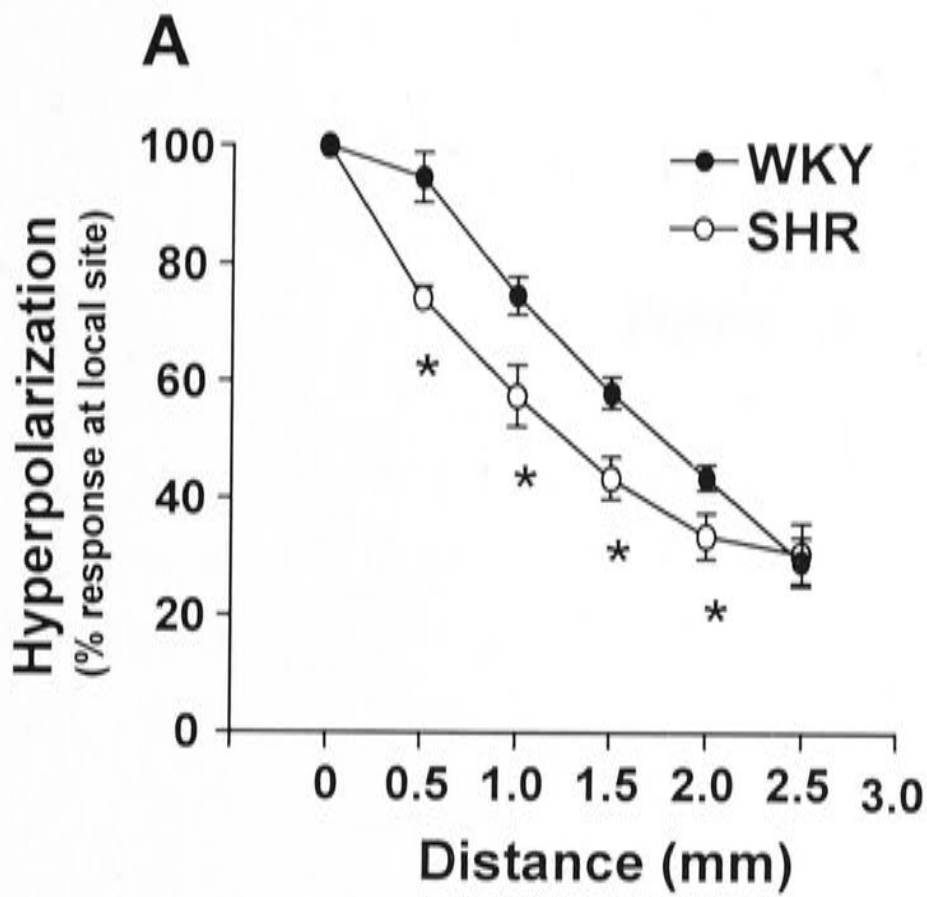
Figure 7.6
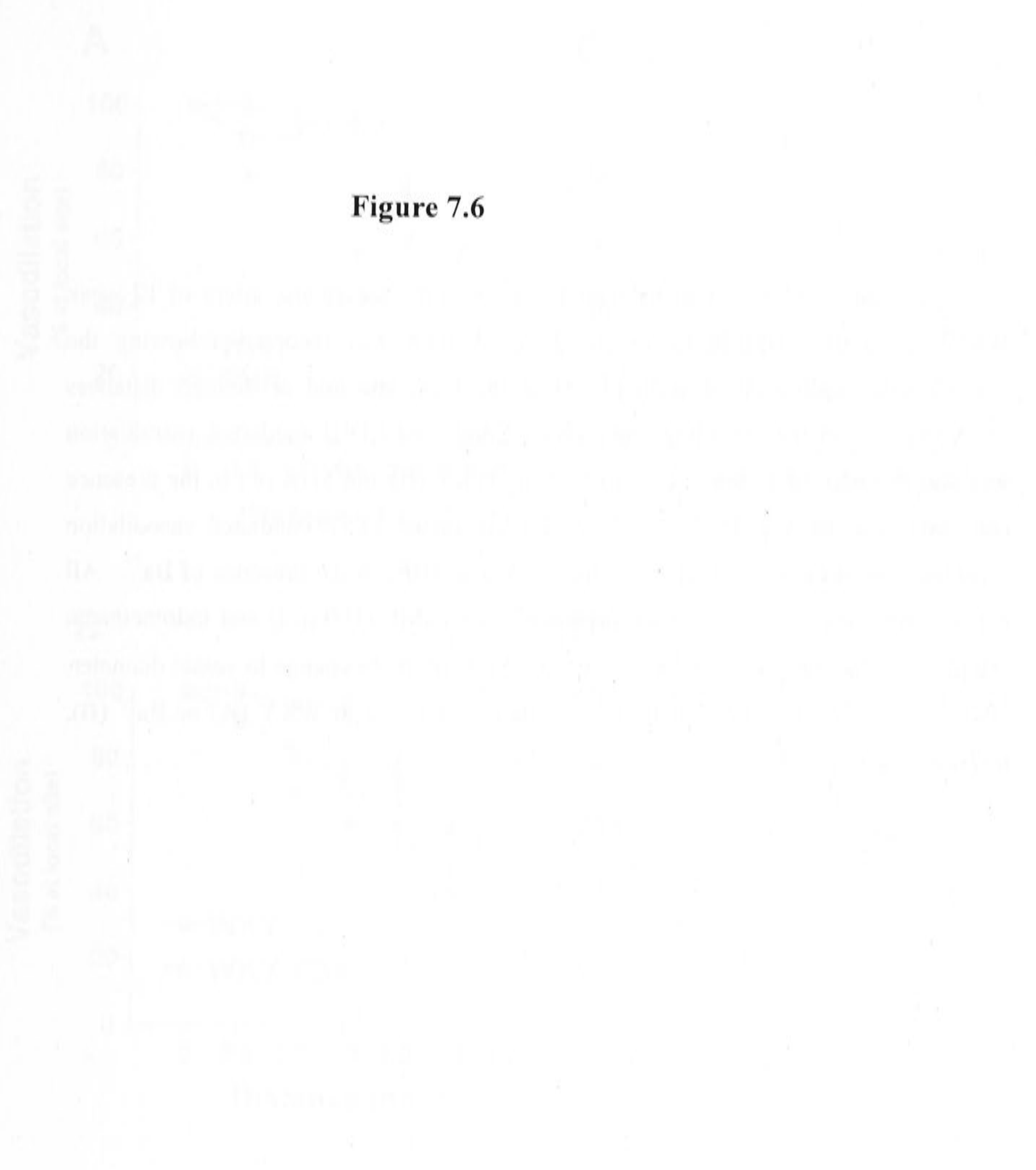
Figure 7.6.

Conducted EDHF-mediated vasodilatation in the mesenteric artery of 12 week WKY and SHR.   (A) EDHF-mediated vasodilation was recorded following the iontophoretic application of ACh (1 M) at the local site and at defined distances downstream from the recording site. (B,C) Conducted EDHF-mediated vasodilation was also recorded in mesenteric arteries of the WKY (B) and SHR (C) in the presence and absence of barium (Ba^{2+}, 30 μM). (D) Conducted EDHF-mediated vasodilation recorded from mesenteric arteries of the WKY and SHR, in the presence of Ba^{2+}. All experiments were performed in the presence of L-NAME (100 μM) and indomethacin (10 μM). Values are expressed as the mean ± SEM of the % change in vessel diameter. $^{*}P<0.05$, significantly different from vasodilation recorded in WKY (A) or Ba^{2+} (B). n=7-8 animals.
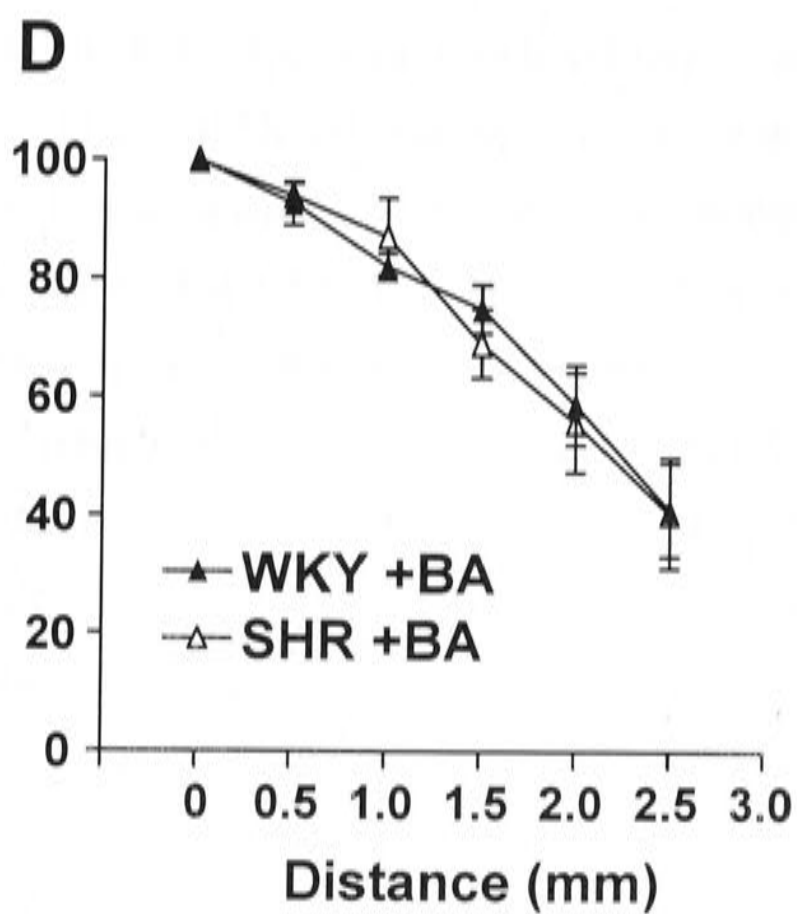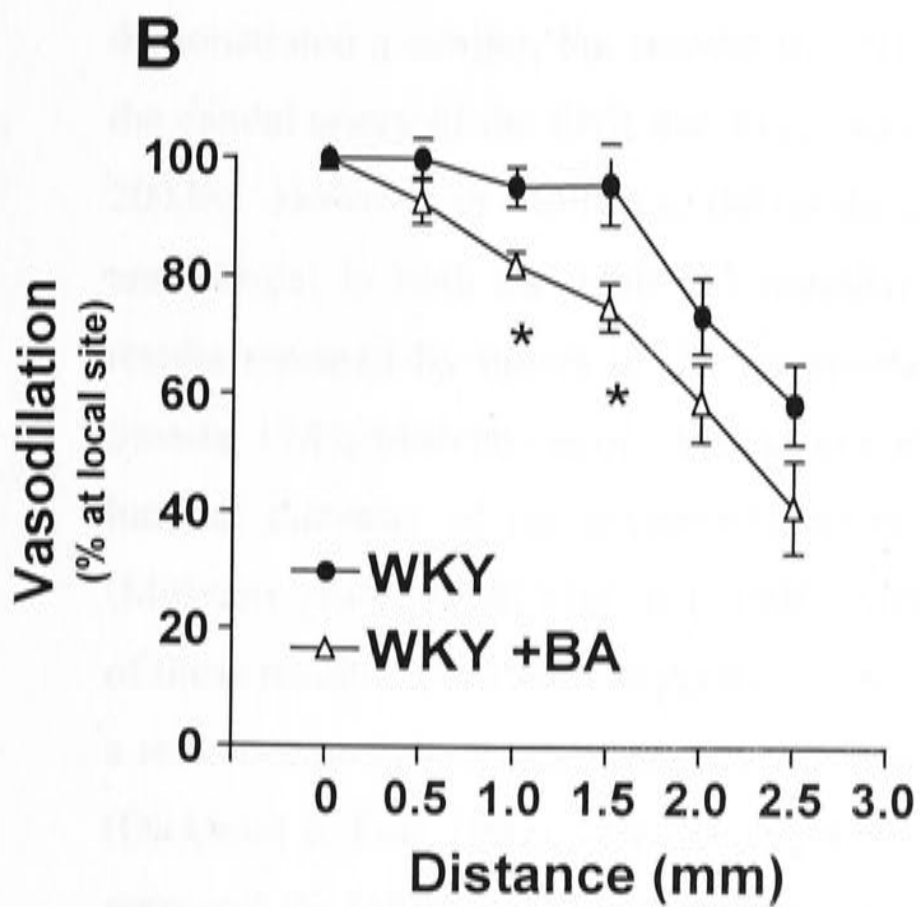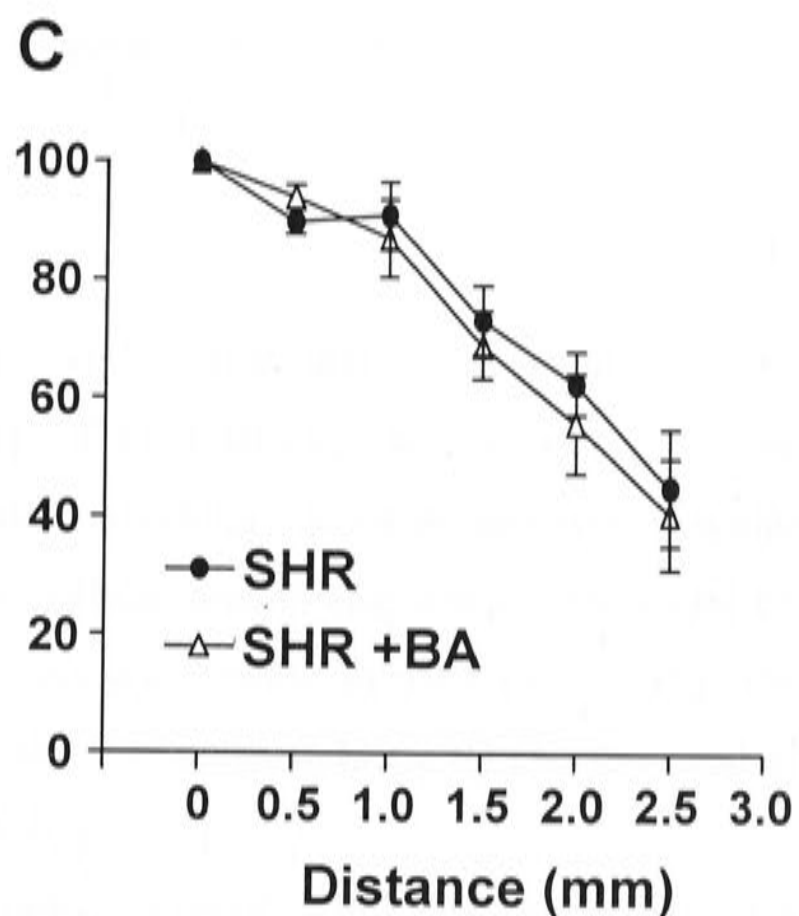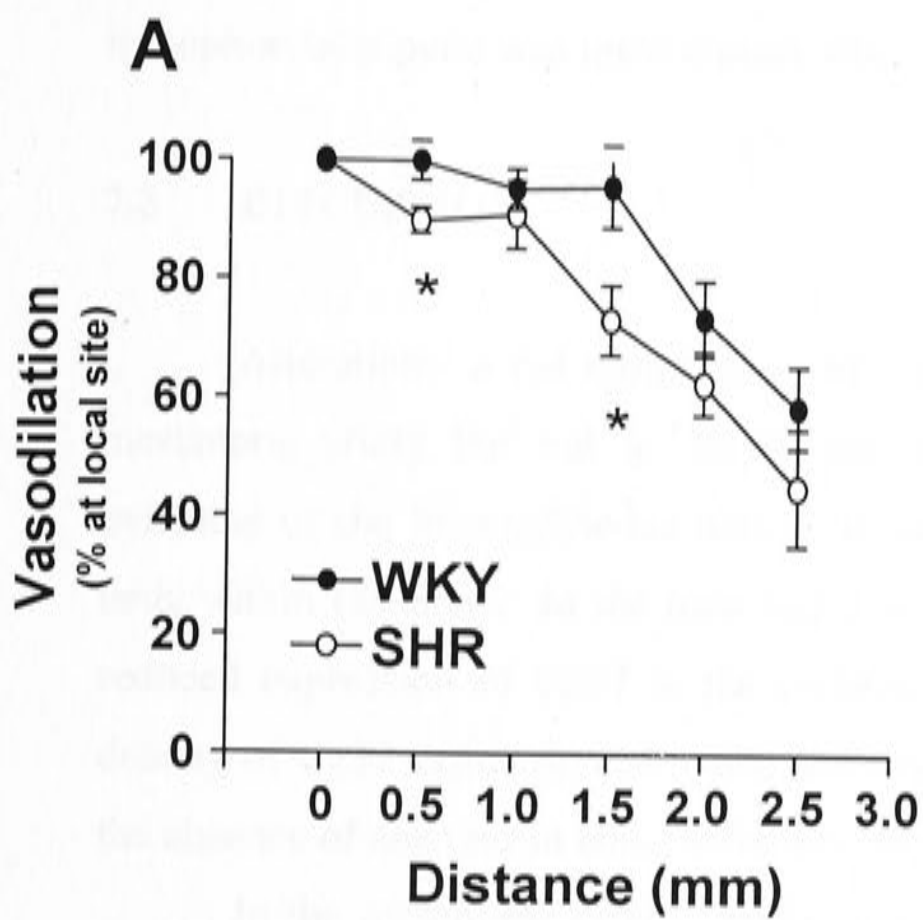
strains ($P>0.05$, Figure 7.5D, 7.6D). Responses were completely abolished when the iontophoretic pipette was moved away from the preparation by 0.5 mm.

7.3   DISCUSSION

Alterations in the morphology of both the endothelium and media occurred in the mesenteric artery but not in the basilar artery of hypertensive rats, providing further evidence of the heterogeneous nature of vascular remodeling amongst different vascular beds within the SHR. In the mesenteric artery, cellular remodeling was accompanied by reduced expression of Cx37 in the endothelial cell layer, while in the basilar artery, the density of Cx37 expression was also reduced in the endothelium, however this occurred in the absence of changes in endothelial cell morphology.

In the mesenteric artery, medial hypertrophy occurred in the SHR as a result of a doubling in the number of smooth muscle cell layers. The results presented in Chapter 5, demonstrated a similar, but smaller increase in the number of smooth muscle cell layers in the caudal artery of the SHR due to increases in smooth muscle cell number (Sandow et al. 2003b). However in contrast to the caudal artery, luminal diameter of the mesenteric artery was similar in both the adult (>3 months) WKY and SHR. These results are similar to results reported by others in the mesenteric artery of the SHR (Lee et al. 1983; Lee & Smeda, 1985; Mulvany et al. 1985). In contrast, other studies have reported a reduction in luminal diameter of the mesenteric artery of the adult (>3 months) SHR and SHR-SP (Mulvany et al. 1978; Mulvany, 1986; Arribas et al. 1997; Rizzoni et al. 1998). In light of these results, it has been suggested by some that due to the elasticity of the vascular wall, a reduction in lumen diameter may occur only in the event of changes in wall compliance (Dickhout & Lee, 1997). The results presented for the mesenteric artery in this study may represent the initial stages of more extensive vascular remodeling in the SHR.

In contrast to the mesenteric and caudal arteries, no evidence of medial remodeling was found in the basilar artery of hypertensive rats. These results suggest that hypertrophic remodeling is present in systemic vessels of the SHR but not in vessels of the cerebral circulation or in large conduit vessels such as the thoracic aorta (Chapter 5). Medial remodeling within the basilar artery may occur in response to prolonged increases in blood pressure or in more severe forms of hypertension as described for the thoracic aorta. Indeed, vascular remodeling has been demonstrated in cerebral vessels of the 12 week old

SHR-SP and in the aging SHR (Mulvany, 1986; Baumbach & Heistad, 1989; Arribas *et al.* 1996; Baumbach & Hajdu, 1993; Hajdu & Baumbach, 1994; Baumbach *et al.* 2003). The heterogeneity seen here between the basilar and mesenteric arteries may reflect different functional properties of each vascular bed. Within the cerebral circulation the mechanisms underlying the regulation of vascular tone differ from systemic vessels in several ways (Faraci, 1992; Faraci & Heistad, 1998). Unlike the systemic circulation, large vessels are the primary site of peripheral vascular resistance in the cerebral circulation, thus flow-mediated dilation is likely to be more important in these vessels than in smaller arteries and arterioles (Faraci & Heistad, 1998). Furthermore, several studies have shown that the activity of vasodilatory factors is increased in cerebral vessels of the SHR while the reverse is true for the mesenteric vessels. Indeed, the activity of large conductance K_{Ca} is increased in the basilar artery of the SHR compared to the WKY (Paternò *et al.* 1997). Similarly, the expression of NADPH-oxidase and the production of superoxide is greater in the basilar artery of the SHR compared to the WKY (Sobey, 2003), while in the basilar artery of the adult (>6 months) SHR-SP, vasodilatory function of NO is impaired (Kitazono *et al.* 1996). Thus, the lack of morphological changes in the cerebral vasculature of the 12 week SHR may reflect the up-regulation of vasodilatory factors and the maintenance of near normal blood pressure in this vascular bed ensuring adequate blood flow to the brain (Faraci & Heistad, 1990).

A decrease in endothelial cell size was found in the mesenteric artery but not the basilar artery of the SHR. Similarly, in Chapter 5, a reduction in the size of endothelial cells was found in the caudal artery of the SHR, while there was no change in endothelial cell size in the thoracic aorta. Together these results suggest that during hypertension, cellular remodeling within the endothelium may be heterogeneous, like the changes in the media of functionally different vascular beds. In the mesenteric artery, endothelial cells were smaller in the SHR compared to the WKY, but there was no significant change to lumen diameter, suggesting hyperplasia within the intimal layer. In contrast to these studies Arribas *et al.* (1997) demonstrated a reduction in the total number of endothelial cells in the mesenteric artery of the SHR-SP however this study reported large areas devoid of endothelial cells, suggesting damage to the luminal surface of the blood vessel during tissue preparation. In other studies, ligation of the mouse carotid artery resulted in hyperplasia of intimal cells and a reduction in lumen diameter (Emanueli *et al.* 2000). The vascular endothelium is exposed to varying hemodynamic forces arising from the flow of

blood (Davies & Tripathi, 1992; DePola *et al.* 1992). Changes in blood flow and consequently shear stress have been shown to affect both endothelial cell morphology and function (Davies *et al.* 1992; Resnick *et al.* 2003). For example, during atherosclerosis, diseased regions of the blood vessel are subject to turbulent blood flow (Davies, 1989), and display altered endothelial cell morphology and gene expression (Garbriels & Paul, 1998; DePaola *et al.* 1999). In a similar manner, during hypertension, increased peripheral reistance and blood viscosity can result in altered haemodynamic forces and subsequent vascular remodeling (Pries & Secomb, 2002). Furthermore, several studies have shown that shear stress dependent dilation is impaired in arterioles of the SHR (Koller & Huang, 1999). Taken together, the results presented here suggest that when the endothelium is subject to altered hemodynamic forces as a result of ligation or increased peripheral resistance endothelial cell morphology may be altered in some blood vessels. The lack of endothelial cell remodeling in the basilar artery of the SHR suggests that similar alterations in hemodynamic forces described above are not present in this vascular bed.

In the caudal artery, Cx40 was found to be significantly decreased in the endothelium of the SHR compared to the WKY (Chapter 5). In contrast, Cx37 was decreased in the endothelium of both the mesenteric and basilar arteries during hypertension, and in the thoracic aorta as demonstrated in Chapter 5. Interestingly in the aorta (Chapter 5), mesenteric and basilar arteries, the density of Cx40 showed a trend to be decreased during hypertension, although this did not reach significance in any vessel. Similarly, in the caudal artery of the SHR, expression of Cx37 also showed a trend to be decreased, again this did not reach significance (Chapter 5). Such results suggest an important role for both Cxs 37 and 40 in the endothelium of both elastic and muscular arteries. Indeed, recent studies have demonstrated a co-dependent relation between expression of Cxs 37 and 40 within the vascular endothelium (Simon & McWhorter, 2003).

As discussed in Chapters 1 and 5, longitudinal conduction of vasodilatory responses is known to occur in the vascular endothelium via the gap junctional coupling of adjacent endothelial cells (Segal *et al.* 1999; Emerson & Segal, 2001). Therefore it seems likely that a reduction in endothelial cell size and Cx expression would result in reduced cellular coupling and conduction of vasomotor responses. It is known that junctional resistance is greater than axial resistance, thus reduced endothelial cell size would increase the number of gap junctions an electrical signal must pass through as it is conducted longitudinally along the endothelium resulting in the attenuation of the conducted response (Zaniboni *et*

al. 2003). Indeed, in the SHR hyperpolarization and relaxation seen within the mesenteric artery was significantly reduced at sites downstream of ACh stimulation compared to the WKY. However, further investigation found that the reduction in conducted responses was due to the decreased involvement of K_{IR} channels in the SHR. Blockade of K_{IR} channels with Ba^{2+} in the WKY, reduced both the conducted hyperpolarization and the relaxation to the same level as the SHR. In contrast, blockade of K_{IR} channels in the mesenteric artery of the SHR had no effect on either the conducted hyperpolarization or relaxation. Indeed, studies by Chrissobolis *et al.* (2002), show decreased activity of K_{IR} channels in the basilar artery of the SHR. Hence, unlike studies in the Cx40 deficient mouse (de Wit *et al.* 2000) reduced Cx37 expression within the endothelium of the mesenteric artery during hypertension did not result in reduced conducted vasodilation. The absence of an effect on conduction may be due to the magnitude of the change in Cx37 expression, i.e. 25% in the present study versus 100% in Cx40 deficient mice, or to the nature of the Cx altered. In this context, it is interesting that deletion of Cx40 in the mouse aortic endothelium inhibited intercellular dye transfer to a much greater extent than did deletion of Cx37 (Simon & McWhorter, 2003). Together these results suggest that Cx40 may play a more important role than Cx37 in conducted responses. Alternatively, since the hyperpolarization and relaxation at the local site did not differ between the WKY and SHR, while the conducted responses due to K_{IR} were reduced in the SHR, it is possible that conduction of these responses may be mediated by Cx37 however, this hypothesis requires further examination. Finaly, recent studies in rat cerebral arteries demonstrate that K_{IR} channels present within the smooth muscle, not the endothelium, are involved in conducted K^+ induced relaxation (Horiuchi *et al.* 2002), suggesting that altered Cx expression may not be involved in the reduced conducted responses in this vessel.

From the above results, it is clear that cellular remodeling occurs in both the endothelial and smooth muscle cell layers of different blood vessels during hypertension, however the nature of such remodeling depends on the particular vascular bed examined. Remodeling is more extensive in muscular arteries of the systemic circulation rather than in cerebral vessels. Changes in coupling within the endothelium are accompanied by cellular remodeling in muscular arteries of the systemic circulation. It is likely that such changes may be involved in the development of hypertension, given that medial remodeling has been described in the mesenteric arteries of pre-hypertensive rats and changes in endothelial cell morphology and Cx expression were found in the caudal artery prior to the

onset of hypertension. However, whether such changes within the endothelium are present in the mesenteric artery before the onset of hypertension, awaits further studies. In contrast, in the basilar artery, reduced Cx expression occurred in the absence of altered endothelial cell morphology. The lack of anatomical remodeling within the basilar artery in this study may suggest that cerebral vessels undergo other functional alterations, which protect them from the systemic increase in blood pressure. More prolonged or severe changes in blood pressure, as occurs in aged rats and within the SHR-SP, may be required before secondary structural changes take place in cerebral vessels.

CHAPTER 8
GENERAL DISCUSSION

The results presented in this thesis demonstrate distinct differences in the expression of Cxs between functionally different blood vessels. This expression is significantly altered during hypertension. During hypertension, morphological changes were observed in the endothelium and media of some, but not all blood vessels examined, while Cx expression was reduced in all vessels. The nature of the medial remodeling and the specific Cx isotype altered during hypertension was heterogeneous depending on the vascular bed. These and several other important issues have arisen from the work presented in this thesis and these will be addressed in the following discussion.

8.1 GAP JUNCTION EXPRESSION IN VASCULAR TISSUE

To date, studies examining gap junction coupling within the blood vessel wall have reported significant heterogeneity in Cx expression amongst different vascular beds. Indeed, the results of Chapter 4, which examined the expression of Cx mRNA and protein in the thoracic aorta and caudal artery of the Wistar rat, found a profile of Cx expression that was different in the smooth muscle, but not the endothelium of the two vessels. The thoracic aorta and caudal artery were chosen as they represent functionally different blood vessels, thus providing the first systematic investigation of the expression of all four vascular Cxs in arteries of the rat. Expression of Cxs 37, 40 and 43 was found in the endothelium of both the thoracic aorta and caudal artery, thus confirming reports by others indicating that all three Cxs are expressed within the endothelium throughout the vasculature (Severs, 1999; Hill *et al.* 2001). Similar expression was also found in mesenteric and basilar arteries. The expression of Cx43 within the aortic endothelium has been shown by some to vary along the length of the vessel. For example, Cx43 expression was greater in the thoracic versus the abdominal aorta and expression was higher in regions of increased shear stress (Gabriels & Paul, 1999). Such variation was not evident in the regions of thoracic aorta examined in this study. This discrepancy may simply reflect differences in experimental technique or in the affinity of the antibodies used.

In contrast to the expression of Cxs within the endothelium, in the smooth muscle, Cx expression was much more variable between vascular beds. Expression of Cx43 within

94

the smooth muscle of the rat thoracic aorta has been extensively reported (Hill *et al.* 2001), and this was confirmed in the current study. In contrast, it has been noted in this and other studies that Cx43 labeling is not detectable in the media of both large and small muscular arteries (Hill *et al.* 2001). In these arteries, reports suggest that the predominant Cx present varies throughout the vasculature (Severs, 1999; Hill *et al.* 2001). In this study, Cx 37 was the principal Cx expressed within the media of the caudal artery. The differences in Cx expression amongst different arteries are likely to reflect the functional significance of each Cx and its specific role in arteries throughout the vasculature.

8.2 VASCULAR REMODELING AND CONNEXIN EXPRESSION DURING HYPERTENSION

Gap junctions play an important role in the control of vasomotor tone (Christ *et al.* 1996) and thus altered Cx expression has been implicated in the mechanisms underlying altered vascular function of many disease states including hypertension. Indeed, Cx expression is altered in the aorta of various rat hypertensive models including the SHR (Haefliger *et al.* 1997a,b, 1999, 2001; Haefliger & Meda, 2000). However, results presented in Chapters 5 and 7 provide the first comprehensive examination of all four vascular Cxs in other arteries of greater physiological relevance to hypertension.

During hypertension, changes in Cx expression were present in the thoracic aorta, caudal, mesenteric and basilar arteries, indicating that the effects of hypertension on the vasculature are widespread, affecting a number of functionally distinct blood vessels. However, the Cx isotype involved varied with each vascular bed. In the endothelium, expression of Cx37 was decreased in the thoracic aorta, mesenteric and basilar arteries of the SHR, while in the caudal artery, Cx40 expression was decreased. It is interesting to note that in all four vessels, both Cxs 37 and 40 were reduced in the SHR, although in some cases this did not reach significance. However, it is clear that both Cxs play an important role in the endothelium of both elastic and muscular arteries. On the other hand, Cx43 was not altered in any of the four vessels during hypertension, suggesting that this Cx is unlikely to have an important role in the vascular endothelium in this disease state. In contrast, changes in Cxs 43 and 45 were found in the smooth muscle of the thoracic aorta during hypertension, while Cx45 was also altered in the media of the caudal artery.

During hypertension, vascular remodeling has been described in a number of blood vessels throughout the vasculature (Mulvany *et al.* 1996; Intengan & Schiffrin, 2000). In

the present study, morphological changes occurring in association with hypertension were found to be restricted to the caudal and mesenteric arteries, which are both muscular arteries. Vascular remodeling was absent in both the thoracic aorta and basilar arteries. It is possible that these blood vessels have distinct functional characteristics that preclude the necessity for vascular remodeling. The thoracic aorta is purely a conduit vessel with extensive elastic laminae, while the basilar artery is essential for normal vascular hemodynamics in the brain, and therefore may be more resistant to changes that occur in the systemic circulation in response to altered blood pressure, due to the up-regulation of compensatory vasodilatory mechanisms (Paternò *et al.* 1997; Sobey, 2003).

8.3 VASCULAR REMODELING, CONNEXIN EXPRESSION AND THE ONSET OF HYPERTENSION

Vascular remodeling has been described both before and after the onset of hypertension however, the underlying nature of the remodeling varies with the blood vessel being examined and the specific stages in the development of hypertension (Lee & Smeda, 1985; Lee, 1987). In Chapter 6, no changes in vessel morphology were found in either the thoracic aorta or the caudal artery of pre-hypertensive SHR. Taken together, these results suggest that during the development of hypertension, morphological changes may be either primary or secondary in nature. Primary changes are present shortly after the onset of hypertension, while secondary changes occur following prolonged periods of increased blood pressure, and therefore represent adaptive changes in response to increased peripheral resistance. Whether or not changes in cellular coupling might contribute to the development of hypertension has been examined for the first time in this study.

In the pre-hypertensive SHR, altered Cx expression was observed in the endothelium and media of the caudal artery, but not in the thoracic aorta. In the endothelium of the caudal artery, this reduction was present despite the absence of cellular remodeling, suggesting that a reduction in Cx expression may play a causative role in the development of hypertension in this vessel, whilst cellular remodeling may be a consequence of increased blood pressure. On the other hand, in the thoracic aorta, the absence of morphological differences in the pre-hypertensive SHR suggest that alterations observed at 12 weeks of age occur secondarily to increased blood pressure and thus reflect an adaptive response to hypertension.

The results presented in Chapter 6 concerning pre-hypertensive animals may be complicated by developmental differences between the WKY and SHR. It is possible that within the caudal artery, the decrease in Cx expression in the endothelium observed at 3 weeks may simply reflect inherent differences between the 2 strains. Indeed, strain variation between the WKY and SHR is recognized to present potential problems in comparing data between the two types of rat (Louis & Howes, 1990). Future studies, whereby hypertensive animals are treated with anti-hypertensive drugs, are required to address this hypothesis. Reversal of vascular remodeling and the changes in Cx expression following the reduction of blood pressure with anti-hypertensive drugs would confirm the relationship between hypertension, vascular remodeling and altered Cx expression. In contrast, any differences remaining following anti-hypertensive treatment, consistent with those seen in the pre-hypertensive phase, would be indicative of differences between the two strains. Various drugs have been used to lower blood pressure in hypertensive animals. These included ACE inhibitors, AT receptor antagonists, Ca^{2+} channel blockers, and inhibition of superoxide anion production. Inhibition of ACE has been shown to reverse vascular remodeling and blood pressure in various vascular beds of the SHR (Otsuka *et al.* 1998; Sharifi *et al.* 1998b; Intengan *et al.* 1999; Saleh & Jurjus, 2001). However the underlying mechanisms by which ACE inhibitors reverse vascular remodeling vary depending on the vascular bed (Kett *et al.* 1995; Bergstrom *et al.* 1998). In a similar manner, AT_1 receptor antagonists, Ca^{2+} channel blockers, ET_A receptor antagonists and the inhibition of superoxide anion also reduce blood pressure and vascular remodeling in the SHR (Rao & Berk, 1992; Lacolley *et al.* 1995; Levy *et al.* 1996; Otsuka *et al.* 1998; Fujii *et al.* 1999; Koffi *et al.* 1999; Park *et al.* 2002).

8.4   GAP JUNCTIONS AND VASCULAR FUNCTION DURING HYPERTENSION

Cellular remodeling and changes in Cx expression have potentially important implications for the propagation of vascular responses within both the endothelium and smooth muscle. Reduced electrical coupling within the media of the caudal artery demonstrated here during hypertension was consistent with the observed increase in the number of smooth muscle cell layers and reduction in Cx expression. However, EDHF-mediated relaxation was not affected in this vessel during hypertension, despite the significant reduction in Cx40 within the endothelium and the reduction in EDHF-mediated

hyperpolarization. The maintenance of this response results from the increased incidence of MEGJs coupling the endothelium and smooth muscle of the SHR (Sandow *et al.* 2003b). Several studies have reported a reduction in EDHF-mediated hyperpolarization and relaxation in the mesenteric artery of the aged SHR compared to WKY (Fujii *et al.* 1992; Onaka *et al.* 1998) and therefore an absence of such a response in this study may simply reflect the age of animals or the nature of the vascular bed examined. The incidence of MEGJs in aged animals is unknown and thus requires further examination.

Given that the conduction of vasodilator responses occurs principally in the endothelium (Dora, 2001; Segal *et al.* 2001; Yamamoto *et al.* 2001; Sandow *et al.* 2003d), a reduction in endothelial cell size and Cx expression is likely to result in reduced conducted vasodilation. Indeed, reduced conducted vasodilation has been reported in cremaster arterioles of the Cx40 knockout mouse (de Wit *et al.* 2000). In contrast, the results of Chapter 7 demonstrate that while the involvement of K_{IR} channels in conduction is altered in the mesenteric artery during hypertension, the residual conducted vasodilation was unaltered. From these results it may be hypothesised that Cx40 may have greater functional importance than Cx37 within the endothelium. In contrast, since conducted responses due to K_{IR} were reduced in the SHR, it is possible that conduction of these responses may involve Cx37, although, this hypothesis requires further examination. Alternatively, the reduction in Cx37 expression observed in the mesenteric artery (25%) may not be sufficiently significant to impact on endothelial function. Studies in Cx knockout mice, whereby Cx37 can be abolished specifically in the endothelium, in a similar manner to Cx43 endothelial knockout mice (Liao *et al.* 2001; Theis *et al.* 2001), may provide further answers to these questions. Furthermore, experiments examining conducted vasodilation within the caudal artery of the SHR, where a 31% reduction in endothelial expression of Cx40 was observed, will be required to determine whether this reduction is sufficient to compromise conducted vasodilatory responses.

8.5 EXPERIMENTAL HYPERTENSION

Worldwide, essential hypertension in humans affects 25-35% of the population (Staessen *et al.* 2003). Several animal models are used in the study of hypertension, with the SHR being most commonly used as a model for human essential hypertension (Stoll & Jacob, 2001). In this model of hypertension, the renin-angiotensin system plays a major role in both the development and maintenance of hypertension (Li & Jackson, 1987).

Inbred WKY rats were initially developed as a normotensive control for the SHR (Hansen *et al.* 1973), however, the validity of using the WKY as a genetic control for the SHR has recently been questioned. The distribution of both WKY and SHR animals before they were fully inbred, has lead to significant genetic diversity between the two strains (Louis & Howes, 1990; Johnson *et al.* 1992; Kurtz & Morris, 1987; Kurtz *et al.* 1989; Alemayehu *et al.* 2002). Given these concerns, it may be argued that the SHR is not the most appropriate model for the examination of hypertension. Given the impracticalities of re-deriving the SHR and its normotensive WKY control, one way to overcome the genetic variability between the two strains in comparative studies, is to use several normotensive rat strains. A complementary approach is to use models whereby hypertension within a normotensive rat is induced with drug treatment, thus permitting the untreated rat to serve as the normotensive control. Induced models of hypertension include, DOCA-salt, adrenocorticotropic hormone (ACTH) and 2, kidney, 1 clip hypertensive rats, which represent models of glucocorticoid-induced hypertension, mineralocorticoid-induced hypertension and renovascular hypertension respectively (Whitworth, 1990; Hollenber *et al.* 1992; Webb *et al.* 1984). Unfortunately however, these types of hypertension comprise only a minority of hypertension cases in humans and therefore, their use as models for human essential hypertension, which is multifactorial in nature, is limited. Alternatively, like the SHR, it has been suggested that L-NAME induced hypertension in the rat represents a renin-angiotensin model of hypertension (Takemoto *et al.* 1997a,b) and this may represent a suitable model for relevant studies of hypertension in the future.

8.6   CONCLUSION

In conclusion, the results presented in this thesis have outlined clear evidence supporting a link between reduced Cx expression, vascular remodeling and altered cellular coupling in the hypertensive rat. In muscular arteries of the systemic circulation, but not in elastic arteries, some of these changes in Cx expression may precede the development of hypertension and thus contribute to the increase in blood pressure. Changes in cellular coupling were found to occur throughout the vasculature and were not limited to vessels involved in peripheral resistance. However, the heterogeneous nature of changes occurring within the vasculature during hypertension is likely to reflect the functional properties of each vascular bed. The regulation of gap junction channels and thus cellular coupling may provide potential therapeutic targets for the future treatment of hypertension.

REFERENCE LIST

Ahmad S, Diez JA, George CH, Evans WH. (1999) Synthesis and assembly of connexins in vitro into homomeric and heteromeric functional gap junction hemichannels. *Biochem J.* 339:247-253.

Alcoléa S, Theveniau RM, Jarry GT, Marics I, Tzouanacou E, Chauvin JP, Briand JP, Moorman AF, Lamers WH, Gros DB. (1999) Downregulation of connexin 45 gene products during mouse heart development. *Circ Res.* 84:1365-1379.

Alemayehu A, Breen L, Printz MP. (2002) A new inbred Wistar-Kyoto rat substrain exhibiting apparent salt sensitivity and borderline hypertension. *Am J Physiol.* 283:H1181-H1190.

Allen T, Iftinca M, Cole WC, Plane F. (2002) Smooth muscle membrane potential modulates endothelium-dependent relaxation of rat basilar artery via myo-endothelial gap junctions. *J Physiol.* 545:975-986.

Amann K, Gharehbaghi H, Stephen S, Mall G. (1995) Hypertrophy and hyperplasia of smooth muscle cells of small intramyocardial arteries in spontaneously hypertensive rats. *Hypertension.* 25:124-131.

Amann K, Wolf B, Nichols C, Tornig J, Schwarz U, Zeier M, Mall G, Ritz E. (1997) Aortic changes in experimental renal failure: hyperplasia or hypertrophy of smooth muscle cells? *Hypertension.* 29:770-775.

Arensbak B, Mikkelsen HB, Gustafsson F, Christensen T, Holstein-Rathlou N-H. (2001) Expression of connexin 37, 40, and 43 mRNA and protein in renal preglomerular arterioles. *Histochem and Cell Biol* 115:479-487.

Arribas SM, Gordon JF, Daly CJ, Dominiczak AF, McGrath JC. (1996) Confocal microscopic characterization of a lesion in a cerebral vessel of the stroke-prone spontaneously hypertensive rat. *Stroke.* 27:1118-1122.

Arribas SM, Hillier C, Gonzalez C, McGrory S, Dominiczak AF, McGrath JC. (1997) Cellular aspects of vascular remodeling in hypertension revealed by confocal microscopy. *Hypertension.* 30:1455-1464.

Aydin F, Rosenblum WI, Povlishock JT. (1991) Myoendothelial junctions in human brain arterioles. *Stroke.* 22:1592-1597.

Barbee KA, Davies PF, Lal R. (1994) Shear stress-induced reorganization of the surface topography of living endothelial cells imaged by atomic force microscopy. *Circ Res.* 74:163-171.

Bartlett IS, Segal SS. resolution of smooth muscle and endothelial pathways for conduction along hamster cheek pouch arterioles. *Am J Physiol.* 2000;278:H604-H612.

Bastide B, Neyses L, Ganten D, Paul M, Willecke K, Traub O. (1993) Gap junction protein connexin40 is preferentially expressed in vascular endothelium and conductive bundles of rat myocardium and is increased under hypertensive conditions. *Circ Res.* 73:1138-1149.

Bauersachs J, Hecker M, Busse R. (1994) Display of the characteristics of endothelium-derived hyperpolarizing factor by cytochrome P450-derived arachidonic acid metabolite in the coronary microcirculation. *Br J Pharmac.* 113:1548-1553.

Bauersachs J, Popp R, Fleming I, Busse R. (1997) Nitric oxide and endothelium-derived hyperpolarizing factor: formation and interactions. *Prostaglandins Leukot Essent Fatty Acids.* 57:439-446.

Baumbach GL, Heistad DD. (1989) Remodeling of cerebral arterioles in chronic hypertension. *Hypertension.* 13:968-972.

Baumbach GL, Hajdu MA. (1993) Mechanics and composition of cerebral arterioles in renal and spontaneously hypertensive rats. *Hypertension.* 21:816-826.

Baumbach GL, Sigmund CD, Faraci FM. (2003) Cerebral arteriolar structure in mice overexpressing human renin and angiotensinogen. *Hypertension.* 41:50-55.

Beardslee MA, Laing JG, Beyer EC, Saffitz JE. (1998) Rapid turnover of connexin43 in the adult rat heart. *Circ Res.* 83:629-635.

Beblo DA, Wang HZ, Beyer EC, Westphale EM, Veenstra RD. (1995) Unique conductance, gating, and selective permeability properties of gap junction channels formed by connexin40. *Circ Res.* 77:813-822.

Beny J-L, von der Weid P-Y. (1991) Hyperpolarising factors. *Curr Sci.* 2:300-306.

Beny J-L, Connat JL. (1992) An electron-microscopic study of smooth muscle cell dye coupling in the pig coronary arteries. Role of gap junctions. *Circ Res.* 70:49-55.

Beny J-L. Electrical coupling between smooth muscle cells and endothelial cells in pig coronary arteries. (1997) *Pflugers Archivs.* 433:364-367.

Beny J-L. (1999) Information networks in the arterial wall. *News in Physiol Sci.* 14:68-73.

Bergstrom G, Johansson I, Stevenson KM, Kett MM, Anderson WP. (1998) Perindopril treatment affects both preglomerular renal vascular lumen dimensions and in vivo responsiveness to vasoconstrictors in spontaneously hypertensive rats. *Hypertension*. 31:1007-1013.

Berman RS, Martin PE, Evans WH, Griffith TM. (2002) Relative contributions of NO and gap junctional communication to endothelium-dependent relaxations of rabbit resistance arteries vary with vessel size. *Microvasc Res*. 63:115-128.

Berne RM, Rubio R. (1979) Coronary circulation. In: The cardiovascular system. Berne RM, Sperelakis N, Geiger SR, eds. Williams and Williams, Baltimore, MD.

Beyer EC, Steinberg TH. (1991) Evidence that the gap junction protein connexin-43 is the ATP-induced pore of mouse macrophages. *J Biol Chem*. 266:7971-7974.

Beyer EC, Reed KE, Westphale EM, Kanter HL, Larson DM. (1992) Molecular cloning and expression of rat connexin40, a gap junction protein expressed in vascular smooth muscle. *J Membrane Biol*. 127:69-76.

Beyer EC, Gemel J, Seul KH, Larson DM, Banach K, Brink PR. (2000) Modulation of intercellular communication by differential regulation and heteromeric mixing of co-expressed connexins. *Braz J Med Biol Res*. 33:391-397.

Beyer EC, Berthoud VM. (2002) Gap junction synthesis and degradation as therapeutic targets. *Curr Drug Targets*. 3:409-416.

Blackburn JP, Connat JL, Severs NJ, Green CR. (1997) Connexin43 gap junction levels during development of the thoracic aorta are temporarily correlated with elastic laminae deposition and increased blood pressure. *Cell Biol Int*. 21:87-97.

Blackburn JP, Peters NS, Yeh H-I, Rothery S, Green CR, Severs NJ. (1995) Upregulation of connexin43 gap junctions during early stages of human coronary atherosclerosis. *Arterioscler Thromb Vasc Biol*. 15:1219-1228.

Bolton TB, Lang RJ, Takewaki T. (1984) Mechanisms of action of noradrenaline and carbachol on smooth muscle of guinea-pig anterior mesenteric artery. *J Physiol*. 351:549-572.

Bolz S-S, Pieperhoff S, de Wit C, Pohl U. (2001) Intact endothelial and smooth muscle function in small resistance arteries after 48 h in vessel culture. *Am J Physiol* 279:H1434-H1439.

Boulanger CM. (1999) Secondary endothelial dysfunction: hypertension and heart failure. *J Mol Cell Cardiol*. 31:39-49.

Bouloumie A, Bauersachs J, Linz W, Scholkens BA, Wiemer G, Fleming I, Busse R. (1997) Endothelial dysfunction coincides with an enhanced nitric oxide synthase expression and superoxide anion production. *Hypertension*. 30:934-941.

Brink PR, Cronin K, Banach K, Peterson E, Westphale EM, Seul KH, Ramanan SV, Beyer EC. (1997) Evidence for heteromeric gap junction channels formed from rat connexin43 and human connexin37. *Am J Physiol*. 273:C1386-C1396.

Brink PR. (1998) Gap junctions in vascular smooth muscle. *Acta physiol scand*. 164:349-356.

Brink PR, Ricotta J, Christ GJ. (2000) Biophysical characteristics of gap junctions in vascular wall cells: implications for vascular biology. *Braz J Med Biol Res*. 33:415-422.

Brink PR. (2002) Are gap junction channels a therapeutic target and if so what properties are best exploited? *Curr Drug Targets*. 3:417-425.

Brock JA, van Helden DF. (1995) Enhanced excitatory junction potentials in mesenteric arteries from spontaneously hypertensive rats. *Pflugers Arch*. 430:901-908.

Bruzzone R, Haefliger JA, Gimlich RL, Paul DL. (1993) Connexin40, a component of gap junctions in vascular endothelium, is restricted in its ability to interact with other connexins. *Mol Biol Cell*. 4:7-20.

Budel S, Bartlett IS, Segal SS. (2003) Homocellular conduction along endothelium and smooth muscle of arterioles in hamster cheek pouch: unmasking an NO wave. *Circ Res*. 93:61-68.

Bukauskas FF, Jordan K, Bukauskiene A, Bennett MVL, Lampe PD, Laird DW, Verselis VK. (2000) Clustering of connexin 43-enhanced green fluorescent protein gap junction channels and functional coupling in living cells. *Proc Natl Acad Sci USA*. 97:2556-2561.

Burt JM. (1987) Block of intercellular communication: interaction of intracellular H^+ and Ca^{2+}. *Am J Physiol*. 253:C607-C612.

Burt JM, Fletcher AM, Steele TD, Wu Y, Cottrell T, Kurjiaka DT. (2001) Alteration of Cx43:Cx40 expression ratio in A7r5 cells. *Am J Physiol*. 280:C500-C508.

Busse R, Mulsch A. (1990) Induction of nitric oxide synthase by cytokines in vascular smooth muscle cells. *FEBS Lett*. 275:87-90.

Bussemaker E, Popp R, Binder J, Busse R, Fleming I. (2003) Characterization of the endothelium-derived hyperpolarizing factor (EDHF) response in the human interlobar artery. *Kidney Int.* 63:1749-1755.

Cai W-J, Koltai S, Kocsis E, Scholz D, Schaper W, Schaper J. (2001) Connexin37, not Cx40 and Cx43, is induced in vascular smooth muscle cells during coronary arteriogenesis. *J Mol Cell Cardiol.* 33:957-967.

Calero G, Kanemitsu M, Taffet SM, Lau AF, Delmar M. (1998) A 17mer peptide interferes with acidification-induced uncoupling of connexin43. *Circ Res.* 82:929-935.

Campbell DJ, Duncan A, Kladis A, Harrap SB. (1995) Angiotensin peptides in spontaneously hypertensive and normotensive donryu rats. *Hypertension.* 25:928-934.

Campbell WB, Harder DR. (1999) Endothelium-derived hyperpolarizing factors and vascular cytochrome P450 metabolites of arachidonic acid in the regulation of tone. *Circ Res.* 84:484-488.

Carter TD, Chen XY, Carlie G, Kalapothakis E, Ogden D, Evans WH. (1996) Porcine aoetic endothelial gap junctions: identification and permaeation by caged InsP$_3$. *J Cell Sci.* 109:1765-1773.

Cassis LA, Stitzel RE, Head RJ. (1985) Hypernoradrenergic innervation of the caudal artery of the spontaneously hypertensive rat: an influence upon neuroeffector mechanisms. *J Pharmacol Exp Ther.* 234:792-803.

Chauhan S, Rahman A, Nilsson H, Clapp L, MacAllister R, Ahluwalia A. (2003) NO contributes to EDHF-like responses in rat small arteries: a role for NO stores. *Cardiovasc Res.* 57:207-216.

Chaytor AT, Evans WH, Griffith TM. (1997) Peptides homologous to extracellular loop motifs of connexin 43 reversibly abolish rhythmic contractile activity in rabbit arteries. *J Physiol.* 503:99-110.

Chaytor AT, Evans WH, Griffith TM. (1998) Central role of heterocellular gap junctional communication in endothelium-dependent relaxations of rabbit arteries. *J Physiol.* 508:561-573.

Chaytor AT, Martin PEM, Edwards DH, Griffith TM. (2001) Gap junctional communication underpins EDHF-type relaxations evoked by Ach in the rat hepatic artery. *Am J Physiol.* 280:H2441-H2450.

Chaytor AT, Taylor HJ, Griffith TM. (2002) Gap junction-dependent and -independent EDHF-type relaxations may involve smooth muscle cAMP accumulation. *Am J Physiol.* 282:H1548-H1555.

Chrissobolis S, Ziogas J, Anderson CR, Chu Y, Faraci FM, Sobey CG. (2002) Neuronal NO mediates cerebral vasodilator responses to K^+ in hypertensive rats. *Hypertension.* 39:880-885.

Christ GJ, Spray DC, el-Sabban M, Moore LK, Brink PR. (1996) Gap junctions in vascular tissues. Evaluating the role of intercellular communication in the modulation of vasomotor tone. *Circ Res.* 79:631-646.

Christensen KL, Mulvany M. (2001) Location of resistance arteries. *J Vasc Res.* 38:1-12.

Churchill GC, Lurtz MM, Louis CF. (2001) Ca(2+) regulation of gap junctional coupling in lens epithelial cells. *Am J Physiol.* 281:C972-C981.

Coleman HA, Tare M, Parkington HC. (2001) EDHF is not K^+ but may be due to spread of currnet from the endothelium in guinea pig arterioles. *Am J Physiol.* 280:H2478-H2483.

Coppen SR, Dupont E, Rothery S, Severs NJ. (1998) Connexin45 expression is preferentially associated with the ventricular conduction system in mouse and rat heart. *Circ Res.* 82:232-243.

Coppen SR, Kodama I, Boyett MR, Dobrzynski H, Takagishi Y, Honjo H, Yeh H-I, Severs NJ. (1999) Connexin45, a major connexin of the rabbit sinoatrial node, is co-expressed with connexin43 in a restricted zone at the nodal-crista terminalis border. *J Histochem Cytochem.* 47:907-918.

Cottrell GT, Burt JM. (2001) Heterotypic gap junction channel formation between heteromeric and homomeric Cx40 and Cx43 connexons. *Am J Physiol.* 281:C1559-C1567.

Cottrell GT, Wu Y, Burt JM. (2002) Cx40 and Cx43 expression ratio influences heteromeric/ heterotypic gap junction channel properties. *Am J Physiol.* 282:C1469-C1482.

Cowan DB, Lye SJ, Langille BL. (1998) Regulation of vascular connexin43 gene expression by mechanical loads. *Circ Res.* 82:786-793.

Crow DS, Beyer EC, Paul DL, Kobe SS, Lau AF. (1990) Phosphorylation of connexin43 gap junction protein in uninfected and Rous sarcoma virus-transformed mammalian fibroblasts. *Mol Cell Biol.* 10:1754-1763.

Crow JM, Atkinson MM, Johnson RG. (1994) Micromolar levels of intracellular calcium reduce gap junctional permeability in lens cultures. *Invest Ophthalmol Vis Sci.* 35:3332-3341.

Dahl G, Nonner W, Werner R. (1994) Attempts to define functional domains of gap junction proteins with synthetic peptides. *Biophys J.* 67:1816-1822.

Daniel RE, Boitnott JK, Brown GD, Heptinstall RH. (1982) Aortic endothelial cell activity in high renin and normal renin models of hypertension in the rat. *Lab Invest.* 47:451-458.

Darrow BJ, Fast VG, Kleber AG, Beyer EC, Saffit JE. (1996) Functional and structural assesment of intercellular communication. Increased conduction velocity and enhanced connexin expression in dibutyryl cAMP-treated cultured cardiac myocytes. *Circ Res.* 79:174-183.

Davies PF, Remuzzi A, Gordon EJ, Dewey CF, Jr, Gimbrone MA, Jr. (1986) Turbulent fluid shear stress induces vascular endothelial cell turnover in vitro. *Proc Natl Acad Sci U S A.* 83:2114-2117.

Davies PF, Robotewskyj A, Griem ML, Dull RO, Polacek DC. (1992) Hemodynamic forces and vascular cell communication in arteries. *Arch Pathol Lab Med.* 116:1301-1306.

Davies PF, Tripathi SC. (1993) Mechanical stress mechanisms and the cell. An endothelial paradigm. *Circ Res.* 72:239-245.

Davies PF. (1997) Haemodynamic influences on vascular remodelling. *Transpl Immunol.* 5:243-245.

Davis LM, Rodefeld ME, Green K, Beyer EC, Saffitz JE. (1995) Gap junction protein phenotypes of the human heart and conduction system. *J Cardiovasc Electrophysiol.* 6:813-822.

Davis MJ. (1993) Myogenic response gradient in an arteriolar network. *Am J Physiol.* 264:H2168-H2179.

Davis MJ, Hill MA. (1999) Signaling mechanisms underlying the vascular myogenic response. *Physiol Rev.* 79:387-423.

De Chastonay C, Gabbiani G, Elemer G, Hüttner I. (1983) Remodeling of the rat aortic endothelial layer during experimental hypertension: changes in replication rate, cell density, and surface morphology. *Lab Invest.* 48:45-52.

De Vriese AS, Van d, V, Lameire NH. (2002) Effects of connexin-mimetic peptides on nitric oxide synthase- and cyclooxygenase-independent renal vasodilation. *Kidney Int*. 61:177-185.

de Wit C, Roos F, Bolz S-S, Kirchhoff S, Krüger O, Willecke K, Pohl U. (2000) Impaired conduction of vasodilation along arterioles in connexin40-deficient mice. *Circ Res*. 86:649-655.

Delorme B, Dahl E, Jarry-Guichard T, Briand JP, Willecke K, Gros D, Theveniau-Ruissy M. (1997) Expression pattern of connexin gene products at the early developmental stages of the mouse cardiovascular system. *Circ Res*. 81:423-437.

DePaola N, Gimbrone MA, Jr., Davies PF, Dewey CF, Jr. (1992) Vascular endothelium responds to fluid shear stress gradients. *Arterioscler Thromb*. 12:1254-1257.

DePaola N, Davies PF, Pritchard WF, Jr., Florez L, Harbeck N, Polacek DC. (1999) Spatial and temporal regulation of gap junction connexin43 in vascular endothelial cells exposed to controlled disturbed flows in vitro. *Proc Natl Acad Sci U S A*. 96:3154-3159.

DeWitt DL, Day JS, Sonnenburg WK, Smith WL. (1983) Concentrations of prostaglandin endoperoxide synthase and prostaglandin I_2 synthase in the endothelium and smooth muscle of bovine aorta. *J Clin Invest*. 72:1882-1888.

Dickhout JG, Lee RM. (1997) Structural and functional analysis of small arteries from young spontaneously hypertensive rats. *Hypertension*. 29:781-789.

Dickhout JG, Lee RM. (1998) Blood pressure and heart rate development in young spontaneously hypertensive rats. *Am J Physiol*. 274:H794-H800.

Dickhout JG, Lee RMKW. (1999) Apoptosis in the muscular arteries from young spontaneously hypertensive rats. *J Hypertens*. 17:1413-1419.

Dickhout JG, Lee RMKW. (2000) Increased medial smooth muscle cell length is responsible for vascular hypertrophy in young hypertensive rats. *Am J Physiol*. 279:H2085-H2094.

Diez J, Panizo A, Hernandez M, Pardo J. (1997) Is the regulation of apoptosis altered in smooth muscle cells of adult spontaneously hypertensive rats? *Hypertension*. 29:776-780.

Dohi Y, Kojima M, Sato K. (1996) Endothelial modulation of contractile responses in arteries from hypertensive rats. *Hypertension*. 28:732-737.

Dora KA. (2001) Cell-cell communication in the vessel wall. *Vascular Medicine*. 6:43-50.

Dora KA, Sandow SL, Gallager NT, Takano H, Rummery NM, Hill CE, Garland CJ. (2003) Myoendothelial gap junctions may provide the pathway for EDHF in mouse mesenteric artery. *J Vasc Res.* In press.

Dupont E, el Aoumari A, Fromaget C, Briand J-P, Gros D. (1991) Affinity purification of a rat-brain junctional protein, connexin 43. Euro J Biochem. 200:263-270.

Edwards G, Dora KA, Gardner MJ, Garland CJ, Weston AH. (1998) K$^+$ is an endothelium-derived hyperpolarizing factor in rat arteries. *Nature.* 396:269-272.

Edwards G, Weston AH. (1998) Endothelium-derived hyperpolarizing factor - a critical appraisal. *Prog Drug Res.* 50:107-133.

Ek JF, Delmar M, Perzova R, Taffet SM. (1994) Role of histidine 95 on pH gating of the cardiac gap junction protein connexin43. *Circ Res.* 74:1058-1064.

Ek-Vitorin JF, Calero G, Morley GE, Coombs W, Taffet SM, Delmar M. (1996) PH regulation of connexin43: molecular analysis of the gating particle. *Biophys J.* 71:1273-1284.

el Aoumari A, Dupont E, Fromaget C, Jarry T, Briand JP, Kreitman B, Gros D. (1991) Immunolocalization of an extracellular domain of connexin43 in rat heart gap junctions. *Eur J Cell Biol.* 56:391-400.

Elfgang C, Eckert R, Lichtenberg-Frate H, Butterweck A, Traub O, Klein RA, Hulser DF, Willecke K. (1995) Specific permeability and selective formation of gap junction channels in connexin-transfected HeLa cells. *J Cell Biol.* 129:805-817.

Emanueli C, Bonaria SM, Figueroa C, Chao J, Chao L, Gaspa L, Capogrossi MC, Madeddu P. (2000) Participation of kinins in the captopril-induced inhibition of intimal hyperplasia caused by interruption of carotid blood flow in the mouse. *Br J Pharmacol.* 130:1076-1082.

Emerson GG, Segal SS. (2000a) Electrical coupling between endothelial cells and smooth muscle cells in hamster feed arteries: role in vasomotor control. *Circ Res.* 87:474-479.

Emerson GG, Segal SS. (2000b) Endothelial cell pathway for conduction of hyperpolarization and vasodilation along hamster feed arteries. *Circ Res.* 86:94-100.

Emerson GG, Segal S. (2001) Electrical activation of endothelium evokes vasodilation and hyperpolarization along hamster feed arteries. *Am J Physiol.* 280:H160-H167.

Emerson GG, Neild TO, Segal SS. (2002) Conduction of hyperpolarization along hamster feed arteries: augmentation by acetylcholine. *Am J Physiol.* 283:H102-H109.

Evans WH, Boitano S. (2001) Connexin mimetic peptides: specific inhibitors of gap-junctional intercellular communication. *Biochem Soc Trans*. 29:606-612.

Falk MM, Kumar NM, Gilula NB. (1994) Membrane insertion of gap junction connexins: polytopic channel forming membrane proteins. *J Cell Biol*. 127:343-355.

Falk MM, Buehler LK, Kumar NM, Gilula NB. (1997) Cell-free synthesis and assembly of connexins into functional gap junction membrane channels. *EMBO J*. 16:2703-2716.

Falk MM. (2000a) Biosynthesis and structural composition of gap junction intercellular membrane channels. *Eur J Cell Biol*. 79:564-574.

Falk MM. (2000b) Connexin-specific distribution within gap junctions revealed in living cells. *J Cell Sci*. 113:4109-4120.

Faraci FM, Heistad DD. (1990) Regulation of large cerebral arteries and cerebral microvascular pressure. *Circ Res*. 66:8-17.

Faraci FM. (1992) Regulation of the cerebral circulation by endothelium. *Pharmacol Ther*. 56:1-22.

Faraci FM, Heistad DD. (1998) Regulation of the cerebral circulation: role of endothelium and potassium channels. *Physiol Rev*. 78:53-97.

Ferro TJ, Parker DM, Commins LM, Phillips PG, Johnson A. (1993) Tumor necrosis factor-alpha activates pulmonary artery endothelial protein kinase C. *Am J Physiol*. 264:L7-14.

Figueroa XF, Paul DL, Simon AM, Goodenough DA, Day KH, Damon DN, Duling BR. (2003) Central role of connexin40 in the propagation of electrically activated vasodilation in mouse cremasteric arterioles in vivo. *Circ Res*. 92:793-800.

Fleming I, Busse R. Control and consequences of endothelial nitric oxide formation. (1995) *Adv Pharmacol*. 34:187-206.

Folkow B. Physiological aspects of primary hypertension. (1982) *Physiol Rev*. 62:347-504.

Fujii K, Heistad DD, Faraci FM. (1990) Vasomotion of basilar arteries in vivo. *Am J Physiol*. 258:H1829-H1834.

Fujii K, Tominaga M, Ohmori S, Kobayashi K, Takata Y, Fujishima M. (1992) Decreased endothelium-dependent hyperpolarization to acetylcholine in smooth muscle of the mesenteric artery of spontaneously hypertensive rats. *Circ Res*. 70:660-669.

Fujii K, Umemoto S, Fujii A, Yonezawa T, Sakumura T, Matsuzaki M. (1999) Angiotensin II type 1 receptor antagonist downregulates nonmuscle myosin heavy chains in spontaneously hypertensive rat aorta. *Hypertension.* 33:975-980.

Gabbiani G, Elemer G, Vallotton GMB, Badonnel M-C, Hüttner I. (1979) Morphological and functional changes of the aortic intima during experimental hypertension. *Am J Pathol.* 96:399-422.

Gabriels JE, Paul DL. (1998) Connexin43 is highly localized to sites of disturbed flow in rat aortic endothelium but connexin37 and connexin40 are more uniformly distributed. *Circ Res.* 83:636-643.

Gaietta G, Deerinck TJ, Adams SR, Bouwer J, Tour O, Laird DW, Sosinsky GE, Tsien RY, Ellisman MH. (2002) Multicolor and electron microscopic imaging of connexin trafficking. *Science.* 296:503-507.

Garland CJ, Plane F, Kemp BK, Cox TM. (1995) Endothelium-dependent hyperpolarization: a role in the control of vascular tone. *Trends Pharmacol Sci.* 16:23-30.

Ge T, Hughes H, Junquero DC, Wu KK, Vanhoutte PM, Boulanger CM. (1995) Endothelium-dependent contractions are associated with both augmented expression of prostaglandin H synthase-1 and hypersensitivity to prostaglandin H2 in the SHR aorta. *Circ Res.* 76:1003-1010.

George CH, Kendall JM, Evans WH. (1999) Intracellular trafficking pathways in the assembly of connexins into gap junctions. *J Biol Chem.* 274:8678-8685.

Gilula NB, Reeves OR, Steinbach A. (1972) Metabolic coupling, ionic coupling and cell contacts. *Nature.* 235:262-265.

Giummelly P, Lartaud-Idjouadiene I, Marque V, Niederhoffer N, Chillon J-M, Capdeville-Atkinson C, Atkinson J. (1999) Effects of aging and antihypertensive treatement on aortic internal diameter in spontaneously hypertensive rats. *Hypertension.* 34:207-211.

Goldberg GS, Moreno AP, Bechberger JF, Hearn SS, Shivers RR, MacPhee DJ, Zhang YC, Naus CC. (1996) Evidence that disruption of connexon particle arrangements in gap junction plaques is associated with inhibition of gap junctional communication by a glycyrrhetinic acid derivative. *Exp Cell Res.* 222:48-53.

Goldman LA, Cutrone EC, Kotenko SV, Krause CD, Langer JA. (1996) Modifications of vectors pEF-BOS, pcDNA1 and pcDNA3 result in improved convenience and expression. *Biotechniques.* 21:1013-1015.

Goodenough DA, Goliger JA, Paul DL. (1996) Connexins, connexons, and intercellular communication. *Annu Rev Biochem*. 65:475-502.

Goto K, Fujii K, Kansui Y, Abe I, Iida M. (2002) Critical role of gap junctions in endothelium-dependent hyperpolarization in rat mesenteric arteries. *Clin Exp Pharmacol Physiol*. 29:595-602.

Gourdie RG, Severs NJ, Green CR, Rothery S, Germroth P, Thompson RP. (1993) The spatial distribution and relative abundance of gap-junctional connexin40 and connexin43 correlate to functional properties of components of the cardiac atrioventricular conduction system. *J Cell Sci*. 105:985-991.

Gratton RJ, Gandley RE, McCarthy JF, Michaluk WK, Slinker BK, McLaughlin MK. (1998) Contribution of vasomotion to vascular resistance: a comparison of arteries from virgin and pregnant rats. *J Appl Physiol*. 85:2255-2260.

Green CR, Peters NS, Gourdie RG, Rothery S, Severs NJ. (1993) Validation of immunohistochemical quantification in confocal scanning laser microscopy: a comparative assessment of gap junction size with confocal and ultrastructural techniques. *J Histochem Cytochem*. 41:1339-1349.

Griffith TM, Chaytor AT, Taylor HJ, Giddings BD, Edwards DH. (2002) cAMP facilitates EDHF-type relaxations in conduit arteries by enhancing electrotonic conduction via gap junctions. *Proc Natl Acad Sci U S A*. 99:6392-6397.

Gropper R, Brandt RA, Elias S, Bearer CF, Mayer A, Schwartz AL, Ciechanover A. (1991) The ubiquitin-activating enzyme, E1, is required for stress-induced lysosomal degradation of cellular proteins. *J Biol Chem*. 266:3602-3610.

Gros D, Jarry-Guichard T, Ten Velde I, de Maziere A, van Kempen MJA, Davoust J, Briand JP, Moorman AFM, Jongsma HJ. (1994) Restricted distribution of connexin40, a gap junctional protein, in mammalian heart. *Circ Res*. 74:839-851.

Gros DB, Jongsma HJ. (1996) Connexins in mammalian heart function. *Bioessays*. 18:719-730.

Grunfeld S, Hamilton CA, Mesaros S, McClain SW, Dominiczak AF, Bohr DF, Malinski T. (1995) Role of superoxide in the depressed nitric oxide production by the endothelium of genetically hypertensive rats. *Hypertension*. 26:854-857.

Gu H, Ek-Vitorin JF, Taffet SM, Delmar M. (2000) Coexpression of connexins 40 and 43 enhances the pH sensitivity of gap junctions: a model for synergistic interactions among connexins. *Circ Res*. 86:e98-e103.

Guan X, Wilson S, Schlender KK, Ruch RJ. (1996) Gap-junction disassembly and connexxin 43 dephosphorylation induced by 18 beta-glycyrrhetinic acid. *Mol Carcinogensis*. 16:157-164.

Guerrero PA, Schuessler RB, Davis LM, Beyer EC, Johnson CM, Yamada KA, Saffitz JE. (1997) Slow ventricular conduction in mice heterozygous for a connexin43 null mutation. *J Clin Invest*. 99:1991-1998.

Guo YH, Martinez-Williams C, Gilbert KA, Rannels DE. (1999) Inhibition of gap junction communication in alveolar epithelial cells by 18a-glycyrrhetinic acid. *Am J Physiol*. 276:L1018-L1026.

Gustafsson H, Mulvany MJ, Nilsson H. (1993) Rhythmic contractions of isolated small arteries from rat: influence of the endothelium. *Acta physiol scand*. 148:153-163.

Gustafsson F, Mikkelsen HB, Arensbak B, Thuneberg L, Neve S, Jensen LJ, Holstein-Rathlou NH. (2003) Expression of connexin 37, 40 and 43 in rat mesenteric arterioles and resistance arteries. *Histochem Cell Biol*. 119:139-148.

Gustincich S, Batalov S, Beisel KW, Bono H, Carninci P, Fletcher CF, Grimmond S, Hirokawa N, Jarvis ED, Jegla T, Kawasawa Y, LeMieux J, Miki H, Raviola E, Teasdale RD, Tominaga N, Yagi K, Zimmer A, Hayashizaki Y, Okazaki Y. (2003) Analysis of the mouse transcriptome for genes involved in the function of the nervous system. *Genome Res*. 13:1395-1401.

Gutstein DE, Morley GE, Tamaddon H, Vaidya D, Schneider MD, Chen FL, Chien KR, Stuhlmann H, Fishman GI. (2001a) Conduction slowing and sudden arrhythmic death in mice with cardiac-restricted inactivation of connexin43. *Circ Res*. 88:333-339.

Gutstein DE, Morley GE, Vaidya D, Liu F, Chen FL, Stuhlmann H, Fishman GI. (2001b) Heterogeneous expression of gap junction channels in the heart leads to conduction defects and ventricular dysfunction. *Circulation*. 104:1194-1199.

Haas TL, Duling BR. (1997) Morphology favors an endothelial cell pathway for longitudinal conduction within arterioles. *Microvasc Res*. 53:113-120.

Haddock RE, Hill CE. (2002) Differential activation of ion channels by inositol 1,4,5-trisphosphate (IP_3)- and ryanodine-sensitive calcium stores in rat basilar artery vasomotion. *J Physiol*. 545:615-627.

Haefliger J-A, Bruzzone R, Jenkins NA, Gilbert DJ, Copeland NG, Paul DL. (1992) Four novel members of the connexin family of gap junction proteins. Molecular cloning, expression, and chromosome mapping. *J Biol Chem*. 267:2057-2064.

Haefliger J-A, Castillo E, Waeber G, Aubert J-F, Waeber B, Meda P. (1997a) Hypertension differentially affects the expression of the gap junction protein connexin43 in cardiac myocytes and aortic smooth muscle cells. *Adv Exp Med Biol.* 432:71-82.

Haefliger J-A, Castillo E, Waeber G, Bergonzelli GE, Aubert JF, Sutter E, Nicod P, Waeber B, Meda P. (1997b) Hypertension increases connexin43 in a tissue-specific manner. *Circulation.* 95:1007-1014.

Haefliger J-A, Meda P, Fromenton A, Wiesel P, Zanchi A, Brunner HR, Nicod P, Hayoz D. (1999) Aortic connexin43 is decreased during hypertension induced by inhibition of nitric oxide synthase. *Arterioscler Thromb Vasc Biol.* 19:1615-1622.

Haefliger J-A, Meda P. (2000) Chronic hypertension alters the expression of Cx43 in cardiovascular muscle cells. *Braz J Med Biol Res.* 33:431-438.

Haefliger J-A, Demotz S, Braissant O, Suter E, Waeber B, Nicod P, Meda, P. (2001) Connexins 40 and 43 are differentially regulated within the kidneys of rats with renovascular hypertension. *Kid Int.* 60:190-201.

Hajdu MA, Baumbach GL. (1994) Mechanics of large and small cerebral arteries in chronic hypertension. *Am J Physiol.* 266:H1027-H1033.

Halushka PV, Mais DE, Mayeux PR, Morinelli TA. (1989) Thromboxane, prostaglandin and leukotriene receptors. *Annu Rev Pharmacol Toxicol.* 29:213-239.

Hanesn CT, Judge FJ, and Whitney RA. (1973) Catalogue of NIH rodents. (DREW 74-606). Washington USA, Department of Health and Human Services.

Hayakawa H, Hirata Y, Suzuki E, Kakoki M, Kikuchi K, Nagano T, Hirobe M, Omata M. (1995) Endothelium-derived relaxing factors in the kidney of spontaneously hypertensive rats. *Life Sci.* 56:L401-L408.

Hayakawa H, Raij L. (1998) Nitric oxide synthase activity and renal injury in genetic hypertension. *Hypertension.* 31:266-270.

He DS, Jiang JX, Taffet SM, Burt JM. (1999) Formation of heterotrimeric gap junction channels by conneins 40 and 43 in vascular smooth muscle cells. *Proc Natl Acad Sci USA.* 96:6495-6500.

Heagerty AM, Aalkjaer C, Bund SJ, Korsgaard N, Mulvany MJ. (1993) Small artery structure in hypertension. Dual processes of remodeling and growth. *Hypertension.* 21:391-397.

Hennemann H, Schwarz HJ, Willecke K. (1992a) Characterization of gap junction genes expressed in F9 embryonic carcinoma cells: molecular cloning of mouse connexin31 and -45 cDNAs. *Eur J Cell Biol.* 57:51-58.

Hennemann H, Suchyna T, Lichtenberg-Frate H, Jungbluth S, Dahl E, Schwarz J, Nicholson BJ, Willecke K. (1992b) Molecular cloning and functional expression of mouse connexin40, a second gap junction gene preferentially expressed in lung. *J Cell Biol*. 117:1299-1310.

Hermans MM, Kortekaas P, Jongsma HJ, Rook MB. (1995) pH sensitivity of the cardiac gap junction proteins, connexin 45 and 43. *Pflugers Arch*. 431:138-140.

Hertlein B, Butterweck A, Haubrich S, Willecke K, Traub O. (1998) Phosphorylated carboxy terminal serine residues stabilize the mouse gap junction protein connexin45 against degradation. *J Membrane Biol*. 162:247-257.

Hill CE, Eade J, Sandow SL. (1999) Mechanisms underlying spontaneous rhythmical contractions in irideal arterioles of the rat. *J Physiol (Lond)*. 521:507-516.

Hill CE, Phillips JK, Sandow SL. (2001) Heterogeneous control of blood flow amongst different vascular beds. *Med Res Rev*. 21:1-60.

Hill CE, Rummery N, Hickey H, Sandow SL. (2002) Heterogeneity in the distribution of vascular gap junctions and connexins: implications for function. *Clin Exp Pharmacol Physiol*. 29:620-625.

Hirst GDS, Choate JK, Cousins HM, Edwards FR, Klemm MF. (1996) Transmission by postganglionic axons of the autonomic nervous system: the importance of the specialized neuroeffector junction. *Neuroscience*. 73:7-23.

Hoepfl B, Rodenwaldt B, Pohl U, de Wit C. (2002) EDHF, but not NO or prostaglandins, is critical to evoke a conducted dilation upon ACh in hamster arterioles. *Am J Physiol*. 283:H996-H1004.

Hollenberg NK, Coletti C, Passan D. (1992) Hypertension, volume and vasoconstriction: studies on the renal blood supply in SHR, WKY and DOCA-salt rat models. *Hypertension Res*. 15:3-11.

Hong T, Hill CE. (1998) Restricted expression of the gap junctional protein connexin 43 in the arterial system of the rat. *J Anat*. 193:583-593.

Honjo H, Boyett MR, Coppen SR, Takagishi Y, Opthof T, Severs NJ, Kodama I. (2002) Heterogeneous expression of connexins in rabbit sinoatrial node cells: correlation between connexin isotype and cell size. *Cardiovasc Res*. 53:89-96.

Horiuchi T, Dietrich HH, Hongo K, Dacey RG. (2002) Mechanism of extracellular K+-induced local and conducted responses in cerebral penetrating arterioles. *Stroke*. 33:2692-2699.

Hossain MZ, Murphy LJ, Hertzberg EL, Nagy JI. (1994) Phosphorylated forms of connexin43 predominate in rat brain: demonstration by rapid inactivation of brain metabolism. *J Neurochem.* 62:2394-2403.

Hu J, Cotgreave IA. (1997) Differential regulation of gap junctions by proinflammatory mediators in vitro. *J Clin Invest.* 99:2312-2316.

Hungerford JE, Sessa WC, Segal SS. (2000) Vasomotor control in arterioles of the mouse cremaster muscle. *FASEB J.* 14:197-207.

Hüttner I, Badonnel M-C, Elemer G, Gabbiani G. (1979) Aortic intima of the rat in various phases of hypertension. *Exp Mol Path.* 31:191-200.

Hüttner I, Costabella PM, De Chastonay C, Gabbiani G. (1982) Volume, surface, and junctions of rat aortic endothelium during experimental hypertension. *Lab Invest.* 46:489-504.

Inoguchi T, Yu HY, Imamura M, Kakimoto M, Kuroki T, Maruyama T, Nawata H. (2001) Altered gap junction activity in cardiovascular tissues of diabetes. *Med Electron Microsc.* 34:86-91.

Intengan HD, Thibault G, Li JS, Schiffrin EL. (1999) Resistance artery mechanics, structure, and extracellular components in spontaneously hypertensive rats: effects of angiotensin receptor antagonism and converting enzyme inhibition. *Circulation.* 100:2267-2275.

Intengan HD, Schiffrin EL. (2000) Structure and mechanical properties of resistance arteries in hypertension: role of adhesion molecules and extracellular matrix determinants. *Hypertension.* 36:312-318.

Jacob A, Beyer EC. (2001) Mouse connexin 45: genomic cloning and exon usage. *DNA and Cell Biology.* 20:11-19.

Jobling P, McLachlan EM. (1992) An electrophysiological study of responses evoked in isolated segments of rat tail artery during growth and maturation. *J Physiol.* 476:83-205.

Johnson CM, Kanter EM, Green KG, Laing JG, Betsuyaku T, Beyer EC, Steinberg TH, Saffitz JE, Yamada KA. (2002) Redistribution of connexin45 in gap junctions of connexin43-deficient hearts. *Cardiovasc Res.* 53:921-935.

Johnson PC, Hanson KM. (1962) Effect of arterial pressure on arterial and venous resistance of intestine. *J Appl Physiol.* 17:503-508.

Jongen WM, Fitzgerald DJ, Asamoto M, Piccoli C, Slaga TJ, Gros D, Takeichi M, Yamasaki H. (1991) Regulation of connexin 43-mediated gap junctional

intercellular communication by Ca^{2+} in mouse epidermal cells is controlled by E-cadherin. *J Cell Biol.* 114:545-555.

Jordan K, Chodock R, Hand AR, Laird DW. (2001) The origin of annular junctions: a mechanism of junction internalization. *J Cell Sci* . 114:763-773.

Kadle R, Zhang JT, Nicholson BJ. (1991) Tissue-specific distribution of differentially phosphorylated forms of Cx43. *Mol Cell Biol.* 11:363-369.

Kanemitsu MY, Lau AF. (1993) Epidermal growth factor stimulates the disruption of gap junctional communication and connexin43 phosphorylation independent of 12-0-tetradecanoylphorbol 13-acetate-sensitive protein kinase C: the possible involvement of mitogen-activated protein kinase. *Mol Biol Cell.* 4:837-848.

Kanemitsu MY, Loo LW, Simon S, Lau AF, Eckhart W. (1997) Tyrosine phosphorylation of connexin 43 by v-Src is mediated by SH2 and SH3 domain interactions. *J Cell Biol.* 272:22824-22831.

Kanter HL, Saffitz JE, Beyer EC. (1992) Cardiac myocytes express multiple gap junction proteins. *Circ Res.* 70:438-444.

Kerr S, Brosnan J, McIntyre M, Reid JL, Dominiczak AF, Hamilton CA. (1999) Superoxide anion production is increased in a model of genetic hypertension: role of the endothelium. *Hypertension.* 33:1353-1358.

Kett MM, Alcorn D, Bertram JF, Anderson WP. (1995) Enalapril does not prevent renal arterial hypertrophy in spontaneously hypertensive rats. *Hypertension.* 25:335-342.

Kihara M, Horie R, Lovenberg W, Yamori Y. (1993) Comparative study of various genetic hypertensive rat strains: blood pressure, body weight, growth and organ weights. *Heart Vessels.* 8:7-15.

Kirchhoff S, Nelles E, Hagendorff A, Kruger O, Traub O, Willecke K. (1998) Reduced cardiac conduction velocity and predisposition to arrhythmias in connexin40-deficient mice. *Curr Biol.* 8:299-302.

Kirchhoff S, Kim JS, Hagendorff A, Thonnissen E, Kruger O, Lamers WH, Willecke K. (2000) Abnormal cardiac conduction and morphogenesis in connexin40 and connexin43 double-deficient mice. *Circ Res.* 87:399-405.

Kitazono T, Faraci FM, Heistad DD. (1996) L-arginine restores dilator responses of the basilar artery to acetylcholine during chronic hypertension. *Hypertension.* 27:893-896.

Ko Y-S, Yeh H-I, Rothery S, Dupont E, Coppen SR, Severs NJ. (1999a) Connexin make-up of endothelial gap junctions in the rat pulmonary artery as revealed by immunoconfocal microscopy and triple-label immunogold electron microscopy. *J Histochem Cytochem.* 47:683-691.

Ko Y-S, Yeh HI, Haw M, Dupont E, Kaba R, Plenz G, Robenek H, Severs NJ. (1999b) Differential expression of connexin43 and desmin defines two subpopulations of medial smooth muscle cells in the human internal mammary artery. *Arterioscler Thromb Vasc Biol.* 19:1669-1680.

Ko Y-S, Coppen SR, Dupont E, Rothery S, Severs NJ. (2001) Regional differentiation of desmin, connexin43, and connexin45 expression patterns in rat aortic smooth muscle. *Arterioscler Thromb Vasc Biol.* 21:355-364.

Koffi I, Safar ME, Labat C, Lacolley P, Benetos A, Mourad JJ. (1999) Arterial structural changes with verapamil in spontaneously hypertensive rats. *Am J Hypertens.* 12:732-738.

Koller A, Huang A. (1999) Development of nitric oxide and prostaglandin mediation of shear stress-induced arteriolar dilation with aging and hypertension. *Hypertension.* 34:1073-1079.

Kost CK, Jr, Jackson EK. (1993) Enhanced renal angiotensin II subtype 1 receptor responses in the spontaneously hypertensive rat. *Hypertension.* 21:420-431.

Kowala MC, Cuenoud HF, Nicolosi R, Joris I, Majno G. (1988) Intimal changes in the aorta of prehypertensive rats. *Exp Mol Path.* 49:171-184.

Krüger O, Plum A, Kim J-S, Winterhager E, Maxeiner S, Hallas G, Kirchhoff S, Traub O, Lamers WH, Willecke K. (2000) Defective vascular development in connexin 45-deficient mice. *Development.* 127:4179-4193.

Kumai M, Nishii K, Nakamura K, Takeda N, Suzuki M, Shibata Y. Loss of connexin45 causes a cushion defect in early cardiogenesis.(2000) *Development.* 127:3501-3512.

Kumar NM, Friend DS, Gilula NB. (1995) Synthesis and assembly of human beta 1 gap junctions in BHK cells by DNA transfection with the human beta 1 cDNA. *J Cell Sci.* 108:3725-3734.

Kumar NM, Gilula NB. (1996) The gap junction communication channel. *Cell.* 84:381-388.

Kurtz TW, Morris RC, Jr. (1987) Biological variability in Wistar-Kyoto rats. Implications for research with the spontaneously hypertensive rat. *Hypertension.* 10:127-131.

Kurtz TW, Montano M, Chan L, Kabra P. (1989) Molecular evidence of genetic heterogeneity in Wistar-Kyoto rats: implications for research with the spontaneously hypertensive rat. *Hypertension*. 13:188-192.

Kwak BR, Jongsma HJ. (1996) Regulation of cardiac gap junction channel permeability and conductance by several phosphorylating conditions. *Mol Cell Biochem*. 157:93-99.

Kwak BR, Jongsma HJ. (1999) Selective inhibition of gap junction channel activity by synthetic peptides. *J Physiol*. 516:679-685.

Kwak BR, Mulhaupt F, Veillard N, Gros DB, Mach F. (2002) Altered pattern of vascular connexin expression in atherosclerotic plaques. *Arterioscler Thromb Vasc Biol*. 22:225-230.

Kwak BR, Veillard N, Pelli G, Mulhaupt F, James RW, Chanson M, Mach F. (2003) Reduced connexin43 expression inhibits atherosclerotic lesion formation in low-density lipoprotein receptor-deficient mice. *Circulation*. 107:1033-1039.

Lacolley P, Ghodsi N, Glazer E, Challande P, Brissac AM, Safar ME, Laurent S. (1995) Influence of graded changes in vasomotor tone on the carotid arterial mechanics in live spontaneously hypertensive rats. *Br J Pharmacol*. 115:1235-1244.

Lagaud G, Davies KP, Venkateswarlu K, Christ GJ. (2002a) The physiology, pathophysiology and therapeutic potential of gap junctions in smooth muscle. *Curr Drug Targets*. 3:427-440.

Lagaud G, Karicheti V, Knot HJ, Christ GJ, Laher I. (2002b) Inhibitors of gap junctions attenuate myogenic tone in cerebral arteries. *Am J Physiol*. 283:H2177-H2186.

Laing JG, Westphale EM, Engelmann GL, Beyer EC. (1994) Characterization of the gap junction protein, connexin45. *J Membrane Biol*. 139:31-40.

Laing JG, Beyer EC. (1995) The gap junction protein connexin43 is degraded via the ubiquitin proteasome pathway. *J Biol Chem*. 270:26399-26403.

Laing JG, Tadros PN, Westphale EM, Beyer EC. (1997) Degradation of connexin43 gap junctions involves both the proteasome and the lysosome. *Exp Cell Res*. 236:482-492.

Laing JG, Tadros PN, Green K, Saffitz JE, Beyer EC. (1998) Proteolysis of connexin43-containing gap junctions in normal and heat-stressed cardiac myocytes. *Cardiovasc Res*. 38:711-718.

Laird DW, Puranam KL, Revel JP. (1991) Turnover and phosphorylation dynamics of connexin43 gap junction protein in cultured cardiac myocytes. *Biochem J.* 273:67-72.

Lais LT, Rios LL, Boutelle S, DiBona GF, Brody MJ. (1977) Arterial pressure development in neonatal and young spontaneously hypertensive rats. *Blood Vessels.* 14:277-284.

Lampe PD, Lau AF. (2000) Regulation of gap junctions by phosphorylation. *Arch Biochem Biophy.* 384: 205-215.

Lampe PD, TenBroek EM, Burt JM, Kurata WE, Johnson RG. (2000) Phosphorylation of connexin43 on serine368 by protein kinase C regulates gap junctional communication. *J Cell Biol.* 149:1503-1512.

Lampe PD, Qiu Q, Meyer RA, TenBroek EM, Walseth TF, Starich TA, Grunenwald HL, Johnson RG. (2001) Gap junction assembly: PTX-sensitive G proteins regulate the distribution of connexin43 within cells. *Am J Physiol.* 281:C1211-C1222.

Larson DM, Haudenschild CC. (1988) Junctional transfer in wounded cultures of bovine aortic endothelial cells. *Lab Invest.* 59:373-379.

Lash JA, Critser ES, Pressler ML. (1990) Cloning of a gap junctional protein from vascular smooth muscle and expression in two-cell mouse embryos. *J Biol Chem.* 265:13113-13117.

Lau AF, Kurata WE, Kanemitsu MY, Loo LW, Warn-Cramer BJ, Eckhart W, Lampe PD. (1996) Regulation of connexin43 function by activated tyrosine protein kinases. *J Bioenerg Biomembr.* 28:359-368.

Lauf U, Giepmans BN, Lopez P, Braconnot S, Chen SC, Falk MM. (2002) Dynamic trafficking and delivery of connexons to the plasma membrane and accretion to gap junctions in living cells. *Proc Natl Acad Sci U S A.* 99:10446-10451.

Lee RM, Garfield RE, Forrest JB, Daniel DD. (1983) Morphometric study of structural changes in the mesenteric blood vessels of spontaneously hypertensive rats. *Blood Vessels.* 20:57-71.

Lee RM. (1985) Vascular changes at the prehypertensive phase in the mesenteric arteries from spontaneously hypertensive rats. *Blood Vessels.* 22:105-126.

Lee RM, Smeda JS. (1985) Primary versus secondary structural changes of the blood vessels in hypertension. *Can J Physiol Pharmacol.* 63:392-401.

Lee RM. (1987) Structural alterations of blood vessels in hypertensive rats. *Can J Physiol Pharmacol.* 65:1528-1535.

Lefer DJ, Lynch CD, Lapinski KC, Hutchins PM. (1990) Enhanced vasomotion of cerebral arterioles in spontaneously hypertensive rats. *Microvasc Res.* 39:129-139.

Levy BI, Benessiano J, Henrion D, Caputo L, Heymes C, Duriez M, Poitevin P, Samuel JL. (1996) Chronic blockade of AT2-subtype receptors prevents the effect of angiotensin II on the rat vascular structure. *J Clin Invest.* 98:418-425.

Li P, Jackson EK. (1987) A possible explanation of genetic hypertension in the spontaneously hypertensive rat. *Life Sci.* 41:1903-1908.

Li X, Simard JM. (1999) Multiple connexins form gap junction channels in rat basilar artery smooth muscle cells. *Circ Res.* 84:1277-1284.

Li X, Simard JM. (2002) Increase in Cx45 Gap Junction Channels in Cerebral Smooth Muscle Cells from SHR. *Hypertension.* 40:940-946.

Liao Y, Day KH, Damon DN, Duling BR. (2001) Endothelial cell-specific knockout of connexin 43 causes hypotension and bradycardia in mice. *PNAS.* 98:9989-9994.

Lidington D, Ouellette Y, Tyml K. (2000) Endotoxin increases intercellular resistance in microvascular endothelial cells by a tyrosine kinase pathway. *J Cell Physiol.* 185:117-125.

Lidington D, Tyml K, Ouellette Y. (2002) Lipopolysaccharide-induced reductions in cellular coupling correlate with tyrosine phosphorylation of connexin 43. *J Cell Physiol.* 193:373-379.

Lidington D, Ouellette Y, Li F, Tyml K. (2003) Conducted vasoconstriction is reduced in a mouse model of sepsis. *J Vasc Res.* 40:149-158.

Little TL, Beyer EC, Duling BR. (1995a) Connexin 43 and connexin 40 gap junctional proteins are present in arteriolar smooth muscle and endothelium *in vivo. Am J Physiol.* 268:H729-H739.

Little TL, Xia J, Duling BR. (1995b) Dye tracers define differential endothelial and smooth muscle coupling patterns within the arteriolar wall. *Circ Res.* 76:498-504.

Loewenstein WR. (1979) Junctional intercellular communication and the control of growth. *Biochim Biophys Acta.* 560:1-65.

Lou YK, Wen C, Li M, Adams DJ, Wang MX, Yang F, Morris BJ, Whitworth JA. (2001) Decreased renal expression of nitric oxide synthase isoforms in

adrenocorticotropin-induced and corticosterone-induced hypertension. *Hypertension*. 37:1164-1170.

Louis WJ, Howes LG. (1990) Genealogy of the spontaneously hypertensive rat and Wistar-Kyoto rat strains: implications for studies of inherited hypertension. *J Cardiovasc Pharmacol*. 16:S1-S5.

Mangos GJ, Fraser TB, Turner SW, Whitworth JA. (1999) The role of the parathyroid glands in adrenocorticotrophin-induced hypertension in the rat. *Clin Exp Hypertens*. 21:1083-1096.

Marque V, Kieffer P, Atkinson J, Lartaud-Idjouadiene I. (1999) Elastic properties and compostion of the aortic wall in old spontaneously hypertensive rats. *Hypertension*. 34:415-422.

Martin PE, Blundell G, Ahmad S, Errington RJ, Evans WH. (2001) Multiple pathways in the trafficking and assembly of connexin 26, 32 and 43 into gap junction intercellular communication channels. *J Cell Sci*. 114:3845-3855.

Martinez AD, Hayrapetyan V, Moreno AP, Beyer EC. (2002) Connexin43 and connexin45 form heteromeric gap junction channels in which individual components determine permeability and regulation. *Circ Res*. 90:1100-1107.

Masuda H, Kawamura K, Nanjo H, Sho E, Komatsu M, Sugiyama T, Sugita A, Asari Y, Kobayashi M, Ebina T, Hoshi N, Singh TM, Xu C, Zarins CK. (2003) Ultrastructure of endothelial cells under flow alteration. *Microsc Res Tech*. 60:2-12.

Matoba T, Shimokawa H, Kubota H, Morikawa K, Fujiki T, Kunihiro I, Mukai Y, Hirakawa Y, Takeshita A. (2002) Hydrogen peroxide is an endothelium-derived hyperpolarizing factor in human mesenteric arteries. *Biochem Biophys Res Commun*. 290:909-913.

McGee TP, Cheng HH, Kumagai H, Omura S, Simoni RD. (1996) Degradation of 3-hydroxy-3-methylglutaryl-CoA reductase in endoplasmic reticulum membranes is accelerated as a result of increased susceptibility to proteolysis. *J Biol Chem*. 271:25630-25638.

McGuire JJ, Ding H, Triggle CR. (2001) Endothelium-derived relaxing factors: a focus on endothelium-derived hyperpolarizing factor(s). *Can J Physiol Pharmacol*. 79:443-470.

McGuire PG, Twietmeyer TA. (1985) Aortic endothelial junctions in developing hypertension. *Hypertension*. 7:483-490.

McNutt NS, Weinstein RS. (1970) The ultrastructure of the nexus. A correlated thin-section and freeze-cleave study. *J Cell Biol.* 47:666-688.

Meyer RA, Laird DW, Revel JP, Johnson RG. (1992) Inhibition of gap junction and adherens junction assembly by connexin and A-CAM antibodies. *J Cell Biol.* 119:179-189.

Mombouli JV, Vanhoutte PM. (1999) Endothelial dysfunction: from physiology to therapy. *J Mol Cell Cardiol.* 31:61-74.

Momose N, Fukuo K, Morimoto S, Ogihara T. (1993) Captopril inhibits endothelin-1 secretion from endothelial cells through bradykinin. *Hypertension.* 21:921-924.

Moncada S, Herman AG, Higgs EA, Vane JR. (1977) Differential formation of prostacyclin (PGX or PGI_2) by layers of the arterial wall. An explanation for the anti-thrombotic properties of vascular endothelium. *Thromb Res.* 11:323-344.

Moncada S, Palmer RMJ, Higgs EA. (1991) Nitric oxide: physiology, pathophysiology, and pharmacology. *Pharmacol Rev.* 43:109-142.

Moreno AP, Saez JC, Fishman GI, Spray DC. (1994) Human connexin43 gap junction channesl: regulation of unitary conductances by phosphorylation. *Circ Res.* 74:1050-1057.

Moreno AP, Laing JG, Beyer EC, Spray DC. (1995) Properties of gap junction channels formed of connexin 45 endogenously expressed in human hepatoma (SKHep1) cells. *Am J Physiol.* 268:C356-C365.

Morley GE, Taffet SM, Delmar M. (1996) Intramolecular interactions mediate pH regulation of connexin43 channels. *Biophys J.* 70:1294-1302.

Morley GE, Ek-Vitorin JF, Taffet SM, Delmar M. (1997) Structure of connexin43 and its regulation by pHi. *J Cardiovasc Electrophysiol.* 8:939-951.

Morley GE, Vaidya D, Samie FH, Lo C, Delmar M, Jalife J. (1999) Characterization of conduction in the ventricles of normal and heterozygous Cx43 knockout mice using optical mapping. *J Cardiovasc Electrophysiol.* 10:1361-1375.

Mukai Y, Shimokawa H, Matoba T, Kandabashi T, Satoh S, Hiroki J, Kaibuchi K, Takeshita A. (2001) Involvement of Rho-kinase in hypertensive vascular disease - a novel therapeutic target in hypertension. *FASEB J.* 15:1062-1064.

Mulvany MJ, Halpern W. (1977) Contractile properties of small arterial resistance vessels in spontaneously hypertensive and normotensive rats. *Circ Res.* 41:19-26.

Mulvany MJ, Hansen PK, Aalkjaer C. (1978) Direct evidence that the greater contractility of resistance vessels in spontaneously hypertensive rats is associated with a narrowed lumen, a thickened media, and an increased number of smooth muscle cell layers. *Circ Res.* 43:854-864.

Mulvany MJ, Korsgaard N. (1983) Correlations and otherwise between blood pressure, cardiac mass and resistance vessel characteristics in hypertensive, normotensive and hypertensive/normotensive hybrid rats. *J Hypertens.* 1:235-244.

Mulvany MJ, Baandrup U, Gundersen HJG. (1985) Evidence for hyperplasia in mesenteric resistance vessels of spontaneously hypertensive rats using a three-dimensional disector. *Circ Res.* 57:794-800.

Mulvany MJ. (1986) Role of vascular structure in blood pressure development of the spontaneously hypertensive rat. *J Hypertens Suppl.* 4:S61-S63.

Mulvany MJ, Aalkjaer C. (1990) Structure and function of small arteries. *Physiol Rev.* 70:921-961.

Mulvany MJ. (1995) Resistance vessel growth and remodelling: cause or consequence in cardiovascular disease. *J Hum Hypertens.* 9:479-485.

Mulvany MJ, Baumbach GL, Aalkjaer C, Heagerty AM, Korsgaard N, Schiffrin EL, Heistad DD. (1996) Vascular remodeling. *Hypertension.* 28:505-506.

Munster PN, Weingart R. (1993) Effects of phorbol ester on gap junctions of neonatal rat heart cells. *Pflugers Arch.* 423:181-188.

Musil LS, Cunningham BA, Edelman GM, Goodenough DA. (1990) Differential phosphorylation of the gap junction protein connexin43 in junctional communication-competent and -deficient cell lines. *J Cell Biol.* 111:2077-2088.

Musil LS, Goodenough DA. (1991) Biochemical analysis of connexin43 intracellular transport, phosphorylation, and assembly into gap junctional plaques. *J Cell Biol.* 115:1357-1374.

Musil LS, Goodenough DA. (1993) Multisubunit assembly of an integral plasma membrane channel protein, gap junction connexin43, occurs after exit from the ER. *Cell.* 74:1065-1077.

Musil LS, Le A-CN, VanSlyke JK, Roberts LM. (2000) Regulation of connexin degradation as a mechanism to increase gap junction assembly and function. *J Biol Chem.* 275:25207-25215.

Nagy JI, Li WE, Roy C, Doble BW, Gilchrist JS, Kardami E, Hertzberg EL. (1997) Selective monoclonal antibody recognition and cellular localization of an unphosphorylated form of connexin43. *Exp Cell Res.* 236:127-136. Nakamura H. (1988) Electron microscopic study of the prenatal development of the thoracic aorta in the rat. *Am J Anat.* 181:406-418.

Nakamura K, Inai T, Shibata Y. (1999) Distribution of gap junction protein connexin 37 in smooth muscle cells of the rat trachea and pulmonary artery. *Arch Histol Cytol.* 62:27-37.

Nakashima M, Vanhoutte PM. (1993) Endothelin-1 and -3 cause endothelium-dependent hyperpolarization in the rat mesenteric artery. *Am J Physiol.* 265:H2137-H2141.

Nakazono K, Watanabe N, Matsuno K, Sasaki J, Sato T, Inoue M. (1991) Does superoxide underlie the pathogenesis of hypertension? *Proc Natl Acad Sci U S A.* 88:10045-10048.

Naus CC, Hearn S, Zhu D, Nicholson BJ, Shivers RR. (1993) Ultrastructural analysis of gap junctions in C6 glioma cells transfected with connexin43 cDNA. *Exp Cell Res.* 206:72-84.

Nava E, Noll G, Luscher TF. (1995) Increased activity of constitutive nitric oxide synthase in cardiac endothelium in spontaneous hypertension. *Circulation.* 91:2310-2313.

Nicholson B, Dermietzel R, Teplow D, Traub O, Willecke K, Revel JP. (1987) Two homologous protein components of hepatic gap junctions. *Nature.* 329:732-734.

Nielsen PA, Beahm DL, Giepmans BN, Baruch A, Hall JE, Kumar NM. (2002) Molecular cloning, functional expression, and tissue distribution of a novel human gap junction-forming protein, connexin-31.9. Interaction with zona occludens protein-1. *J Biol Chem.* 277:38272-38283.

Nielsen PA, Kumar NM. (2003) Differences in expression patterns between mouse connexin-30.2 (Cx30.2) and its putative human orthologue, connexin-31.9. *FEBS Lett.* 540:151-156.

Noll G, Tschudi M, Nava E, Lüscher TF. (1997) Endothelium and high blood pressure. *International Journal of Microcirculation.* 17:273-279.

Noris M, Morigi M, Donadelli R, Aiello S, Foppolo M, Todeschini M, Orisio S, Remuzzi G, Remuzzi A. (1995) Nitric oxide synthesis by cultured endothelial cells is modulated by flow conditions. *Circ Res.* 76:536-543.

Norrelund H, Christensen KL, Samani NJ, Kimber P, Mulvany MJ, Korsgaard N. (1994) Early narrowed afferent arteriole is a contributor to the development of hypertension. *Hypertension*. 24:301-308.

Ohnishi Y, Hirano K, Nishimura J, Furue M, Kanaide H. (2001) Inhibitory effects of brefeldin A, a membrane transport blocker, on the bradykinin-induced hyperpolarization-mediated relaxation in the porcine coronary artery. *Br J Pharmacol*. 134:168-178.

Okamoto K, Aokik. (1963) Development of a strain of spontaneously hypertensive rats. *Japan Circ J*. 27:282-293.

Oku H, Kodama T, Sakagami K, Puro DG. (2001) Diabetes-induced disruption of gap junction pathways within the retinal microvasculature. *Invest Ophthalmol Vis Sci*. 42:1915-1920.

Omar BA, Flores SC, McCord JM. (1992) Superoxide dismutase: pharmacological developments and applications. *Adv Pharmacol*. 23:109-161.

Onaka U, Fujii K, Abe I, Fujishima M. (1998) Antihypertensive treatment improves endothelium-dependent hyperpolarization in the mesenteric artery of spontaneously hypertensive rats. *Circulation*. 98:175-182.

Otsuka S, Sugano M, Makino N, Sawada S, Hata T, and Niho Y. (1998) Interaction of mRNAs for angiotensin II type 1 and type 2 receptors to vascular remodeling in spontaneously hypertensive rats. *Hypertension*. 32:467-472.

Palmer RM, Ashton DS, Moncada S. (1988) Vascular endothelial cells synthesize nitric oxide from L-arginine. *Nature*. 333:664-666.

Palmer RM, Moncada S. (1989) A novel citrulline-forming enzyme implicated in the formation of nitric oxide by vascular endothelial cells. *Biochem Biophys Res Commun*. 158:348-352.

Park JB, Touyz RM, Chen X, Schiffrin EL. (2002) Chronic treatment with a superoxide dismutase mimetic prevents vascular remodeling and progression of hypertension in salt-loaded stroke-prone spontaneously hypertensive rats. *Am J Hypertens*. 15:78-84.

Parkington HC, Tare M, Tonta MA, Coleman HA. (1993) Stretch revealed three components in the hyperpolarization of guinea-pig coronary artery in response to acetylcholine. *J Physiol*. 465:459-476.

Paterno R, Heistad DD, Faraci FM. (1997) Functional activity of Ca^{2+}-dependent K^+ channels is increased in basilar artery during chronic hypertension. *Am J Physiol.* 272:H1287-H1291.

Pepper MS, Meda P. (1992a) Basic fibroblast growth factor increases junctional communication and connexin43 expression in microvascular endothelial cells. *J Cell Physiol.* 153:196-205.

Pepper MS, Montesano R, el Aoumari A, Gros D, Orci L, Meda P. (1992b) Coupling and connexin 43 expression in microvascular and large vessel endothelial cells. *Am J Physiol.* 262:C1246-C1257.

Polacek D, Bech F, McKinsey JF, Davies PF. (1997) Connexin43 gene expression in the rabbit arterial wall: effects of hypercholesterolemia, balloon injury and their combination. *J Vasc Res.* 34:19-30.

Pries AR, Secomb TW. (2002) Structural adaption of microvascular networks and development of hypertension. *Microcirculation.* 9:305-314.

Puddu P, Puddu GM, Zaca F, Muscari A. (2000) Endothelial dysfunction in hypertension. *Acta Cardiol.* 55:221-232.

Rajagopalan S, Kurz S, Munzel T, Tarpey M, Freeman BA, Griendling KK, Harrison DG. (1996) Angiotensin II-mediated hypertension in the rat increases vascular superoxide production via membrane NADH/NADPH oxidase activation. Contribution to alterations of vasomotor tone. *J Clin Invest.* 97:1916-1923.

Randall MD, Alexander SP, Bennett T, Boyd EA, Fry JR, Gardiner SM, Kemp PA, McCulloch AI, Kendall DA. (1996) An endogenous cannabinoid as an endothelium-derived vasorelaxant. *Biochem Biophys Res Commun.* 229:114-120.

Rao GN, Berk BC. (1992) Active oxygen species stimulate vascular smooth muscle cell growth and proto-oncogene expression. *Circ Res.* 70:593-599.

Rapoport RM, Murad F. (1983) Agonist-induced endothelium-dependent relaxation in rat thoracic aorta may be mediated through cGMP. *Circ Res.* 52:352-357.

Reaume AG, de Sousa PA, Kulkarni S, Langille BL, Zhu D, Davies TC, Juneja SC, Kidder GM, Rossant J. (1995) Cardiac malformation in neonatal mice lacking connexin43. *Science.* 267:1831-1834.

Reed KE, Westphale EM, Larson DM, Wang HZ, Veenstra RD, Beyer EC. (1993) Molecular cloning and functional expression of human connexin37, an endothelial cell gap junction protein. *J Clin Invest.* 91:997-1004.

Rees D, Ben Ishay D, Moncada S. (1996) Nitric oxide and the regulation of blood pressure in the hypertension-prone and hypertension-resistant Sabra rat. *Hypertension.* 28:367-371.

Rennick RE, Connat JL, Burnstock G, Rothery S, Severs NJ, Green CR. (1993) Expression of connexin43 gap junctions between cultured vascular smooth muscle cells is dependent upon phenotype. *Cell Tissue Res.* 271:323-332.

Resnick N, Yahav H, Shay-Salit A, Shushy M, Schubert S, Zilberman LC, Wofovitz E. (2003) Fluid shear stress and the vascular endothelium: for better and for worse. *Prog Biophys Mol Biol.* 81:177-199.

Rizzoni D, Porteri E, Piccoli A, Castellano M, Bettoni G, Muiesan ML, Pasini G, Guelfi D, Mulvany M, Rosei EA. (1998) Effects of losartan and enalapril on small artery structure in hypertensive rats. *Hypertension.* 32:305-310.

Ross R. (1995) Cell biology of atherosclerosis. *Annu Rev Physiol.* 57:791-804.

Saez JC, Nairn AC, Czernik AJ, Fishman GI, Spray DC, Hertzberger EL. (1997) Phosphorylation of connexin43 and the regulation of neonatal rat cardiac myocyte gap junctions. *Journal of Molecular and Cellular Cardiology.* 29:2131-2145.

Saez JC, Martinez AD, Branes MC, Gonzalez HE. (1998) Regulation of gap junctions by protein phosphorylation. *Braz J Med Biol Res.* 31:593-600.

Saleh FH, Jurjus AR. (2001) A comparative study of morphological changes in spontaneously hypertensive rats and normotensive Wistar Kyoto rats treated with an angiotensin-converting enzyme inhibitor or a calcium-channel blocker. *J Path.* 193:415-420.

Sandow SL, Hill CE. (2000) The incidence of myoendothelial gap junctions in the proximal and distal mesenteric arteries of the rat is suggestive of a role in EDHF-mediated responses. *Circ Res.* 86:341-346.

Sandow SL, Tare M, Coleman HA, Hill CE, Parkington HC. (2002) Involvement of myoendothelial gap junctions in the actions of endothelium-derived hyperpolarizing factor. *Circ Res.* 90:1108-1113.

Sandow SL, Bramich NJ, Bandi HP, Rummery NM, Hill CE. (2003a) Endothelium-derived hyperpolarizing factor, myoendothelial gap junctions and hypertension. In: *EDHF 2002.* Vanhoutte PM, ed. Taylor & Francis, London.

Sandow SL, Bramich NJ, Bandi HP, Rummery NM, Hill CE. (2003b) Structure, Function, and Endothelium-Derived Hyperpolarizing Factor in the Caudal Artery of the SHR and WKY Rat. *Arterioscler Thromb Vasc Biol.* 23:822-828.

Sandow SL, Goto K, Rummery NM, Hill CE. (2003c) Transient developmental appearance of myoendothelial gap junctions and EDHF in rat saphenous artery. *FEPS.* 3:10.

Sandow SL, Looft-Wilson R, Doran B, Grayson TH, Segal SS, Hill CE. (2003d) Expression of homocellular and heterocellular gap junctions in hamster arterioles and feed arteries. *Cardiovasc Res.* In press.

Sarma JD, Wang F, Koval M. (2002) Targeted gap junction protein constructs reveal connexin-specific differences in oligomerization. *J Biol Chem.* 277:20911-20918.

Sato T, Haimovici R, Kao R, Li AF, Roy S. (2002) Downregulation of connexin 43 expression by high glucose reduces gap junction activity in microvascular endothelial cells. *Diabetes.* 51:1565-1571.

Savage D, Perkins J, Lim CH, Bund SJ. (2003) Functional evidence the K^+ is the non-nitric oxide, non-prostanoid endothelium-derived relaxing factor in rat femoral arteries. *Vasc Pharmacol.* 40:23-28.

Schiffrin EL, Thome FS, Genest J. (1984) Vascular angiotensin II receptors in SHR. *Hypertension.* 6:682-688.

Schiffrin EL. (1998) Endothelin: role in hypertension. *Biol Res.* 31:199-208.

Schiffrin EL. (1999) Role of endothelin-1 in hypertension. *Hypertension.* 34:876-881.

Schubert R, Mulvany MJ. (1999) The myogenic response: established facts and attractive hypotheses. *Clin Sci (Lond).* 96:313-326.

Schwartz CJ, Chandler AB, Gerrity RG, Naito HK. (1978) Clinical and pathological aspects of arterial thrombosis and thromboembolism. *Adv Exp Med Biol.* 104:111-126.

Segal SS, Duling BR. (1989) Conduction of vasomotor responses in arterioles: a role for cell-to-cell coupling? *Am J Physiol.* 256:H838-H845.

Segal S, Welsh DG, Kurjiaka DT. (1999) Spread of vasodilation and vasoconstriction along feed arteries and arterioles of hamster skeletal muscle. *J Physiol.* 516:283-291.

Segal S, Emerson GG, Bartlett IS. (2001) Endothelium and smooth muscle pathways for conduction along resistance microvessels. In: *EDHF 2000.* Vanhoutte PM, ed. Taylor & Francis, London.

Seul KH, Beyer EC. (2000) Heterogenous localization of conexin40 in the renal vasculature. *Microvasc Res.* 59:140-148.

Severs NJ, Shovel KS, Slade AM, Powell T, Twist VW, Green CR. (1989) Fate of gap junctions in isolated adult mammalian cardiomyocytes. *Circ Res.* 65:22-42.

Severs NJ, Dupont E, Kaprielian R, Yeh H-I, Rothery S. (1996) Gap junctions and connexins in the cardiovascular system. In: *Annual review of cardiac surgery.* Yacoub MH, Carpentier A, Pepper J, Fabiani JN, eds. Rapid Science, London.

Severs NJ. (1999) Cardiovascular disease. In: *Novartis Foundation Symposium: Gap junction-mediated intercellular signaling in health and disease.* 219:188-211. Norton B Gilula, ed. Wiley, New York.

Severs NJ, Rothery S, Dupont E, Coppen SR, Yeh H-I, Ko Y-S, Matsushita T, Kaba R, Halliday D. (2001) Immunocytochemical analysis of connexin expression in healthy and diseased cardiovascular system. *Micro Res Tech.* 52:301-322.

Sharifi AM, Li JS, Endemann D, Schiffrin EL. (1998) Effects of enalapril and amlodipine on small-artery structure and composition, and on endothelial dysfunction in spontaneously hypertensive rats. *J Hypertens.* 16:457-466.

Sharifi AM, Schiffrin EL. (1998) Apoptosis in vasculature of spontaneously hypertensive rats: effect of an angiotensin converting enzyme inhibitor and a calcium channel antagonist. *Am J Hypertens.* 11:1108-1116.

Shimamura K, Sekiguchi F, Sunano S. (1999) Tension oscillation in arteries and its abnormality in hypertensive animals. *Clin Exp Pharmacol Physiol.* 26:275-284.

Shimizu S, Ishii M, Yamamoto T, Kawanishi T, Momose K, Kuroiwa Y. (1994) Bradykinin induces generation of reactive oxygen species in bovine aortic endothelial cells. *Res Commun Chem Pathol Pharmacol.* 84:301-314.

Shimokawa H, Yasutake H, Fujii K, Owada K, Nakaike R, Fukumoto Y, Takayanagi T, Nagao T, Egashira K, Fujishima M, Takeshita A. (1996) The importance of the hyperpolarizing mechanism increases as the vessel size decreases in endothelium-dependent relaxations in rat mesenteric circulation. *J Cardiovasc Pharmacol.* 28:703-711.

Shimokawa H. (1998) Endothelial dysfunction in hypertension. *J Atheroscler Thromb.* 4:118-127.

Shimokawa H. (1999) Endothelial dysfunction: a novel therapeutic target. Primary endothelial dysfunction: atherosclerosis. *J Mol Cell Cardiol.* 31:23-37.

Sho E, Komatsu M, Sho M, Nanjo H, Singh TM, Xu C, Masuda H, Zarins CK. (2003) High flow drives vascular endothelial cell proliferation during flow-induced arterial

remodeling associated with the expression of vascular endothelial growth factor. *Exp Mol Pathol.* 75:1-11.

Simon AM, Goodenough DA, Li E, Paul DL. (1997) Female infertility in mice lacking connexin 37. *Nature.* 385:525-529.

Simon AM, Goodenough DA, Paul DL. (1998) Mice lacking connexin40 have cardiac conduction abnormalities characteristic of atrioventricular block and bundle branch block. *Curr Biol.* 8:295-298.

Simon AM, McWhorter AR. (2002) Vascular abnormalities in mice lacking the endothelial gap junction proteins connexin37 and connexin40. *Dev Biol.* 251:206-220.

Simon AM, McWhorter AR. (2003) Decreased intercellular dye-transfer and downregulation of non-ablated connexins in aortic endothelium deficient in connexin37 or connexin40. *J Cell Sci.* 116:2223-2236.

Smith WL, Marnett LJ, DeWitt DL. (1991) Prostaglandin and thromboxane biosynthesis. *Pharmacol Ther.* 49:153-179.

Smith WL. (1992) Prostanoid biosynthesis and mechanisms of action. *Am J Physiol.* 263:F181-F191.

Sobey CG. (2003) Potassium channels in the cerebral circulation in health and vascular disease. *Proc Australian Physiol Pharmacol Soc.* 33:9P.

Sofola OA, Knill A, Hainsworth R, Drinkhill M. (2002) Change in endothelial function in mesenteric arteries of Sprague-dawley rats fed a high salt diet. *J Physiol.* 543:255-260.

Sosinsky GE. (1996) Molecular organization of gap junction membrane channels. *J Bioenerg Biomembr.* 28:297-309.

Spagnoli LG, Villaschi S, Neri L, Palmeri G. (1982) Gap junctions in myoendothelial bridges of rabbit carotid arteries. *Exp.* 38:124-125.

Spray DC, Burt JM. (1990) Structure-activity relations of the cardiac gap junction channel. *Am J Physiol.* 258:C195-C205.

Staessen JA, Wang J, Bianchi G, Birkenhager WH. (2003) Essential hypertension. *Lancet.* 361:1629-1641.

Steinberg TH, Civitelli R, Geist ST, Robertson AJ, Hick E, Veenstra RD, Wang HZ, Warlow PM, Westphale EM, Laing JG. (1994) Connexin43 and connexin45 form

gap junctions with different molecular permeabilities in osteoblastic cells. *EMBO J.* 13:744-750.

Stergiopoulos K, Alvarado JL, Mastroianni M, Ek-Vitorin JF, Taffet SM, Delmar M. (1999) Hetero-domain interactions as a mechanism for the regulation of connexin channels. *Circ Res.* 84:1144-1155.

Stoll M, Jacob HJ. (2001) Genetic rat models of hypertension: relationship to human hypertension. *Current Hypertension Reports.* 3:157-164.

Sunano S, Watanabe H, Tanaka S, Sekiguchi F, Shimamura K. (1999) Endothelium-derived relaxing, contracting and hyperpolarizing factors of mesenteric arteries of hypertensive and normotensive rats. *Br J Pharmacol.* 126:709-716.

Suzuki YJ, Ford GD. (1992) Superoxide stimulates IP_3-induced Ca^{2+} release from vascular smooth muscle sarcoplasmic reticulum. *Am J Physiol.* 262:H114-H116.

Takemoto M, Egashira K, Tomita H, Usui M, Okamoto H, Kitabatake A, Shimokawa H, Sueishi K, Takeshita A. (1997) Chronic angiotensin-converting enzyme inhibition and angiotensin II type 1 receptor blockade: effects on cardiovascular remodeling in rats induced by the long-term blockade of nitric oxide synthesis. *Hypertension.* 30:1621-1627.

Takemoto M, Egashira K, Usui M, Numaguchi K, Tomita H, Tsutsui H, Shimokawa H, Sueishi K, Takeshita A. (1997) Important role of tissue angiotensin-converting enzyme activity in the pathogenesis of coronary vascular and myocardial structural changes induced by long-term blockade of nitric oxide synthesis in rats. *J Clin Invest.* 99:278-287.

Takens-Kwak BR, Jongsma HJ. (1992) Cardiac gap junctions: three distinct single channel conductances and their modulation by phosphorylating treatments. *Pflugers Arch.* 422:198-200.

Tamaddon HS, Vaidya D, Simon AM, Paul DL, Jalife J, Morley GE. (2000) High-resolution optical mapping of the right bundle branch in connexin40 knockout mice reveals slow conduction in the specialized conduction system. *Circ Res.* 87:929-936.

Tare M, Coleman HA, Parkington HC. (2002) Glycyrrhetinic derivatives inhibit hyperpolarization in endothelial cells of guinea pig and rat arteries. *Am J Physiol.* 282:H335-H341.

Taylor HJ, Chaytor AT, Edwards DH, Griffith TM. (2001) Gap junction-dependent increases in smooth muscle cAMP underpin the EDHF phenomenon in rabbit arteries. *Biochem Biophys ResComm.* 283:583-589.

Taylor SG, Weston AH. (1988) Endothelium-derived hyperpolarizing factor: a new endogenous inhibitor from the vascular endothelium. *Trends Pharmacol Sci.* 9:272-274.

Tearle A. (2002) The communications gap. *Biologist (London).* 49:29-32.

Theis M, de Wit C, Schlaeger TM, Eckardt D, Krüeger O, Döring B, Risau W, Deutsch U, Pohl U, Willecke K. (2001) Endothelium-specific replacement of the connexin43 coding region by a lacZ reporter gene. *Genesis.* 29:1-13.

Thomas MA, Huang S, Cokoja A, Riccio O, Staub O, Suter S, Chanson M. (2002) Interaction of connexins with protein partners in the control of channel turnover and gating. *Biol Cell.* 94:445-456.

Thomas SA, Schuessler RB, Berul CI, Beardslee MA, Beyer EC, Mendelsohn ME, Saffitz JE. (1998) Disparate effects of deficient expression of connexin43 on atrial and ventricular conduction: evidence for chamber-specific molecular determinants of conduction. *Circulation.* 97:686-691.

Tomioka H, Hattori K, Fukao M, Sakuma I, Sato I, Liu M-Y, Kanno M. (1999) Mechanism why endothelium-derived hyperpolarizing factor-mediated relaxation is more prominent in smaller blood vessels: involvement of Ca^{2+} sensitivity of contractile elements. *Circulation.* 100:I415.

Touyz RM. (2000) Molecular and cellular mechanisms regulating vascular function and structure - implications in the pathogenesis of hypertension. *Can J Cardiol.* 16:1137-1146.

Toyofuku T, Yabuki M, Otsu K, Kuzuya T, Hori M, Tada M. (1998) Direct association of the gap junction protein connexin-43 with ZO-1 in cardiac myocytes. *J Biol Chem.* 273:12725-12731.

Traub O, Eckert R, Lichtenberg-Frate H, Elfgang C, Bastide B, Scheidtmann KH, Hulser DF, Willecke K. (1994) Immunochemical and electrophysiological characterization of murine connexin40 and -43 in mouse tissues and transfected human cells. *Eur J Cell Biol.* 64:101-112.

Tschudi MR, Mesaros S, Luscher TF, Malinski T. (1996) Direct in situ measurement of nitric oxide in mesenteric resistance arteries. Increased decomposition by superoxide in hypertension. *Hypertension.* 27:32-35.

Tsien RW, Weingart R. (1976) Inotropic effect of cyclic AMP in calf ventricular muscle studied by a cut end method. *J Physiol.* 260:117-141.

Tyml K, Wang X, Lidington D, Ouellette Y. (2001) Lipopolysaccharide reduces intercellular coupling in vitro and arteriolar conducted response in vivo. *Am J Physiol*. 281:H1397-H1406.

Ujiie H, Chaytor AT, Bakker LM, Griffith TM. (2003) Essential role of gap junctions in NO- and prostanoid-independent relaxations evoked by acetylcholine in rabbit intracerebral arteries. *Stroke*. 34:544-550.

Ungvari Z, Koller A. (2000) Endothelin and prostaglandin H_2/thromboxane A_2 enhance myogenic constriction in hypertension by increasing sensitivity of arteriolar smooth muscle. *Hypertension*. 36:853-861.

Unwin PNT, Zampighi G. (1980) Structure of the junction between communicating cells. *Nature*. 283:545-549.

Urakami L, Shimokawa H, Nakashima M, Matsumoto N, Owada MK, Takeshita A. (1997) Relative importance of endothelium-derived hyperpolarizing factor and nitric oxide in coronary arteries in pigs and rabbits. *Japan J Pharmacol*. 75:49P.

Valiunas V, Weingart R, Brink PR. (2000) Formation of heterotypic gap junction channels by connexins 40 and 43. *Circ Res*. 86:1-e42.

Valiunas V, Gemel J, Brink PR, Beyer EC. (2001) Gap junction channels formed by coexpressed connexin40 and connexin43. *Am J Physiol*. 281:H1675-H1689.

Valiunas V, Beyer EC, Brink PR. (2002) Cardiac gap junction channels show quantitative differences in selectivity. *Circ Res*. 91:104-111.

Van Gorp AD, Van Ingen Schenau DS, Hoeks APG, Struyker-Boudier HA, De Mey J, Reneman RS. (2000) In spontaneously hypertensive rats alterations in aortic wall properties precede development of hypertension. *Am J Physiol*. 278:H1241-H1247.

van Kempen MJ, Jongsma HJ. (1999) Distribution of connexin37, connexin40 and connexin43 in the aorta and coronary artery of several mammals. *Histochem Cell Biol*. 112:479-486.

Van Rijen H, van Kempen MJ, Analbers LJ, Rook MB, van Ginneken AC, Gros D, Jongsma HJ. (1997) Gap junctions in human umbilical cord endothelial cells contain multiple connexins. *Am J Physiol*. 272:C117-C130.

Van Rijen HV, van Kempen MJ, Postma S, Jongsma HJ. (1998) Tumour necrosis factor alpha alters the expression of connexin43, connexin40, and connexin37 in human umbilical vein endothelial cells. *Cytokine*. 10:258-264.

Van Rijen HV, van Veen TA, Hermans MM, Jongsma HJ. (2000) Human connexin40 gap junction channels are modulated by cAMP. *Cardiovasc Res.* 45:941-951.

van Veen TAB, Van Rijen HVM, Jongsma HJ. (2000) Electrical conductance of mouse connexin45 gap junction channels is modulated by phosphorylation. *Cardiovas Res.* 46:496-510.

van Veen TAB, Van Rijen H, Opthof T. (2001) Cardiac gap junction channels: modulation of expression and channel properties. *Cardiovasc Res.* 51:217-229

Vanhoutte PM. (1989) Endothelium and control of vascular function: state of the art lecture. *Hypertension.* 13:658-667.

Vanhoutte PM, Boulanger CM. (1995) Endothelium-dependent responses in hypertension. *Hypertens Res.* 18:87-98.

Vargas HM, Ignarro LJ, Chaudhuri G. (1990) Physiological release of nitric oxide is dependent on the level of vascular tone. *Eur J Pharmacol.* 190:393-397.

Vaziri ND, Ding Y, Ni Z. (2001) Compensatory up-regulation of nitric-oxide synthase isoforms in lead-induced hypertension; reversal by a superoxide dismutase-mimetic drug. *J Pharmacol Exp Ther.* 298:679-685.

Vaziri ND, Ni Z, Oveisi F. (1998) Upregulation of renal and vascular nitric oxide synthase in young spontaneously hypertensive rats. *Hypertension.* 31:1248-1254.

Vazquez-Perez S, Navarro-Cid J, de Las HN, Cediel E, Sanz-Rosa D, Ruilope LM, Cachofeiro V, Lahera V. (2001) Relevance of endothelium-derived hyperpolarizing factor in the effects of hypertension on rat coronary relaxations. *J Hypertens.* 19:539-545.

Veenstra RD, Wang HZ, Westphale EM, Beyer EC. (1992) Multiple connexins confer distinct regulatory and conductance properties of gap junctions in developing heart. *Circ Res.* 71:1277-1283.

Veenstra RD, Wang H-Z, Beyer EC, Brink PR. (1994a) Selective dye and ionic permeability of gap junction channels formed by connexin45. *Circ Res.* 75:483-490.

Veenstra RD, Wang HZ, Beyer EC, Ramanan SV, Brink PR. (1994b) Connexin37 forms high conductance gap junction channels with subconductance state activity and selective dye and ionic permeabilities. *Biophys J.* 66:1915-1928.

Veenstra RD, Wang HZ, Beblo DA, Chilton MG, Harris AL, Beyer EC, Brink PR. (1995) Selectivity of connexin-specific gap junctions does not correlate with channel conductance. *Circ Res.* 77:1156-1165.

Verheule S, van Kempen MJA, te Welscher PHJA, Kwak BR, Jongsma HJ. (1997) Characterisation of gap junction channels in adult rabbit atrial and ventricular myocardium. *Circ Res.* 80:673-681.

von der Weid P-Y, Beny J-L. (1993) Simultaneous oscillations in the membrane potential of pig coronary artery endothelial and smooth muscle cells. *J Physiol.* 471:13-24.

Vozzi C, Dupont E, Coppen SR, Yeh HI, Severs NJ. (1999) Chamber-related differences in connexin expression in the human heart. *J Mol Cell Cardiol.* 31:991-1003.

Warn-Cramer BJ, Lampe PD, Kurata WE, Kanemitsu MY, Loo LW, Eckhart W, Lau AF. (1996) Characterization of the mitogen-activated protein kinase phosphorylation sites on the connexin-43 gap junction protein. *J Biol Chem.* 271:3779-3786.

Watts SW, Webb RC. (1996) Vascular gap junctional communication is increased in mineralocorticoid-salt hypertension. *Hypertension.* 28:888-893.

Webb DJ, Cumming AM, Adams FC, Hodsman GP, Leckie BJ, Lever AF, Morton JJ, Murray GD, Robertson JI. (1984) Changes in active and inactive renin and in angiotensin II across the kidney in essential hypertension and renal artery stenosis. *J Hypertens.* 2:605-614.

Welsh DG, Segal SS. (1998) Endothelial and smooth muscle cell conduction in arterioles controlling blood flow. *Am J Physiol.* 274:H178-H186.

Werner R, Levine E, Rabadan-Diehl C, Dahl G. (1991) Gating properties of connexin32 cell-cell channels and their mutants expressed in Xenopus oocytes. *Proc R Soc Lond B Biol Sci.* 243:5-11.

White TW, Paul DL. (1999) Genetic diseases and gene knockouts reveal diverse connexin functions. *Annu Rev Physiol.* 61:283-310.

White TW, Srinivas M, Ripps H, Trovato-Salinaro A, Condorelli DF, Bruzzone R. (2002) Virtual cloning, functional expression, and gating analysis of human connexin31.9. *Am J Physiol.* 283:C960-C970.

Whitworth JA, Hewitson TD, Ming L, Wilson RS, Scoggins BA, Wright RD, Kincaid-Smith P. (1990) Adrenocorticotrophin-induced hypertension in the rat: haemodynamic, metabolic and morphological characteristics. *J Hypertens.* 8:27-36.

Wigg SJ, Tare M, Tonta MA, O'Brien RC, Meridith IT, Parkington HC. (2001) Comparison of the effects of diabetes mellitus on an EDHF-dependent and an EDHF-independent artery. *Am J Physiol.* 281:H232-H240.

Willecke K, Heynkes R, Dahl E, Stutenkemper R, Hennemann H, Jungbluth S, Suchyna T, Nicholson BJ. (1991) Mouse connexin37: cloning and functional expression of a gap junction gene highly expressed in lung. *J Cell Biol.* 114:1049-1057.

Willecke K, Eiberger J, Degen J, Eckardt D, Romualdi A, Guldenagel M, Deutsch U, Sohl G. (2002) Structural and functional diversity of connexin genes in the mouse and human genome. *Biol Chem.* 383:725-737.

Xia J, Duling BR. (1995) Electromechanical coupling and the vasomotor response. *Am J Physiol.* 269:H2022-H2030.

Xia J, Little TL, Duling BR. (1995) Cellular pathways of the conducted electrical response in arterioles of hamster cheek pouch in vitro. *Am J Physiol.* 269:H2031-H2038.

Yamamoto H, Fukuta H, Nakahira Y, Suzuki H. (1998) Blockade by 18β-glycyrrhetinic acid of intercellular electrical coupling in guinea-pig arterioles. *J Physiol.* 511:501-508.

Yamamoto Y, Imaeda K, Suzuki H. (1999) Endothelium-dependent hyperpolarization and intercellular electrical coupling in guinea-pig mesenteric arterioles. *J Physiol.* 514:505-513.

Yamamoto Y, Klemm MF, Edwards FR, Suzuki H. (2001) Intercellular electrical communication among smooth muscle and endothelial cells in guinea-pig mesenteric arterioles. *J Physiol.* 535:181-195.

Yeager M, Gilula NB. (1992) Membrane topology and quaternary structure of cardiac gap junction ion channels. *J Mol Biol.* 223:929-948.

Yeager M, Nicholson BJ. (1996) Structure of gap junction intercellular channels. *Curr Opin Struct Biol.* 6:183-192.

Yeager M, Unger VM, Falk MM. (1998) Synthesis, assembly and structure of gap junction intercellular channels. *Curr Opin Struct Biol* . 8:517-524.

Yeh H-I, Dupont E, Coppen S, Rothery S, Severs NJ. (1997a) Gap junction localization and connexin expression in cytochemically identified endothelial cells of arterial tissue. *J Histochem Cytochem.* 45:539-550.

Yeh H-I, Lupu F, Dupont E, Severs NJ. (1997b) Upregulation of connexin43 gap junctions between smooth muscle cells after balloon catheter injury in ther rat carotid artery. *Arterioscler Thromb Vasc Biol.* 17:3174-3184.

Yeh H-I, Rothery S, Dupont E, Coppen S, Severs NJ. (1998) Individual gap junction plaques contain multiple connexins in arterial endothelium. *Circ Res.* 83:1248-1263.

Yeh H-I, Chang H-M, Lu W-W, Lee Y-N, Ko Y-S, Severs NJ, Tsai C-H. (2000) Age-related alteration of gap junction distribution and connexin expression in rat aortic endothelium. *J Histochem Cytochem.* 48:1377-1389.

Yu QC, McNeil PL. (1992) Transient disruptions of aortic endothelial cell plasma membranes. *Am J Pathol.* 141:1349-1360.

Zaniboni M, Rossini A, Swietach P, Banger N, Spitzer KW, Vaughan-Jones RD. (2003) Proton permeation through the myocardial gap junction. *Circ Res.* 93:726-735.

Zygmunt PM, Ryman T, Hogestatt ED. (1995) Regional differences in endothelium-dependent relaxation in the rat: contribution of nitric oxide and nitric oxide-independent mechanisms. *Acta physiol scand.* 155:257-266.